2-D and 3-D ERT surveys and data interpretation

Turin, Italy, 10th. Sept. 2015
Piedmont Regional Order of Geologists
Pasi Geophysics

M.H. Loke
Geotomo Software Pty Ltd
email : geotomosoft@gmail.com
mhloke@geotomosoft.com
www.geotomosoft.com

Workshop outline

1) Brief introduction to the resistivity method.
2) Progress of electrical methods 1930s to 2010s, from 1- D to 4-D
3) 2-D surveys, data and inversion
4) 3-D surveys, data and inversion
5) 4-D surveys, data and inversion
6) Special topics – depending on time limitations

M.H. Loke, geotomosoft@gmail.com

Part 1

Brief introduction to resistivity surveys.

The electrical method – Ohm's Law

Geophysical methods measure some physical (physics) property of materials within the earth (geo). The electrical method measures the resistivity of soils and rocks. The basic physical law used is Ohm's Law. Ohm's Law gives the relationship between the voltage (V), current (I) and resistance (R). It is given by

$$V = R\,I$$

This form of Ohm's Law is for a current flow in an electrical circuit through a resistor.

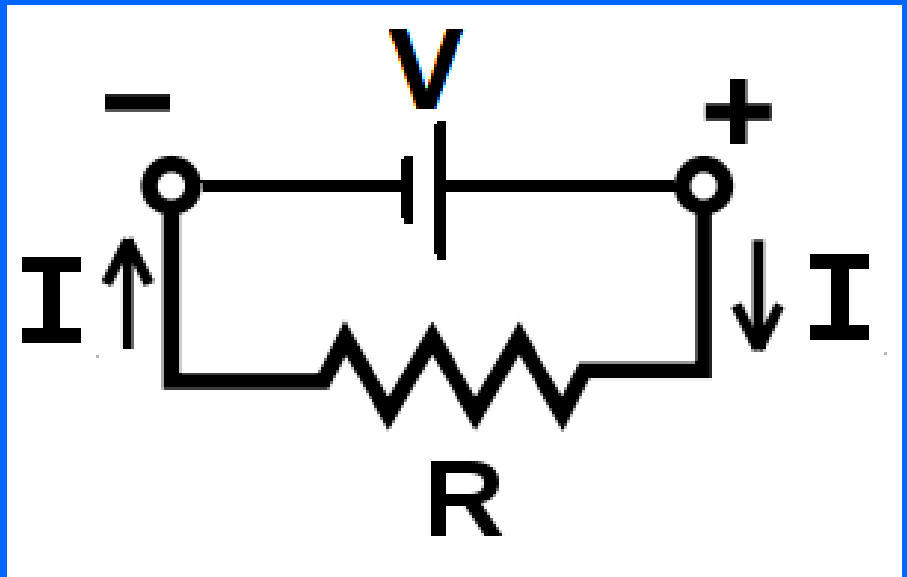

Resistivity measurements in a laboratory

In a laboratory, the resistivity of a material ρ can be determined from the resistance R between two opposite faces of a prism cut out of that material. Each face has surface area A, and the two faces are seperated by distance l. Then $\rho = R A / l$

The unit of resistivity is ohm.meter (Ω.m).

Sometimes the conductivity, s, which is the reciprocal of the resistivity is used.

$$s = 1 / \rho$$

A common unit used for conductivity is milliSeimen/cm (mS/cm).

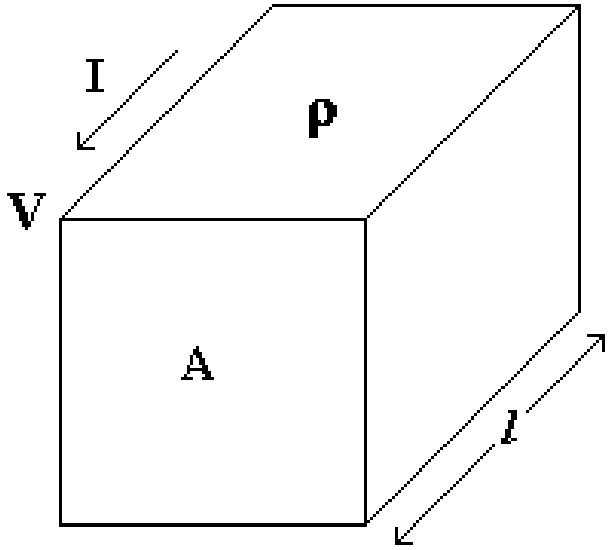

$R = V / I$

$\rho = R A / l$

Ohm's Law in geophysics

In the earth, the current does not pass through a single resistor, but spreads in all directions. The equation for Ohm's Law for current flow through a continuous medium is given by

$$-\nabla \bullet \left[\frac{1}{\rho(x,y,z)} \nabla \Phi(x,y,z) \right] = I_c$$

ρ is the resistivity of the medium, ϕ is the potential due to a current source I.

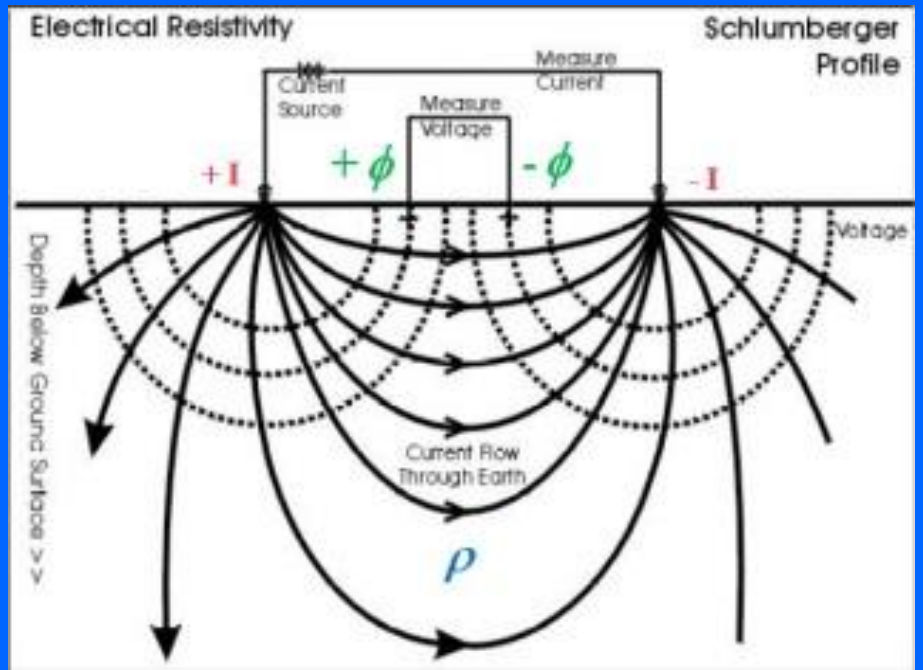

Potential for a homogeneous medium

In a homogeneous half-space, the potential due to a single current electrode has a simple form

$$\phi = I \rho / 2\pi a$$

where 'a' is the distance between the current and potential electrodes.

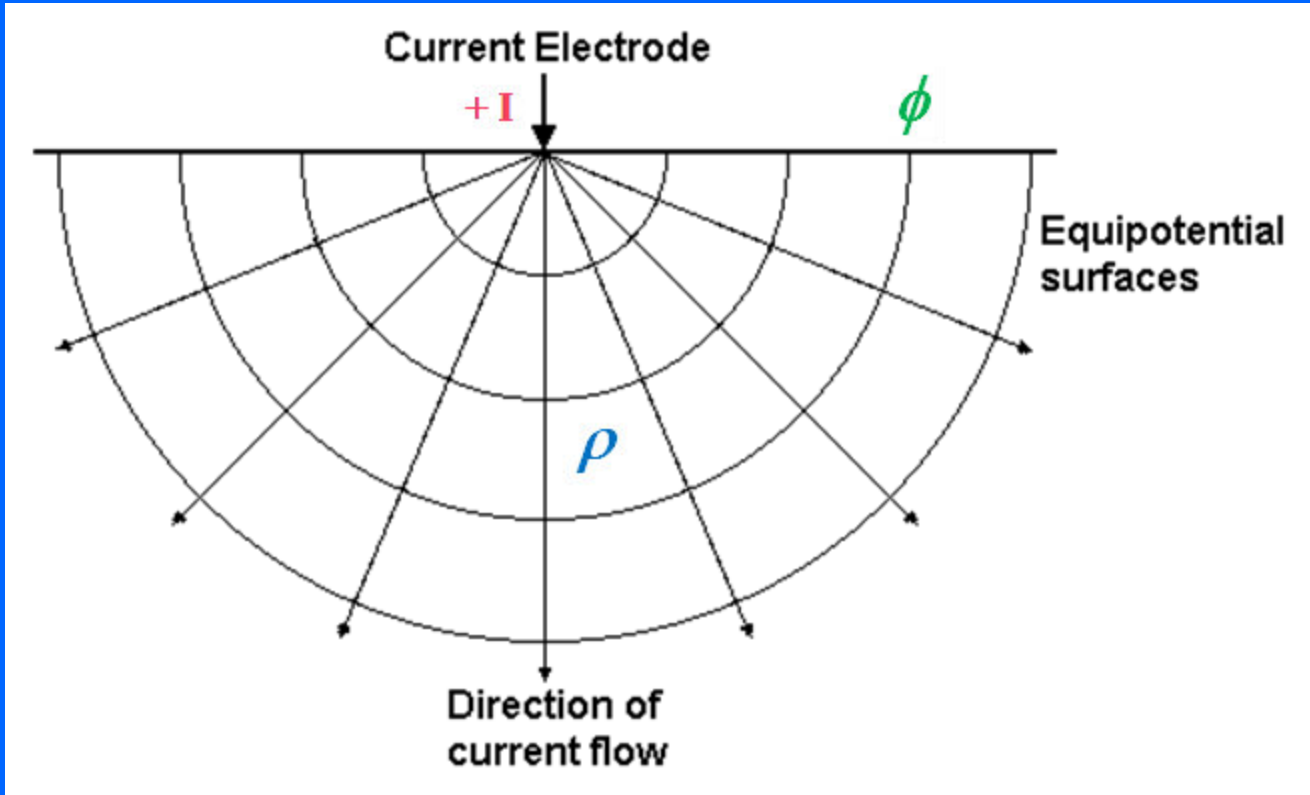

Electrical potentials due to point current sources

In practice, positive and negative current sources area used. The voltage difference between two potential electrode is measured. From the current (I) and potential difference (ΔV) measurements, an apparent resistivity value is calculated. The apparent resistivity value ρ_a is calculated as

$$\rho_a = k\ \Delta V / I = k\ R$$

k = geometric factor, R = resistance

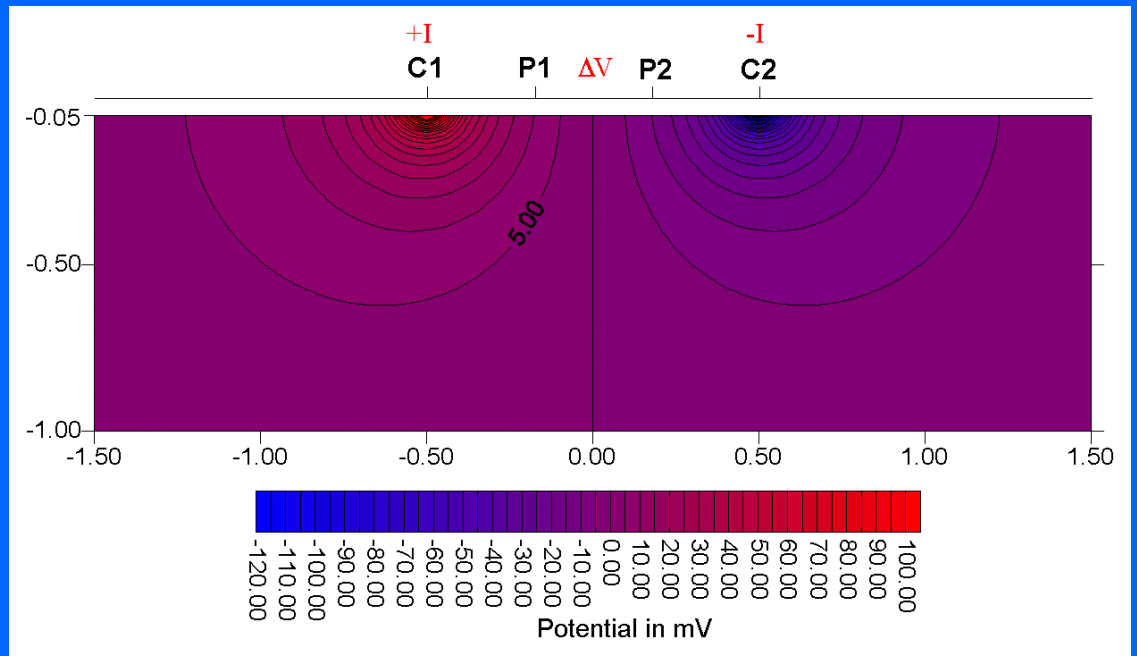

Apparent resistivity

The apparent resistivity value ρ_a calculated by

$$\rho_a = k\ \Delta V / I = k\ R$$

is only equal to the true resistivity for a homogeneous medium. The relationship between the apparent resistivity and the true resistivity is complex for a general non-homogeneous medium, as in all cases for measurements in the earth.

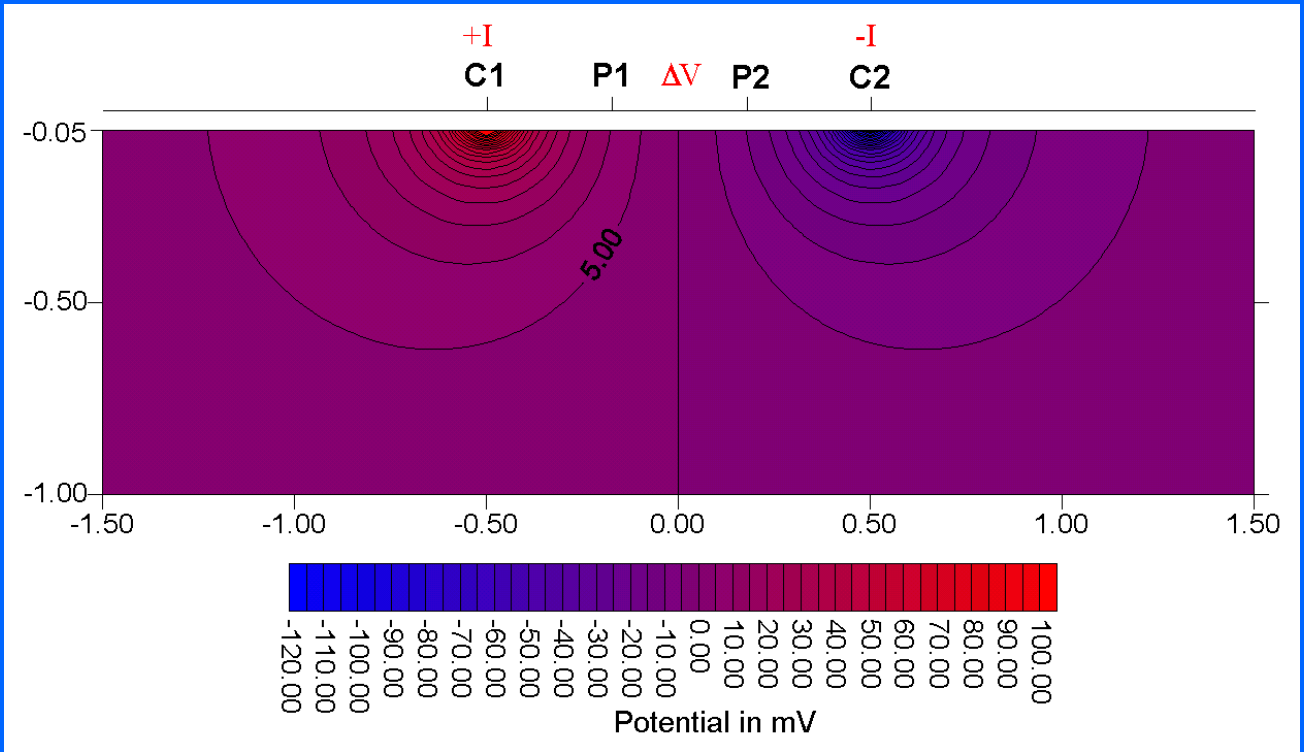

Electrical field survey measurements

In a field survey, the resistivity of the subsurface is measured by passing a current through the ground. Four metal electrodes are planted into the ground. An electric current (10mA to 3 A) is injected into the ground using electrodes C_1 and C_2. The resulting voltage difference at two points on the ground surface is measured using two electrodes, P_1 and P_2. Changes in the ground resistivity will cause deviations in the current flow and the resulting measured voltage difference.

Basic setup for a resistivity survey

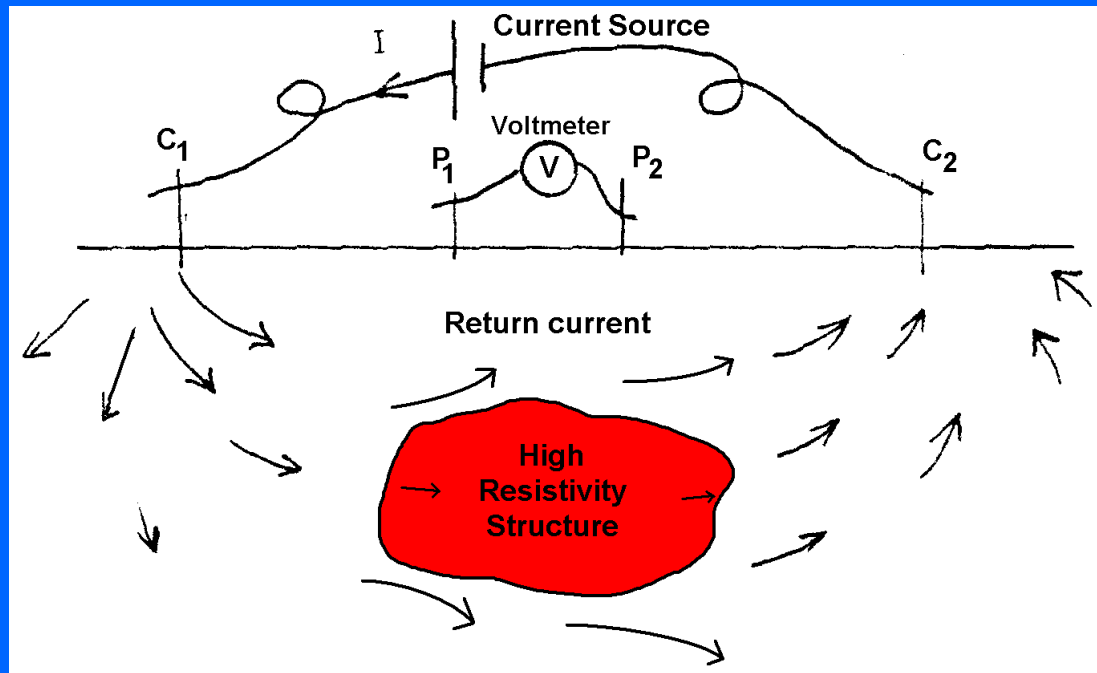

Current flow in the earth

Electric current flows in the earth through two main methods, electronic conduction and electrolytic conduction. The most common method is electrolytic conduction where the current flow is via the movement of ions in groundwater. In environmental and engineering surveys, electrolytic conduction is probably the more common mechanism. Changes in the fluid content causes changes in the electrical conductivity.

This could be due to changes in the porosity, or nature of the fluid (water to hydrocarbons), or solid matrix (sand to clay).

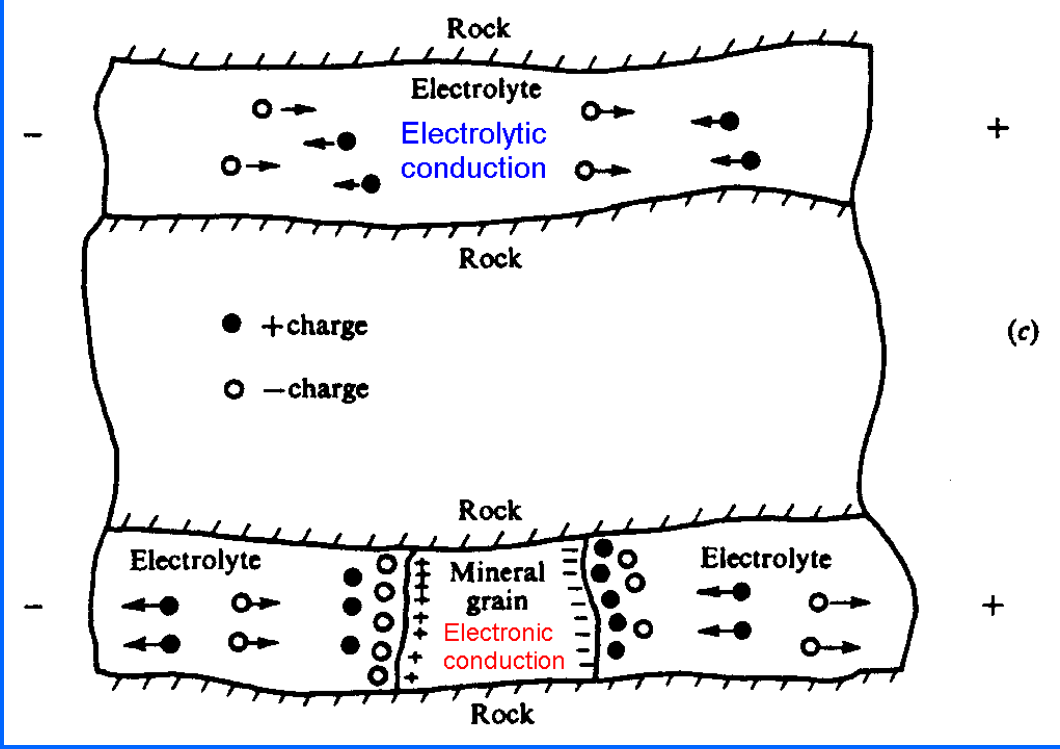

After : Telford, W.M., Geldart, L.P. and Sheriff, R.E., 1990. Applied Geophysics (second edition). Cambridge University Press.

Electronic conduction

In electronic conduction, the current flow is via free electrons, such as in metals. Electronic conduction is important when conductive minerals are present, such metal sulfides and graphite in mineral surveys, and industrial metals in environmental/engineering surveys.

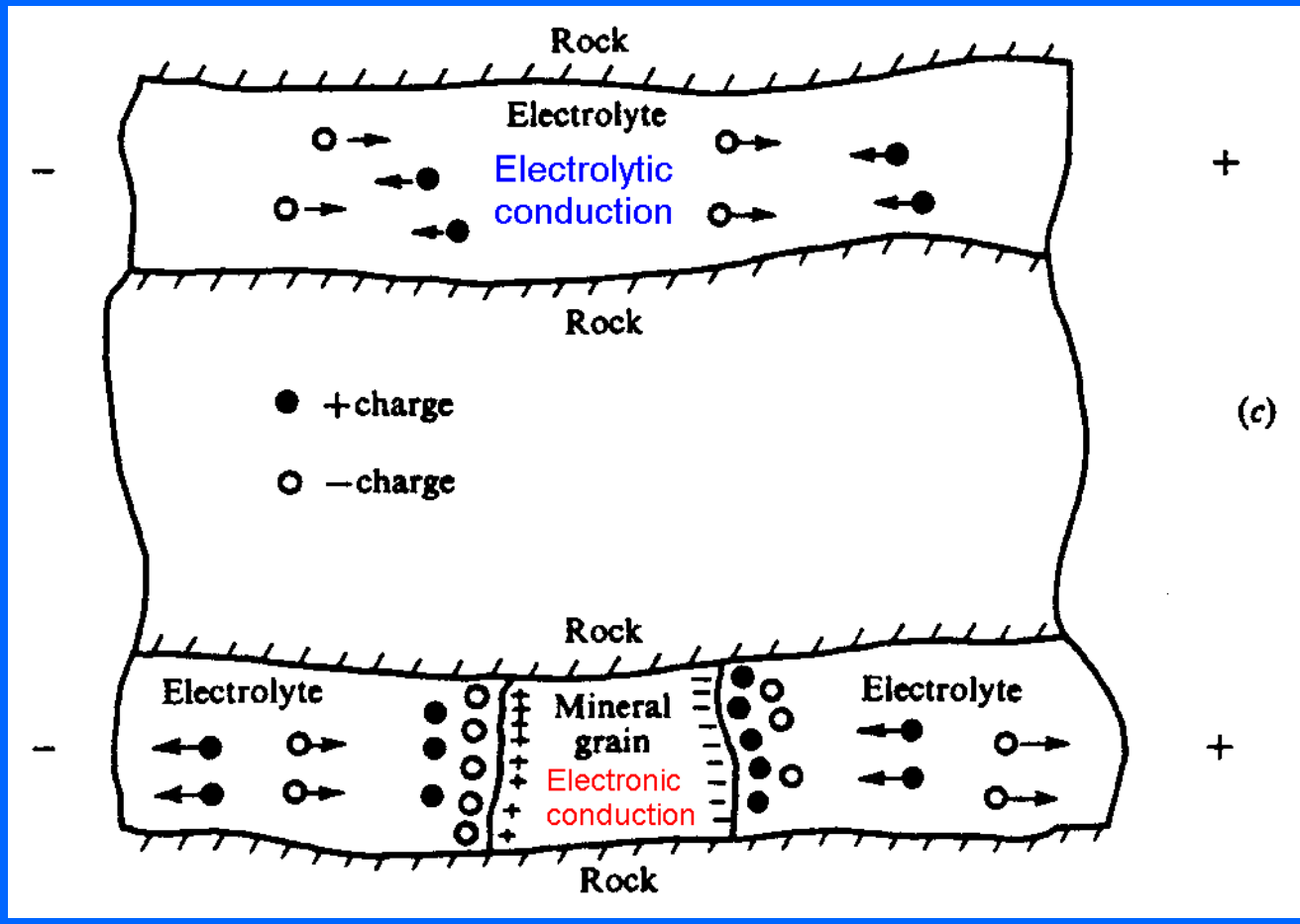

After : Telford, W.M., Geldart, L.P. and Sheriff, R.E., 1990. Applied Geophysics (second edition). Cambridge University Press.

Electrical properties of rocks and soils

The resistivity of a soil or rock depends on the nature of the solid matrix, porosity and pore fluid. Except for conductive minerals (sulfides, graphite, clay, etc) the main effect is the pore fluid (usually water). As a general rule, igneous/metamorphic rocks have the highest resistivity, followed by sedimentary rocks and soils.

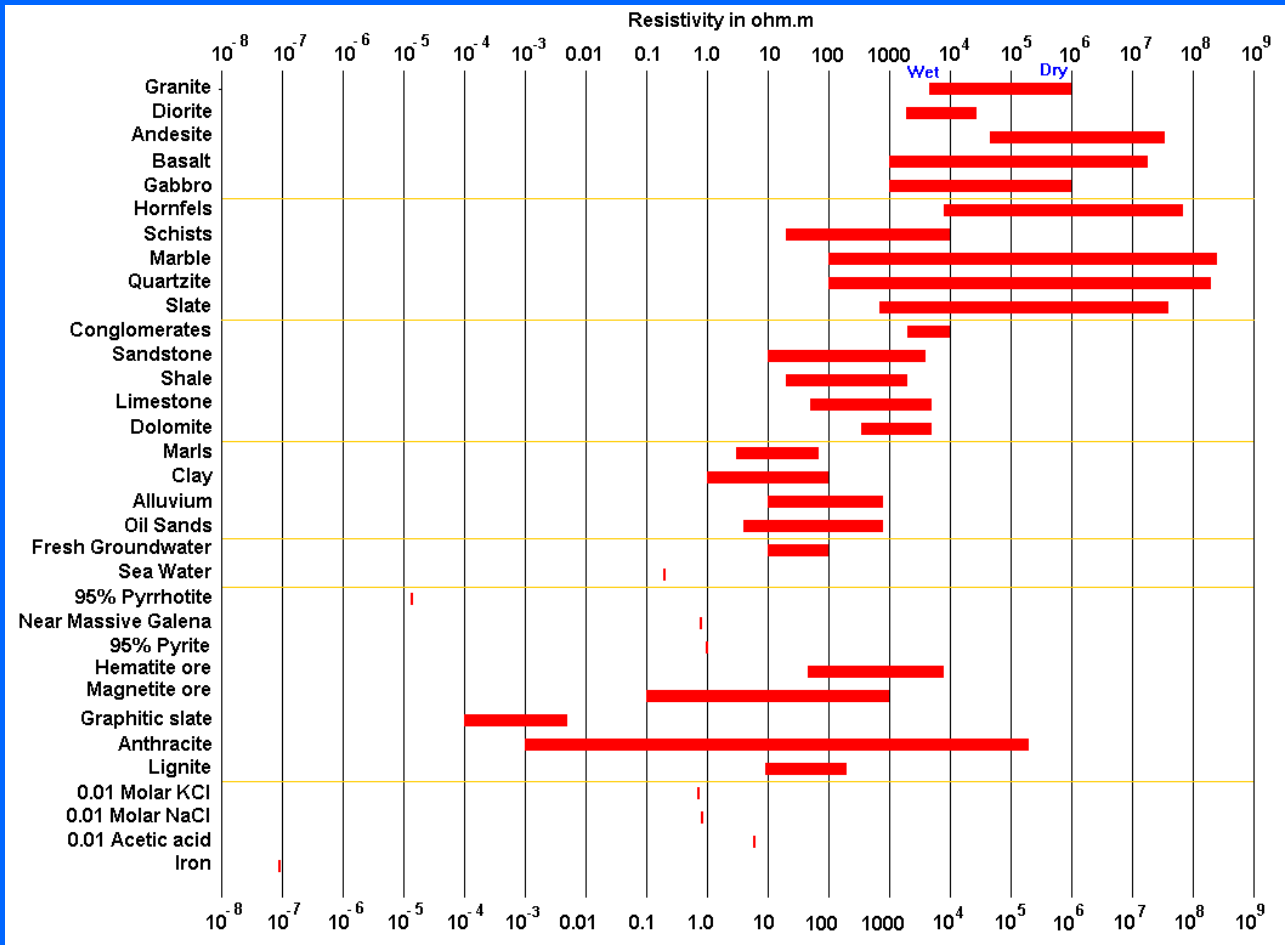

Electrical properties of natural water sources

The resistivity of most types of sediments and rocks depend on the water content. The resistivity of groundwater depends largely on the concentration of dissolved salts. Fresh groundwater has a resistivity of 10 to 100 ohm.m. Seawater has a resistivity of about 0.2 ohm.m. Salty or brackish water has a resistivity in between, generally about 1 to 10 ohm.m.

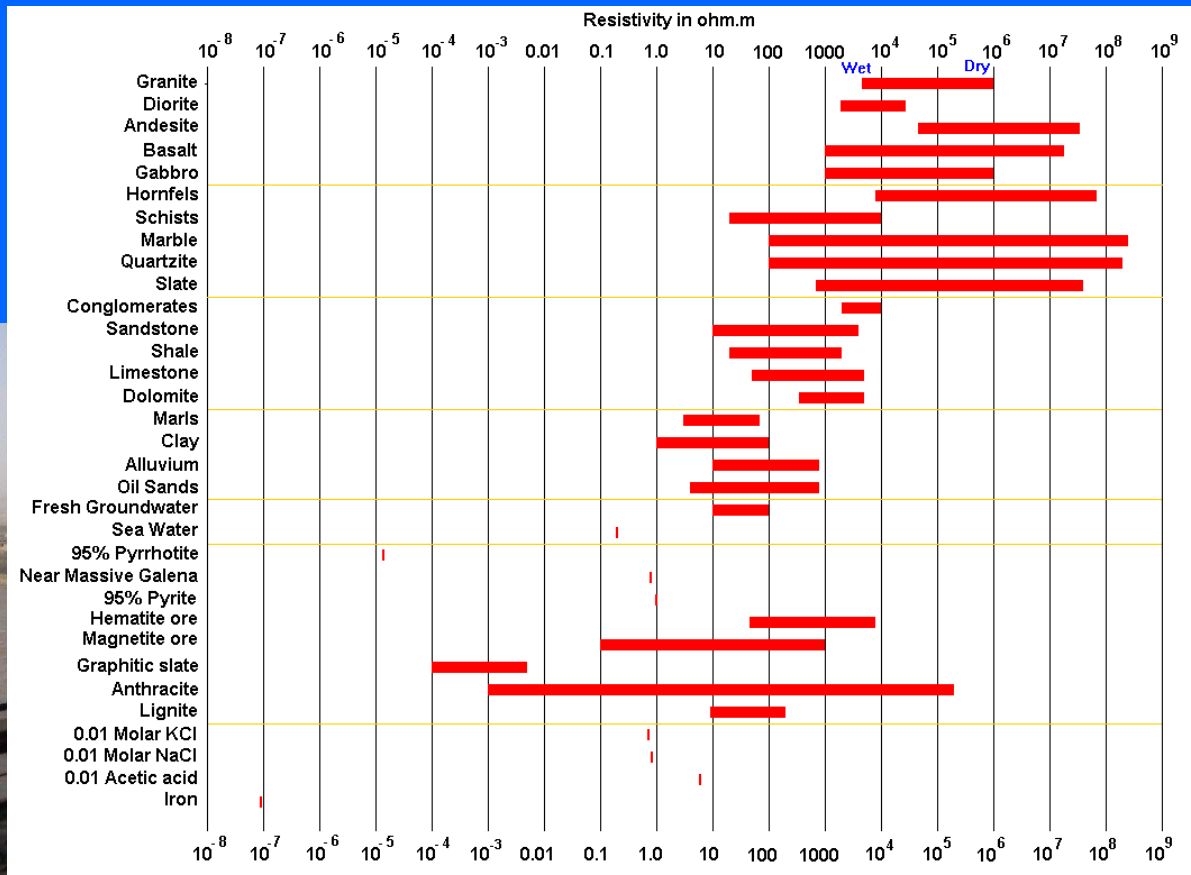

Electrical properties of sediments

The resistivity of sediments/soils depend mainly on the porosity, fluid content and clay content. Most resistivity values range from 10 to 1000 ohm.m. Resistivity decreases with increasing clay content. Most clays have resistivity of 1 to 10 ohm.m. For rocks and sediments with a low clay content, the electrical conduction is mainly through the fluids filling the pores of the rock.

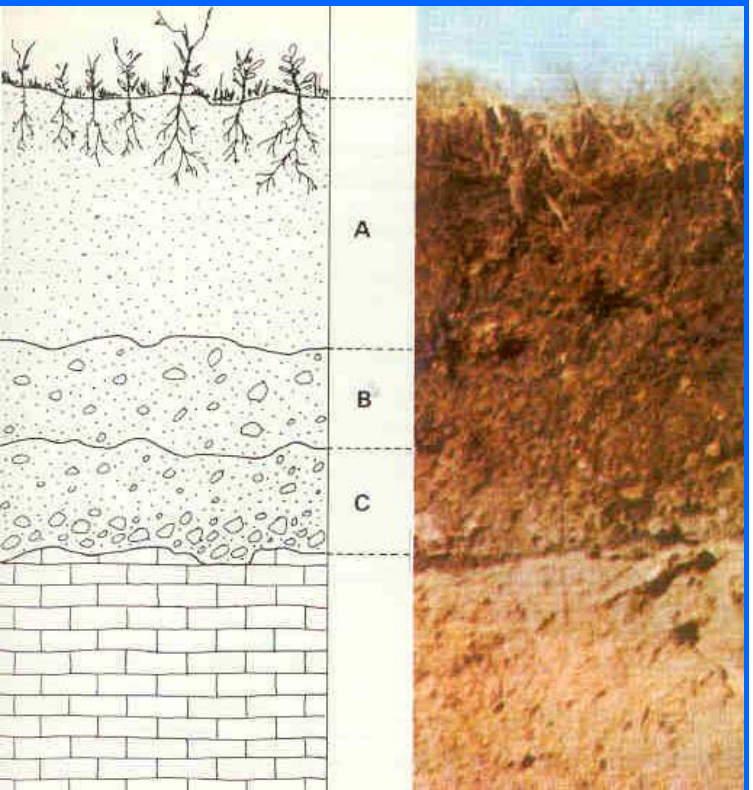

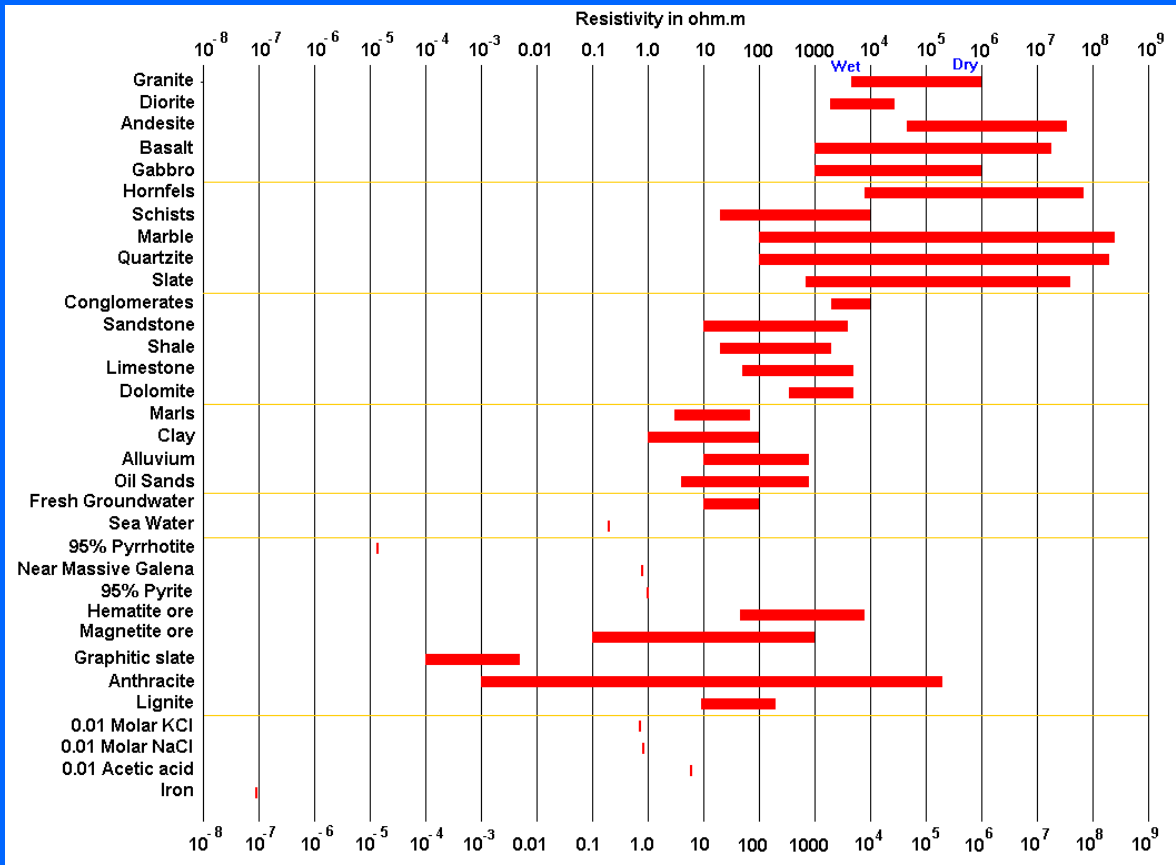

Electrical properties of sedimentary rocks

The resistivity of sedimentary rocks is generally higher than comparable sediments due to compaction and lithification that reduces the porosity in the rocks. For clastic rocks, the resistivity largely depends on the porosity and the resistivity of the fluids within the pores.

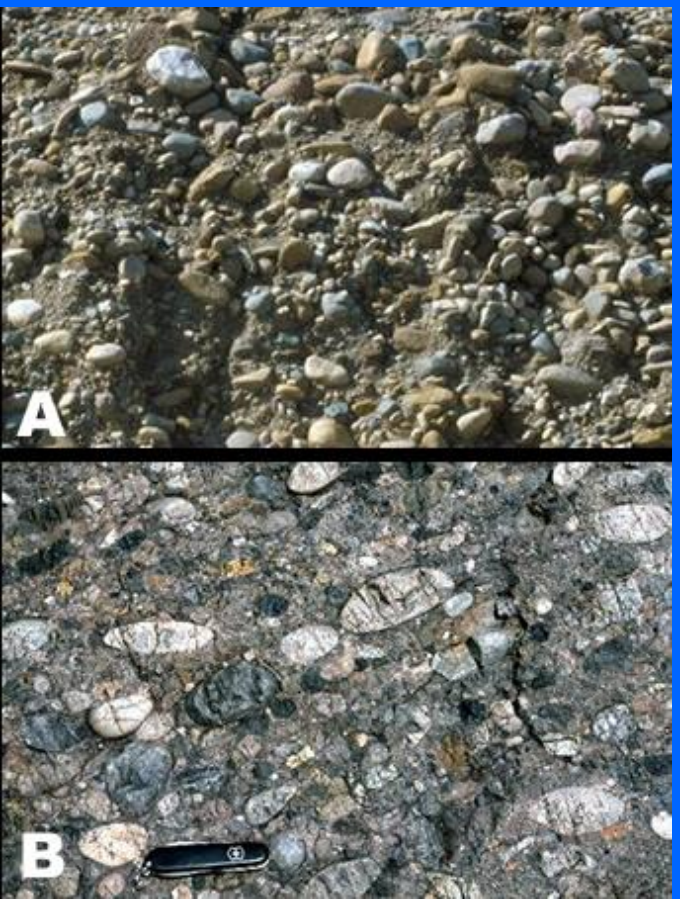

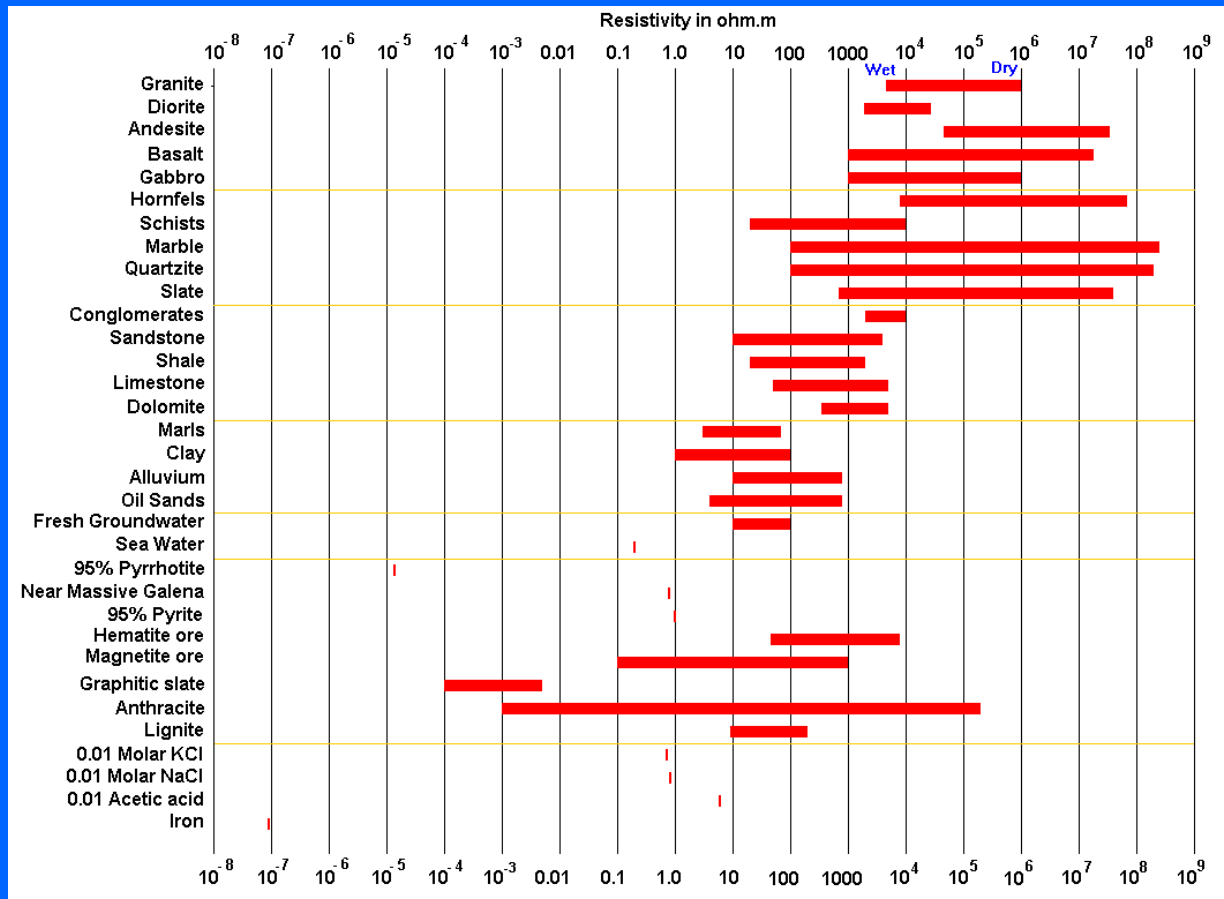

Electrical properties of sediments and sedimentary rocks

The relationship between resistivity and porosity is given by Archie's Law. $\rho_r = a\,\rho_w\,\phi^{-m}$

ρ_r = *rock resistivity,* ρ_w = *fluid resistivity,* $a \approx 1$, $m \approx 2$

ϕ = *fraction of the rock or soil filled with fluid*

Archie's Law is only applicable if the solid material is non-conducting, such as sand. It is not strictly correct if there is conducting material such as clay.

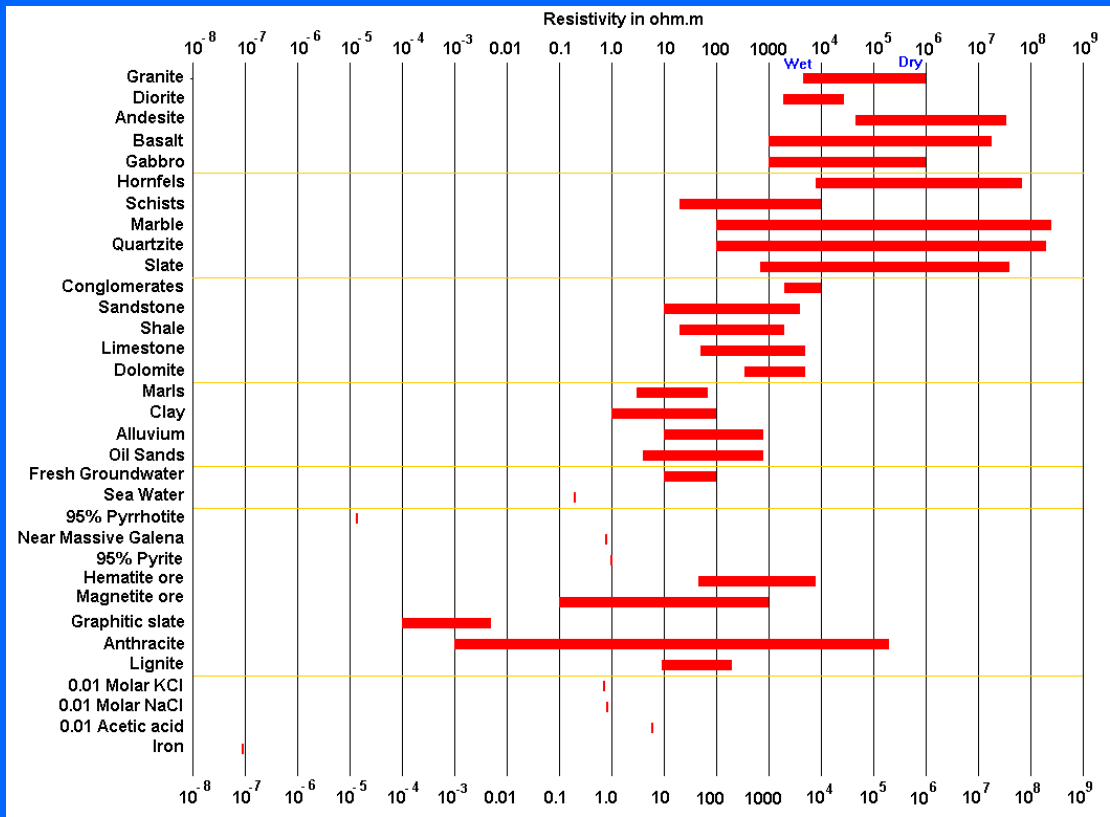

Electrical properties of metamorphic and igneous rocks

Igneous and metamorphic rocks typically have high resistivity values of over 1000 Ω·m. The resistivity of these rocks is greatly dependent on the degree of fracturing, and the percentage of the fractures filled with ground water. A given rock type can have a large range of resistivity, from about 1000 to 10 million Ω·m, depending on whether it is wet or dry.

Quartzite

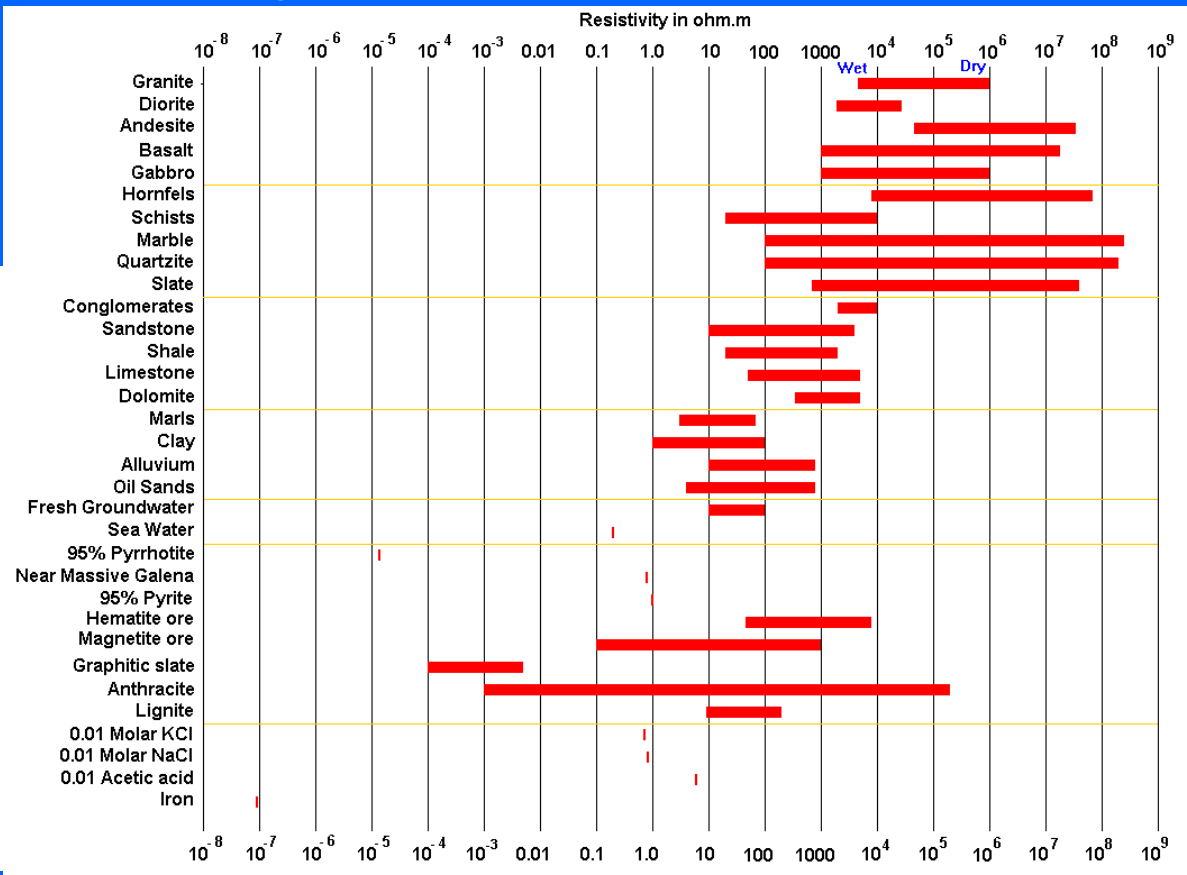

Electrical properties of metamorphic and igneous rocks

The dependence of the resistivity on fractures is useful in the detection of fracture zones and other weathering features, such as in engineering and groundwater surveys. In some areas, groundwater is found in fractures in an igneous or metamorphic bedrock. It is also useful for detecting cavities in karstic areas.

Marble with fractures

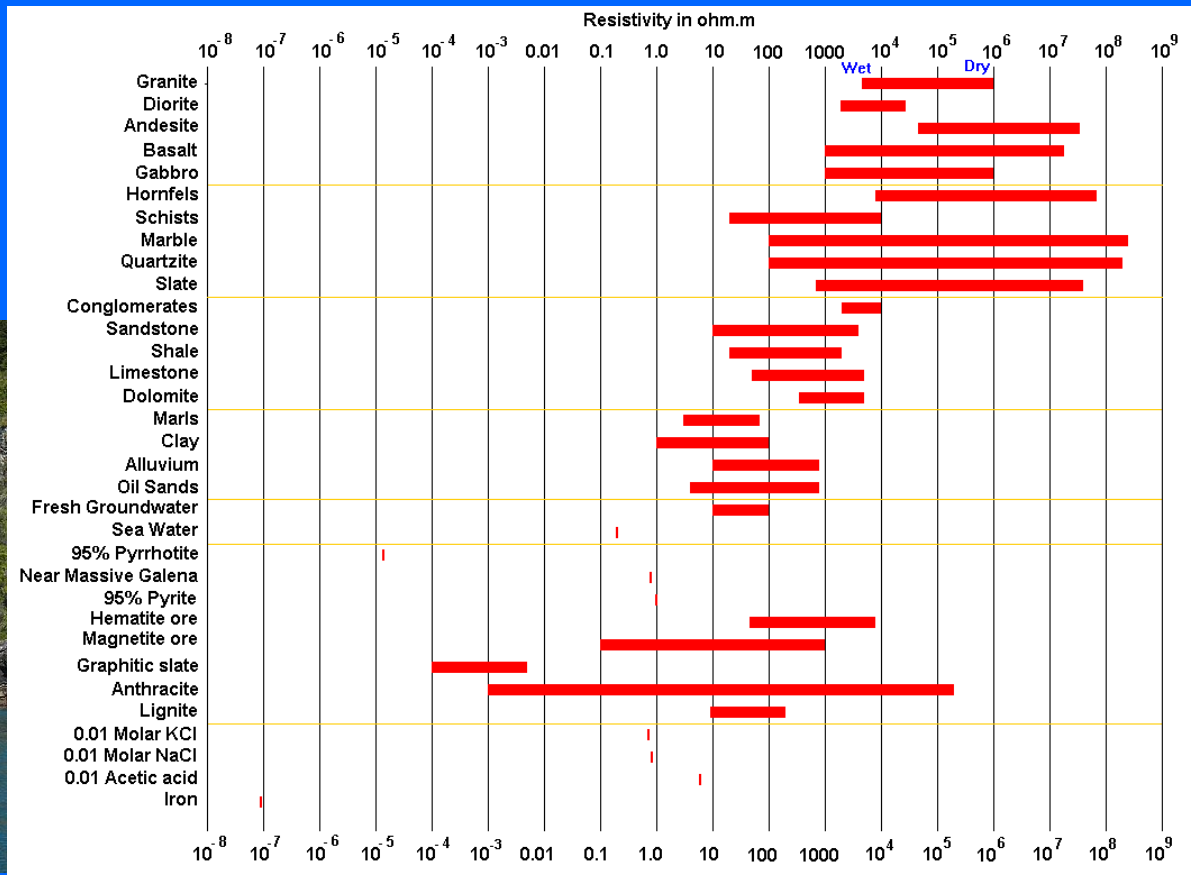

Electrical properties of metallic mineral ores

Metallic sulfides (such as pyrrhotite, galena and pyrite) have typically low resistivity values of less than 1 Ω·m. The resistivity value of a particular ore body can differ greatly from the resistivity of the individual crystals. Other factors, such as the nature of the ore body (massive or disseminated) have a significant effect.

Gold ore

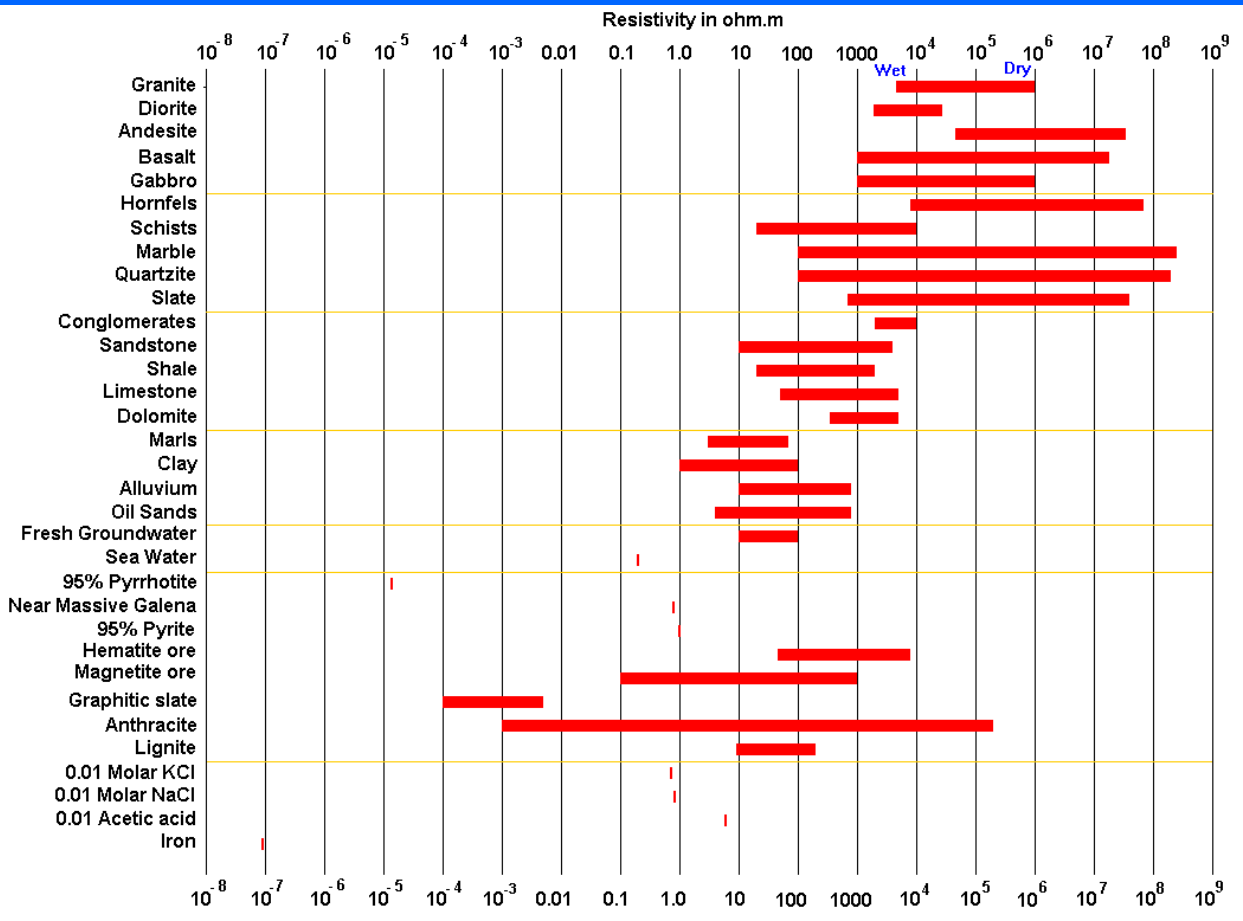

Electrical properties of mineral ores

Graphitic slate have a low resistivity value, similar to the metallic sulfides, which can give rise to problems in mineral surveys.

Most oxides, such as hematite, do not have a significantly low resistivity value. One exception is magnetite.

Iron ore

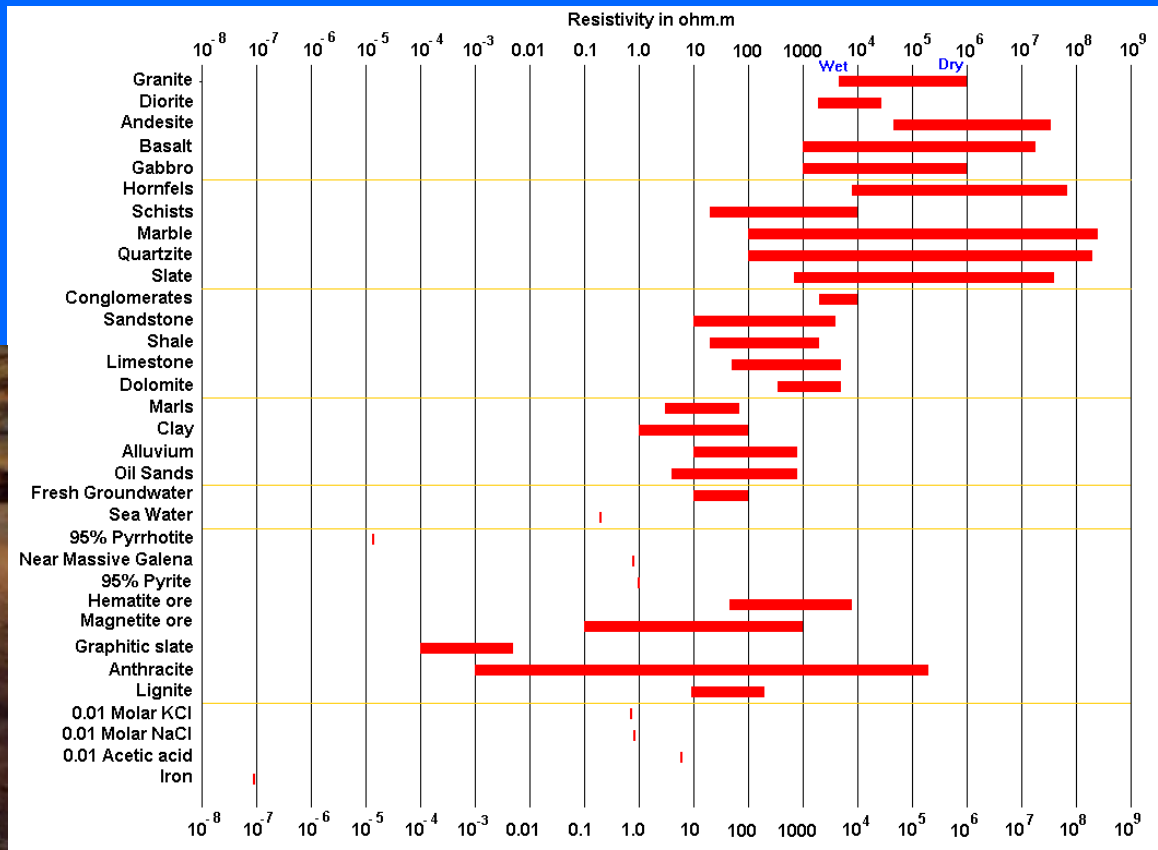

Electrical properties of metals and chemicals

Metals, such as iron, have extremely low resistivity values. Chemicals that are strong electrolytes, such as potassium chloride and sodium chloride, can greatly reduce the resistivity of ground water to less than 1 Ω·m even at fairly low concentrations. The effect of weak electrolytes, such as acetic acid, is comparatively smaller.

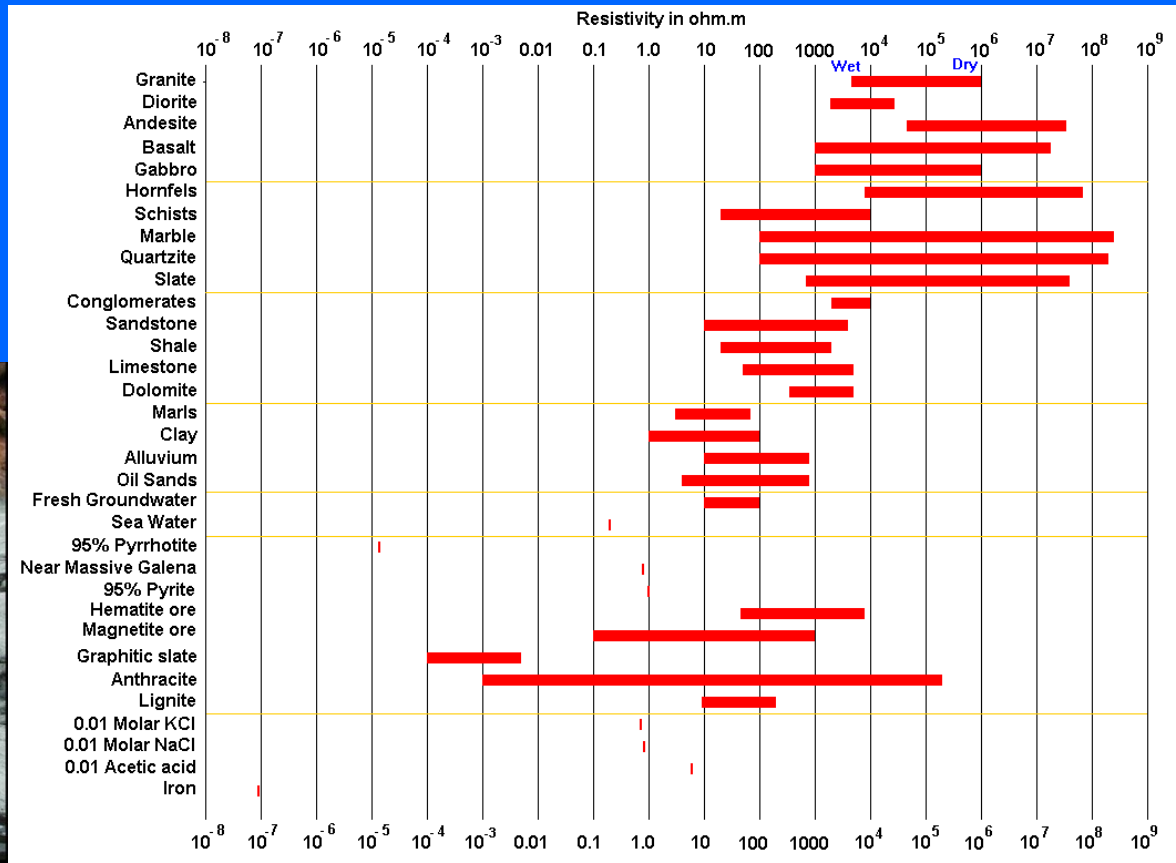

Electrical properties of natural hydrocarbons

Hydrocarbons typically have very high resistivity values. The effect of the hydrocarbons depends on its concentration. Natural occurrences, such as near surface seepage from reservoir or tar sands, can have very high concentrations. Hydrocarbon-bearing tar sands have a significantly higher resistivity so electrical imaging surveys are widely used in its exploration.

Oil shale

Tar sands

Electrical properties of industrial hydrocarbons

The percentage of hydrocarbons in a rock or soil from spillage can be quite small, and might not have a significant effect on the bulk resistivity. In some areas, alteration of insoluble organic compounds by bacteria can produce chemicals that lower the soil resistivity.

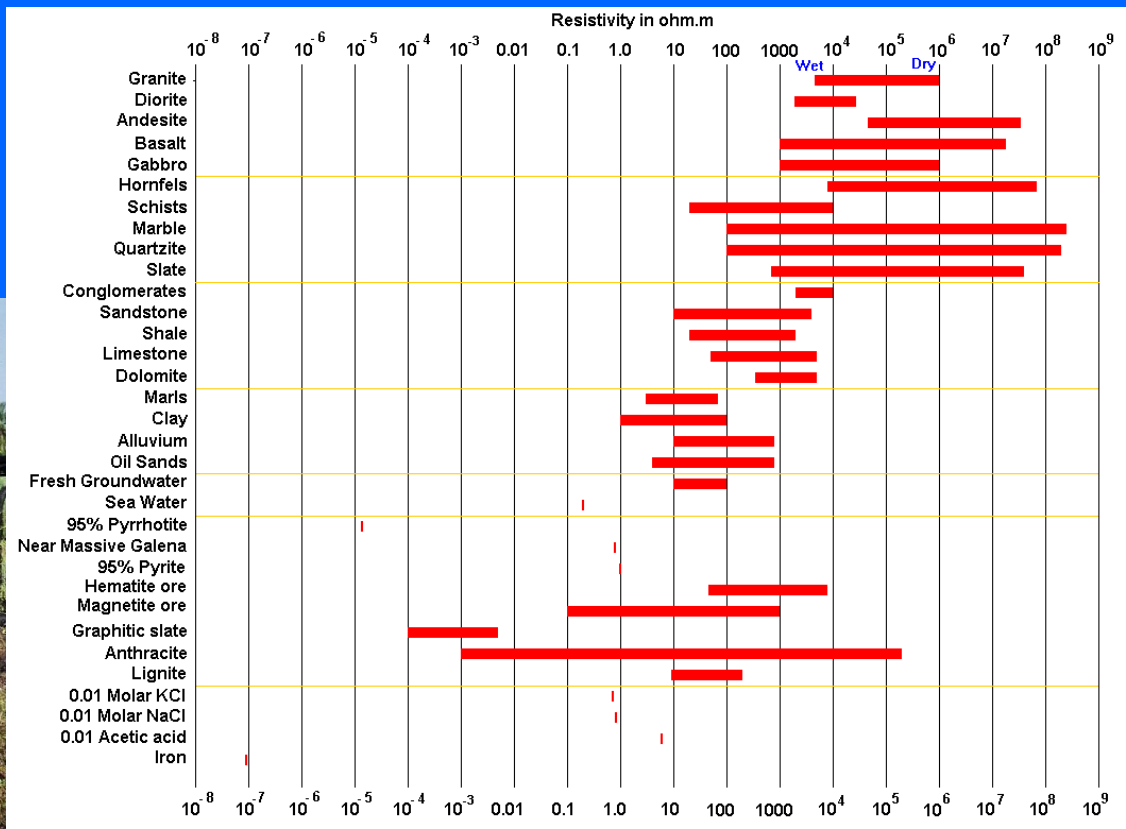

Part 2

Progress of electrical methods 1920s to 2010s, from 1-D to 4-D

Electrical method through the ages : 1920s to 2010s

1920s to 1980s : 1-D. Sounding and profiling surveys using 4 electrode resistivity meters.

1990s : 2-D. Major change with multi-electrode systems. Widespread use, more realistic images.

2000s : 3-D. Multi-channel meters. Dense areal data coverage. Mineral exploration with offset pole-dipole layouts. Able to resolve complex mineral systems.

2010s : 4-D. Environmental monitoring (landslides, aquifers, landfills). Remote systems with wireless control.

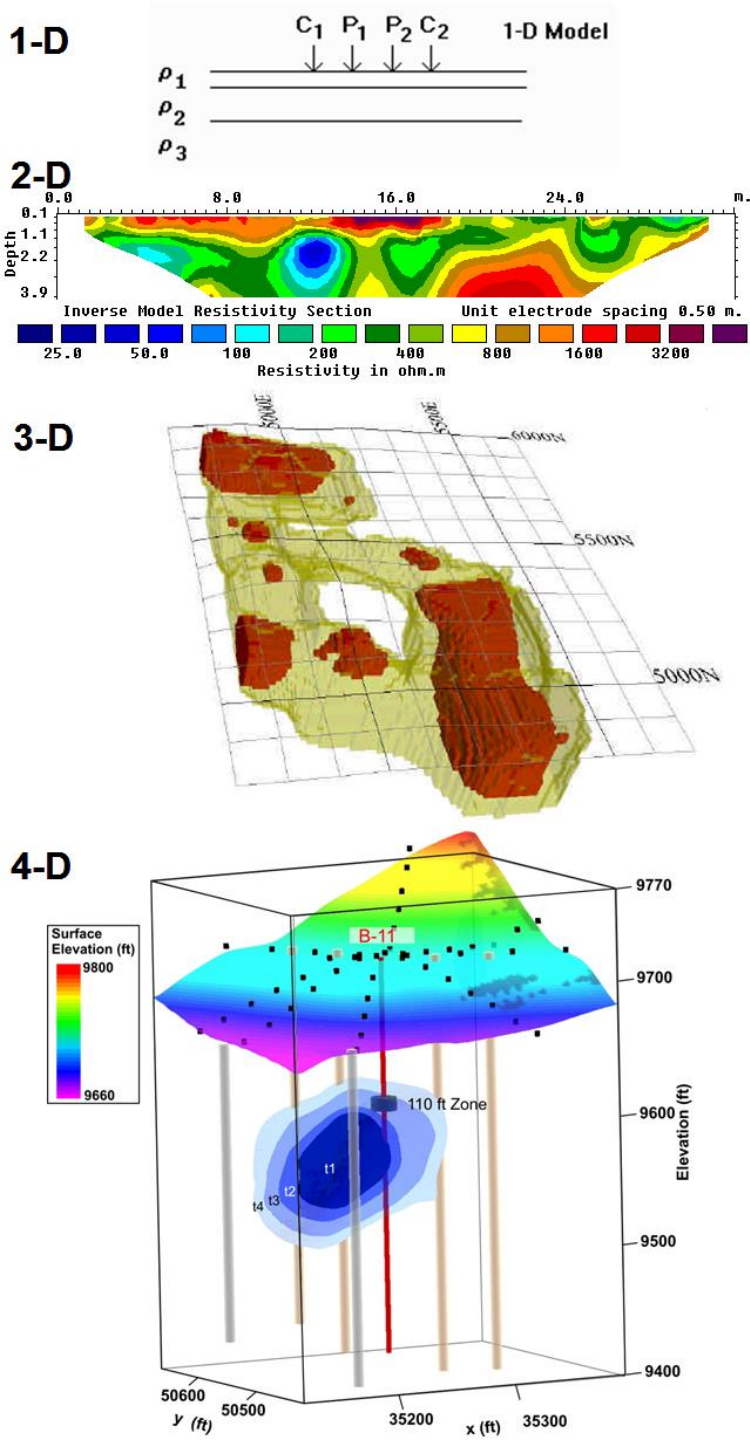

1920s to 1980s : 1-D resistivity method

1-D sounding surveys carry out measurements with different spacings between electrodes but with a common center. The data is usually plotted as a sounding curve.

Assume a simplified mathematical model for the subsurface that consist of horizontal layers.

Correlate model properties with known geology.

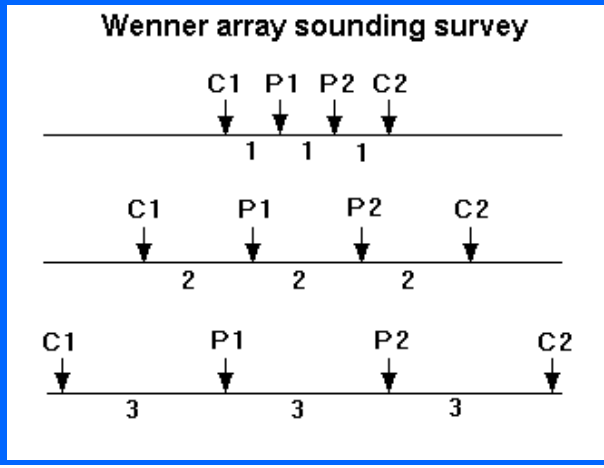

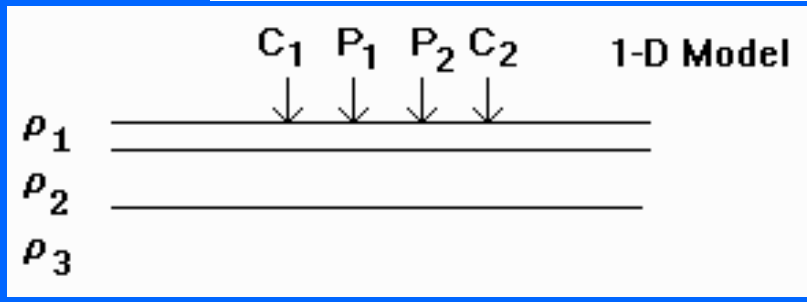

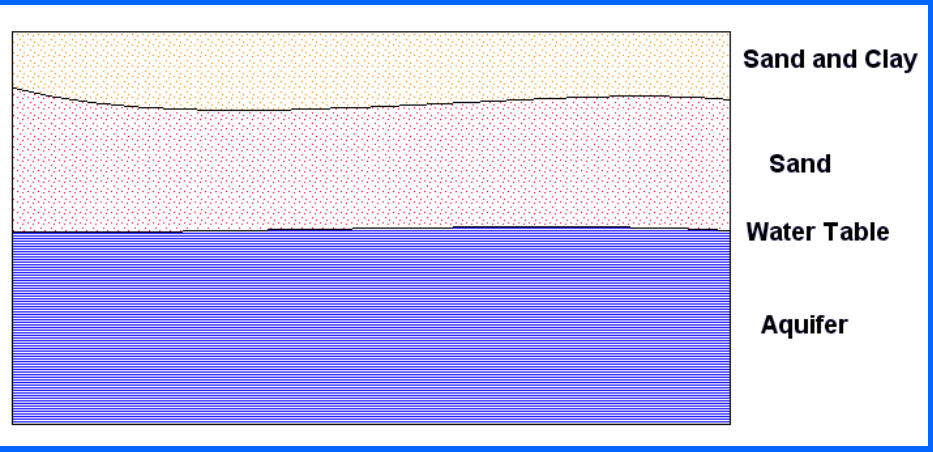

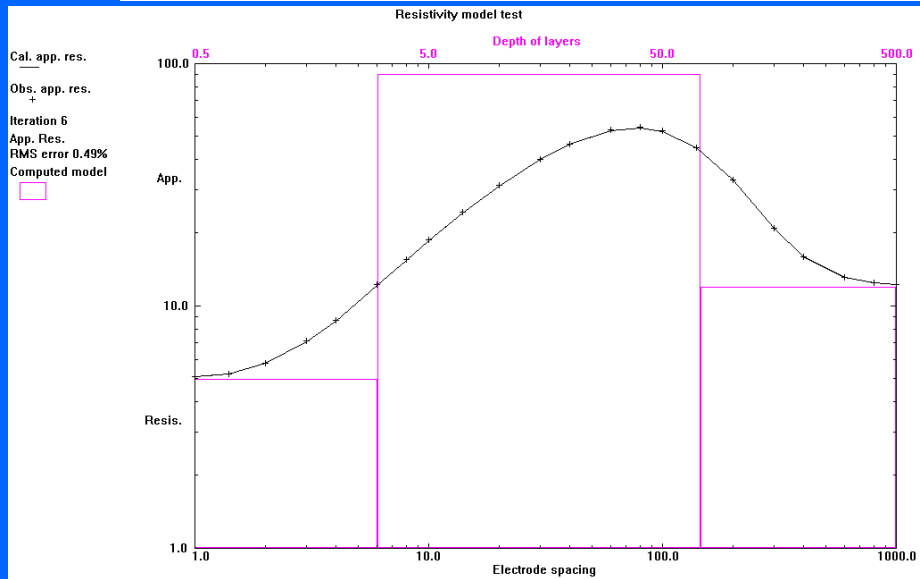

Example of 1-D inversion

The interpretation of data from 1-D sounding surveys can be automatically done using an inversion program. The user enters the data (apparent resistivity values and electrode spacings), together with a starting model (number of layers with estimated thickness and resistivity). The program then automatically adjust the thickness and resistivity of the layers until the calculated apparent resistivity values are 'close' to the measured values.

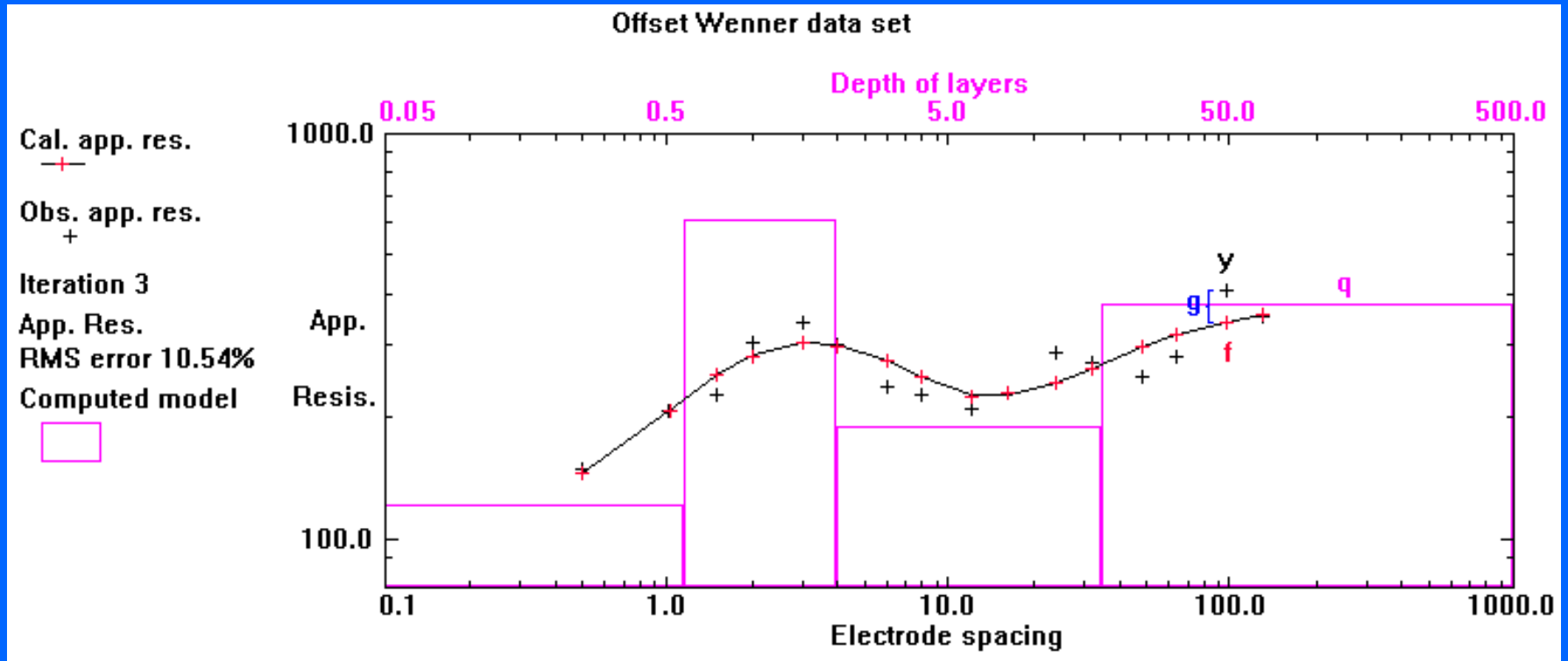

Traditional 1-D profiling surveys

The distances between the electrodes are kept fixed, and the electrodes are moved along the survey line. The data interpretation for profiling surveys was mainly qualitative using profile plots. They illustrate qualitatively the change of resistivity with horizontal distance but gives no depth resolution.

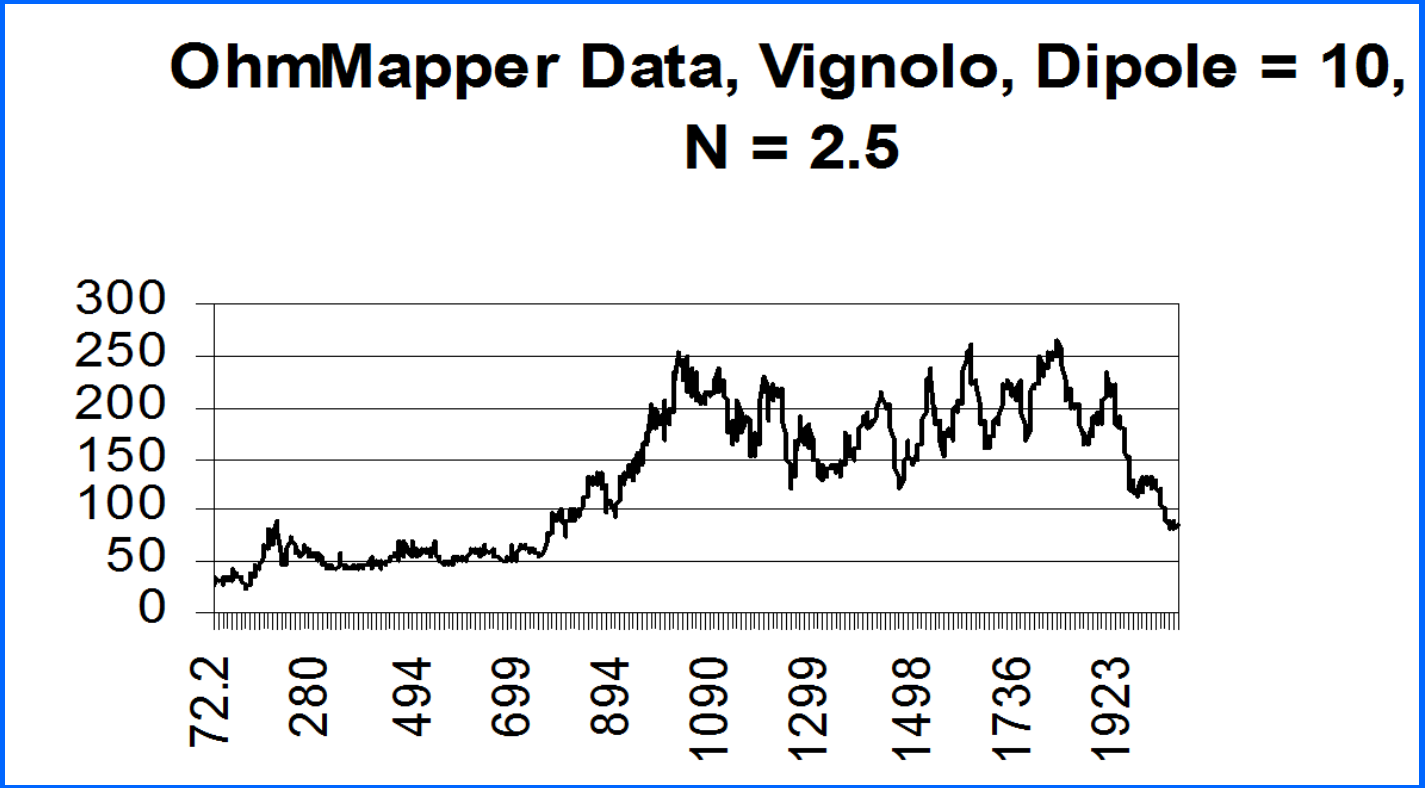

Using the OhmMapper Capacitively Coupled Resistivity System (CCR) from Geometrics

Limitations of 1-D surveys

Traditional resistivity sounding surveys only give a 1-D picture of the subsurface, which is probably too simple in many cases.

Sounding 1-D Picture

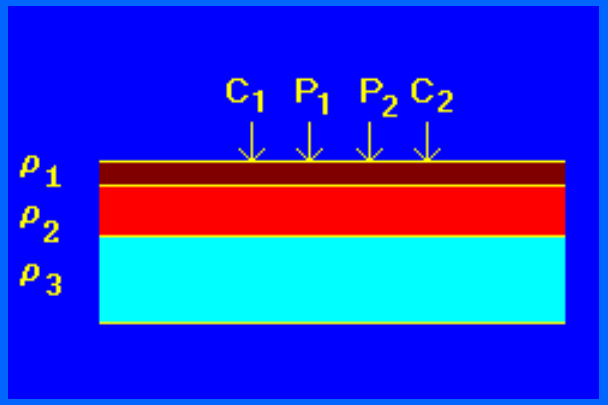

Real Situation

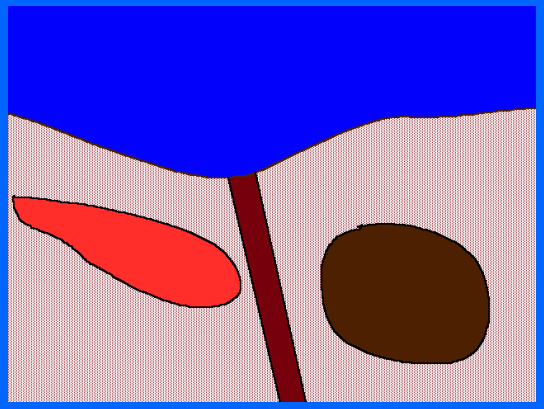

1-D models are probably too inaccurate for most areas where there are significant lateral and vertical variations.

This method is still used for extremely deep aquifers and in many developing parts of the world where access to multi-electrode resistivity meter systems is limited.

1990s - 2-D electrical imaging surveys

The 1990s saw a rapid growth in 2-D surveys driven by availability of multi-electrode instruments, fast PCs and automatic inversion software. A computer control program automatically selects the appropriate 4 electrodes for each measurement to give a 2-D coverage of the subsurface. A large variety of arrays and survey arrangements can be used with such a system.

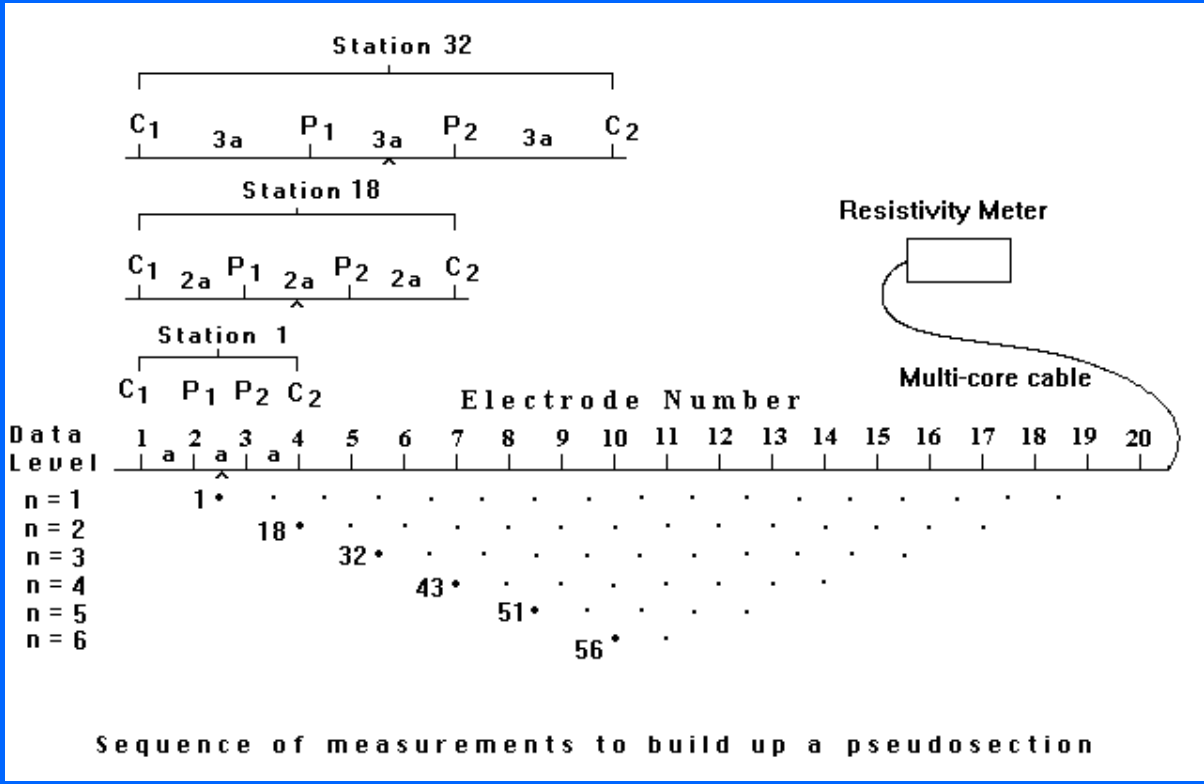

Sequence of measurements to build up a pseudosection

2-D surveys - instrumentation

There are many commercial multi-electrode systems in all shapes and sizes, from US$15,000 to $100,000, from 25 to 128 nodes, single and multi-channels, with and without I.P, on land and at sea.

Environmental/engineering systems – Abem, Iris Syscal, Pasi etc.

I.P. mineral exploration – Iris Elrec, Quantec, Scintrex etc.

2-D survey example - Groundwater

Since the mid-1990s it has become a 'standard' geophysical tool for small companies in the hydrological, environmental and engineering sectors. It has enabled the mapping of complex structures previously not possible with 1-D surveys.

Below is an example of a survey to map fractures filled with groundwater in a hard-rock environment in the Blue Ridge mountain area in eastern USA.

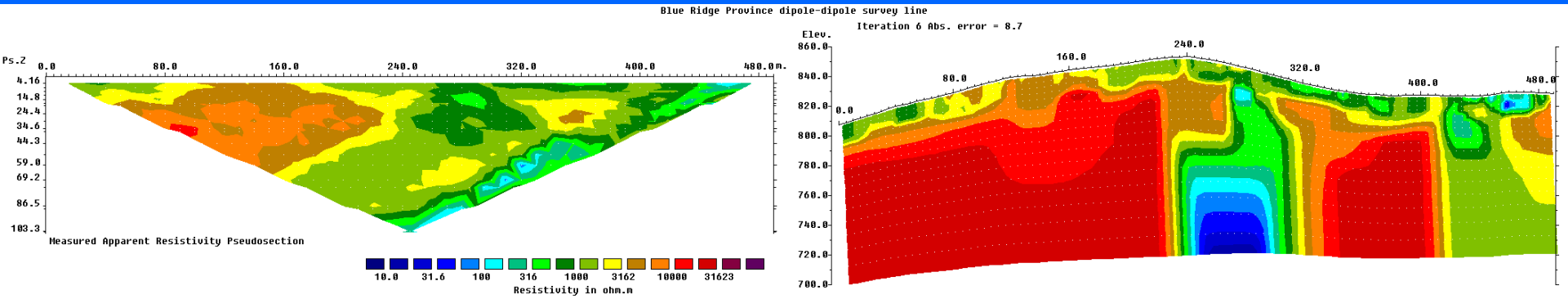

2-D example - Environmental

Another area where 2-D surveys have become popular is mapping pollution from landfills, tailing ponds etc. The contaminants frequently have much lower resistivity than normal groundwater.

Below is an example of a survey to map a pollution plume that has migrated across the boundaries of a landfill.

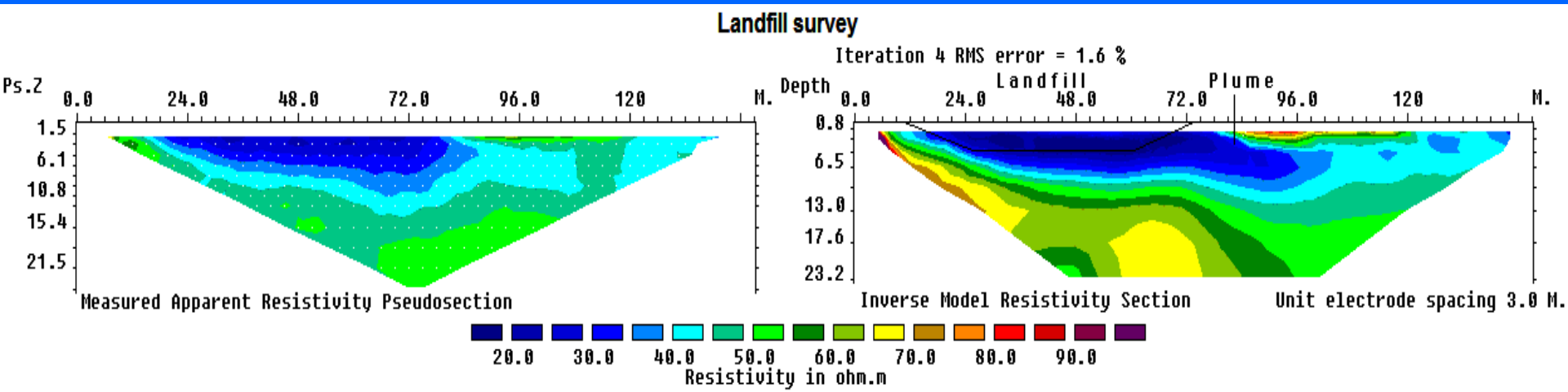

2-D example – Mineral exploration

2-D I.P. surveys have been carried out since the 1950's. However, interpretation was very limited – a matter of hunting for inverted V's in pseudosections. New software tools have enabled the reinterpretation of old data. Below is an example of an I.P. survey over a massive sulfide deposit in Canada. The ore body shows up as a low resistivity and high I.P. anomaly.

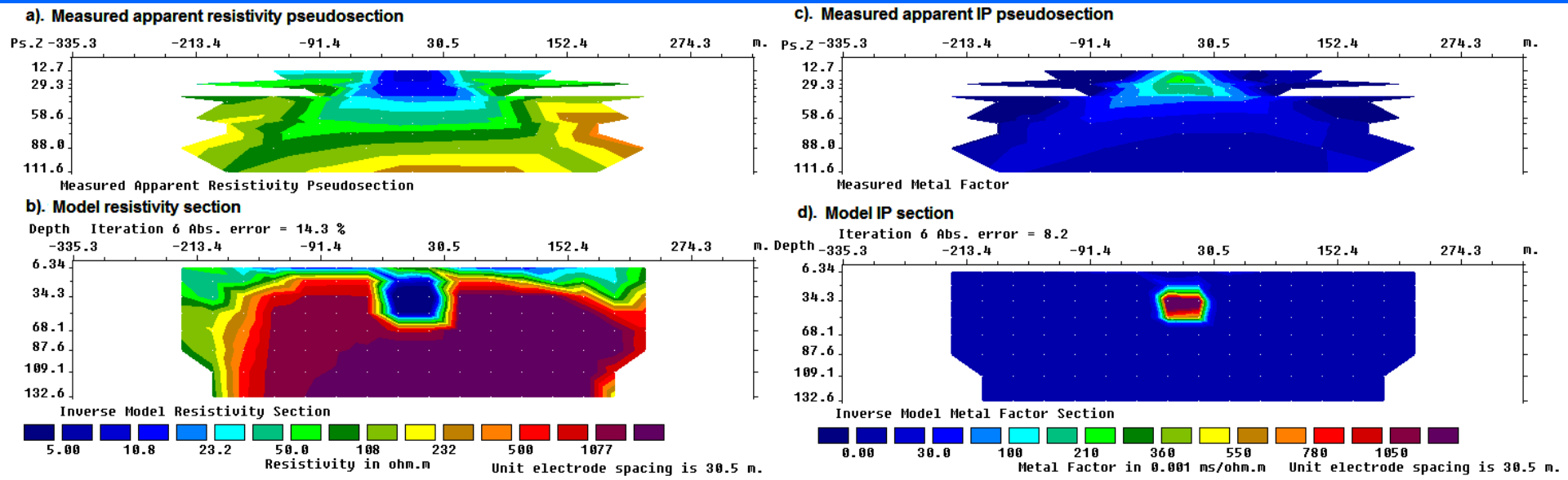

2000s : 3-D surveys

All geological structures are 3-D in nature. For very complex structures, a 3-D resistivity survey and inversion model is required for accurate results. 3-D surveys are not as commonly carried out as 2-D surveys, mainly due higher costs. Recent developments in instrumentation and field techniques have significantly reduced the costs.

The mineral exploration industry was one of the early users of 3-D surveys. The data used was collated from previous 2-D surveys, or measured using new survey protocols such as the offset pole-dipole or dipole-dipole arrays.

3-D example – UK Landfill site (BGS)

3-D surveys are also used in complex environmental problems, usually using a series of 2-D survey lines. In this survey the Wenner-Schlumberger array with an inline electrode spacing of 5m was used, and a 15m spacing between the lines. This is less than ideal, but a common compromise in real world commercial surveys.

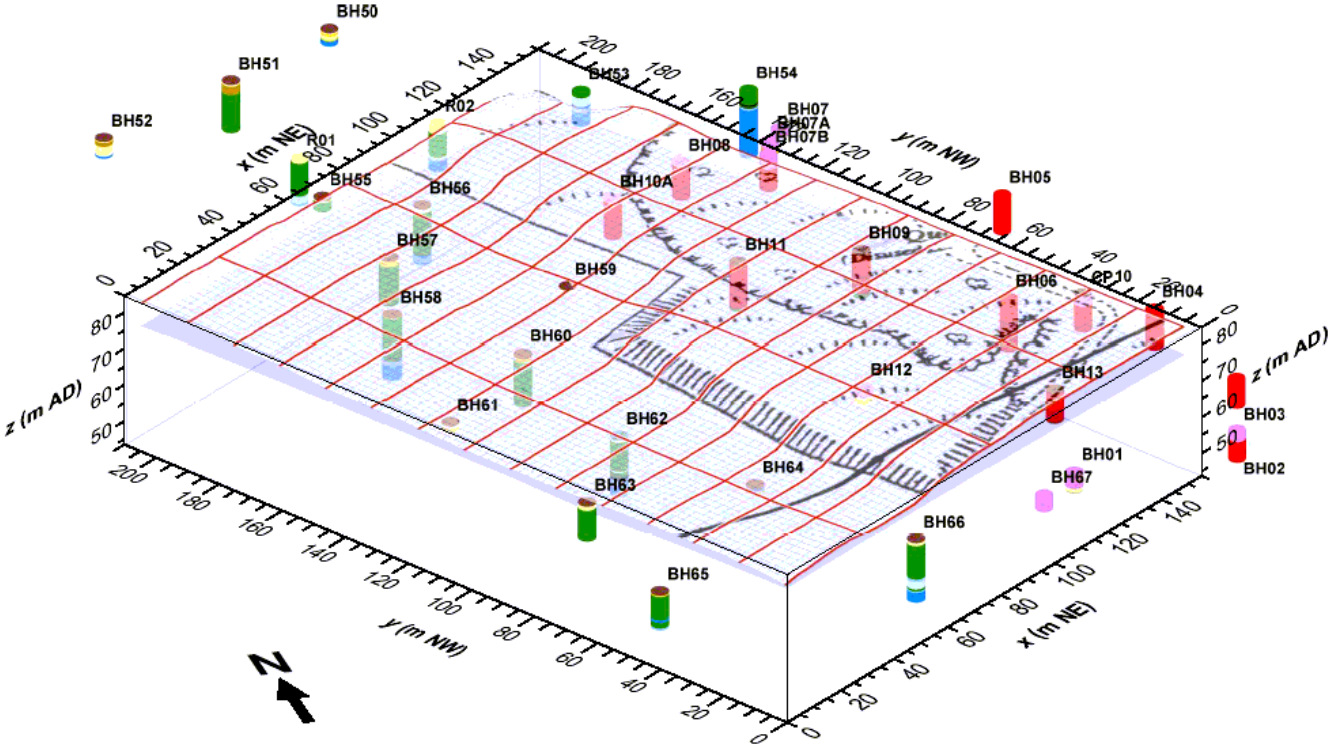

3-D example – UK Landfill site (BGS)

The figure below shows the results from the survey in the form of horizontal sections at different elevations. The dolerite bedrock shows up as high resistivity zones, while the waste materials or contaminated bedrock have much lower resistivity values.

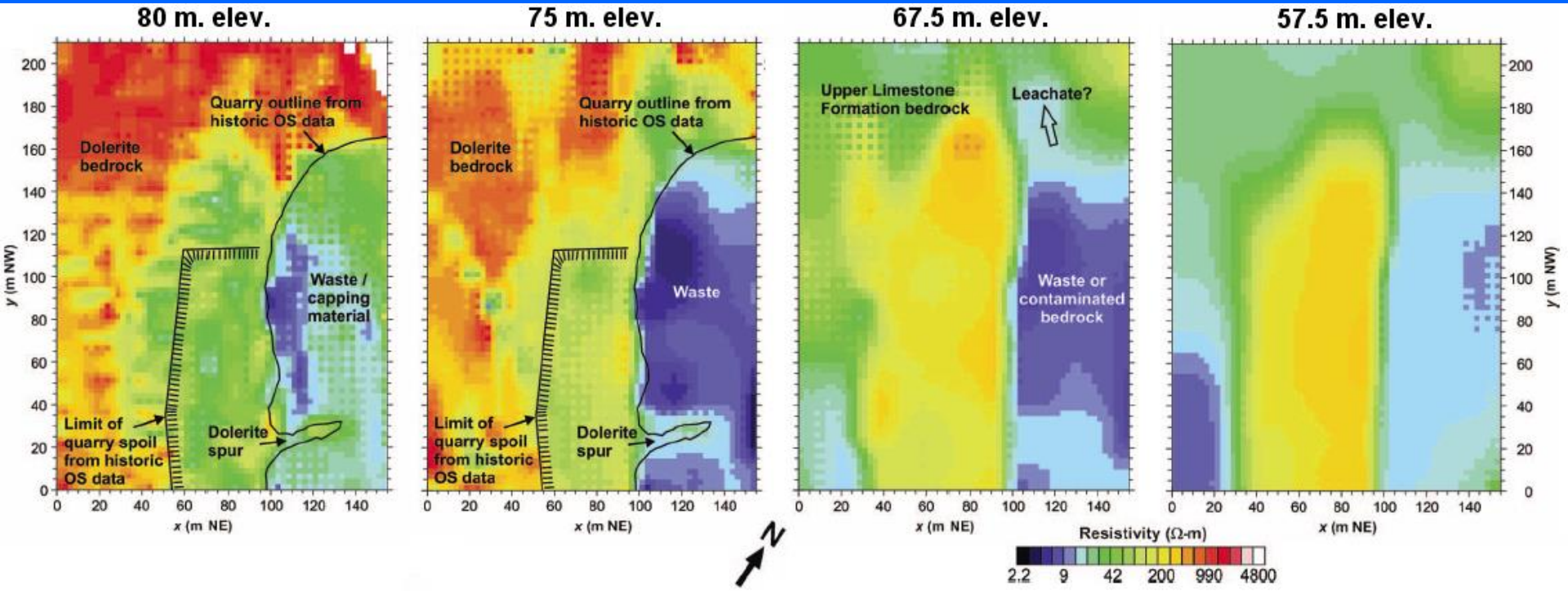

3-D example – UK Landfill site (BGS)

The resistivity model is combined with conventional site data into an integrated 3-D representation. Opaque volumes indicate resistivity values above 50 ohm.m.

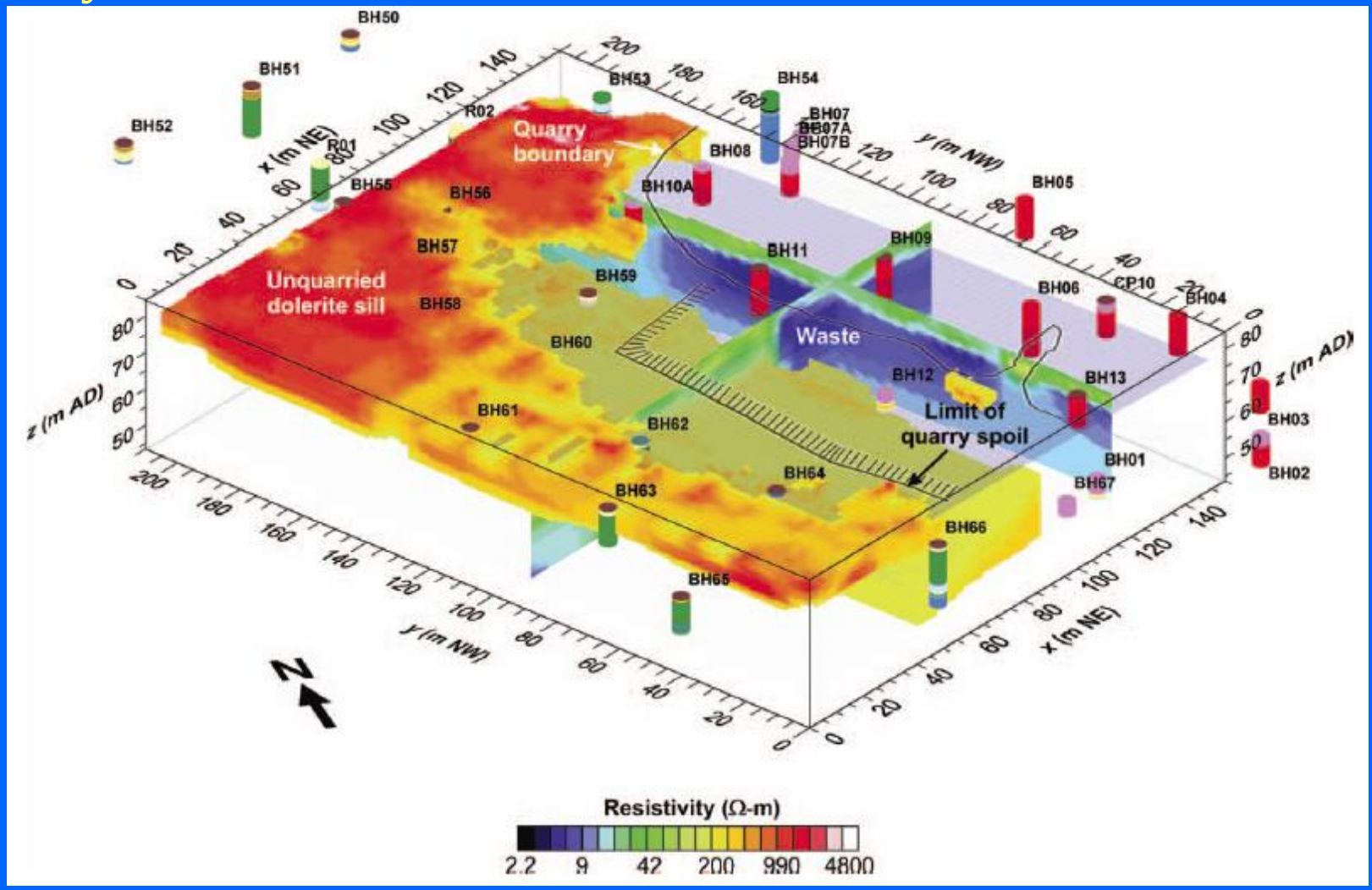

2010s : 4-D surveys

Time-lapse surveys are used to detect changes with time to monitor flow of fluids, possible landslides, landfill changes, leakage from dams. Below is a landslide monitoring example from Austria that shows resistivity change after 1.5 years.

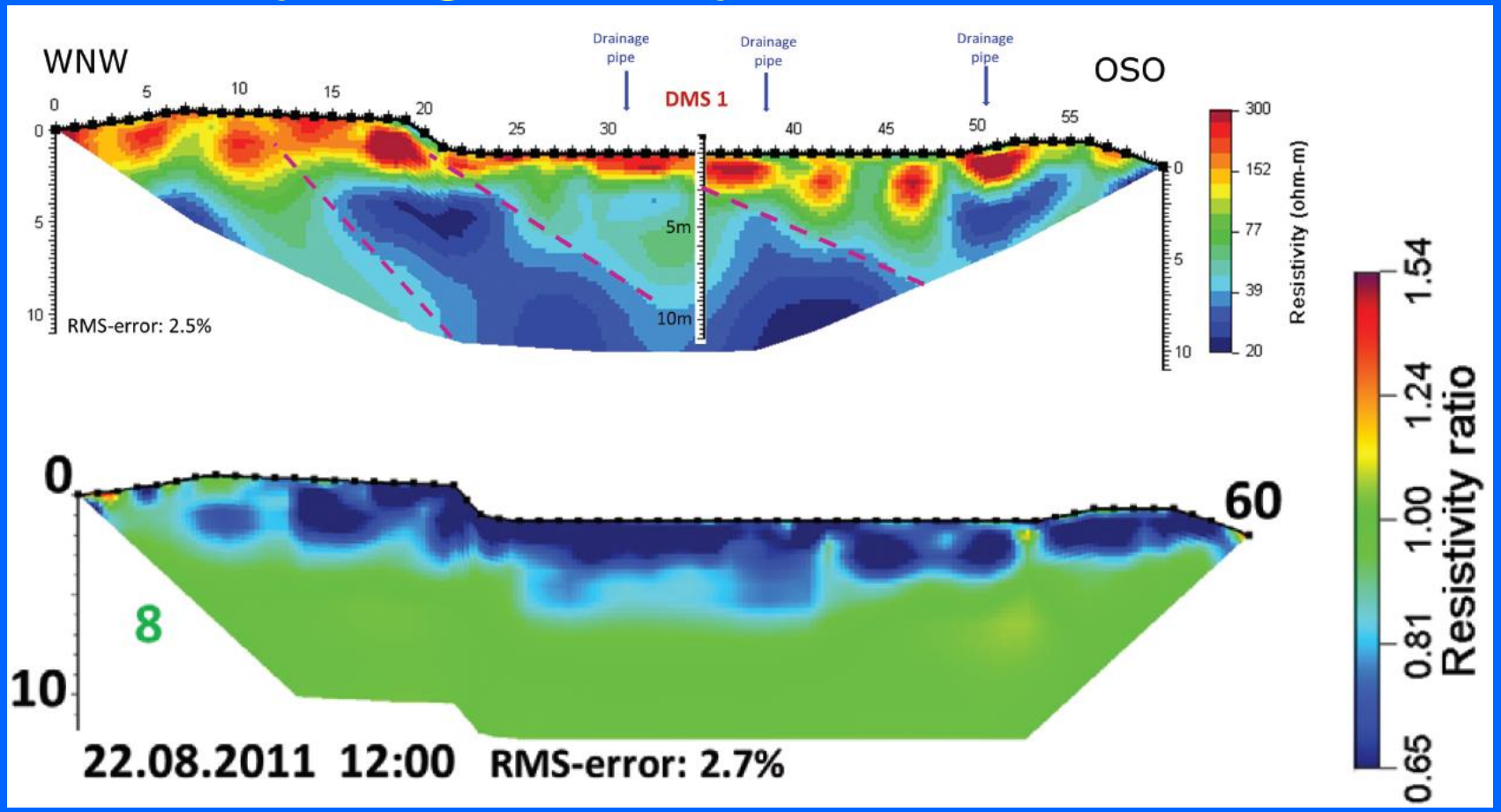

Supper, R., Ottowitz, D., Jochum, B., Kim, J.H., Römer, A., Baron, I., Pfeiler, S., Lovisolo, M., Gruber, S. and Vecchiotti, F., 2014. Geoelectrical monitoring: an innovative method to supplement landslide surveillance and early warning. Near Surface Geophysics, 2014, 12, 133-150

3-D time-lapse example –AnglogoldAshanti USA

This example is from an injection experiment at the Cripple Creek and Victor Gold Mine, in Colorado, USA. A dilute sodium cyanide solution was injected at high pressures into an engineered rock pile to increase the extraction of gold as a means of secondary recovery after surface leaching had ceased. The figure shows an illustration of the Hydro-Jex method with four discrete injection zones. The picture shows Hydro-Jex unit.

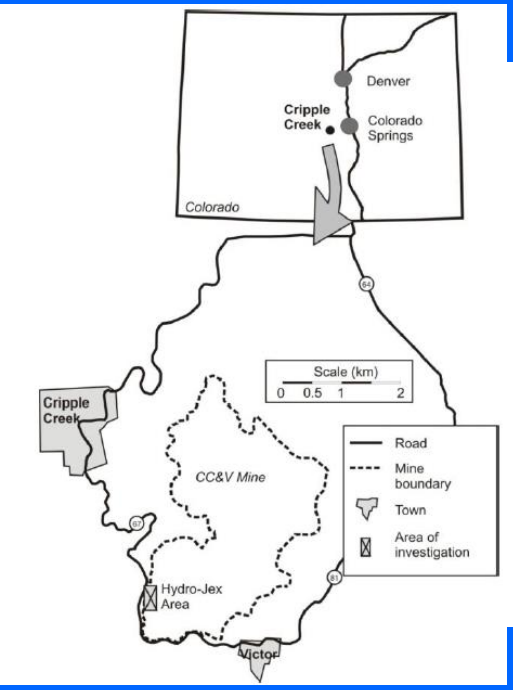

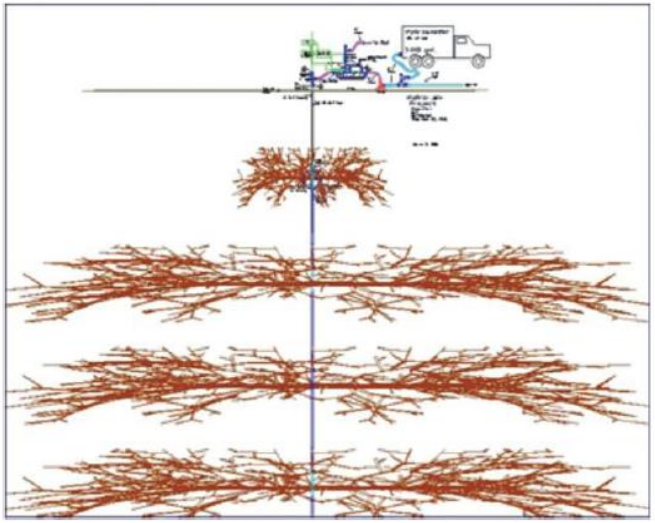

AnglogoldAshanti USA – survey procedure

A resistivity survey was conducted to better understand the direction of flow and area of influence of the pressured injections that is important for optimizing recovery and ensuring safety of the side slopes. Resistivity measurements were made with the pole-pole array using 48 surface electrodes placed along eight radials, 94 electrodes within six boreholes, and eight long electrodes using steel-cased injection wells.

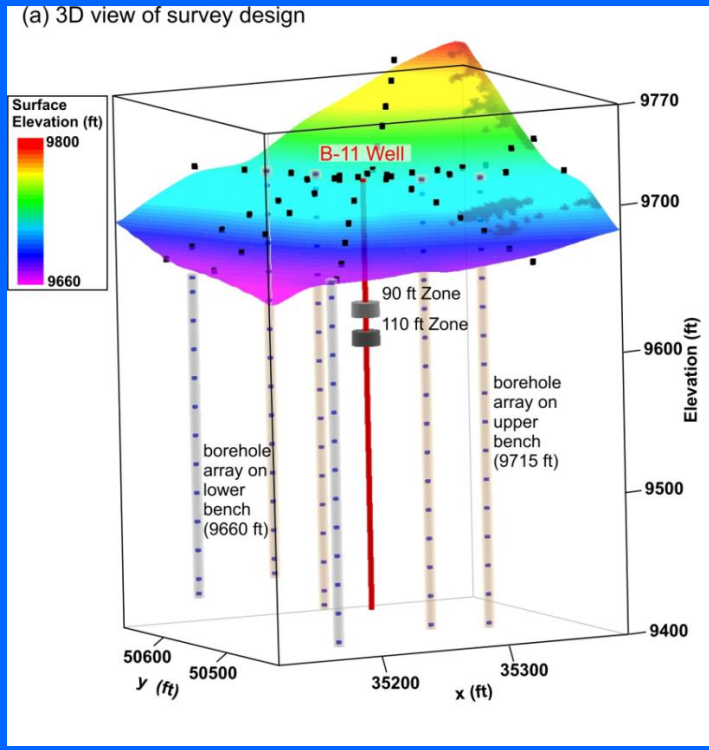

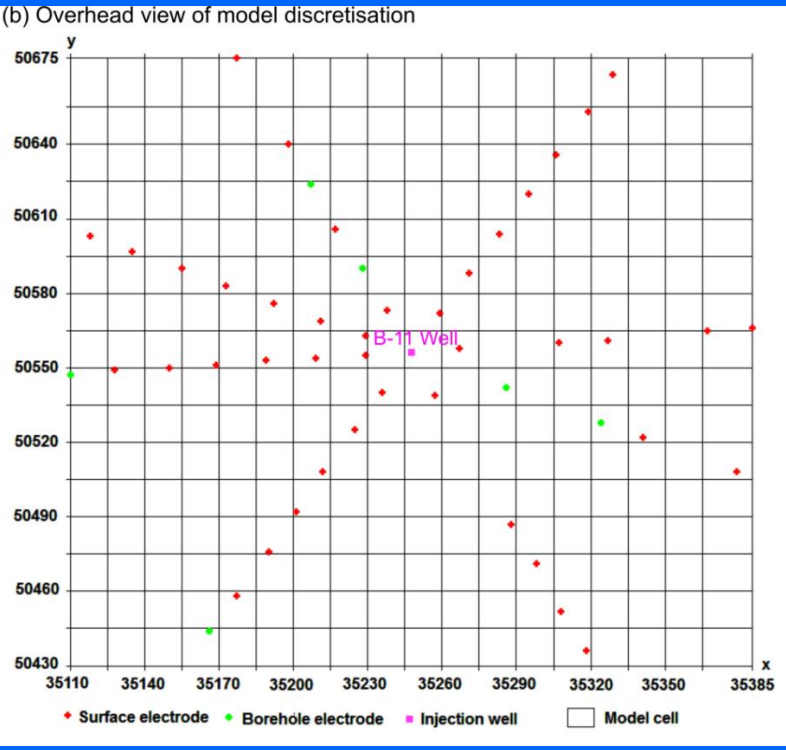

AnglogoldAshanti USA - results

A sample of the injection results is shown. Injections were made at 90 ft and 110 ft below the ground surface. The figure shows the change in the resistivity (of -4%) in the form of 3-D iso-contours that better illustrates the migration of the solution.

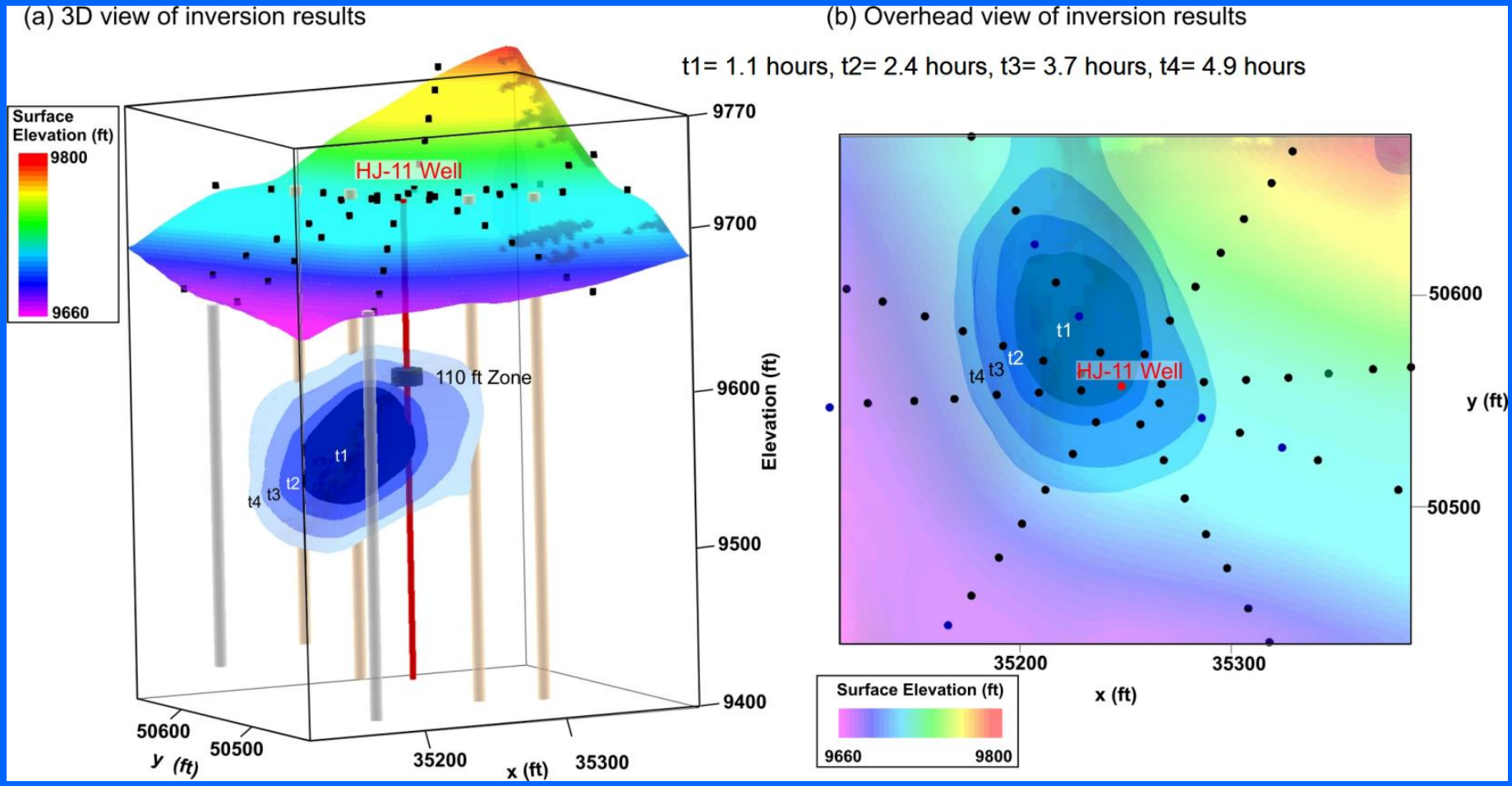

Example 3 – AnglogoldAshanti USA

Below is a time-lapse video constructed from 137 snap-shots.

Break for questions and discussion

Part 3

2-D surveys, data and inversion

How 2-D surveys are carried out, the models used, inversion and interpretation.

What is a 2-D electrical imaging survey?

A 2-D imaging survey is usually carried out with a computer controlled resistivity meter system connected to a multi-electrode cable system. The control software automatically selects the appropriate four electrodes for each measurement to give a 2-D coverage of the subsurface. A large variety of arrays and survey arrangements can be used with such a system.

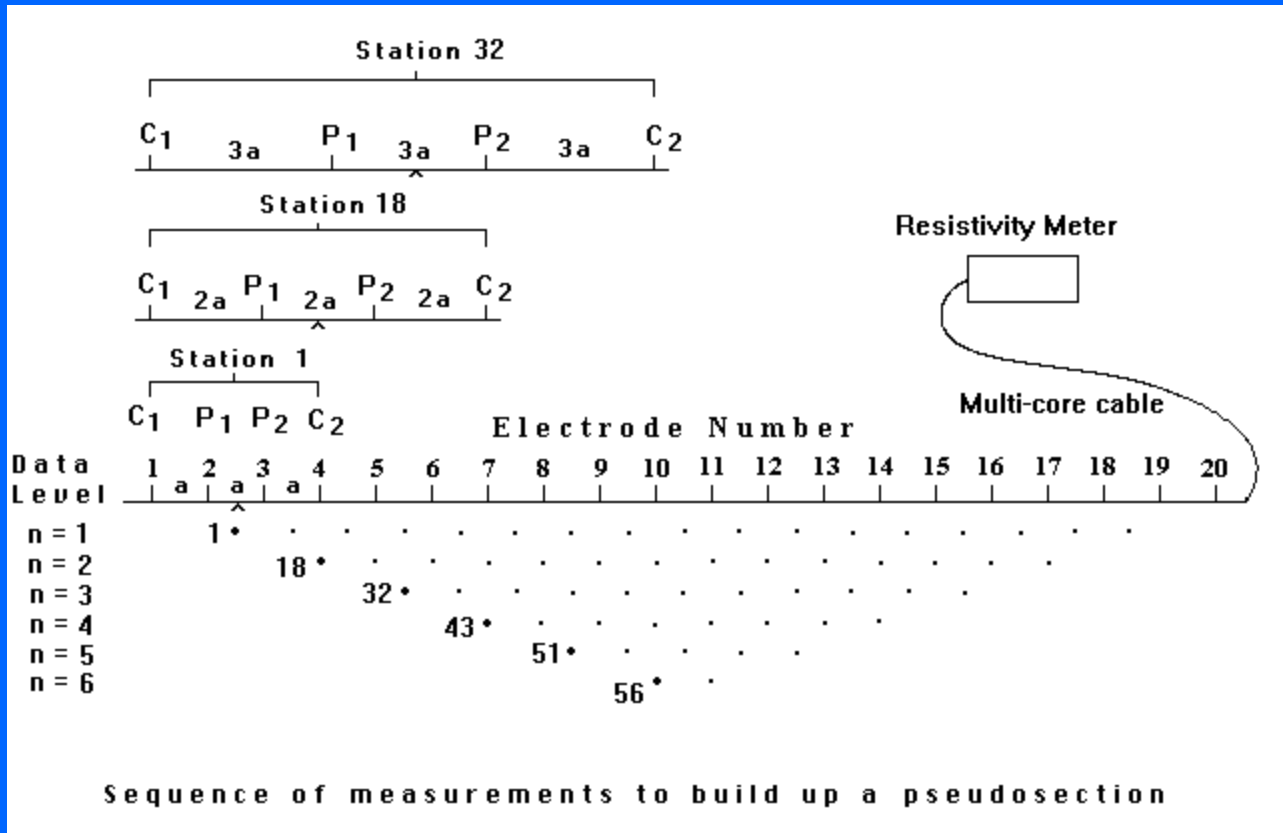

Sequence of measurements to build up a pseudosection

2-D imaging survey - instrumentation

At present, field techniques and equipment to carry out 2-D resistivity surveys are fairly well developed. Commercial multi-electrode systems typically costs from about US$20,000 upwards. The more expensive systems support multi-channel measurements, and I.P. readings.

To obtain a good 2-D picture of the subsurface, the coverage of the measurements must be 2-D as well. The figure shows a sequence of measurements for the Wenner electrode array for a system with 20 electrodes where all the possible spacings from *1a* to *6a* are measured across the line.

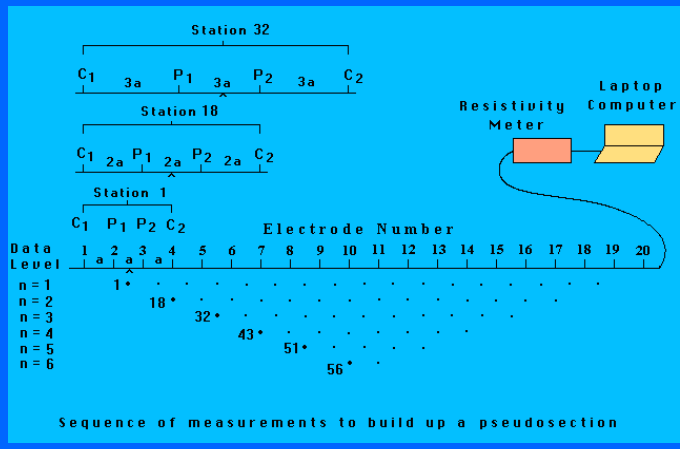

Sequence of measurements to build up a pseudosection

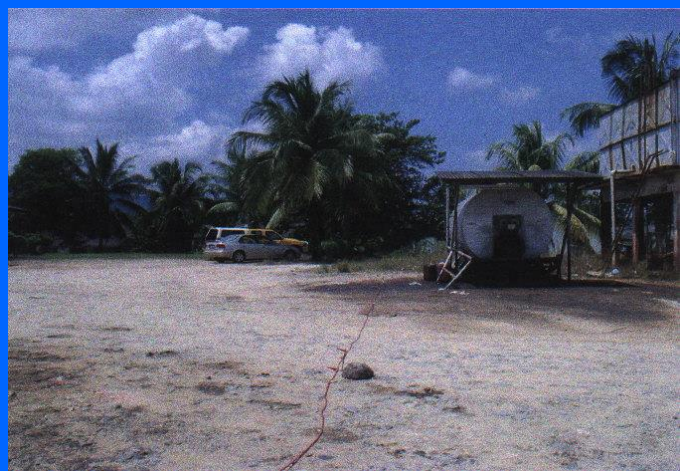

2-D surveys – typical multi-electrode systems

A typical system is the Pasi Polares system. Many system has a 'center-spread' arrangement using two cables with take-outs attached to the main resistivity meter placed at the center. It supports 16 to 256 electrodes, but 32 is probably the practical minimum. An unusual feature is the use of AC current for making frequency-domain I.P. measurements. Another common system is the Abem SAS and LS series that uses a time-domain measuring system.

Prosys system by Iris Instruments

Another example is the Syscal series by Iris Instrument that uses cable segments each with 12 electrodes. Systems come with 48 to 128 electrodes. This is one of the more powerful battery based systems. The multielectrode cable system has been used with node spacings of up to 20 m for surveys up to about 300 m deep.

The **SYSCAL Pro Switch** units use segments (seg) of multi-core cable which are reversible and interchangeable.

For instance, the **SYSCAL Pro Switch 48** with 10m spacing has 4 segments of cable a, b, c, d, with 12 electrodes each, for a total line length of 480m. The SYSCAL is placed in the middle of the line, between segments b and c.

If the profile to measure is longer than the line length, a **ROLL ALONG technique** can be applied where, after a first set of readings with (a, b, c, d), segment a is placed after segment d to form a new (b, c, d, a) combination etc.

SYSCAL Pro Switch	48	72	96	120
5m spacing total line length	2 seg x 24 elect 240m	4 seg x 18 elect 360m	6 seg x 16 elect 480m	12 seg x 10 elect 600m
10m spacing total line length	4 seg x 12 elect 480m	8 seg x 9 elect 720m	12 seg x 8 elect 960m	24 seg x 5 elect 1 200m

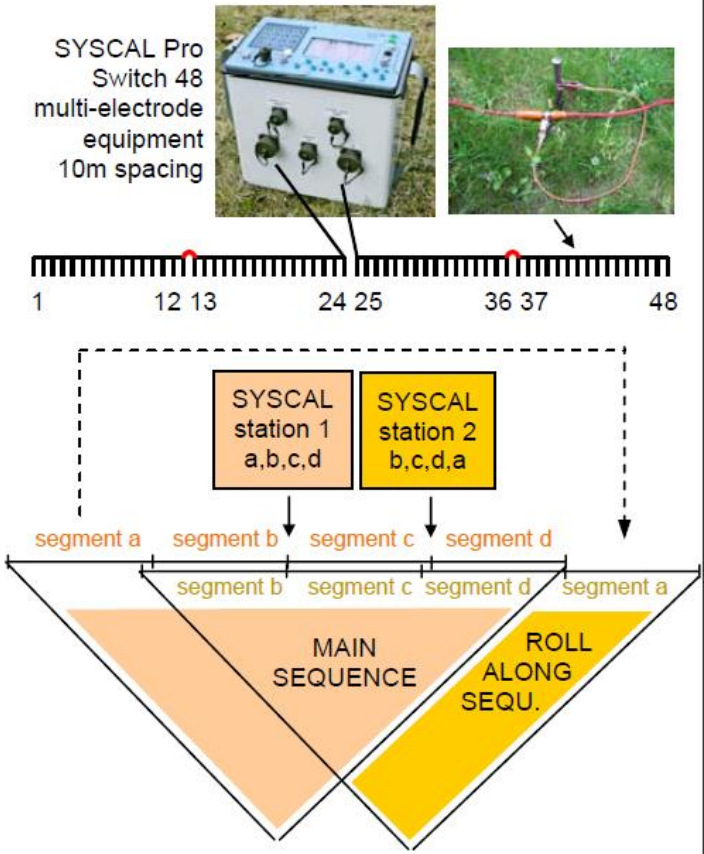

More powerful systems

For deeper surveys using larger spacings, separate current and potential measurement units are used. The current source is usually a petrol generator that can produce high currents of up to about 10 Amps. This arrangement commonly used in I.P. mineral surveys. Example systems are the Iris Elrec, Quantec Geoscience Titan and Scintrex IPR-12 system. They are used for survey depths up to about 500 to 1000 meters for mineral exploration.

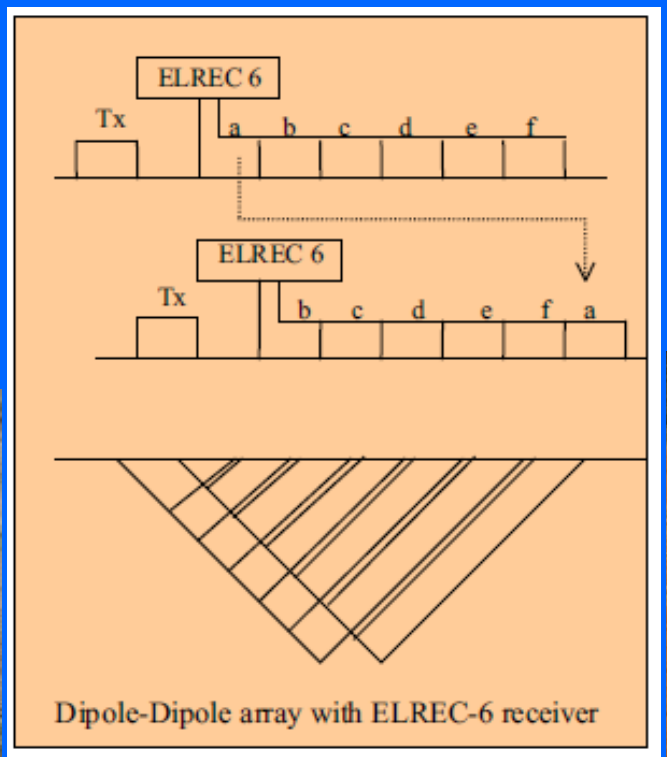

Dipole-Dipole array with ELREC-6 receiver

Other types of 2-D surveys - mobile systems

Static systems, such as the Pasi or Abem systems, use a large number of nodes to get a wide data coverage. In contrast, dynamic systems use a small number of nodes in a fixed configuration but move the entire system to obtain a wide coverage. There are two main types of dynamic systems for land use. One type, such as the Pulled Array System uses direct contact, so it can only be used on open moist ground. The second type based on capacitive coupling, such as the Geometrics OhmMapper, does not require direct contact with the ground and can be used on roads or in houses. These mobile system can cover a very large area in a short time, but has a more limited depth penetration (3-15m).

Pulled Array System

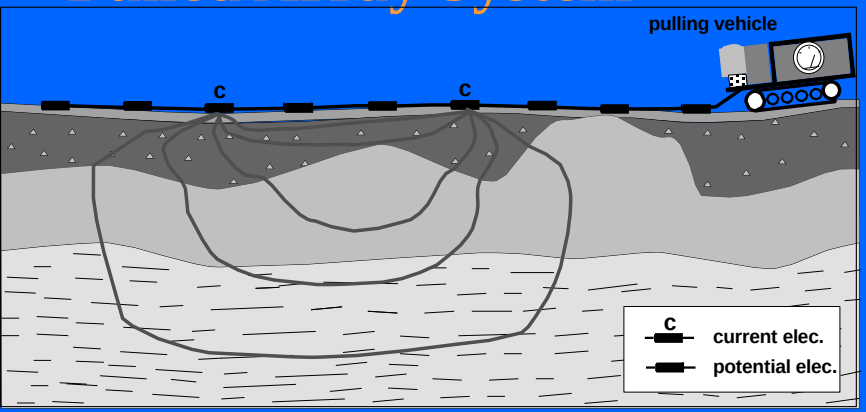

Geometrics OhmMapper System

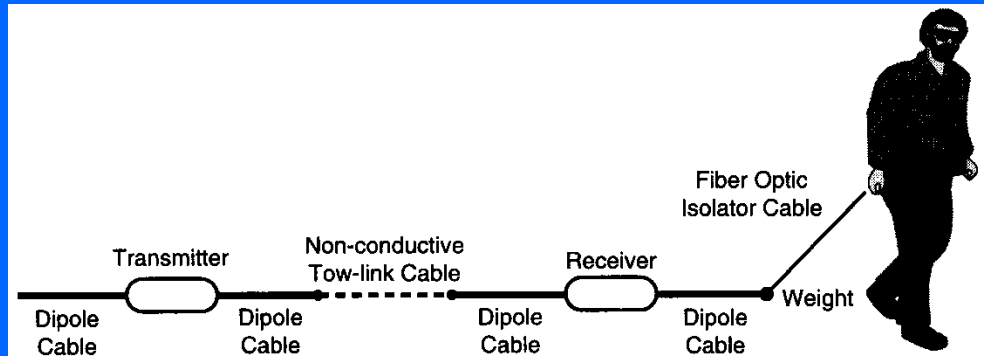

The Syscal Pro continuous land survey system

One commercial system combines the Syscal Pro instrument with a cable using cylindrical steel electrodes. A laptop PC and coupled to the Syscal and a GPS record the readings automatically.

SYSCAL Pro for continuous land survey

DYNAMIC ACQUISITION for LAND SURVEYS

- **The SYSCAL Pro** can be used with a specific cable pulled on the ground by a light vehicle, for a continuous acquisition of resistivity readings.
- **The cable features** 13 cylindrical stainless steel electrodes (8cm diameter, 25cm length, 4.2kg) at *2m spacing*:
  - 2 for transmitting the current,
  - 11 for simultaneously measuring ten potential channels.
- **A PC** continuously records the 10 resistivity values and the GPS data, displays profiles in real time
- **Recommended electrode array:** reciprocal Wenner Schlumberger
- **Penetration depth:** about 5m
- **Best conditions:** wet grounds
- **Acquisition speed:** typ. 3km/h

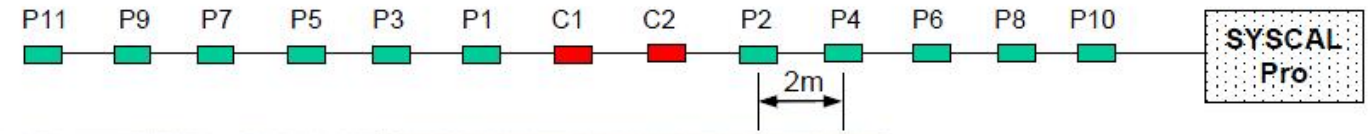

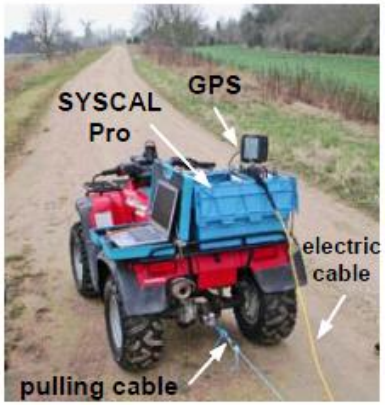

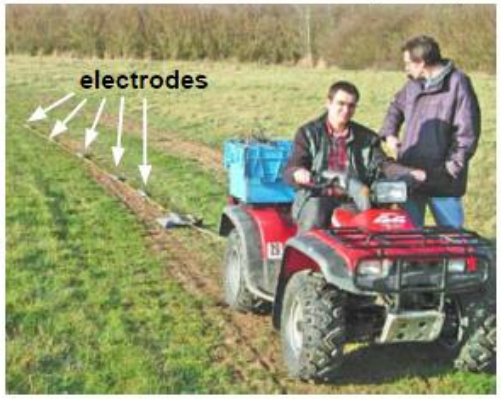

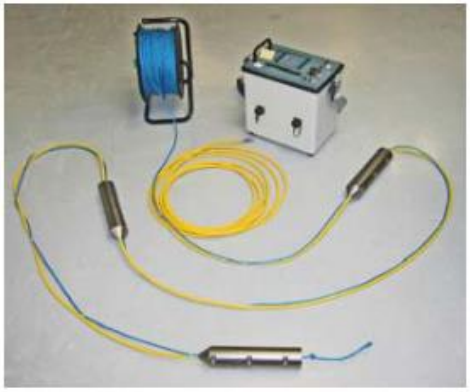

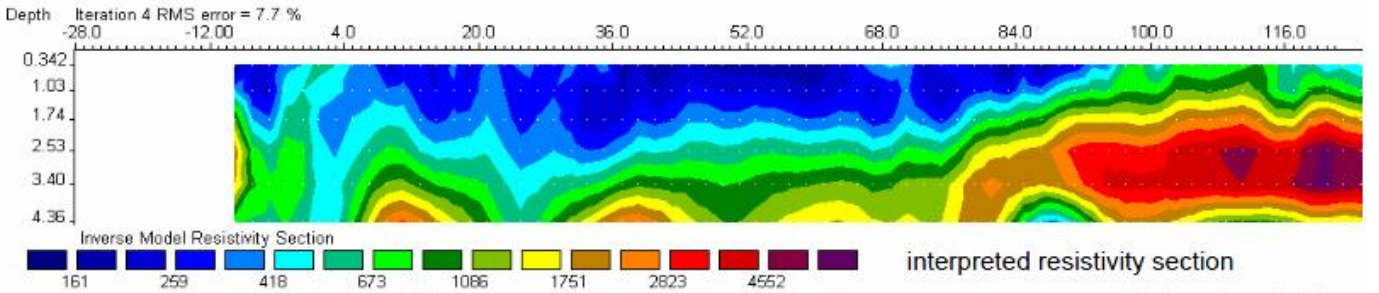

Capacitively coupled systems - the OhmMapper

There are 2 basic types of capacitively coupled system.

The OhmMapper system uses a line antenna arrangement with cylindrical transmitters and receivers which are towed behind an operator.

The receiver and transmitter are attached by a cable and pulled along during the survey. The positions are automatically recorded by a GPS system.

OhmMapper being towed over grass and pavement. Contact is made capacitively with the ground through insulated cables.

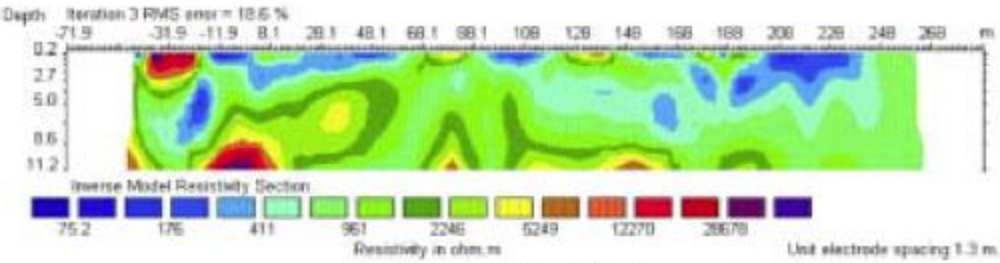

OhmMapper TR data collected over granite with surface weathering. Inversion done with RES2DINV program from MH Loke.

The BGS system

The second type (electrostatic quadrupole) uses flat metallic conductors in an equatorial dipole-dipole configuration. Examples are the Iris Corim and BGS system. 2-D and even 3-D surveys can be rapidly carried out with these mobile systems.

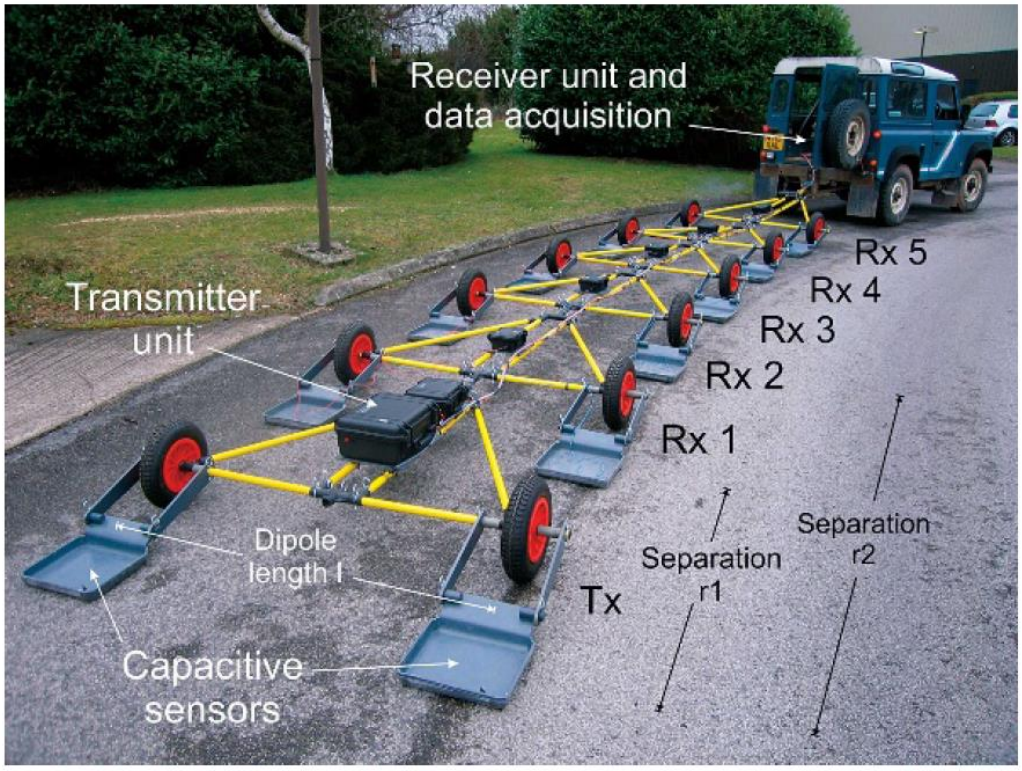

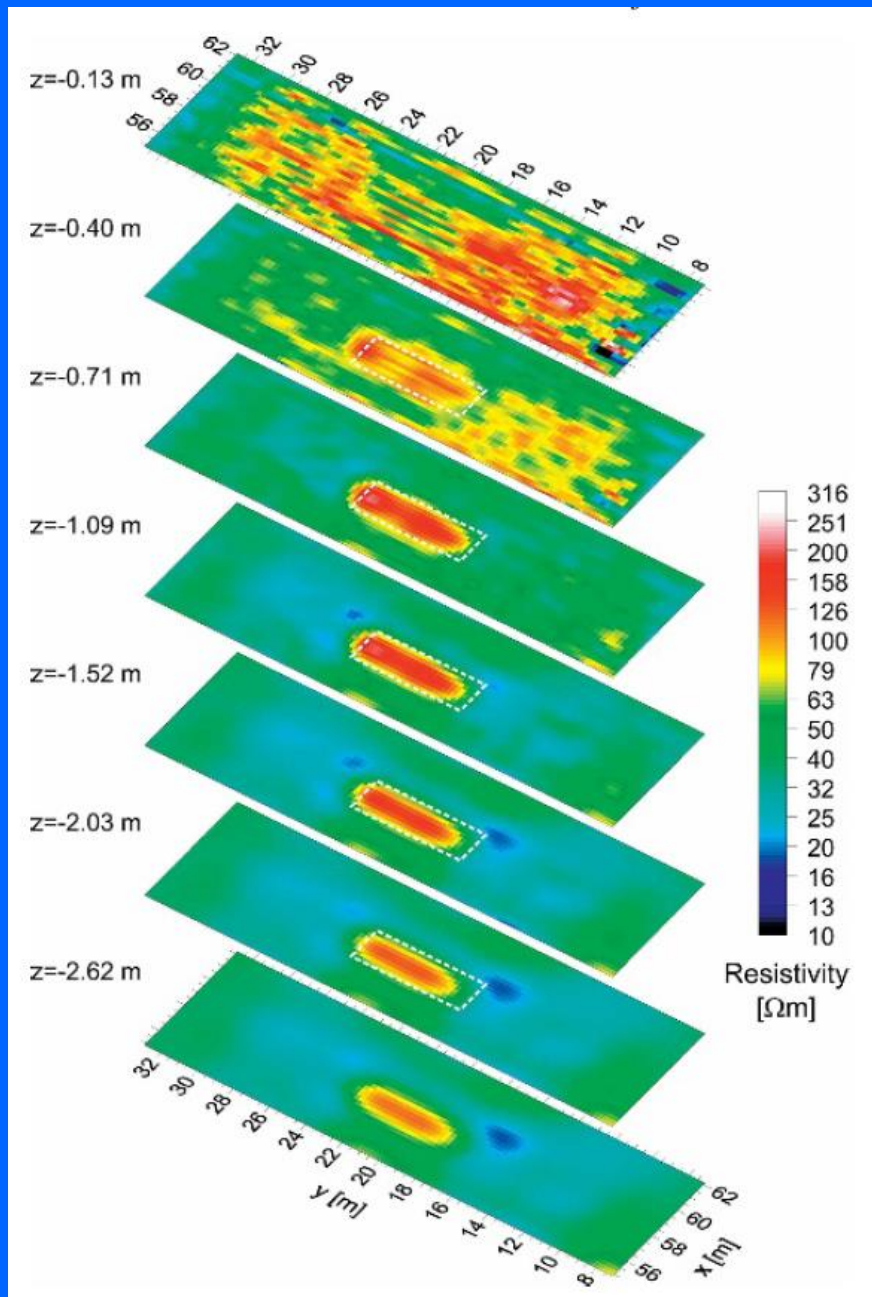

Kuras, O., Meldrum, P. I., Beamish, D., Ogilvy, R. D., and Lala, D., 2007. Capacitive resistivity imaging with towed arrays. *Journal of Environmental and Engineering Geophysics*, 12: 267-279.

Other types of mobile 2-D surveys - aquatic systems

The main problem faced by mobile systems on land is to get sufficient current to flow into the ground, but this is not a problem in aquatic environments. A possible arrangement for an underwater mobile surveying system where a cable with a number of nodes is pulled along the river/lake/sea bottom by a boat is shown below. Two of the nodes are used as current electrodes, while the rest are used as potential electrodes. There are now several multi-channel systems marine systems available. Surveys have also been carried out with the electrodes floating on the surface, or suspended between the water surface and bottom which might be the best arrangement.

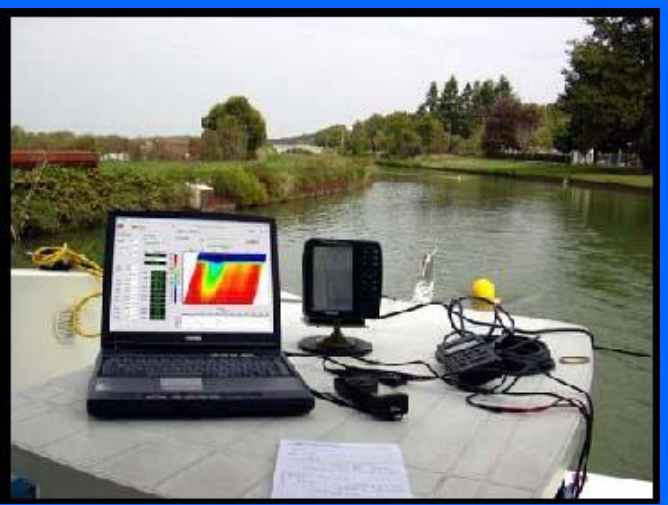

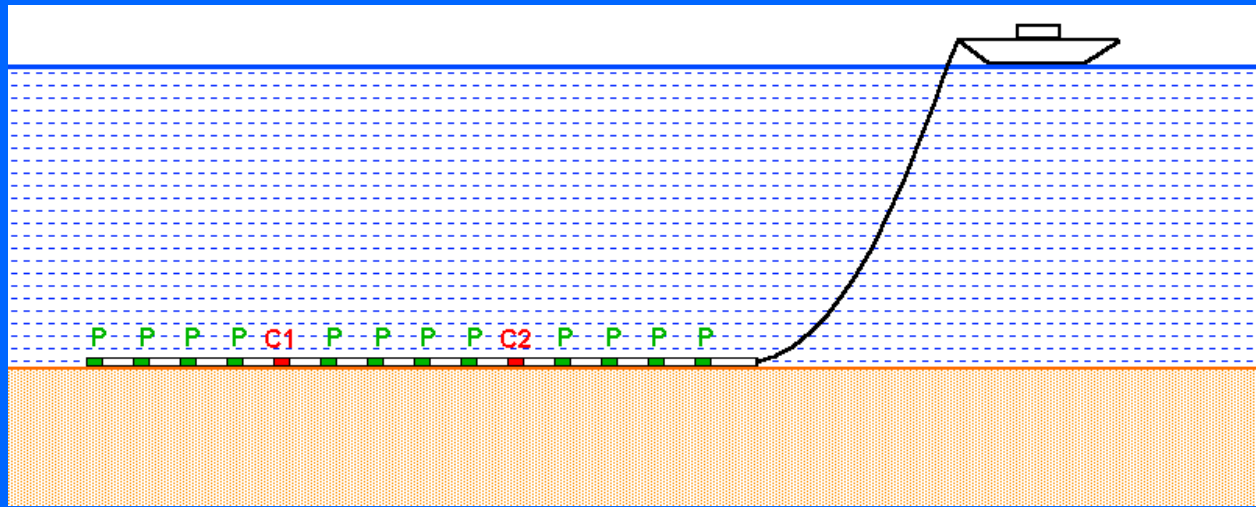

Example of commercial water survey system

Below is an example with the Syscal system with PC and GPS together with a streamer using graphite electrodes used for a water-borne survey.

SYSCAL Pro for river and sea survey

DYNAMIC ACQUISITION for RIVER & SEA SURVEYS

- **The SYSCAL Pro** can be used with a specific cable pulled on the surface of water (lake, river or sea) by a light boat, for a continuous acquisition of resistivity readings.
- **The cable features** 13 cylindrical graphite electrodes (4cm diameter, 10cm length) at *5m spacing*:
  - 2 for transmitting the current,
  - 11 for simultaneously measuring ten potential channels.
- **A PC** continuously records the 10 resistivity / IP values and the GPS data, displays profiles in real time
- **GPS track** vizualisation on Google Earth
- **Recommended electrode array:** reciprocal Wenner Schlumberger
- **Penetration depth:** about 15m with a 100m total length cable
- **Acquisition speed:** typ. 3km/h

cable with graphite electrodes

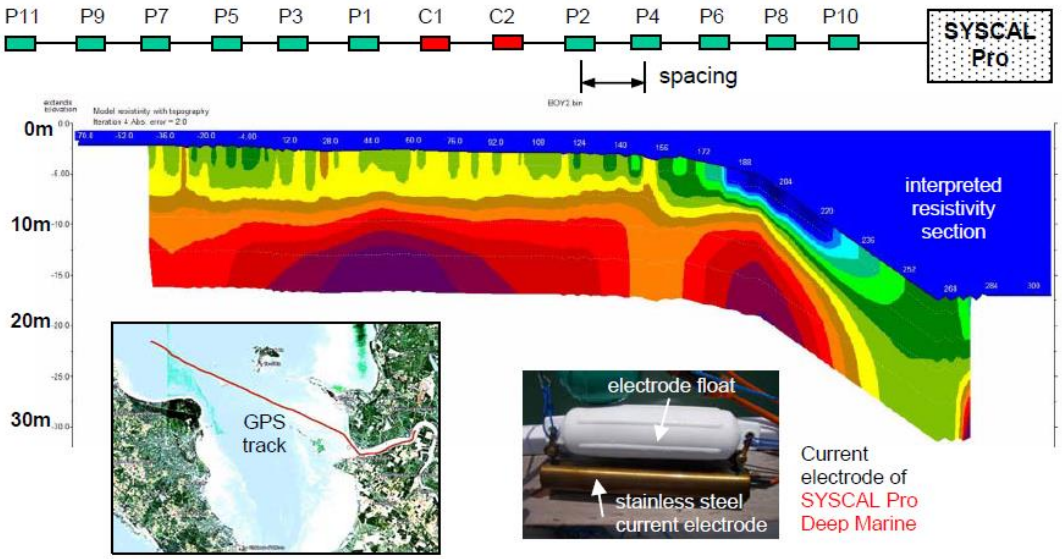

Current electrode of SYSCAL Pro Deep Marine

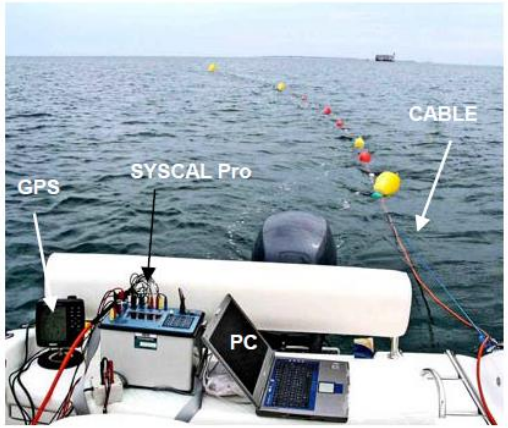

SYSCAL Pro Deep Marine is a SYSCAL Pro dedicated to measurement in sea water:

- **with outputs of 50V, 50A, 2500W**
- **for higher penetration**
- **for higher speed (up to 10km/h)**
- **with reciprocal Wenner-Schlumb & dip-dip**

It uses the same graphite electrode cable as the SYSCAL Pro for the measurement of the potential, but stainless steel electrodes for the current (5cm diameter, 30cm length)

It can be used with a cable of *25m spacing* between electrodes (total cable length 350m), for a depth of penetration of about 60m

Presentation of 2-D survey data

The pseudosection plotting method

Pseudosection data plotting method

To plot the data from a 2-D imaging survey, the pseudosection contouring method is normally used. The horizontal location of the point is placed at the mid-point of the set of electrodes used to make that measurement. The vertical location of the plotting point is placed at the median depth of investigation of the array used. For example, the data point measured by electrodes 1, 2, 3 and 4 are plotted at the mid-point between electrodes 2 and 3 in the diagram below.

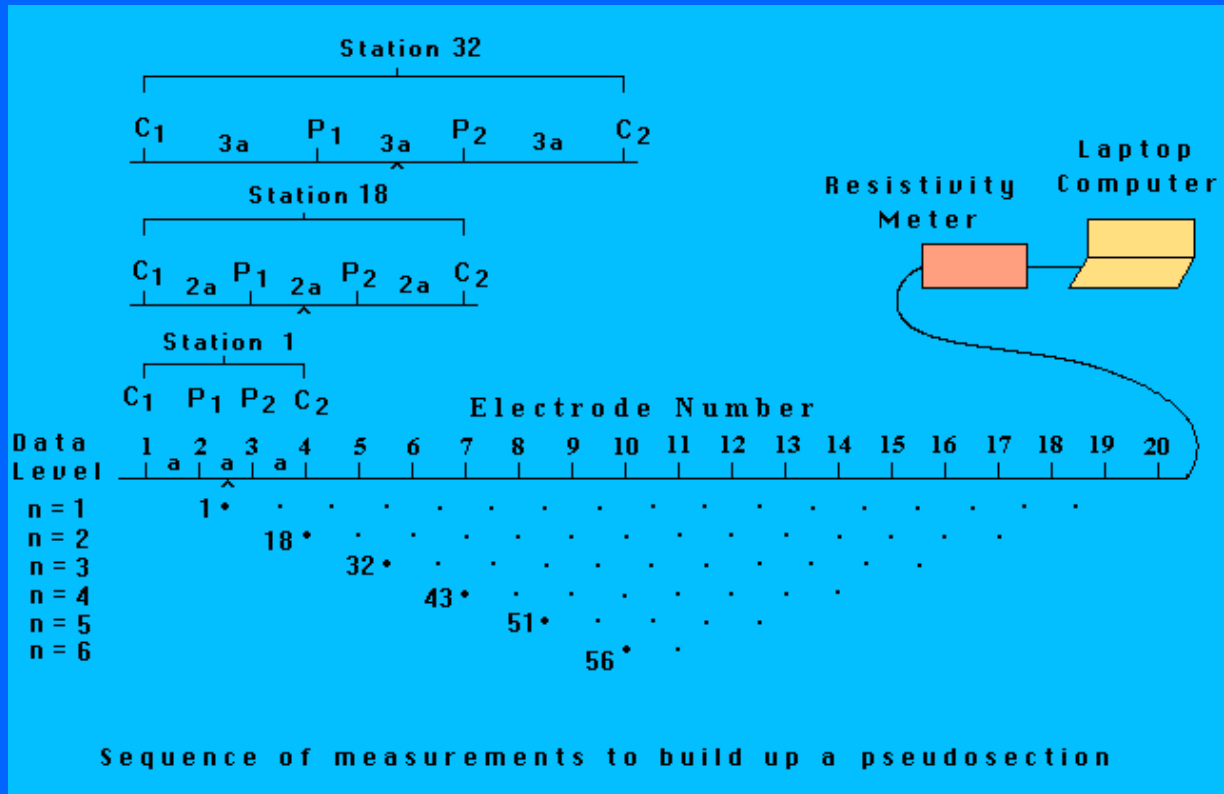

Sequence of measurements to build up a pseudosection

Pseudosection data plotting method - usage

The pseudosection gives a very approximate picture of the true subsurface resistivity distribution, as the shapes of the contours depend on the type of array used as well as the true subsurface resistivity.

The pseudosection is useful as a means to present the measured apparent resistivity values in a pictorial form, and as an initial guide for further quantitative interpretation.

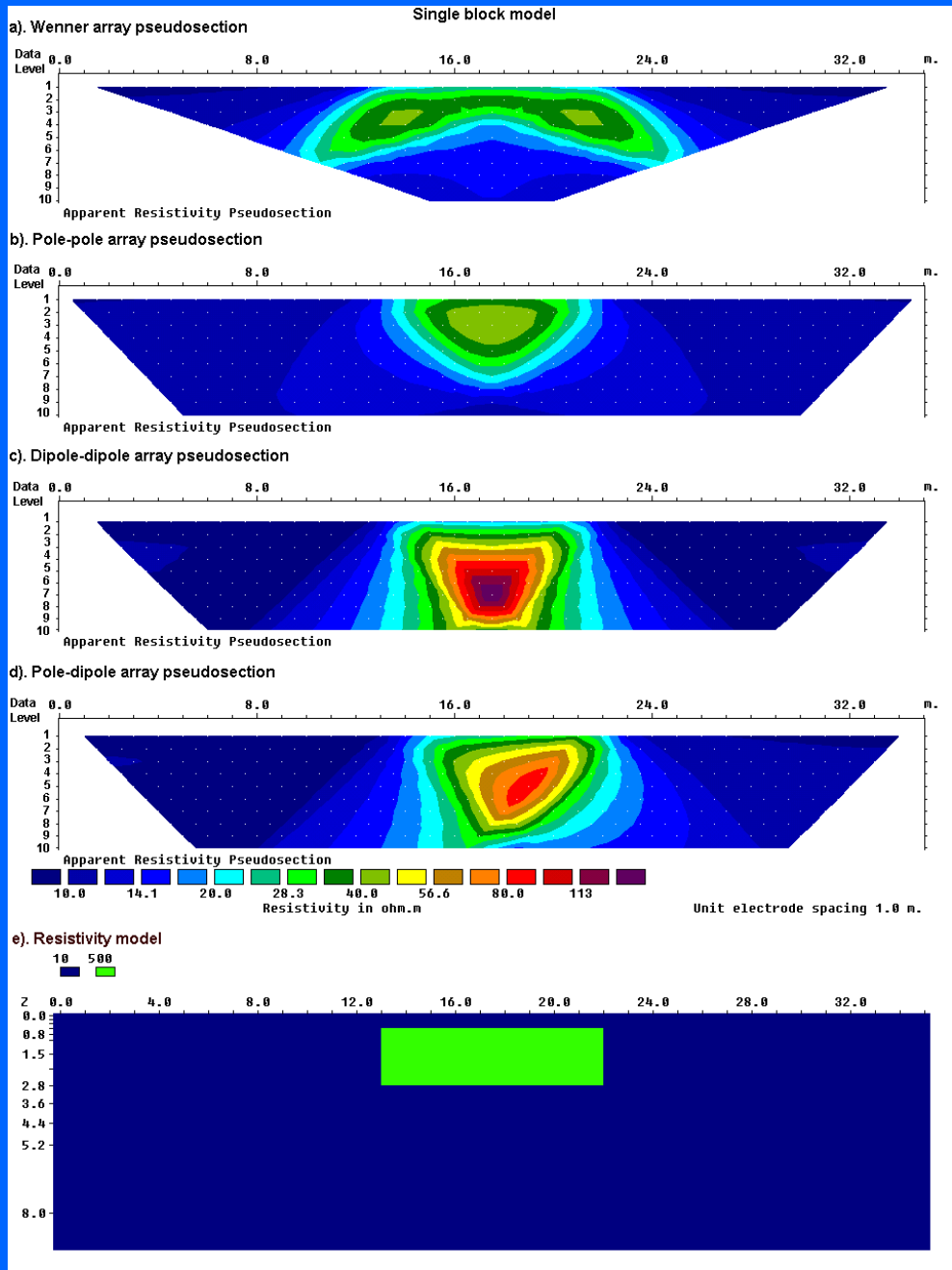

Pseudosection data plotting method - limitations

The figure also gives you an idea of the data coverage that can be obtained with different arrays. The pole-pole array gives the widest horizontal coverage, while the coverage obtained by the Wenner array decreases more rapidly with increasing electrode spacing.

One useful practical application of the pseudosection plot is for picking out bad apparent resistivity data points, which have unusually high or low values. We will look at this in a later section.

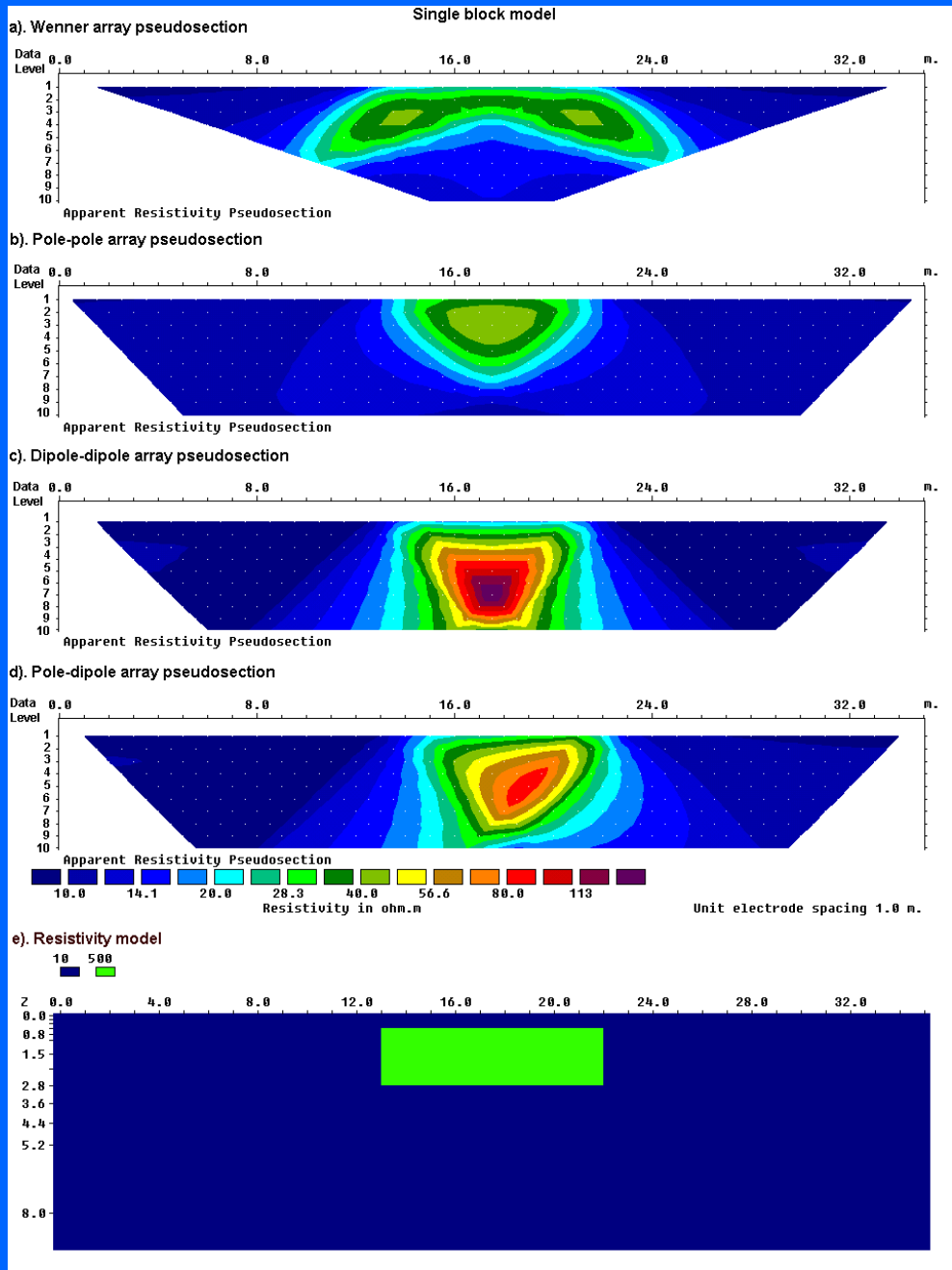

Brief guide to 2-D inversion

This sections gives a very brief guide to inversion of 2-D data sets for non-geophysicists. A more detailed discussion is given in the last part of the talk.

From data to model : 2-D inversion

After the field survey, the resistance measurements are usually changed to apparent resistivity values. The purpose of the inversion is to convert the apparent resistivity values into a model section. For 2-D surveys, the conversion of the apparent resistivity data to a model for the subsurface resistivity is carried out on a microcomputer using an automatic inversion program.

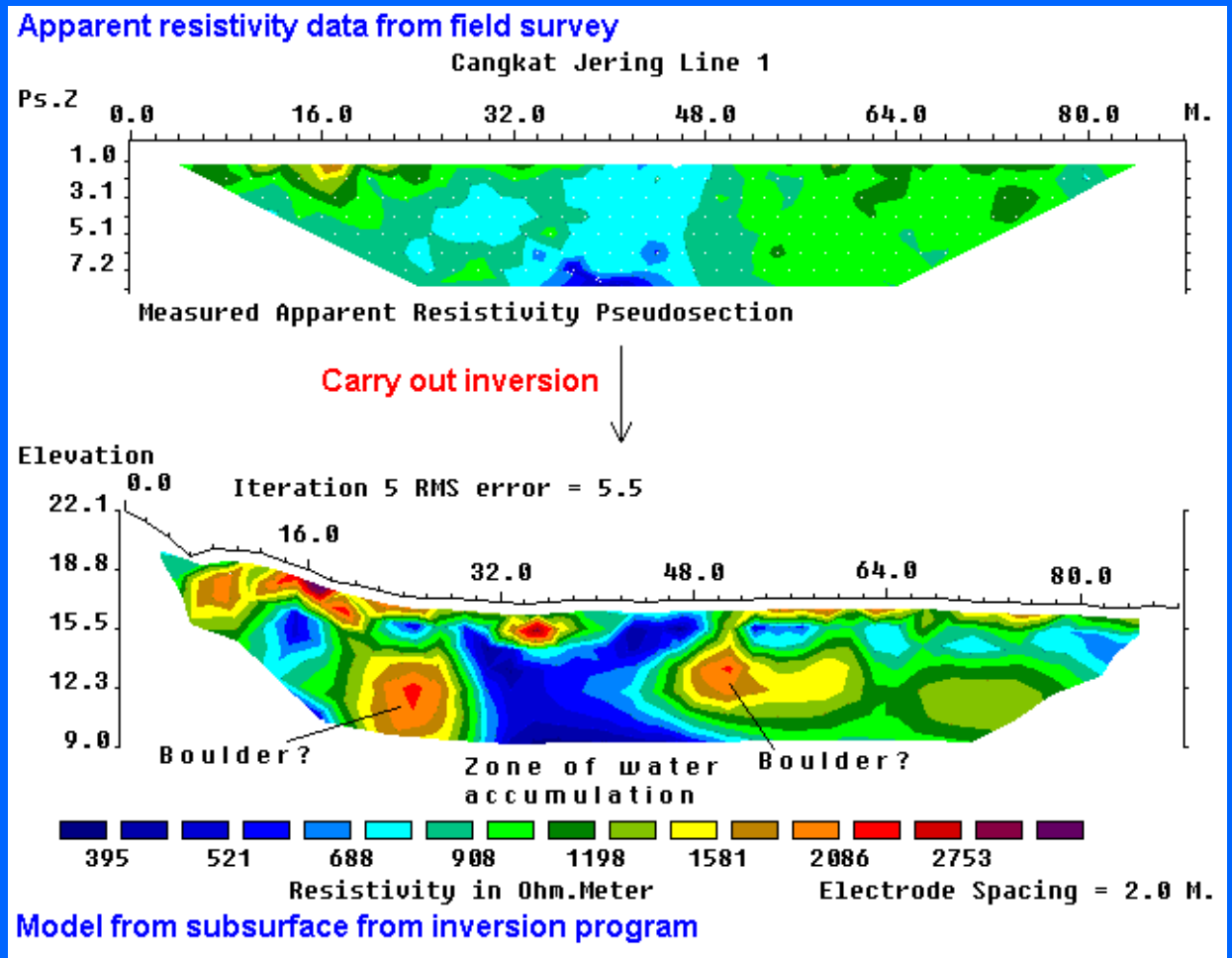

What is a 2-D model?

A 2-D model is used to interpret the data from a 2-D imaging survey. The model usually consists of a large number of rectangular cells. The size and position of each cell is fixed. An inversion program is used to determine the resistivity of the cells from the measured apparent resistivity values.

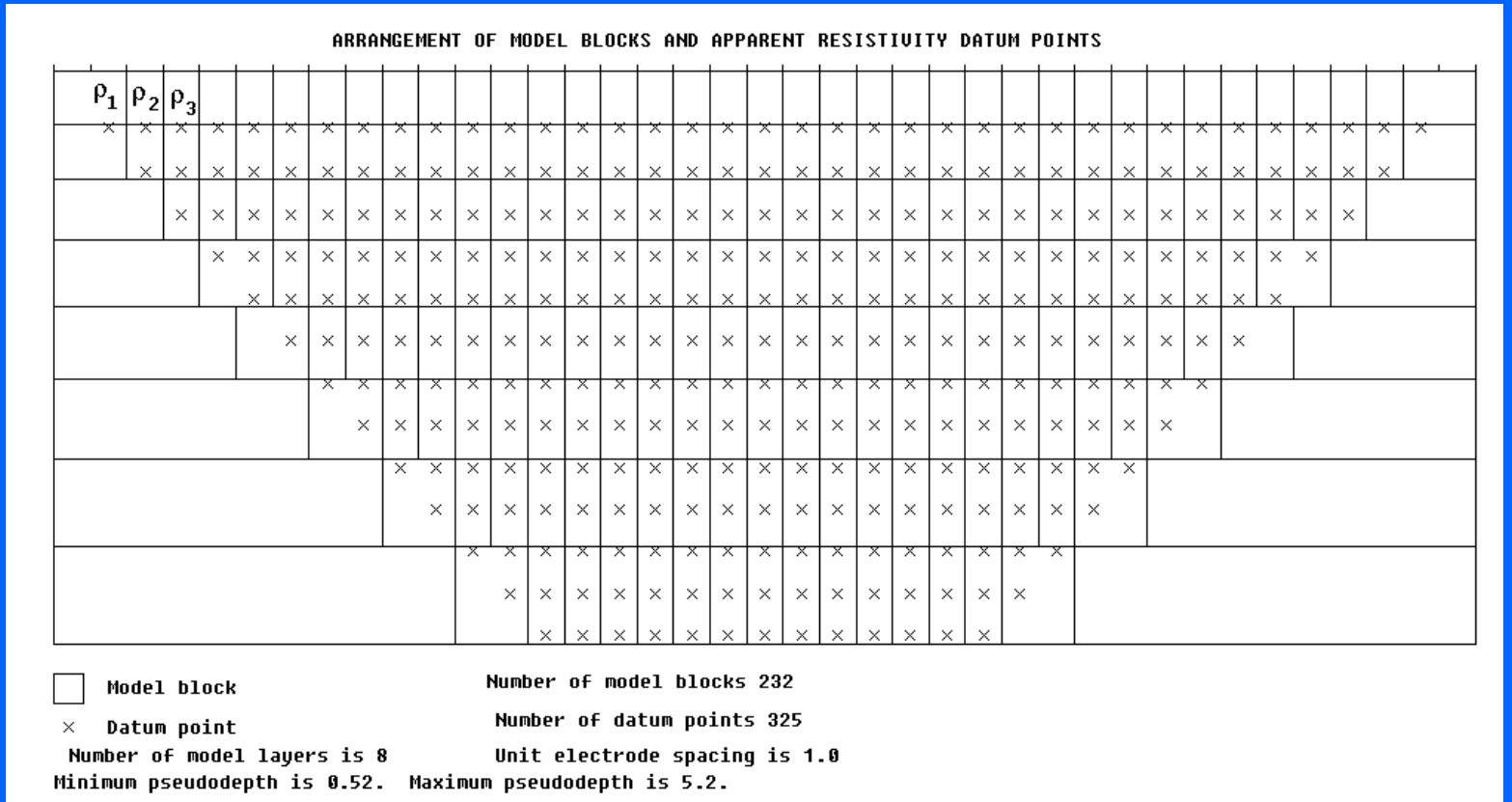

The least-squares optimization method

The smoothness-constrained least-squares optimization method is commonly used in 2-D and 3-D resistivity inversion, using the following equation.

$$\left[\mathbf{J}_i^T\mathbf{J}_i + \lambda_i \mathbf{W}^T\mathbf{W}\right]\Delta\mathbf{q}_i = \mathbf{J}_i^T\mathbf{g}_i - \lambda_i \mathbf{W}^T\mathbf{W}\,\mathbf{q}_{i-1}$$

$\mathbf{W}$ = roughness filter, λ = roughness filter damping factor

$\mathbf{q}_{i-1}$ = current inversion model

$\Delta\mathbf{q}_i$ = change in model resistivity to be calculated

$\mathbf{g}$ = data misfit, difference between measured and calculated apparent resistivity values

$\mathbf{J}$ = Jacobian matrix of partial derivatives, or sensitivity.

Normally the model parameter vector $\mathbf{q}$ contains the (logarithm) of the model resistivity values.

Inversion algorithm

The steps taken are as follows :-

a). Start with a homogenous model q_0 where all the model cells have the same resistivity.

b). Calculate the apparent resistivity values for this model, and thus the data misfit g, put it in the least-squares equation and calculate the change needed Δq.

c). Calculate the new model $q_i = q_{i-1} + \Delta q$, repeat step (b) until the difference between the calculated and measured apparent resistivity values is sufficiently small.

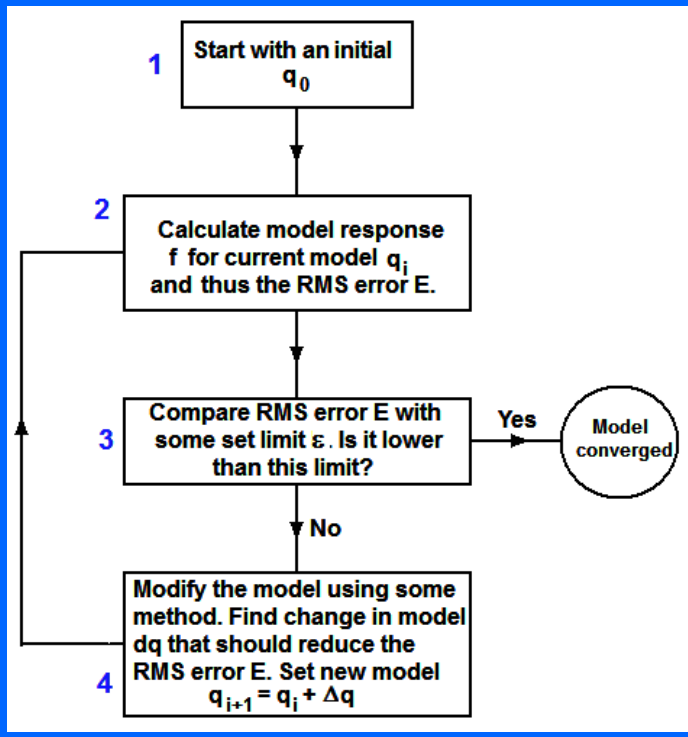

$$\left[\mathbf{J}_i^T\mathbf{J}_i + \lambda_i\mathbf{W}^T\mathbf{W}\right]\Delta\mathbf{r}_i = \mathbf{J}_i^T\mathbf{g}_i - \lambda_i\mathbf{W}^T\mathbf{W}\mathbf{r}_{i-1}$$

Types of arrays used in 2-D surveys

Brief summary of common arrays

1). Wenner

2). Wenner-Schlumberger

3). Dipole-dipole

4). Pole-dipole

5). Pole-pole

6). Multiple gradient

Array types for 2-D surveys

The multi-electrode systems can be programmed to use almost any array. Most surveys use the Wenner (alpha), dipole-dipole, Wenner-Schlumberger, pole-pole and pole-dipole. A new addition for multi-channel systems is the multiple gradient array, which is a non-symmetrical form of the Schlumberger. The dipole-dipole and pole-dipole arrays are also widely used with multi-channel systems.

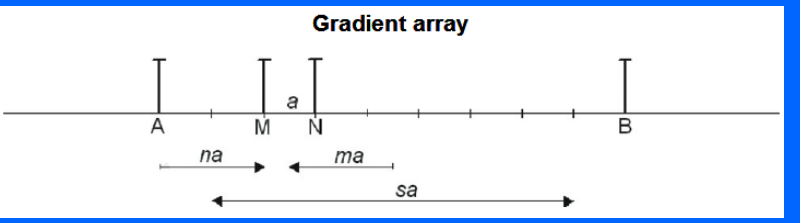

a). Wenner Alpha

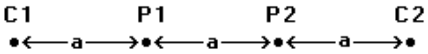

$k = 2 \pi a$

b). Wenner Beta

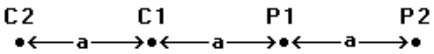

$k = 6 \pi a$

c). Wenner Gamma

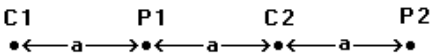

$k = 3 \pi a$

d). Pole - Pole

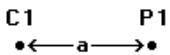

$k = 2 \pi a$

e). Dipole - Dipole

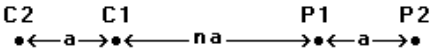

$k = \pi n(n+1)(n+2)a$

f). Pole - Dipole

$k = 2 \pi n(n+1)a$

g). Wenner - Schlumberger

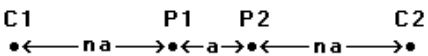

$k = \pi n(n+1)a$

h). Equatorial Dipole - Dipole

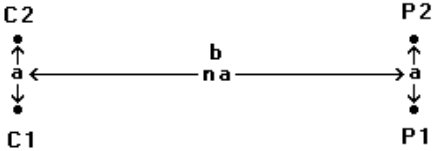

$b = na$

$k = 2 \pi b L / (L - b)$

$L = (a * a + b * b)^{0.5}$

$k = \text{Geometric Factor}$

2D surveys - array types

Among the characteristics of an array that should be considered are (i) the depth of investigation, (ii) the sensitivity of the array to vertical and horizontal changes in the subsurface resistivity, (iii) the horizontal data coverage and (iv) the signal strength.

A new consideration is the efficiency in which it can be implemented for multi-channel systems, i.e. the number of simultaneous readings that can be made with a common pair of current electrodes.

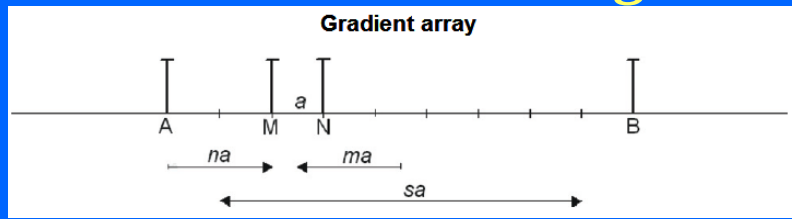

a). Wenner Alpha

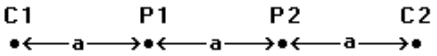

k = 2 π a

b). Wenner Beta

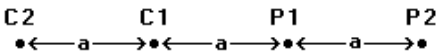

k = 6 π a

c). Wenner Gamma

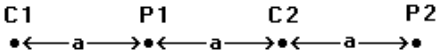

k = 3 π a

d). Pole - Pole

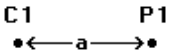

k = 2 π a

e). Dipole - Dipole

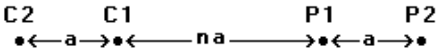

k = π n(n+1)(n+2)a

f). Pole - Dipole

k = 2 π n(n+1)a

g). Wenner - Schlumberger

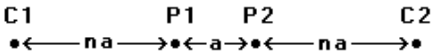

k = π n(n+1)a

h). Equatorial Dipole - Dipole

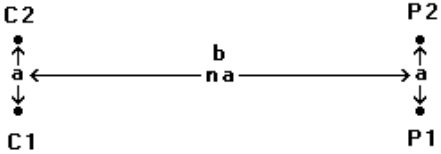

b = na

k = 2 π bL/(L-b)

L = (a*a + b*b)^0.5

k = Geometric Factor

How to select an array? – Signal strength

The signal strength is an important factor in noisy areas, or when large electrode spacings are used or for surveys with conductive material (such as aquatic surveys). The signal strength is inversely proportional to the geometric factor, so it can be easily estimated. The Wenner (alpha) array has the smallest geometric factor, and thus the highest signal strength. This means surveys with the Wenner alpha array are generally less noisy.

The pole-pole array has the same geometric factor but it has higher telluric noise due to the large distance between the potential electrodes.

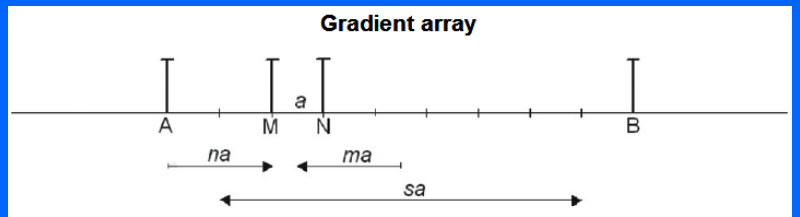

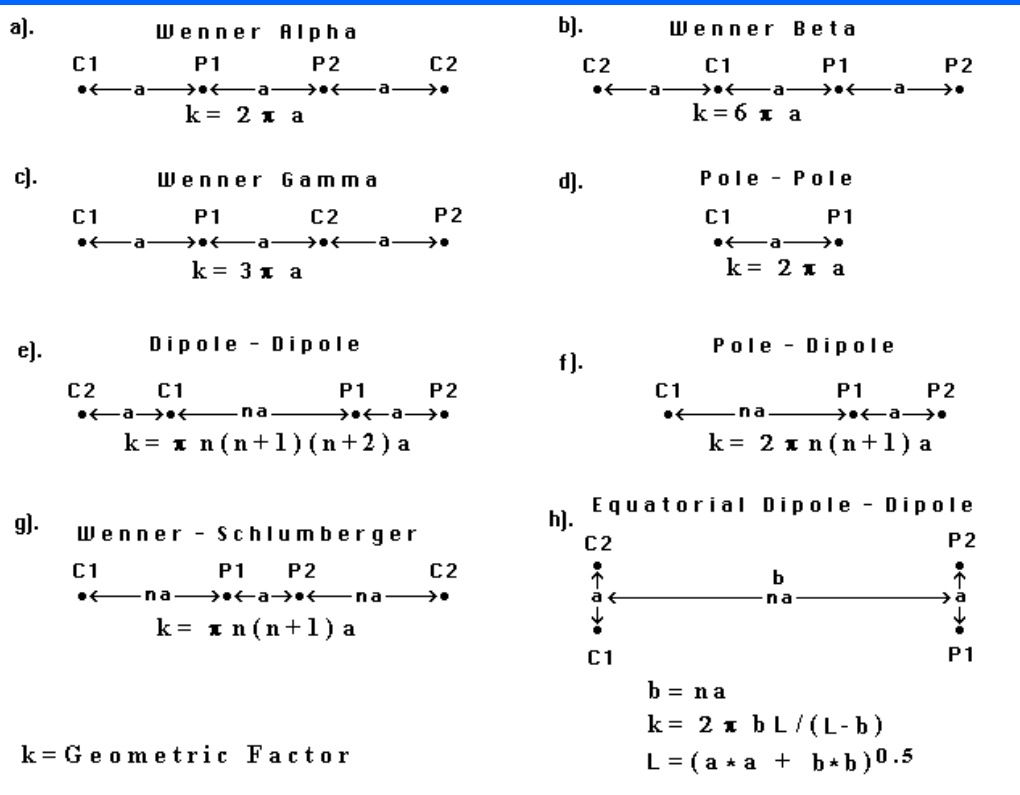

Signal strength of different arrays

The geometric factor for the dipole-dipole array is proportional to n^3, thus dipole-dipole surveys tend to have the most noisy data. As a general rule, the maximum '*n*' value should not exceed 6.

The geometric factors for pole-dipole and Wenner-Schlumberger arrays are proportional to n^2, thus the signal strength is stronger than the dipole-dipole but weaker than the Wenner.

The signal strength for the gradient array is between that of the Schlumberger and pole-dipole arrays.

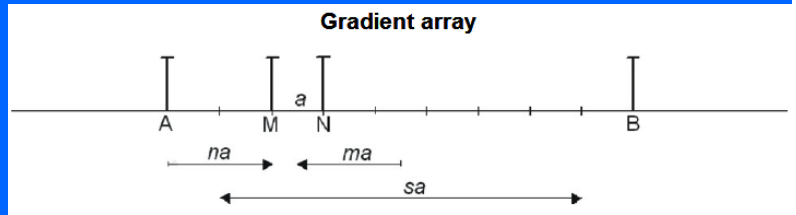

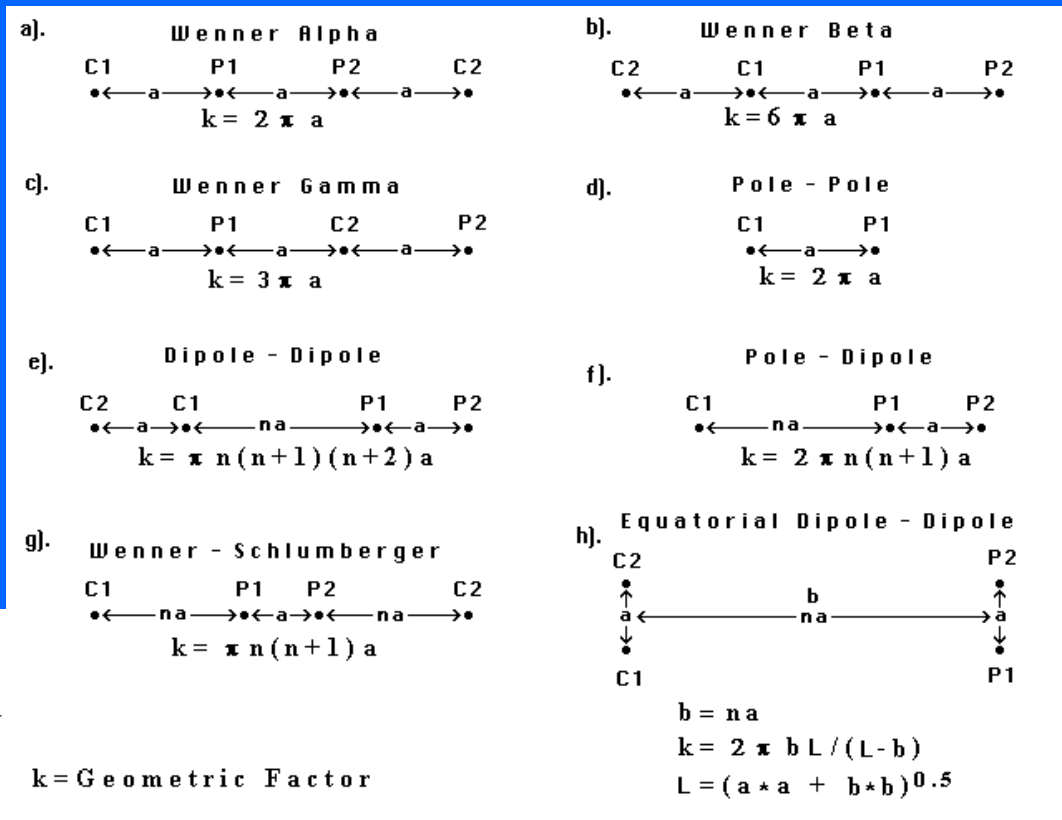

Depth of investigation and sensitivity

These characteristics can be determined from the sensitivity function of the array for a homogeneous earth model. The sensitivity function tells us the degree to which a change in the resistivity of a section of the subsurface will influence the potential measured by the array. The higher the value of the sensitivity function, the greater is the influence of the subsurface region on the measurement.

A current of 1 Amp injected into the ground through the C1 current electrode results in a potential ϕ observed at the potential P1 electrode. If the resistivity within a small volume ($\delta\tau$) of the ground located at (x,y,z) is changed by a small amount, $\delta\rho$, the change in the potential, $\delta\phi$, measured at P1 due to a current source at C1 is given by the equation below. Sensitivity = $\delta\phi / \delta\rho$

$$\delta\phi = \frac{\delta\rho}{\rho^2}\int_V \nabla\phi \cdot \nabla\phi' \, d\tau$$

$$\frac{\delta\phi}{\delta\rho} = F_{3D}(x,y,z) = \frac{1}{4\pi^2} \cdot \frac{x(x-a) + y^2 + z^2}{\left[x^2 + y^2 + z^2\right]^{1.5}\left[(x-a)^2 + y^2 + z^2\right]^{1.5}}$$

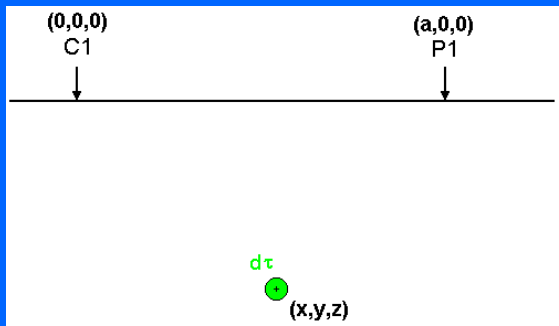

Depth of investigation – the 1-D sensitivity function

In resistivity sounding surveys, it is well known as the separation between the electrodes is increased, the array senses the resistivity of increasingly deeper layers. One method to calculate the depth of investigation is by using the 1-D version of the sensitivity function. The sensitivity function for a thin horizontal layer is obtained by integrating the 3-D sensitivity function in the *x* and *y* directions.

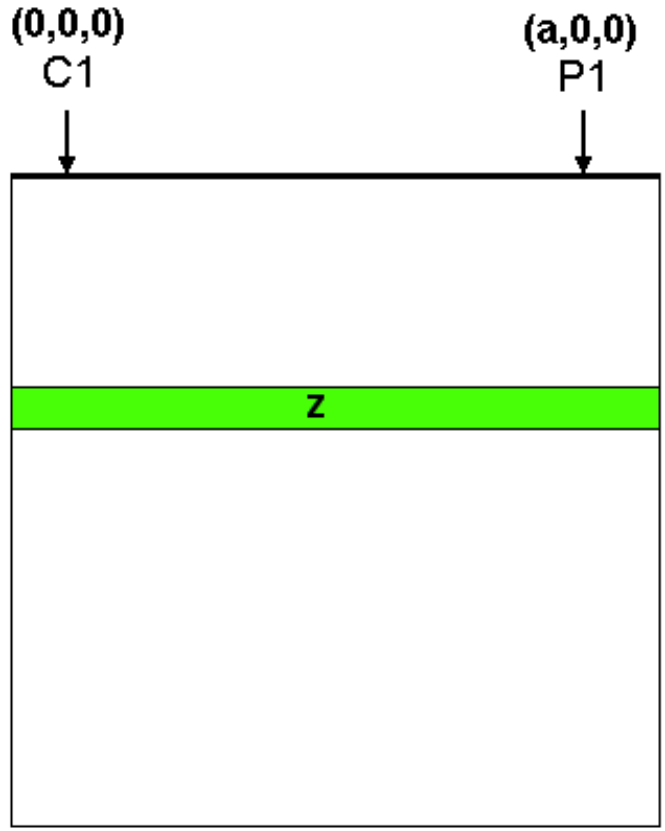

What is the effect of a change in the resistivity of a thin layer on the measured potential on the surface?

$$F_{1D}(z) = \frac{2}{\pi} \cdot \frac{z}{\left(a^2 + 4z^2\right)^{1.5}}$$

Depth of investigation – the 1-D sensitivity function

The 1-D sensitivity function is given by

$$F_{1D}(z) = \frac{2}{\pi} \cdot \frac{z}{\left(a^2 + 4z^2\right)^{1.5}}$$

The "median depth of investigation“ of an array is the depth above which the area under the sensitivity function curve is equal to half the total area under the curve. The upper section of the earth above the "median depth of investigation" has the same influence on the measured potential as the lower section. This is roughly how deep we can see with an array, assuming the subsurface is homogeneous.

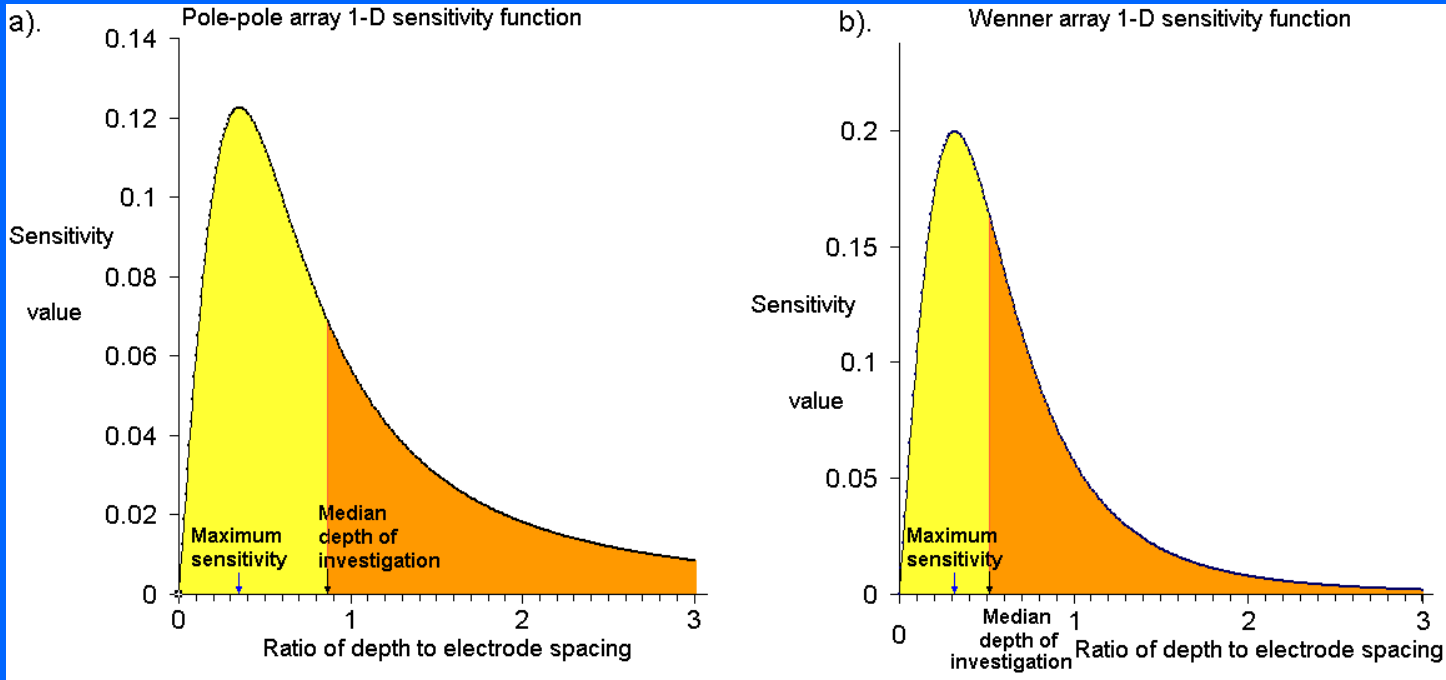

The depth of investigation of different arrays

The "median depth of investigation", z_e, can be easily calculated for different arrays, as listed in the table below. The depths are given as the ratio to the 'a' spacing or the total length 'L' of the array. To calculate the actual depth of investigation, just multiply this ratio by the 'a' spacing or 'L' length used in the field survey.

Array type	z_e/a	z_e/L
Wenner Alpha	0.519	0.173
Wenner Beta	0.416	0.139
Wenner Gamma	0.594	0.198
Dipole-dipole		
n = 1	0.416	0.139
n = 2	0.697	0.174
n = 3	0.962	0.192
n = 4	1.220	0.203
n = 5	1.476	0.211
n = 6	1.730	0.216
n = 7	1.983	0.220
n = 8	2.236	0.224
Equa. dipole-dipole		
n = 1	0.451	0.319
n = 2	0.809	0.362
n = 3	1.180	0.373
n = 4	1.556	0.377
Pole-Pole	0.867	

Array type	z_e/a	z_e/L
Wenner-Schlumberger		
n = 1	0.519	0.173
n = 2	0.925	0.186
n = 3	1.318	0.189
n = 4	1.706	0.190
n = 5	2.093	0.190
n = 6	2.478	0.191
n = 7	2.863	0.191
n = 8	3.247	0.191
n = 9	3.632	0.191
n = 10	4.015	0.191
Pole-dipole		
n = 1	0.519	
n = 2	0.925	
n = 3	1.318	
n = 4	1.706	
n = 5	2.093	
n = 6	2.478	
n = 7	2.863	
n = 8	3.247	

Comparison of the depth of investigation for arrays

Note that the depth of investigation of the Wenner alpha array is about half the 'a' spacing between the electrodes. The pole-pole array has the deepest depth of investigation. The 'median depth of investigation' for the dipole-dipole array is probably an underestimate, due to the extreme form of the shape of the sensitivity function (which we shall see next).

Array type	z_e/a	z_e/L
Wenner Alpha	0.519	0.173
Wenner Beta	0.416	0.139
Wenner Gamma	0.594	0.198
Dipole-dipole		
n = 1	0.416	0.139
n = 2	0.697	0.174
n = 3	0.962	0.192
n = 4	1.220	0.203
n = 5	1.476	0.211
n = 6	1.730	0.216
n = 7	1.983	0.220
n = 8	2.236	0.224
Equa. dipole-dipole		
n = 1	0.451	0.319
n = 2	0.809	0.362
n = 3	1.180	0.373
n = 4	1.556	0.377
Pole-Pole	0.867	

Array type	z_e/a	z_e/L
Wenner-Schlumberger		
n = 1	0.519	0.173
n = 2	0.925	0.186
n = 3	1.318	0.189
n = 4	1.706	0.190
n = 5	2.093	0.190
n = 6	2.478	0.191
n = 7	2.863	0.191
n = 8	3.247	0.191
n = 9	3.632	0.191
n = 10	4.015	0.191
Pole-dipole		
n = 1	0.519	
n = 2	0.925	
n = 3	1.318	
n = 4	1.706	
n = 5	2.093	
n = 6	2.478	
n = 7	2.863	
n = 8	3.247	

The Wenner alpha array : 2-D sensitivity

The plot of the 2-D sensitivity function shows that the sensitivity of an array to 2-D structures at different (x,z) locations. This shows the sensitivity of the array to different types of structures. The sensitivity plot for this array has almost horizontal contours beneath the center of the array. It is relatively sensitive to vertical changes in the subsurface resistivity below the center of the array, but is less sensitive to horizontal changes in the subsurface resistivity. The Wenner is good in resolving vertical changes (horizontal structures), but relatively poor in detecting horizontal changes (narrow vertical structures).

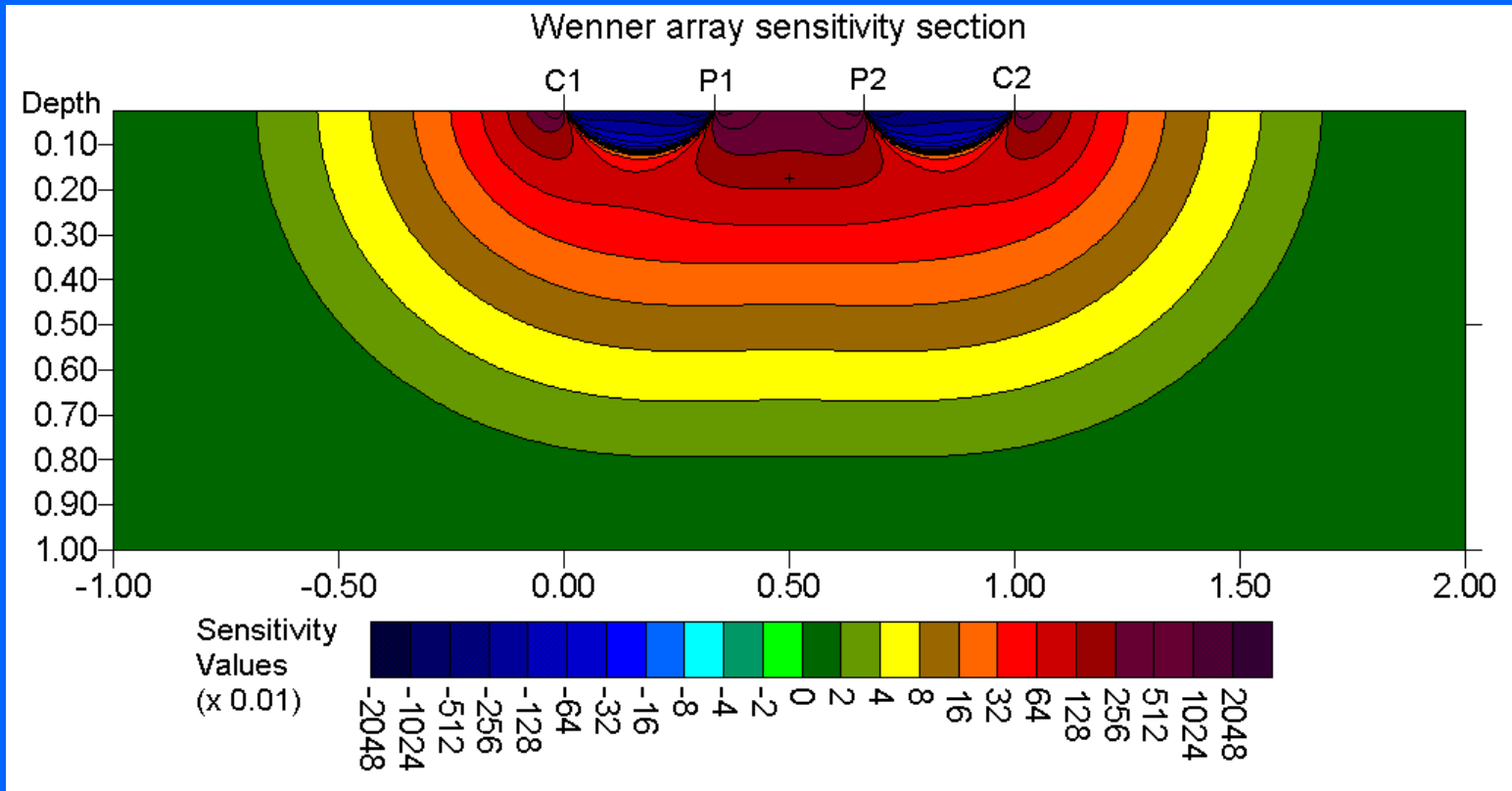

Wenner array – depth of investigation and signal strength

The median depth of investigation for the Wenner Alpha array is approximately 0.5 times the "a" spacing (or one-sixth the array length) used, and this array has a moderate depth of investigation.

Among the common arrays, the Wenner array has the strongest signal strength. This can be an important factor if the survey is carried in areas with high background noise.

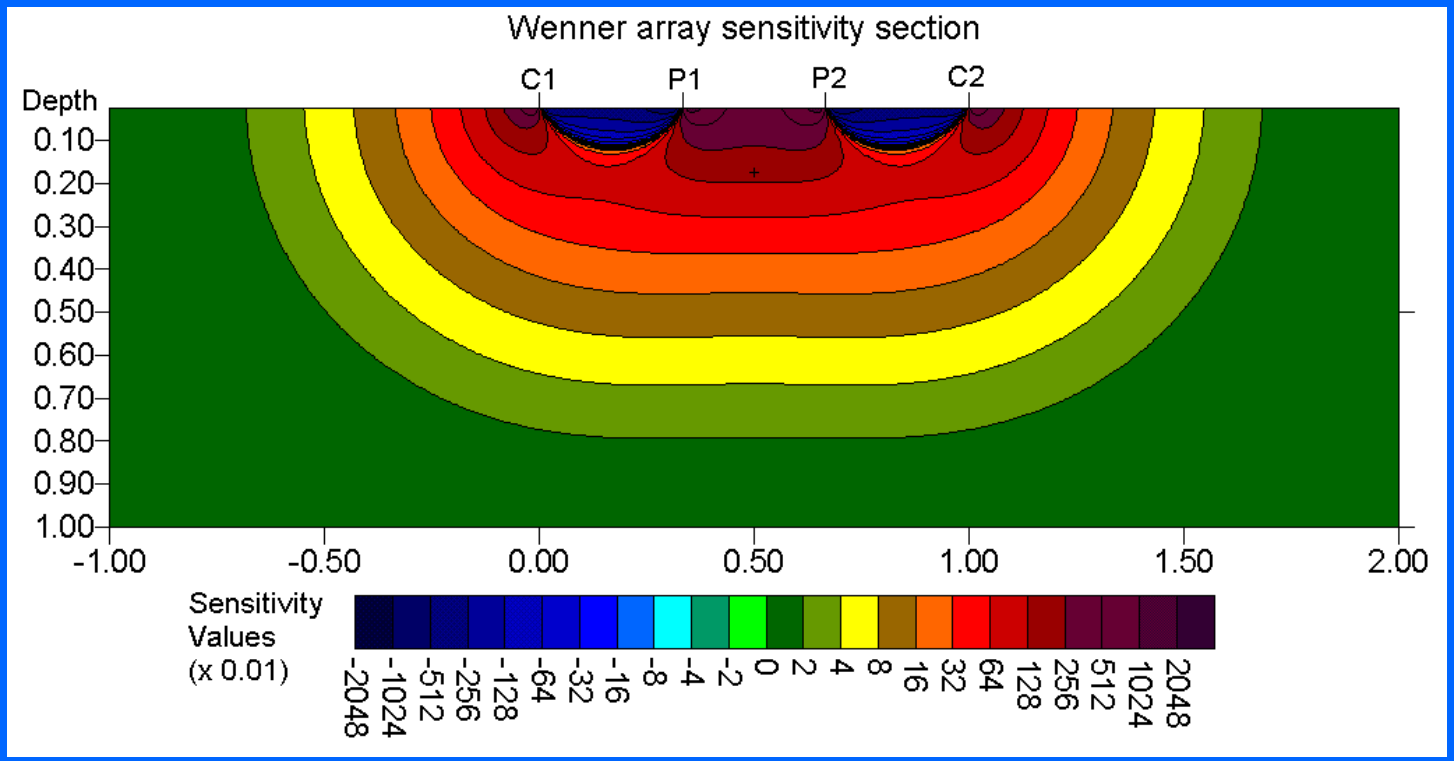

The Wenner alpha array – data coverage

One disadvantage of this array for 2-D surveys is the relatively poor horizontal coverage as the electrode spacing is increased. This could be a problem if you use a system with a relatively small number of nodes. As the 'a' spacing is increased by 1, the number of data points at that data level decreases by 3.

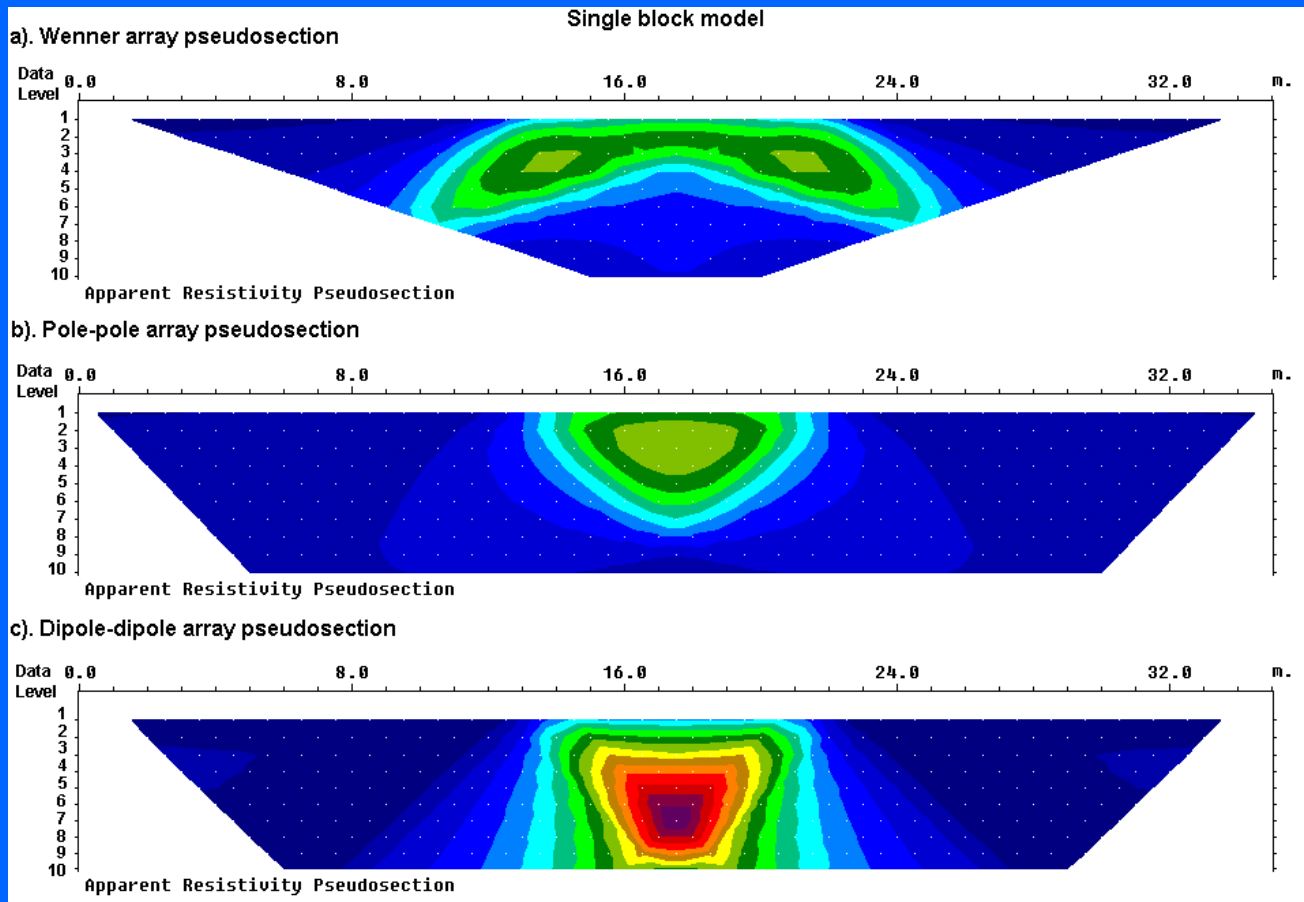

The Wenner-Schlumberger array

This is a combination of the Wenner and Schlumberger arrays. The "n" factor for this array is the ratio of the distance between the C1-P1 (or P2-C2) electrodes to the spacing ("a") between the P1-P2 potential pair.

The median depth of investigation for this array is about 10% larger than that for the Wenner array for the same aray length for large "*n*" values.

The signal strength decreases with n^2. It is weaker than the Wenner array, but higher than the dipole-dipole and pole-dipole arrays. The horizontal data coverage is slightly wider than the Wenner array, but narrower than that obtained with the dipole-dipole and pole-dipole arrays.

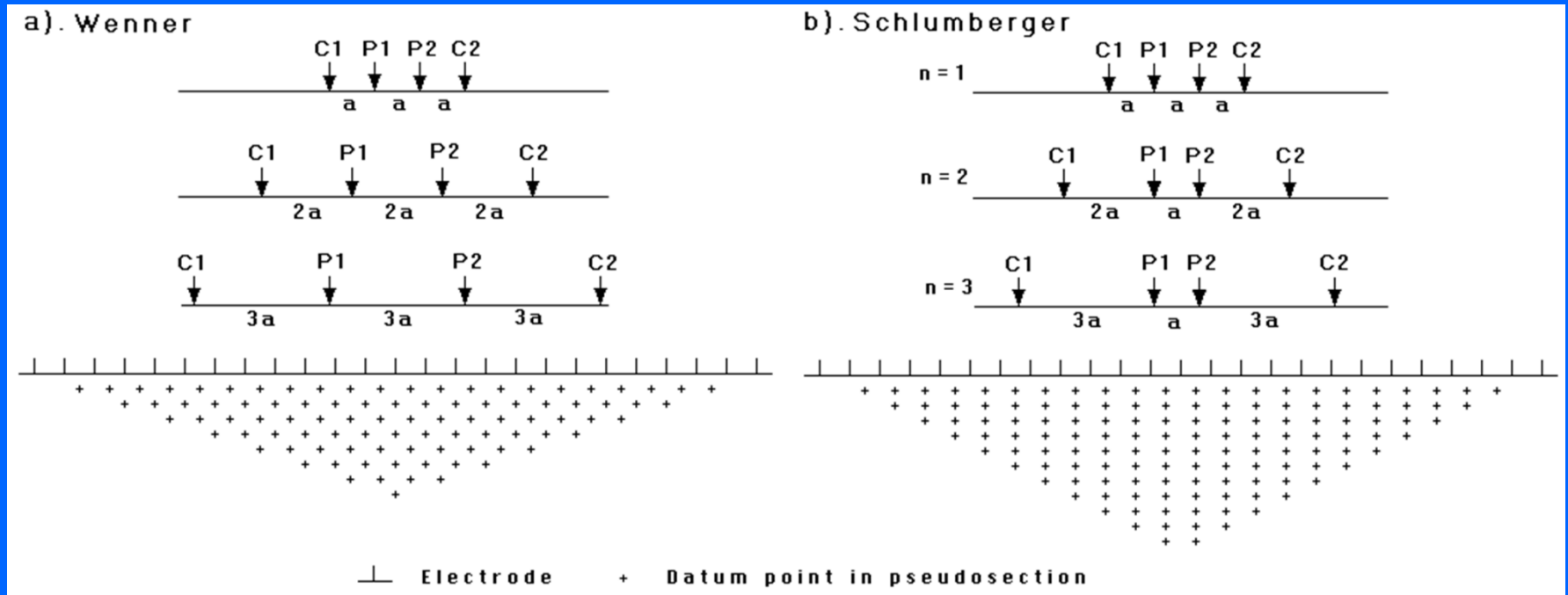

The Wenner-Schlumberger array – sensitivity pattern

The figure shows the sensitivity pattern as the "*n*" factor is increased from 1 (Wenner array) to 6 (the Schlumberger array). The flat sensitivity pattern for low "*n*" values means that this array is moderately sensitive to horizontal structures, and also to vertical structures for high "*n*" values where the pattern is more vertical.

In areas where both types of geological structures are expected, this array might be a good compromise between the Wenner and the dipole-dipole arrays.

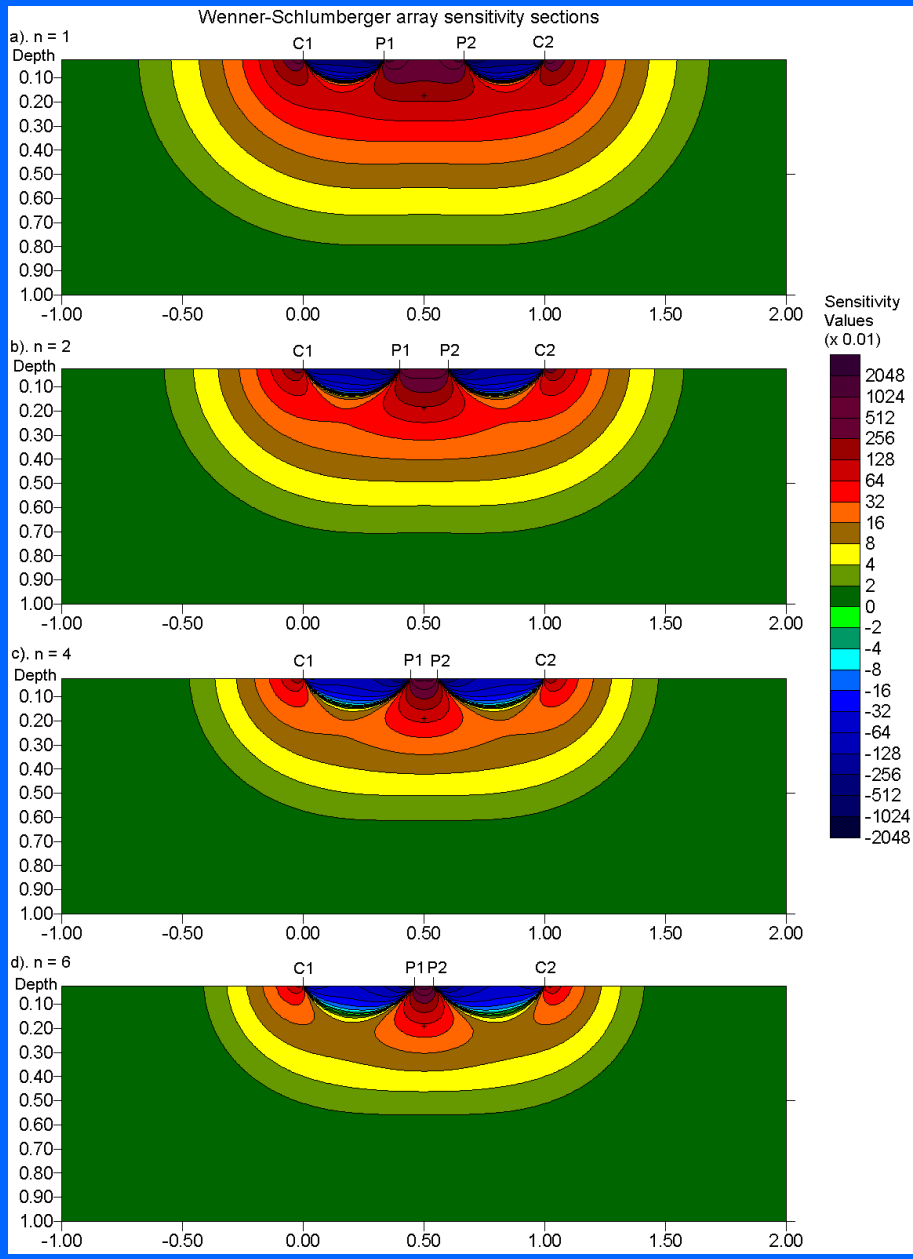

The dipole-dipole array – arrangement

This array is widely used in I.P. surveys because of the low EM coupling between the current and potential circuits. The spacing between the C2-C1 (and P1-P2) electrodes is given as "*a*". The "*n*" factor is the ratio of the C1-P1 distance the dipole length "*a*". For surveys, the "*a*" spacing is initially kept fixed at the smallest unit electrode spacing and the "*n*" factor is increased from 1 to 2 until about 6 to increase the depth of investigation.

One disadvantage of this array is the low signal strength. It decreases with the cube of the "*n*" factor. The voltage measured by the resistivity meter drops by about 56 times when "*n*" is increased from 1 to 6. To overcome this problem, the "*a*" spacing between the C1-C2 (and P1-P2) dipole pair can be increased. The two different arrangements for the dipole-dipole array with the same array length but with different "*a*" and "*n*" factors. The signal strength of the array with the smaller "*n*" factor is about 28 times stronger than the one with the larger "*n*" factor.

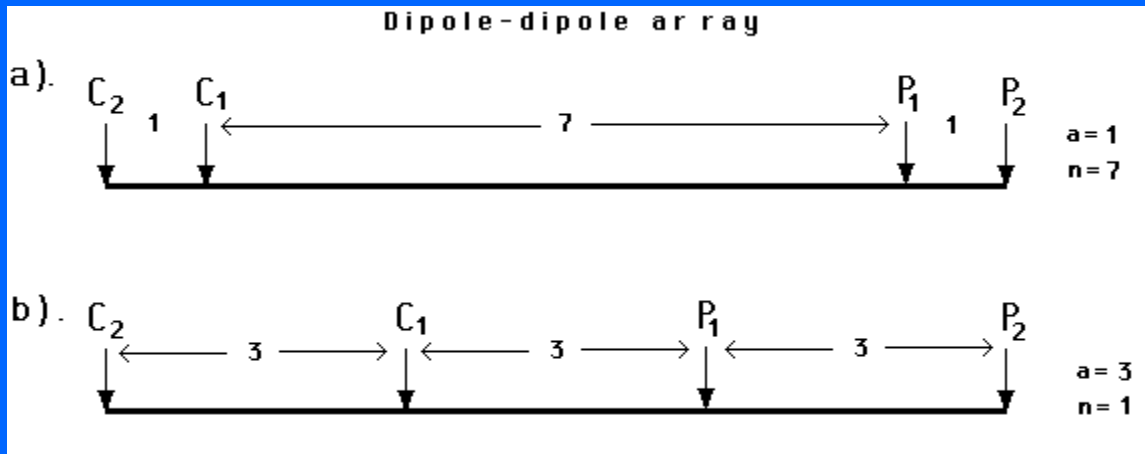

The dipole-dipole array – sensitivity pattern

The figure shows the sensitivity sections for this array for "*n*" values of 1 to 6.

The largest sensitivity values are generally located between the C1-C2 dipole pair, and also between the P1-P2 pair. This means that this array is most sensitive to resistivity changes below each dipole pair.

As the "*n*" factor is increased, the high sensitivity values become increasingly more concentrated beneath the C1-C2 and P1-P2 dipoles, while the sensitivity values beneath the center of the array between the C1-P1 electrodes decreases.

For "*n*" values of greater than 2, the sensitivity values at the pseudosection data plotting point becomes negligible. The sensitivity contour pattern becomes almost vertical for "*n*" values greater than 4.

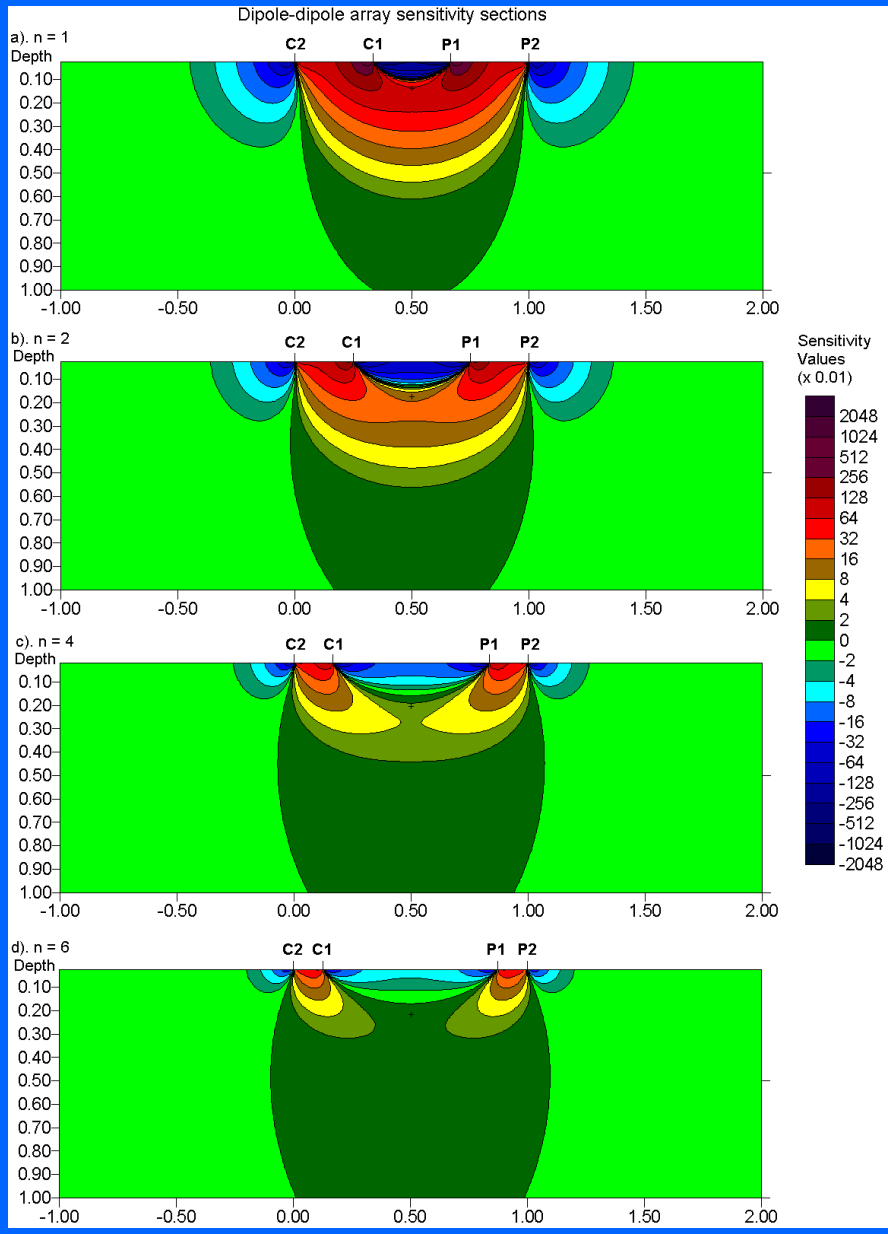

The dipole-dipole array – sensitivity to structures

Due to the almost vertical sensitivity pattern, this array is very sensitive to horizontal changes in resistivity, but relatively insensitive to vertical changes in the resistivity. That means that it is good in mapping vertical structures, such as dykes and cavities, but poorer in mapping horizontal structures such as sedimentary layers.

The depth of investigation of this array depends on both the "*a*" spacing and the "*n*" factor. For "*n*" larger than 3, the depth of investigation is approximately 20% of the array length. Due to the almost vertical pattern of the sensitivity contours, the median depth of investigation might underestimate the depth of structures sensed by this array by about 20% to 30% for large "*n*" factors.

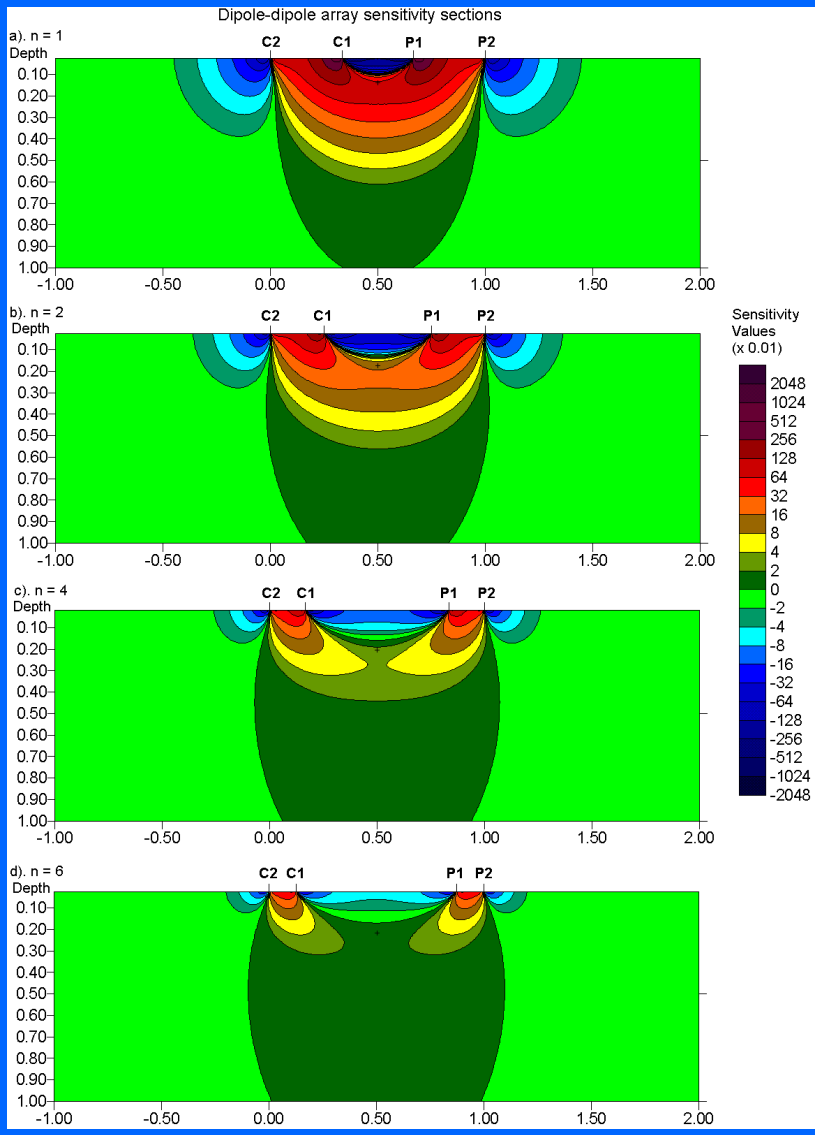

The dipole-dipole array – data coverage and usage

This array has better horizontal data coverage than the Wenner. This can be an important advantage when the number of nodes available with the multi-electrode system is small.

To use this array and there should be good contact between the electrodes and the ground to reduce the contact resistance. A higher current output can be used to partially offset the drop in the voltage due to the high geometric factor.

This array has been successfully used in many areas to detect structures such as cavities where the good horizontal resolution of this array is a major advantage.

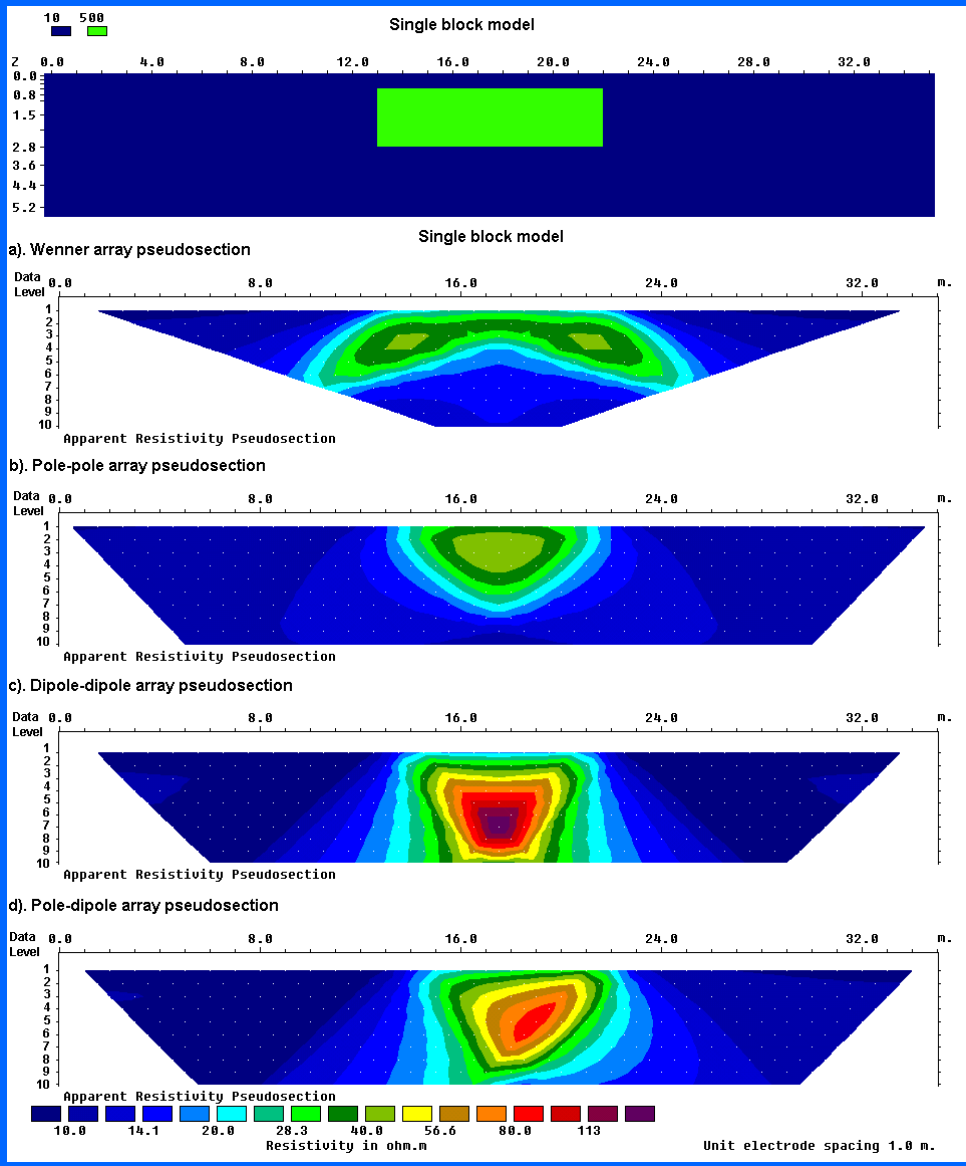

The pole-dipole array – electrode arrangement

The pole-dipole array is an asymmetrical array. The pole-dipole array requires a remote electrode, the C2 electrode, which must be placed sufficiently far from the survey line (at least 5 times the maximum C1-P1 distance used).

Over symmetrical structures the apparent resistivity anomalies in the pseudosection are asymmetrical, which could influence the inversion model. To remove the asymmetry, measurements are repeated with the electrodes arranged in the reverse manner. By combining the measurements with the "forward" and "reverse" pole-dipole arrays, any bias in the model due to the asymmetrical nature of this array would be removed. This will double the number of data points but it is not a significant problem with multi-channel instruments.

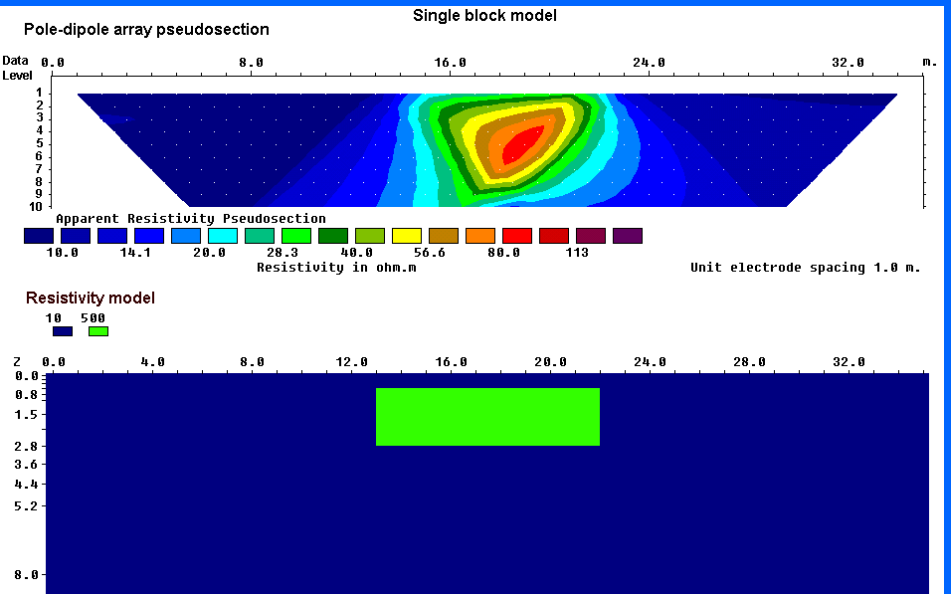

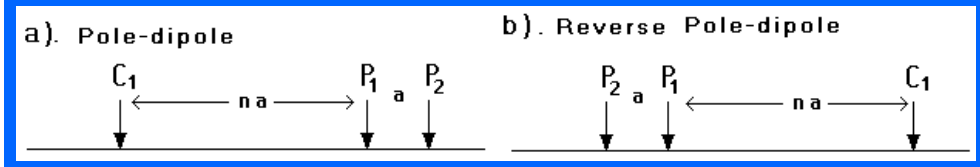

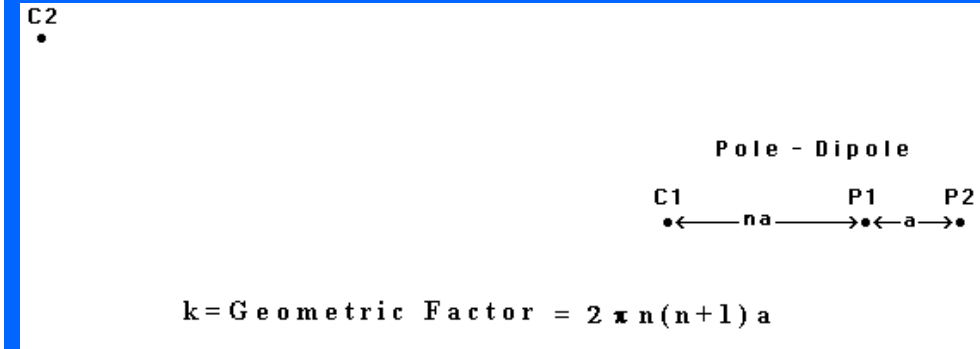

The pole-dipole array – sensitivity pattern

The areas with the greatest sensitivity lies beneath P1-P2 dipole pair, particularly for large "*n*" factors. For "*n*" values of 4 and higher, the high positive sensitive region beneath the P1-P2 dipole becomes increasingly vertical. Thus this array is more sensitive to vertical structures, particularly below the P1-P2 potential dipole.

For very large '*n*' factors, the array becomes very sensitive to near surface features between the P1-P2 electrodes, and less sensitive to deeper structures. This means beyond a certain limit, the effective depth of investigation actually decreases with increasing '*n*'.

One result is that the '*n*' factor used in a field survey should not exceed 8.

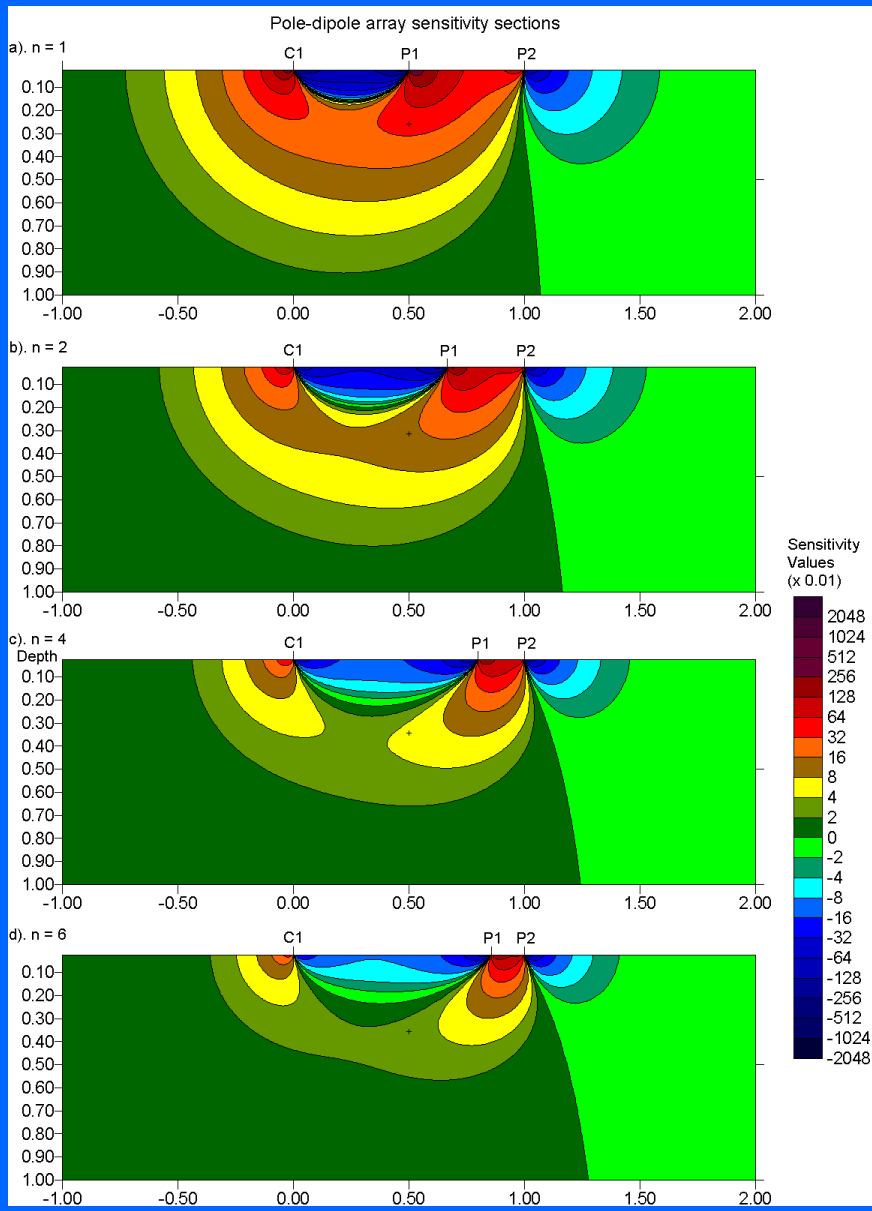

The pole-dipole array – depth and signal strength

The signal strength for the pole-dipole array decreases with the *square* of the "*n*" factor. The maximum "*n*" value used should not exceed 8. Beyond this, the "*a*" spacing between the P1-P2 dipole pair should be increased to obtain a stronger signal strength.

The signal strength is lower compared with the Wenner and Wenner-Schlumberger arrays but higher than the dipole-dipole array. The depth of investigation is about 30% of the C1 to P2 distance.

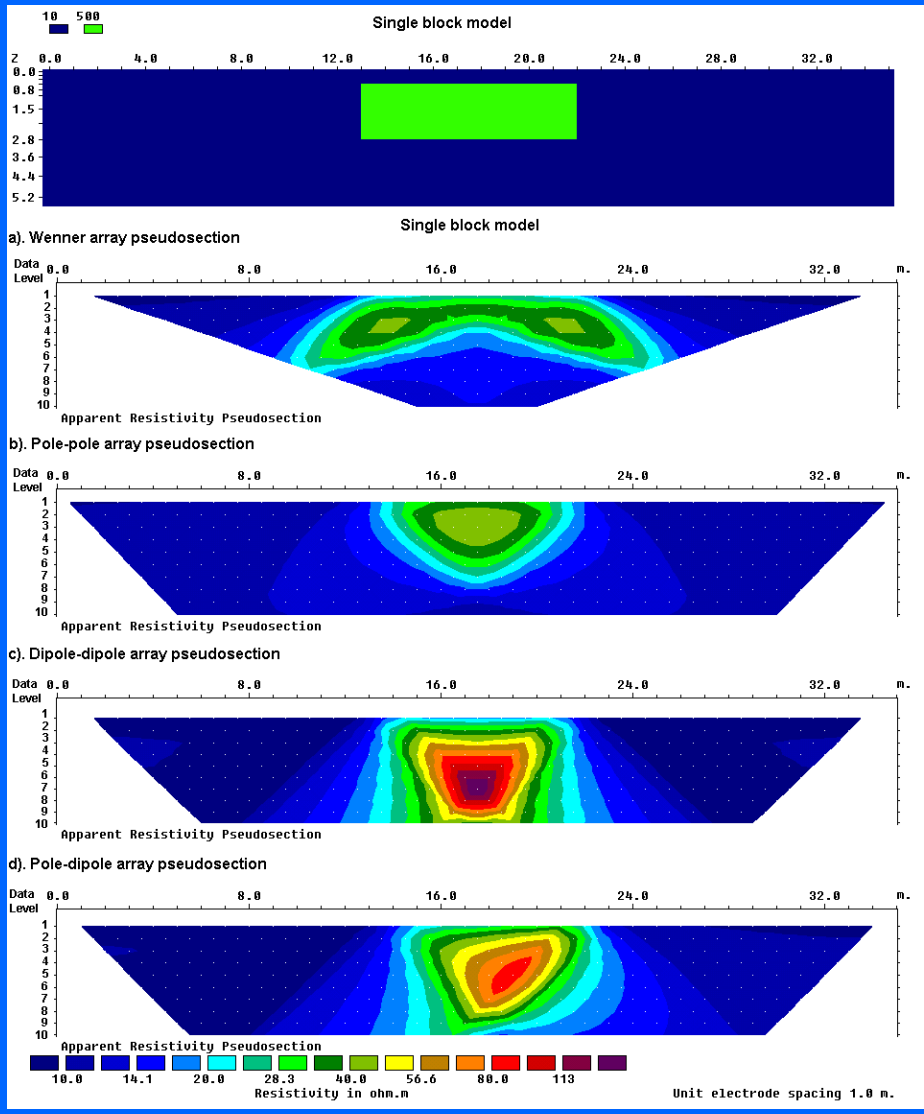

The multiple gradient array array

This is a relatively new array developed primary for multi-channel resistivity meter systems. In the multiple gradient array, different sets of measurements are made with the potential electrodes at different locations for the same current electrodes. As an example, for a system with 32 electrodes, one set of measurements can be made with the current electrodes at nodes 1 and 32. Next, another series of measurements are made with the current electrodes at nodes 1 and 16, as well as another with the current electrodes at 16 and 32. A similar set of measurements can be made with the C1-C2 electrodes at 1-8, 8-16, 16-24 and 2-32. This can be repeated using smaller distances between the current electrodes.

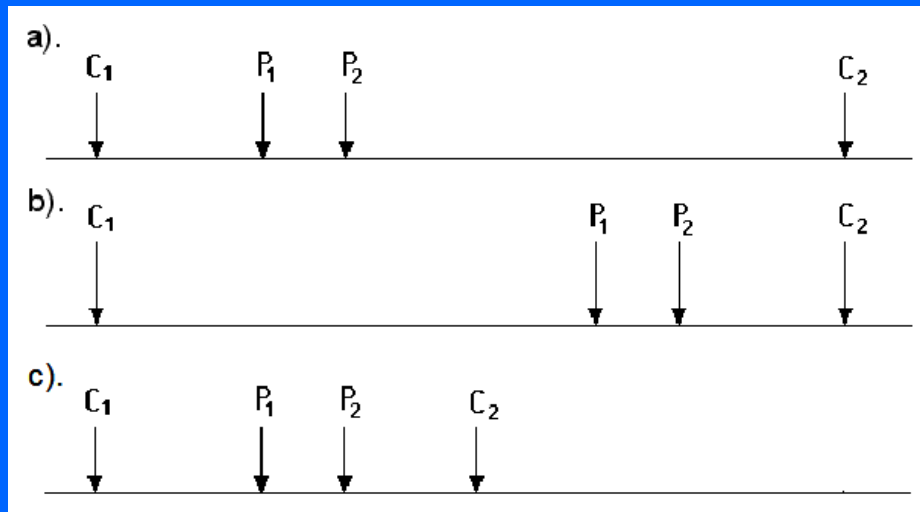

The gradient array array - sensitivity

The figure shows sensitivity sections with the same positions of the C1-C2 current electrodes, but with the potential dipole P1-P2 being moved from the center to one end of the array. The sensitivity contour pattern slowly changes from a Wenner-Schlumberger pattern towards the pole-dipole pattern as the potential dipole moves closer to the current electrode at one end of the array. The results obtained by this array is comparable to those obtained by the Wenner-Schlumberger and pole-dipole arrays, but generally has better signal strength.

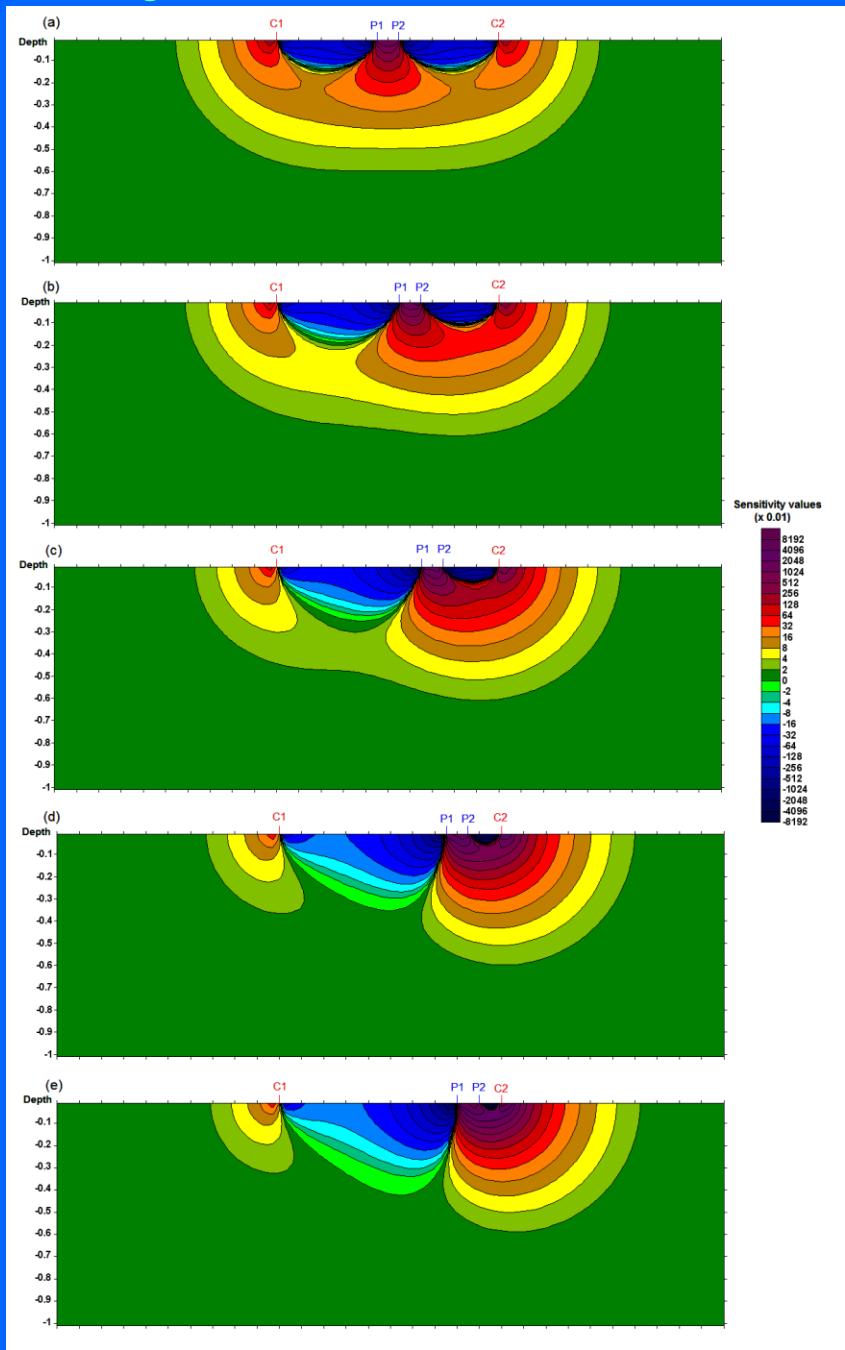

The multiple gradient array array - example

The figure shows the data from a survey using a multiple gradient array was carried out by Aarhus University for the Danish Road and Highway Association. A plot of this data set in the form of profiles is also shown. This array is popular with the new multi-channel instruments. It allows a number of readings to be taken simultaneously with the same current electrodes positions, but gives a stronger signal strength compared to the dipole-dipole and pole-dipole arrays.

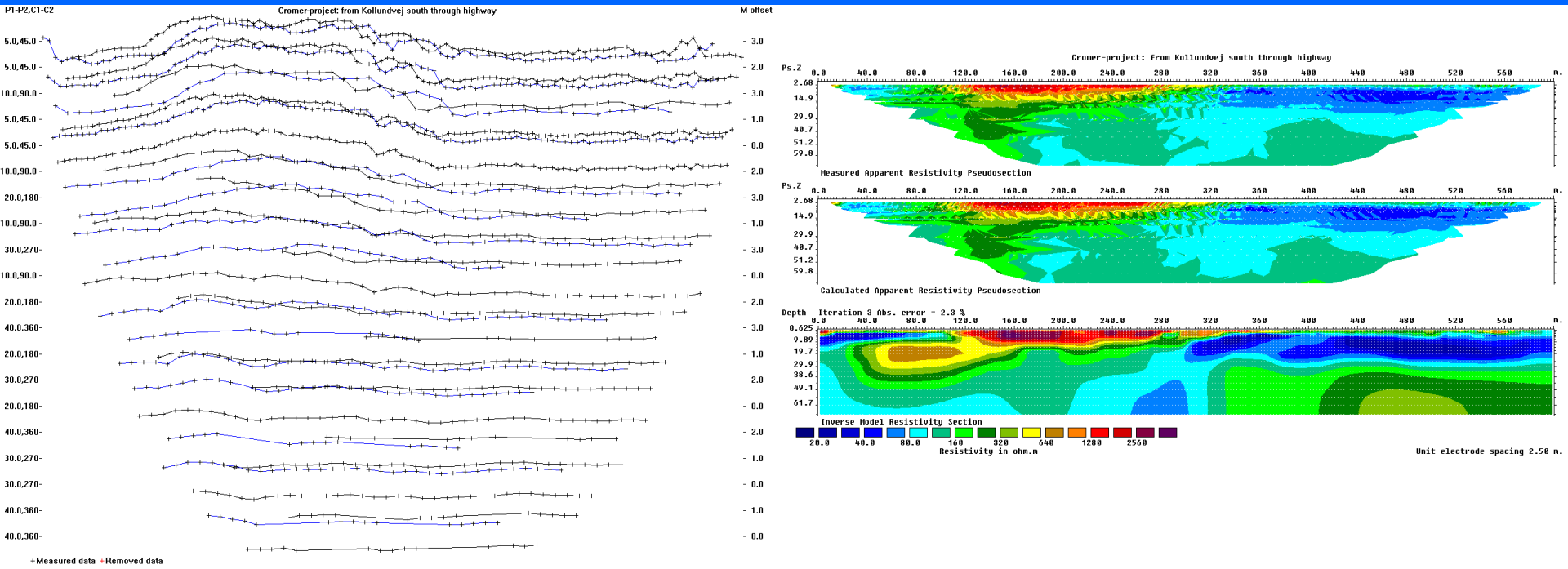

The pole-pole array – arrangement

In practice the ideal pole-pole array, with only one current and one potential electrode, does not exist. To approximate the pole-pole array, the second current and potential electrodes (C2 and P2) must be placed at a distance that is more than 20 times the maximum separation between C1 and P1 electrodes used in the survey. When the inter-electrode spacing along the survey line is more than a few meters, finding suitable locations for the C2 and P2 electrodes to satisfy this requirement could be a major task.

Another possible disadvantage of this array is that because of the large distance between the P1 and P2 electrodes, it is can pick up a large amount of telluric noise (particularly near urban areas) that can severely degrade the quality of the measurements.

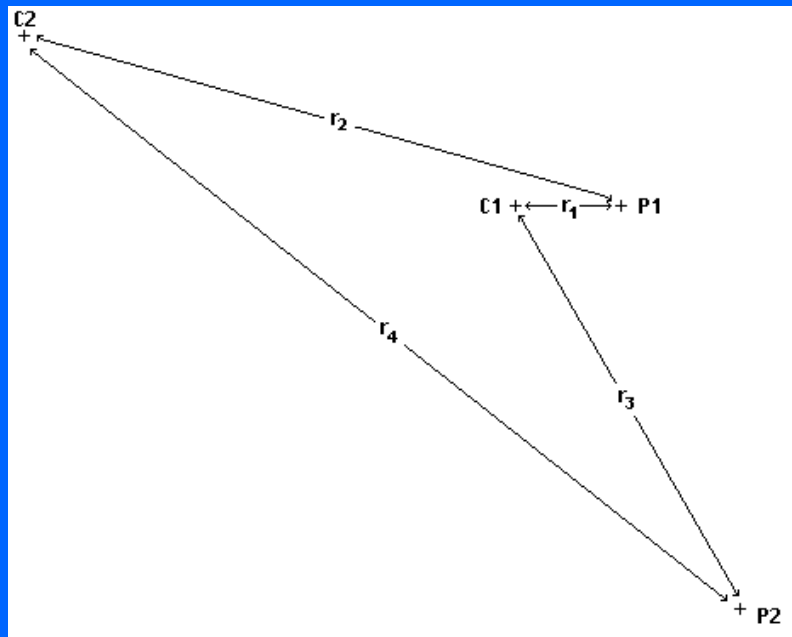

The Pole-pole array – sensitivity pattern

This array is commonly used in surveys where small electrode spacings (less than a few meters) are used, such as archaeological surveys. This array has the widest horizontal coverage and the deepest depth of investigation. However, it has the poorest resolution, which is reflected by the comparatively large spacing between the contours in the sensitivity function plot.

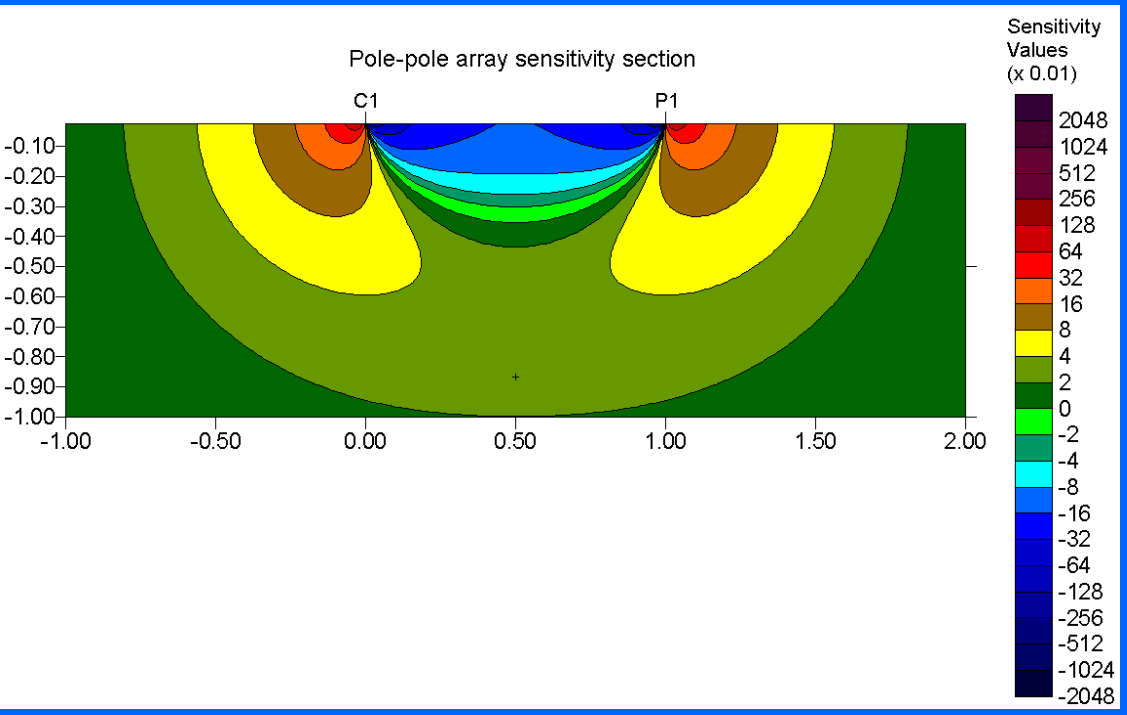

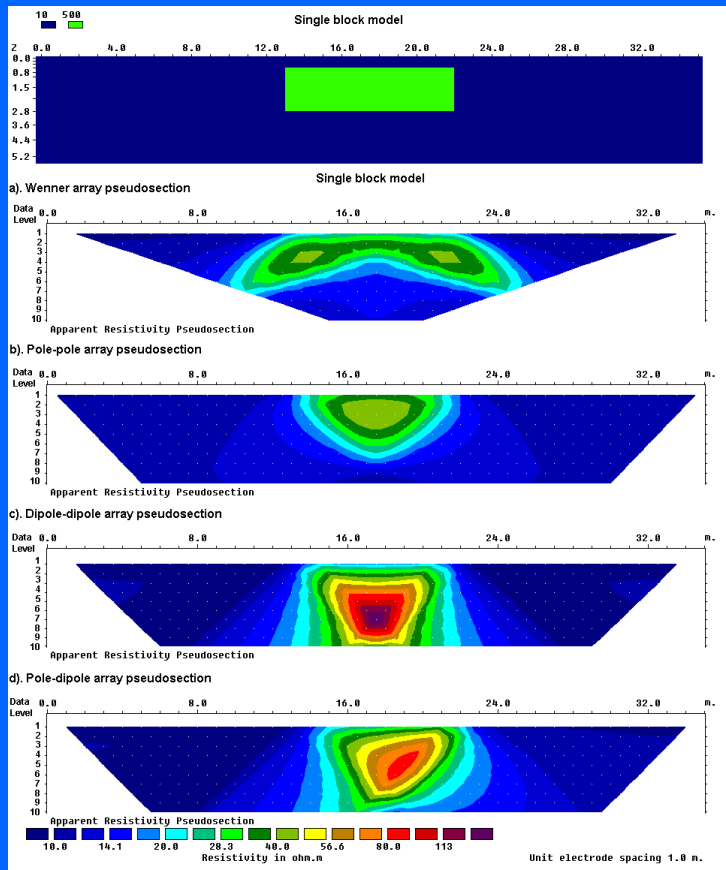

Pole-pole array field example

Despite the potential problems, this arrays has been used in mineral exploration surveys. Below is an example from Peru where an IP survey was conducted to map mining wastes containing metallic sulphides using a 10 m. electrode spacing.

The success of the survey was partly due to the low telluric noise because of the remote location of the site from possible cultural EM noise.

Due to its large depth of investigation compared to the survey line length, it is an attractive alternative in remote areas.

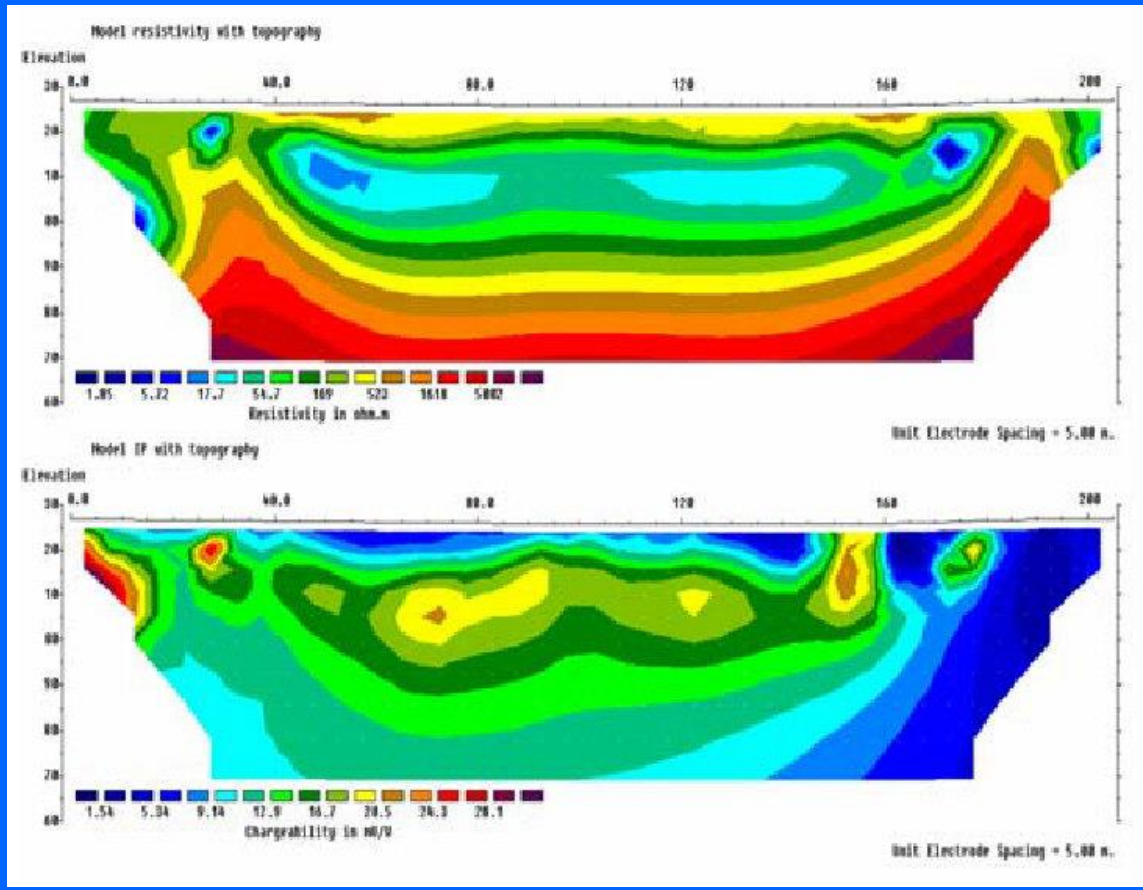

Perfiles, Nov. 2005, Arce-Geophysics, Peru.

Summary of array types

The Wenner array is an attractive choice for a survey carried out in a noisy area (due to its high signal strength) and also if good vertical resolution is required.

The Wenner-Schlumberger array is a reasonable alternative if both good horizontal and vertical resolutions are needed, particularly if good signal strength is also required.

The multiple-gradient array is useful with multi-channel systems.

The dipole-dipole array might be a more suitable choice if good horizontal resolution and data coverage is important (assuming your resistivity meter is sufficiently sensitive and there is good ground contact).

Summary of array types continued

If you have a system with a limited number of electrodes, the **pole-dipole** array with measurements in both the forward and reverse directions might be a suitable choice. It is an alternative to the dipole-dipole for I.P. surveys.

For surveys with small electrode spacings and require a good horizontal coverage, the **pole-pole** array might be a suitable choice. In remote arrays with low cultural noise, it has been used with very large spacings due to its large depth of investigation.

The new multi-electrode systems has modified the criteria for array choice. The arrays that are used are the **dipole-dipole, pole-dipole, pole-pole, reverse Wenner-Schlumberger** and **multiple gradient.**

High resolution surveys with overlapping data levels

The Wenner-Schlumberger, dipole-dipole and pole-dipole arrays have 2 parameters, the '*a*' spacing between the potential electrodes and an '*n*' factor.

A dipole-dipole array with a "*a*" spacing of 10m and "*n*" of 7 will have the same length as an array with *a=30m* and *n=1*. However, the array with n=1 will have a signal strength that is 28 times larger than the array with n=7.

The two dipole-dipole arrays have sensitivity patterns that are also very different. The array with *n=7* will be very sensitive to vertical structures below the C1-C2 and P1-P2 dipoles, while the other array will be more sensitive to deeper structures below the entire array. To make use of both features, a "high-resolution" survey technique can be used by combining measurements with different "*a*" and "*n*" values to give overlapping data levels.

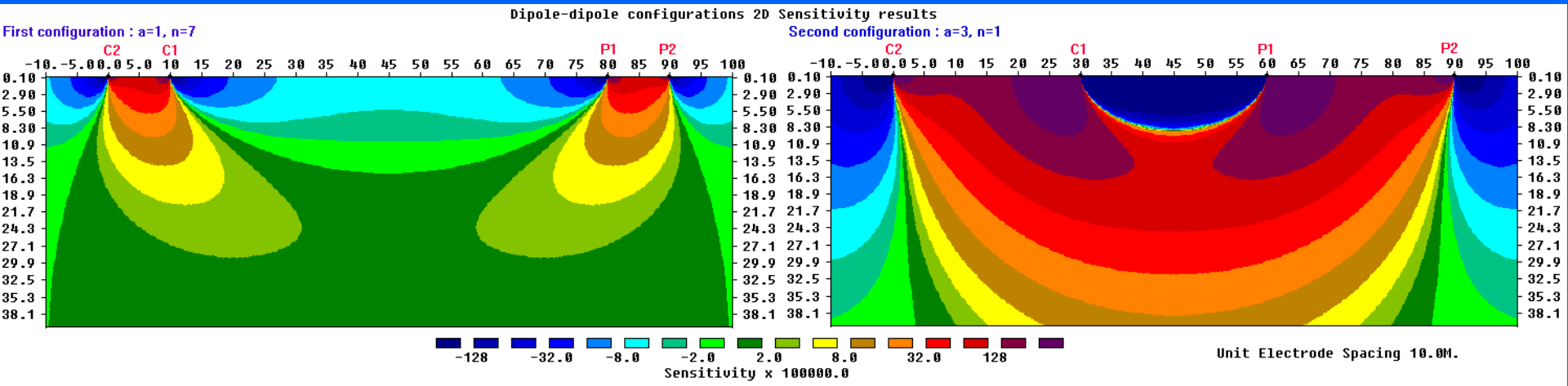

High resolution survey example

The figure shows the apparent resistivity pseudosection for the dipole–dipole array using overlapping data levels over a rectangular prism. Values of 1 to 3 metres are used for the dipole length '*a*', and the dipole separation factor '*n*' varies from 1 to 5.

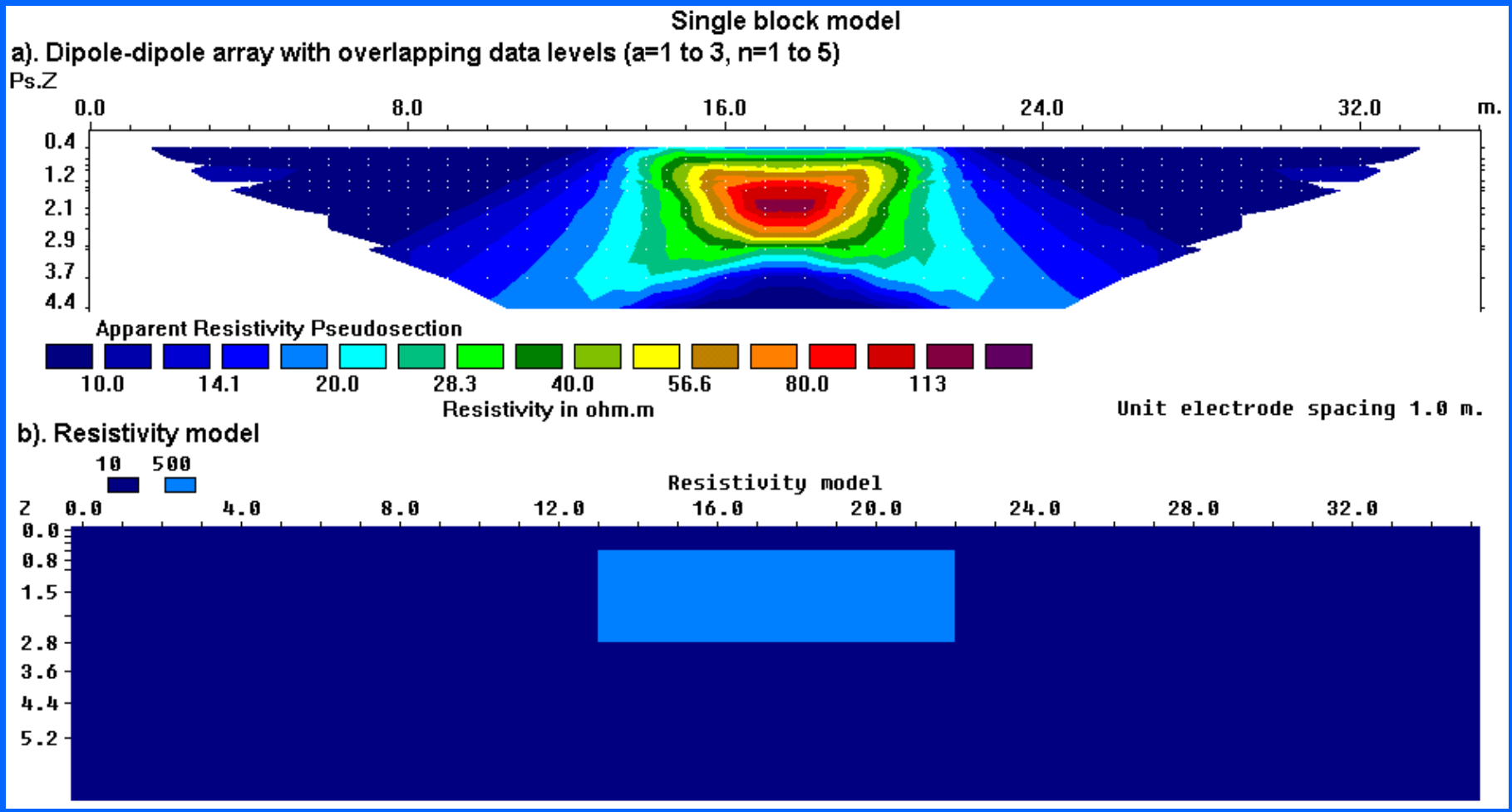

Inversion model settings

Settings that control the subdivision of the subsurface into model cells, and how they affect the inversion results.

1). Trapezoidal versus extended model sections

2). Model cell width

3). Topography modeling

Trapezoidal and extended models

This controls the lateral extent of the model cells in the model. The two options are (i) use a distribution similar to the data points in the pseudosection, (ii) use an extended distribution that extends to the ends of the survey line.

The present preference is to use a uniform extended distribution, and use the model resolution section as a guide to highlight areas that are well constrained by the data. The pseudosection provides an approximate but crude guide to the lateral information in the data set, so using the trapezoidal shape might place too severe limits on the lateral extent of the model.

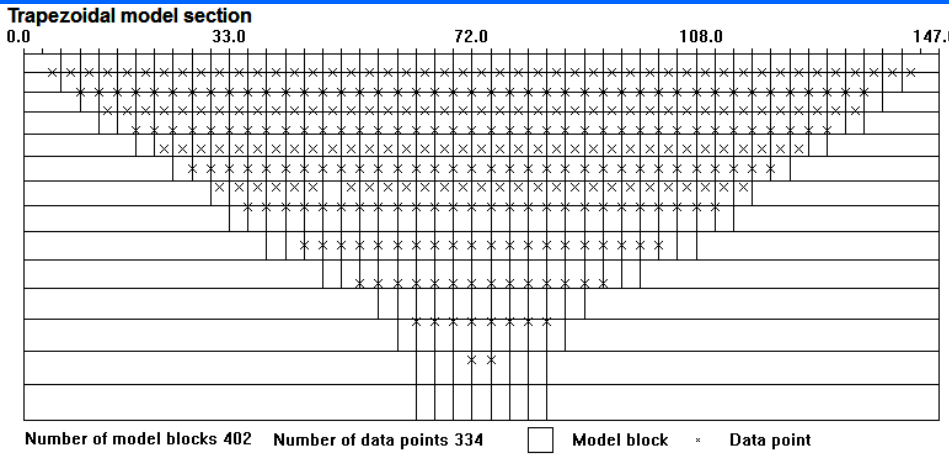

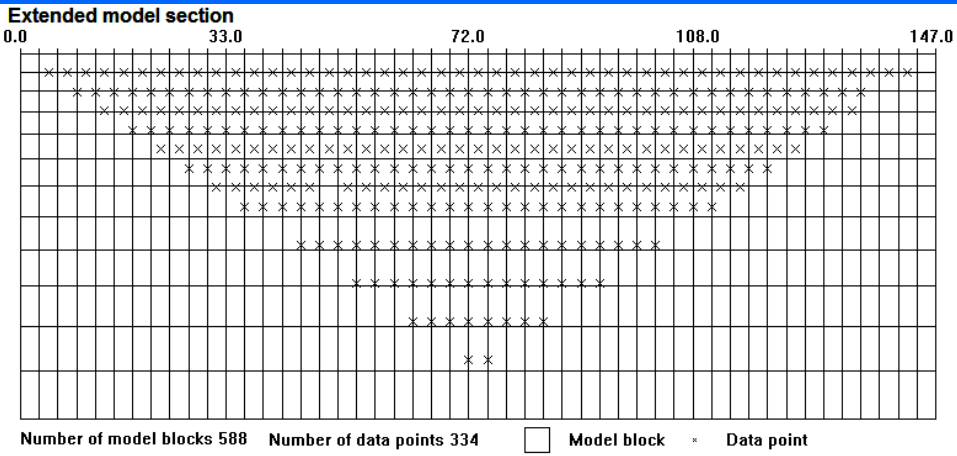

Trapezoidal and extended models - example

The example below is from a dipole-dipole survey over a water-bearing fracture zone that occurs below the middle of the survey line. The trapezoidal model section (b) does not show the sides of the fracture zone clearly as they occur near the edges of the model section. They are more clearly shown in the extended model section (c). The model resolution section (d) shows there is significant information at depth below the 160 to 320 m. marks.

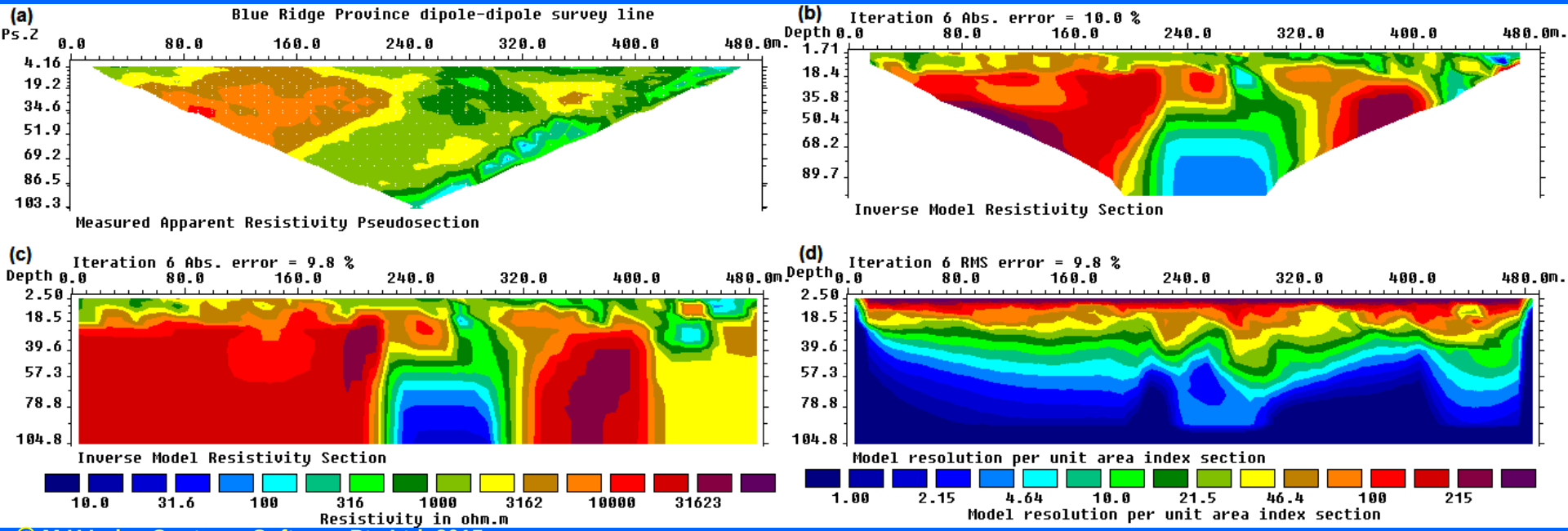

MODEL DISCRETIZATION – Effect of model cell width

The default model uses model cells with the same width as the unit electrode spacing. In situations with large resistivity variations near the ground surface, better results can be obtained by using narrower model cells.

The model with cell width of one electrode spacing has a maximum misfit of one-half the electrode spacing for a near-surface inhomogeneity. The finer model with cell width of half the electrode spacing has a maximum misfit of one-quarter electrode spacing.

In theory, it is possible to reduce the cell width further, but the error due to the misfit becomes increasingly less significant. Reducing the cell width increases the number of model parameters, thus increasing the computer time and memory required.

a). Default model with cell width of one unit electrode spacing

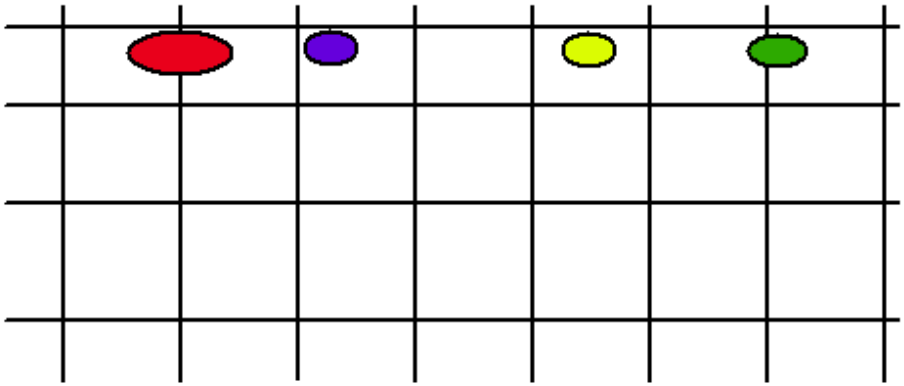

b). Finer model with cell width of one-half unit electrode spacing

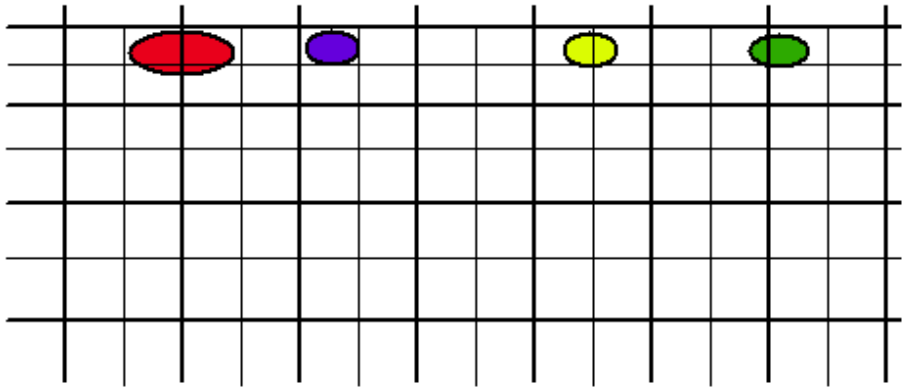

MODEL DISCRETIZATION – Example test model

The main structure is a faulted block of 100 Ω.m and a rectangular prism of 1 ohm.m in a medium of 10 Ω.m. A series of small near-surface high resistivity blocks with widths of 1.0, 0.75, 0.50 and 0.25 m. and resistivity of 300 Ω.m are above the faulted block. A similar series of near-surface low resistivity blocks of 1.0 Ω.m are located on the right.

The pole-dipole array has the P1-P2 spacing ("*a*") fixed at 1.0m, but with "n" factor ranging from 1 to 16. Note the strong anomalies produced by the near-surface inhomogeneties.

The Wenner array is much less affected by the near-surface anomalies.

The reason lies in the sensitivity patterns of the two arrays..

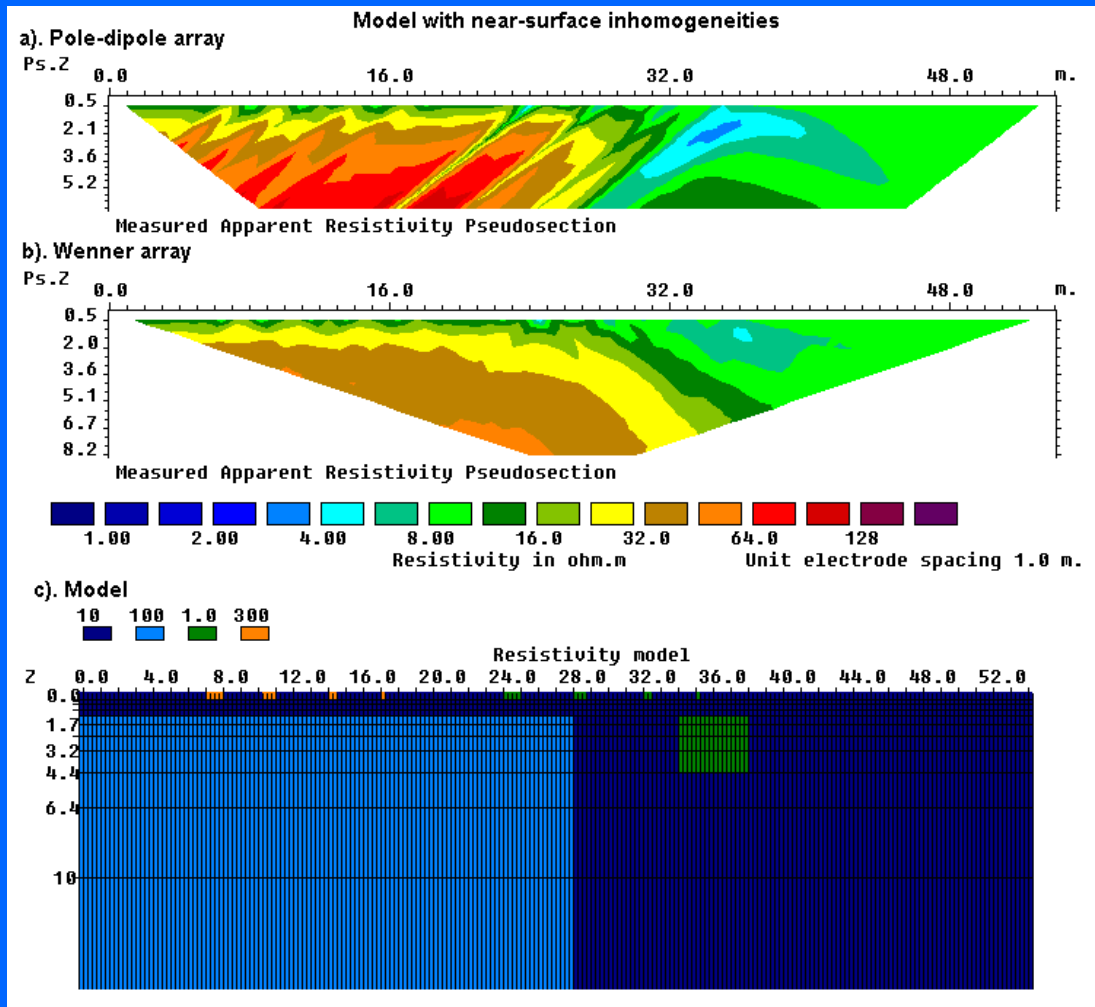

MODEL DISCRETIZATION – Sensitivity sections

The sensitivity sections for the Wenner and pole-dipole arrays with the same array length are shown below. The pole-dipole array has high sensitivity values concentrated below the P1-P2 electrodes. This makes it very sensitive to inhomogeneties below these electrodes. The Wenner array has relatively broad areas near the surface with high sensitivity values that are not as concentrated as the pole-dipole array. Thus it less sensitive to small near surface inhomogeneties.

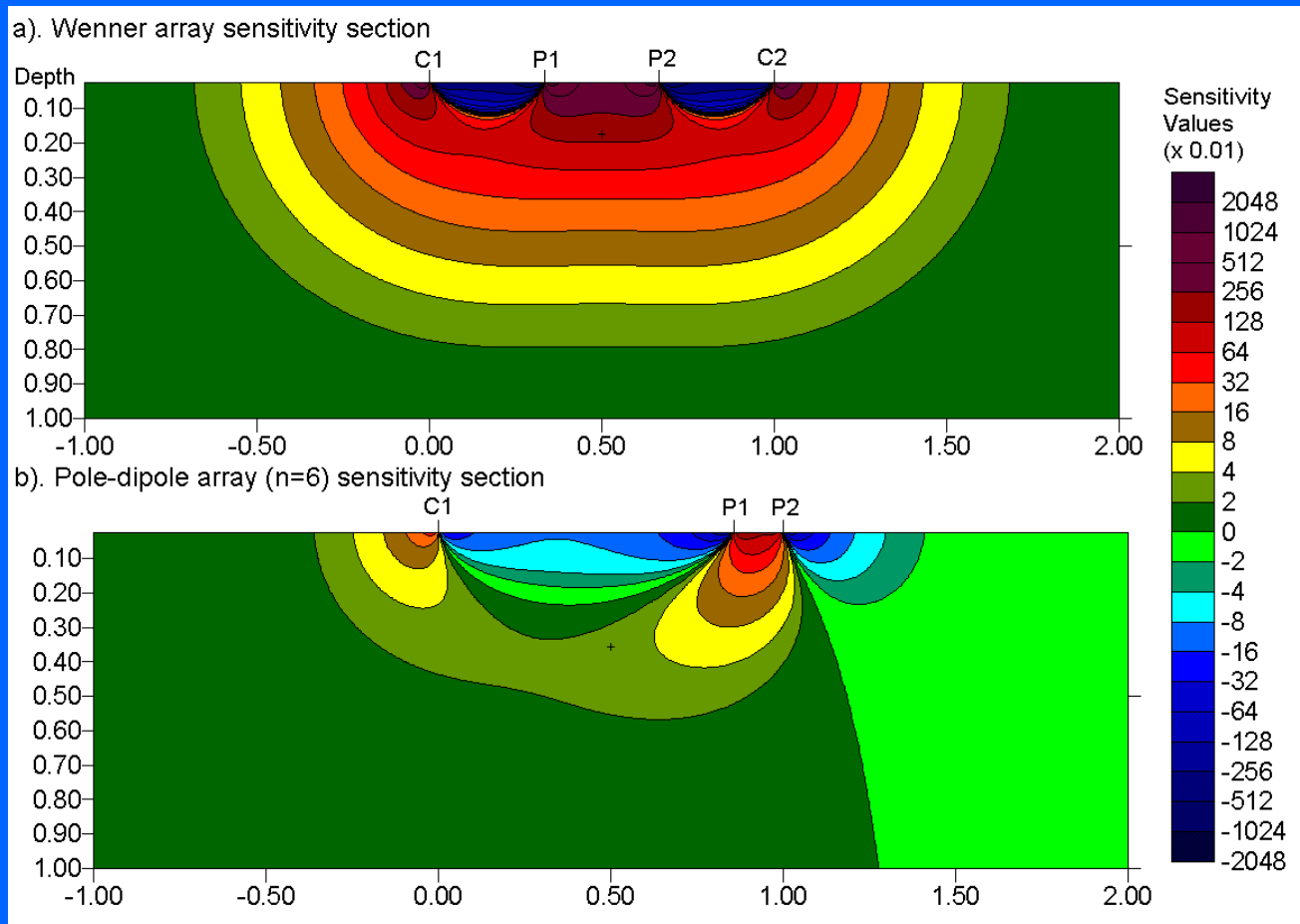

Pole-dipole array model refinement

The model for the pole-dipole array with a cell width of 1.0 m. shows significant distortions near the top of the faulted block. Most of the distortions have been removed in the model with a 0.50 m. cell width.

The model with a 0.25 m. cell width do not show any major improvements over the 0.50 m. cell width model although it should more accurately model the near surface inhomogeneties of less than 0.50 m. width.

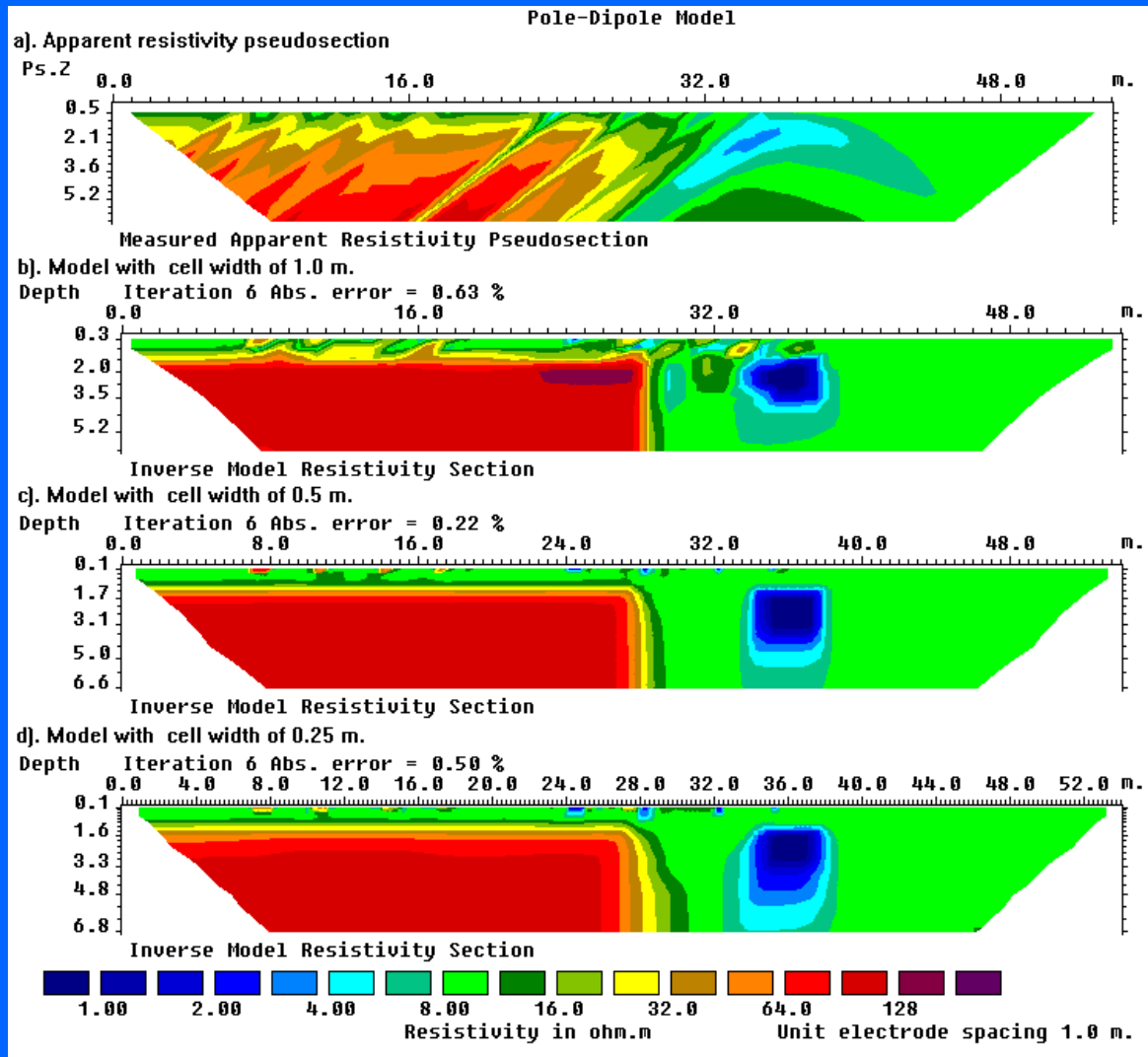

Wenner array model refinement example

The model with a cell width of 1.0 m. shows significant distortions near the top of the faulted block. Note the near-surface high resistivity bodies near the 30 and 33 m. marks near the locations of the low resistivity near-surface inhomogeneties.

Almost all the distortions have been removed in the model with a 0.50 m. cell width.

The model with a 0.25 m. cell width show slightly less distortions on the upper surface of the faulted block.

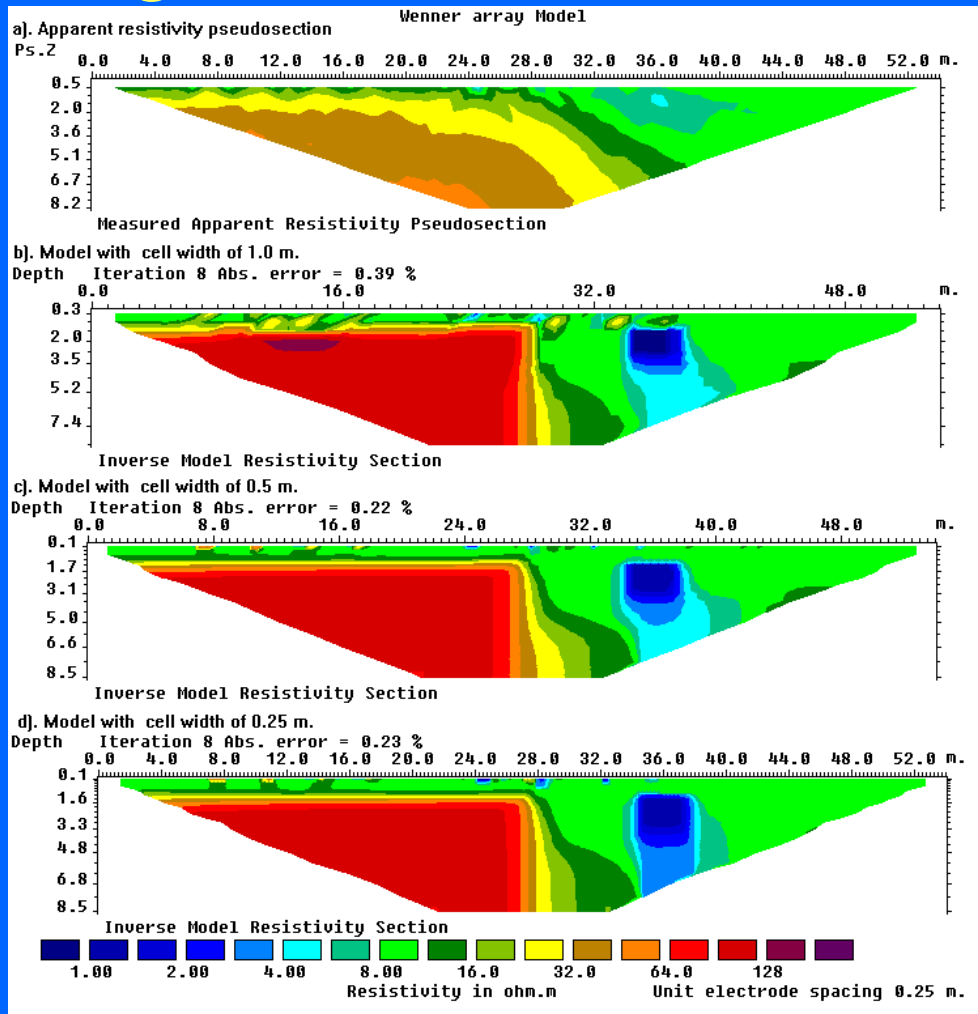

Lateral resolution limit

The pole-dipole and Wenner array models show that reducing the cell width to less than half the unit electrode spacing do not significantly improve the results. The arrays are not sensitive to lateral variations of less than half the '*a*' spacing. We can make use of this property to reduce the time to invert long survey data sets.

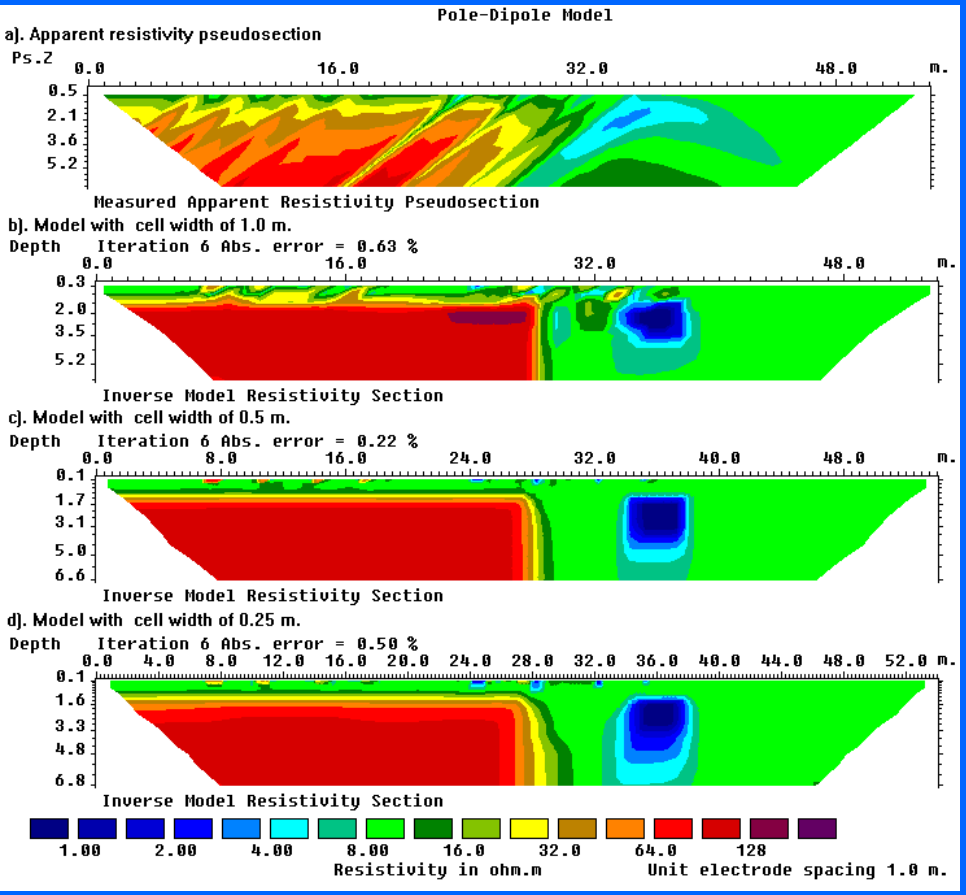

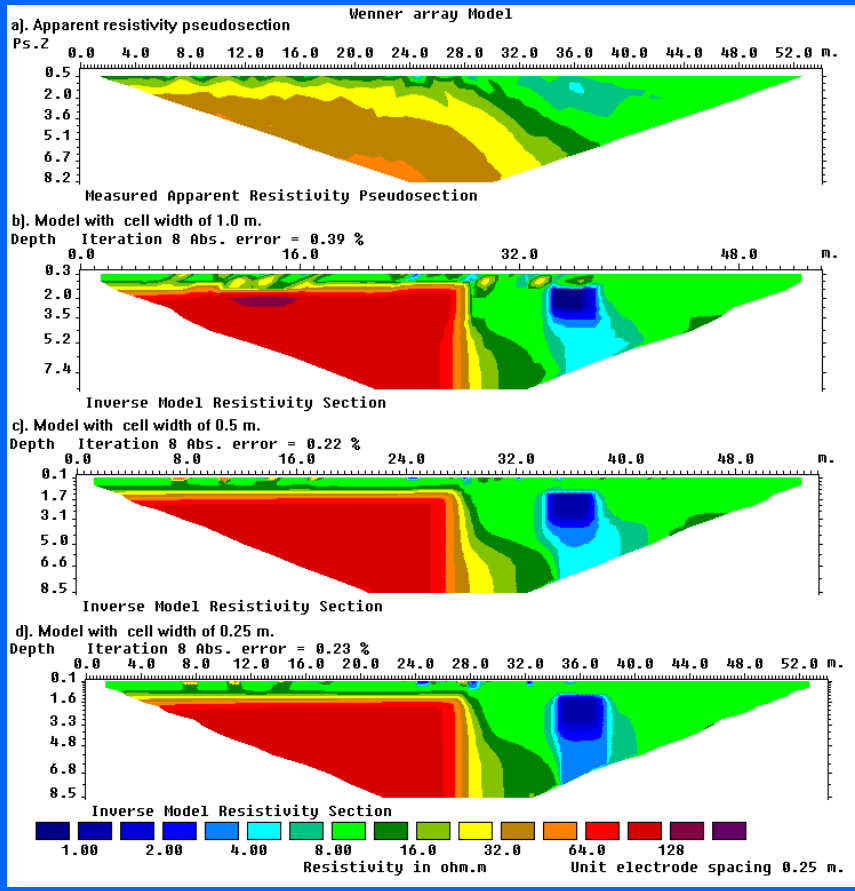

Model Refinement – dipole-dipole field data set example.

The figure shows the models from the Blueridge survey using cell width of 10 m. (the survey electrode spacing) and 5 m. Note the 5 m. cell model has contours that are more regular and structures with the very high resistivity zones near the fracture zone are not present. They are probably caused by a discretization that is too coarse in the 10 m. model that cannot accurately model the large resistivity variations (with widths of less than 10 m) near the surface.

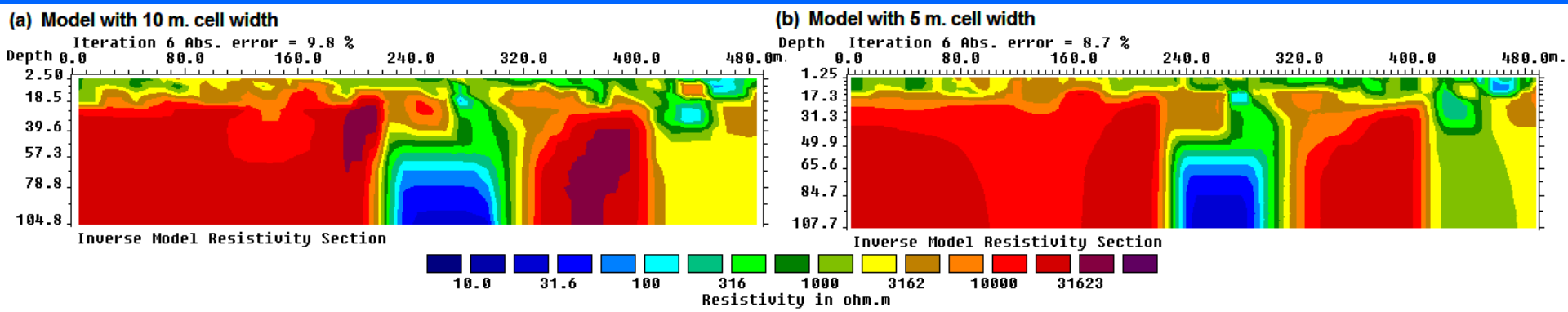

MODEL DISCRETIZATION – General rules

In most cases, using a cell width of half the unit electrode spacing seems to give the optimum results.

Using a cell width of one-third the unit spacing seems to be beneficial only a certain cases with the pole-dipole and dipole-dipole arrays with very large '*n*' values.

A cell width of one-quarter the unit spacing sometimes leads to instability with oscillating model values.

Using finer cells will lead to longer inversion times, so using a width of the half the unit spacing seems to provide the best trade-off. The resistivity method is unlikely to resolve structures less than one-third the '*a*' spacing of the array used. Mobile surveys frequently take consecutive readings with a fixed streamer at positions less than the '*a*' spacing. By combining readings that are less than one-third '*a*' distance apart, the number of readings and electrode positions can be reduced without affecting the results.

Methods to handle topography

The RES2DINV program has three different methods to incorporate the topography into the inversion model. In all these methods, the surface nodes of the mesh are shifted up or down so that they match the actual topography. The topography becomes part of the mesh and is automatically included into the inversion model. The difference between these three methods is the way the subsurface nodes are shifted.

The simplest method is to shift all the subsurface nodes by the same amount as the surface node along the same vertical mesh line. This is probably acceptable for cases with a small to moderate topographic variations. The disadvantage is that every bend in the surface topography is reproduced in all the layers.

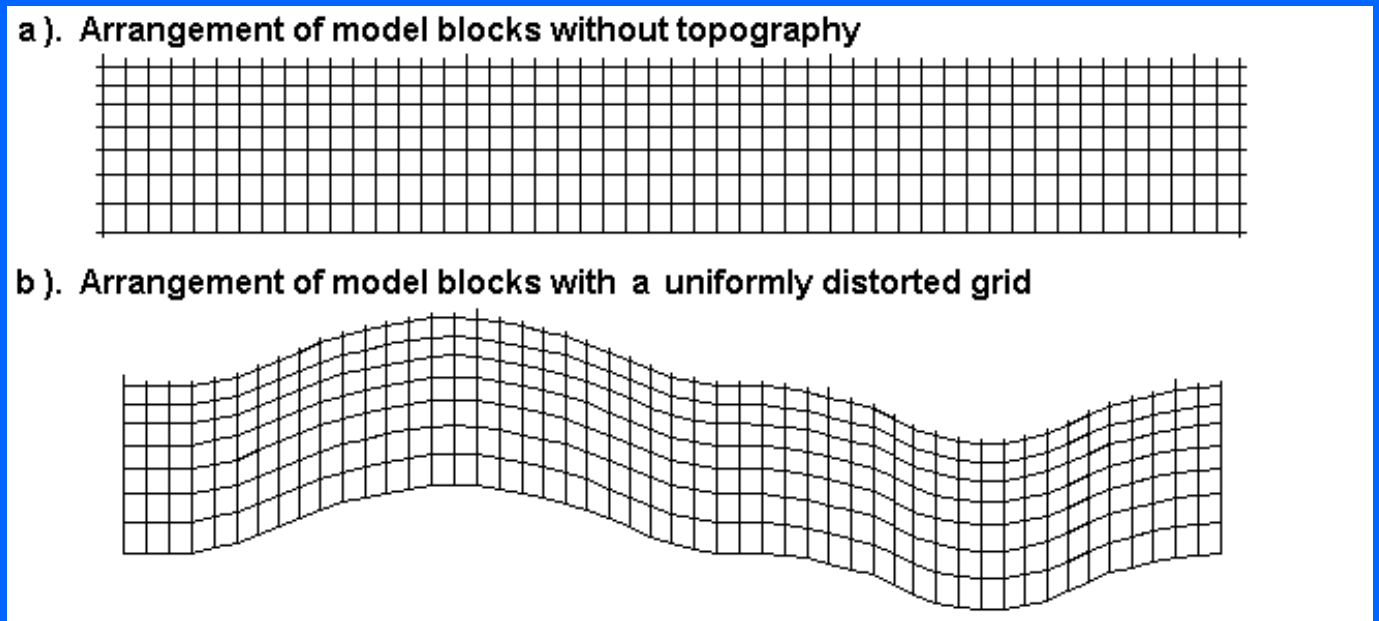

Methods to handle topography – damped grid

In the second method, the amount the subsurface nodes are shifted is reduced exponentially with depth. This is because the effect of the topography decreases with depth. One disadvantage of this method is that it sometimes produces a model that is too thick where the topography curves upwards, and too thin where it curves downwards. The inverse Schwartz-Christoffel transformation method is used to calculate the amount to shift the subsurface nodes. This method takes into account the curvature of the surface topography and usually produces a more "natural" looking model section.

c). Arrangement of model blocks with a moderately damped distorted grid

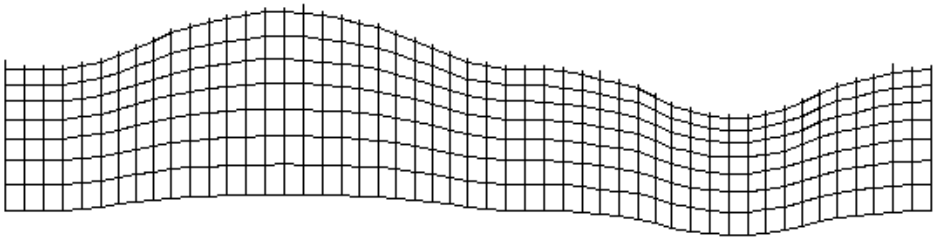

d). Arrangement of model blocks with a highly damped distorted grid

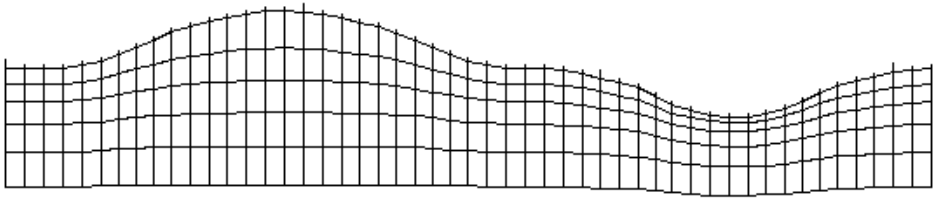

e). Arrangement of model blocks with the inverse Schwartz-Christoffel transformation

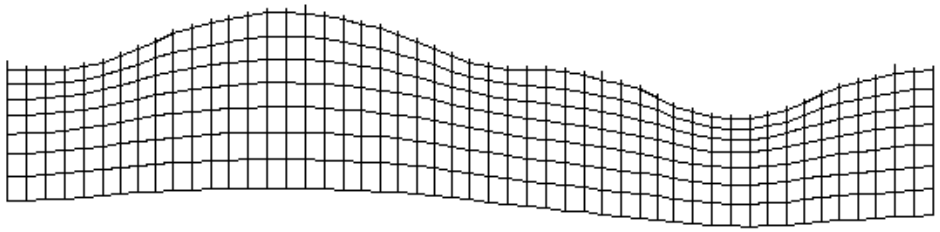

Example of different topographic modeling methods

This example is from a Wenner array survey over a known burial mound with some topography. Note the damped distorted grid model has slightly thicker layers below the center where the topography curves upwards, whereas the inverse Schwartz-Christoffel transformation has a more uniform thickness. However, overall the anomalies are basically the same.

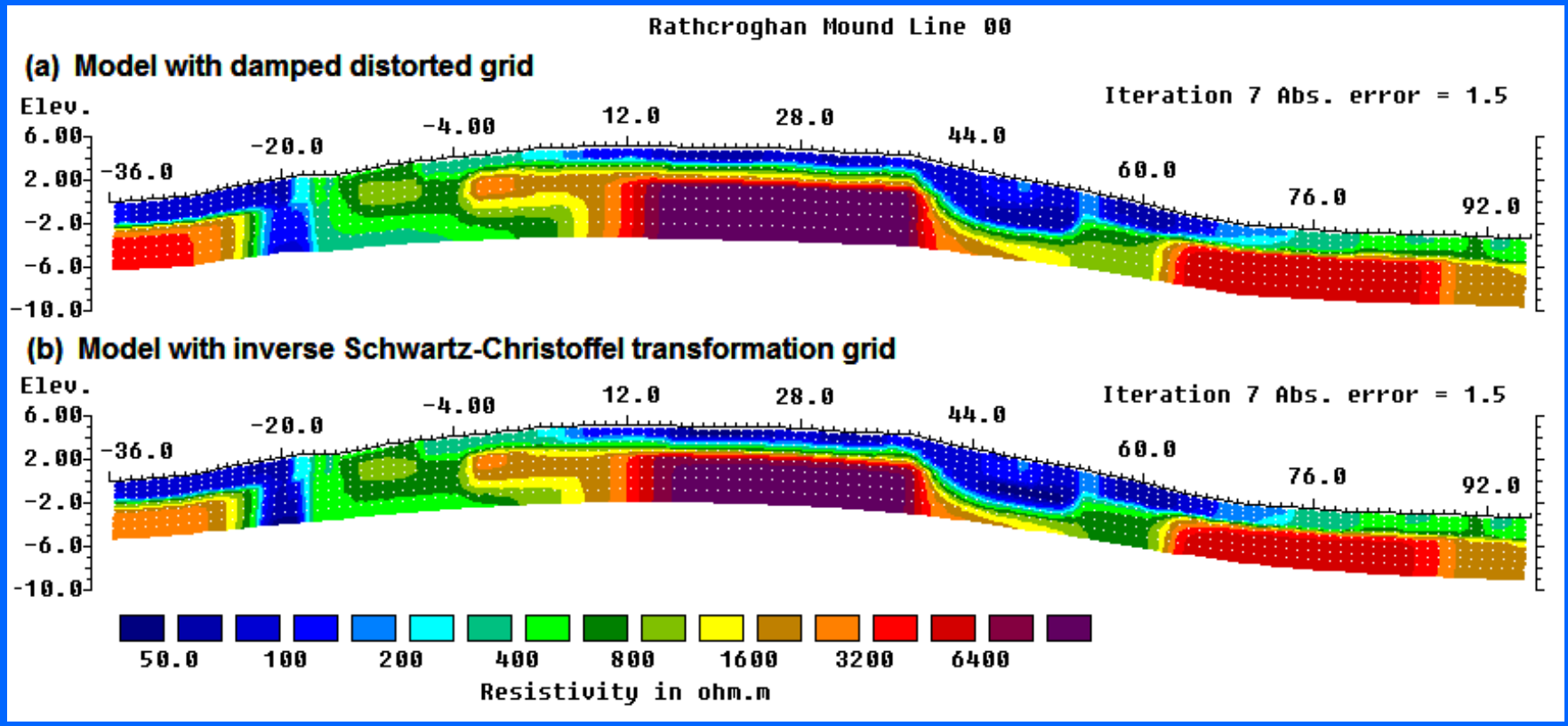

The 2-D electrical imaging method : general conclusions

In most areas, the traditional 1-D sounding survey is probably not sufficiently accurate due to lateral changes in the ground resistivity.

The multi-electrode resistivity meter systems, fast microcomputers and software has made the use of 2-D resistivity imaging surveys possible. It has become a 'standard' geophysical exploration tool for engineering, environmental, hydrological and mineral surveys. The Wenner, Wenner-Schlumberger, pole-pole, dipole-dipole and pole-dipole arrays are the most common arrays used.

It gives sufficiently accurate results in areas of moderately complex geology where the 2-D assumption is reasonably accurate.

Choice of a proper electrode array, survey strategy, data processing and inversion method can significantly affect the results.

It is limited by the rapid decrease of resolution with depth, and in areas with significant 3-D variations near the survey line.

2-D case histories

Examples of 2-D surveys and results.

Example 1 : Cavity under house

This survey was conducted to determine the cause of damage to a home in Florida. The results from an OhmMapper survey provided evidence that proved the damage was the result of a karst cavity under the house. The OhmMapper was used as it does not require direct electrical contact with the soil. The house flooring has a concrete base.

Courtesy of Geometrics Inc.

OhmMapper being towed over grass and pavement. Contact is made capacitively with the ground through insulated cables.

Example 1 : Cavity under house

This slide shows the plan of the house and the location of the survey lines. The bottom figure shows the results from one of the survey lines.

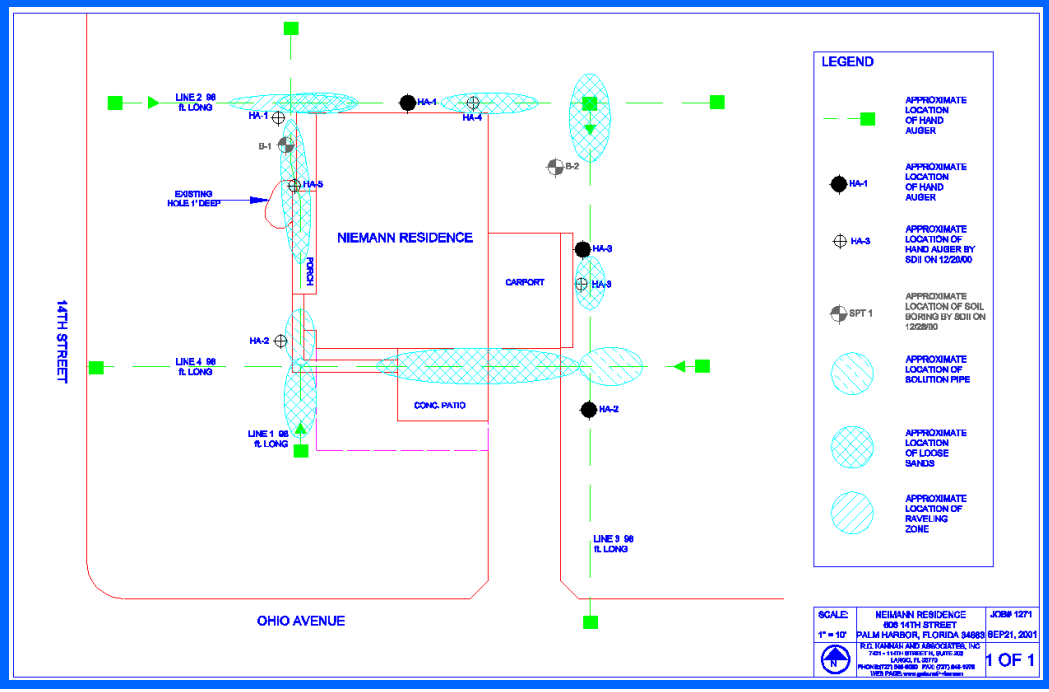

This shows the inversion model from one of the lines. The cavities correspond to the regions with high resistivity values.

Courtesy of R.C.Kannan Assoc.

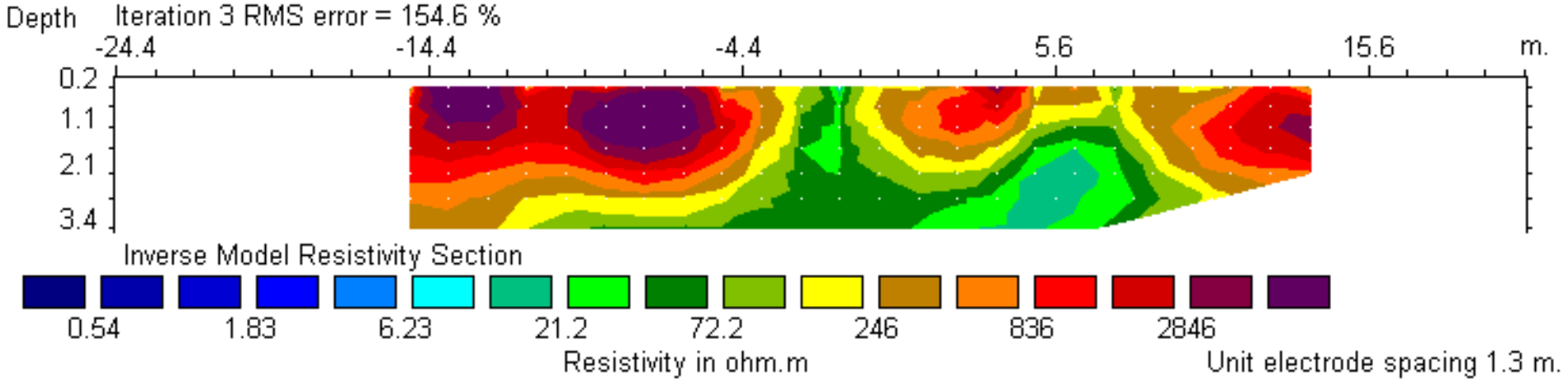

Example 2 : Train tunnel project

This survey was carried out in south-west Sweden along a proposed railway tunnel route. The Hallandsås Horst is one of several uplifted blocks of the Earth's upper crust that are found in Skåne, the southernmost province of Sweden. The horst, composed of Precambrian rocks, is flanked by younger sedimentary rocks and some 8-10 km wide, 30-40 km long and trends NW-SE.

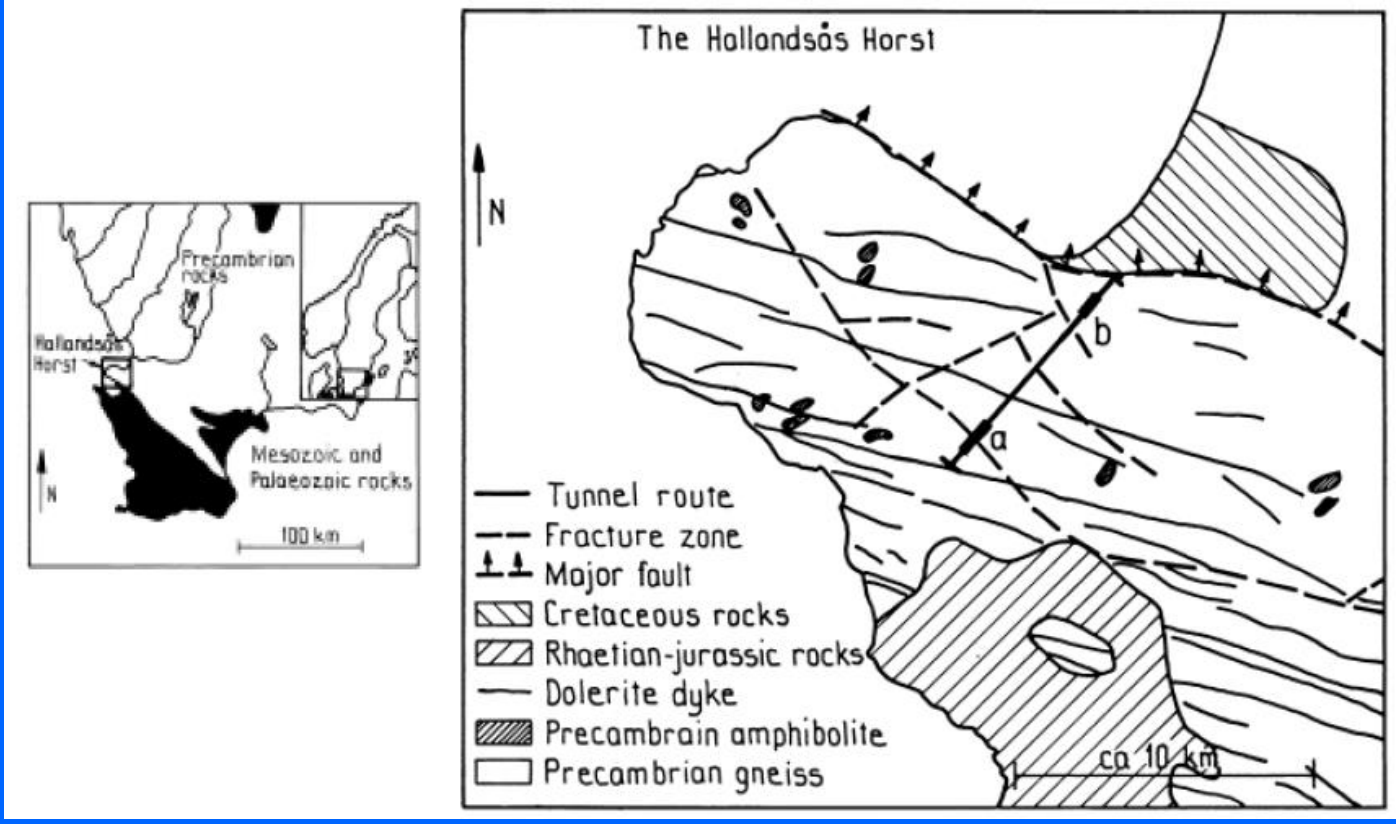

Ref. : Dahlin, T., 1996, 2D resistivity surveying for environmental and engineering applications. First Break, 14, 275-283.

Example 2 : Train tunnel project

The highly weathered sedimentary rocks poses greater problems to the tunnel construction compared to the higher resistivity metamorphic and igneous rocks. A large region with sedimentary rocks (blue region with resistivity values of less than 100 ohm.m) was detected between the 7100 and 7800 meters marks.

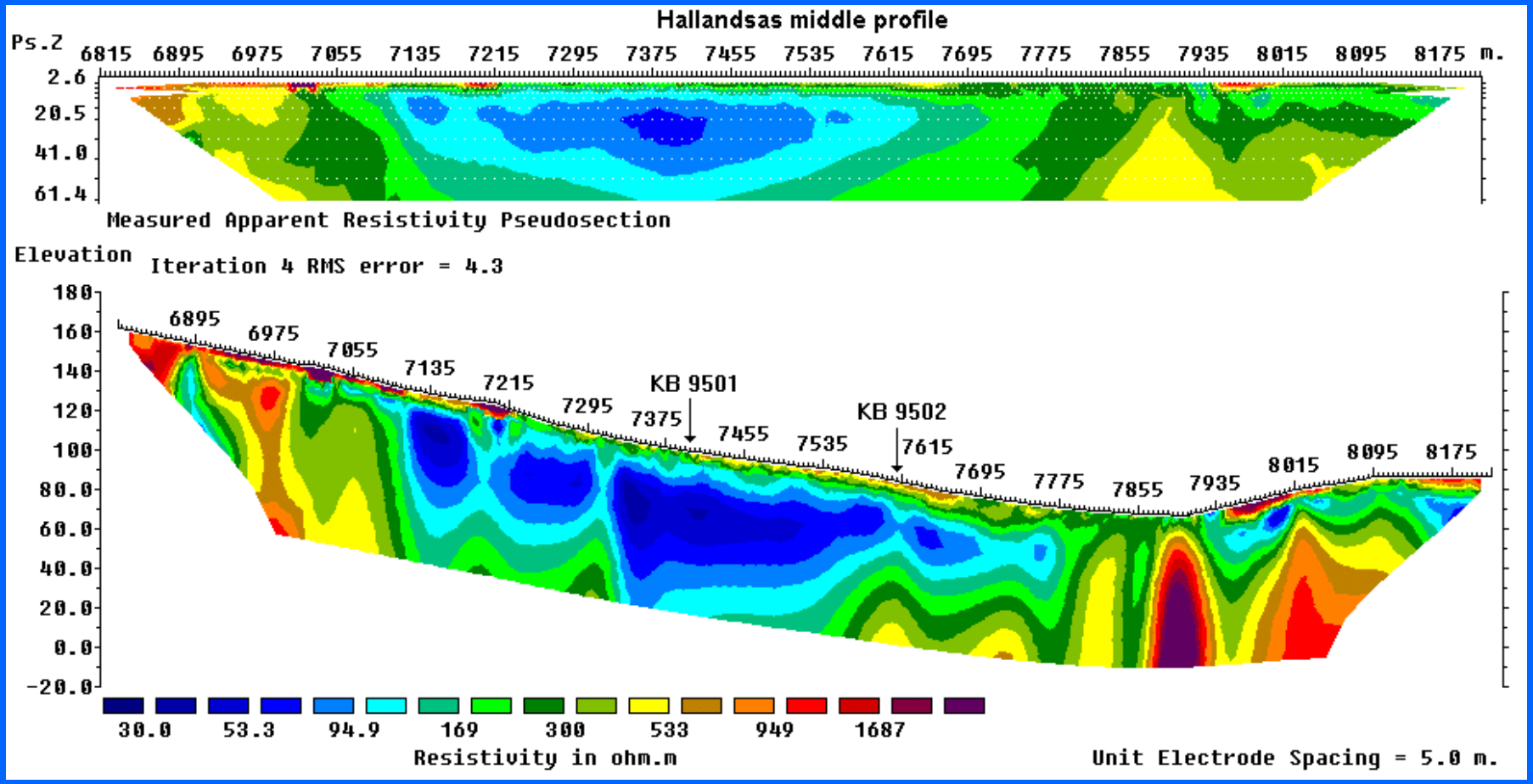

Ref. : Dahlin, T., 1996, 2D resistivity surveying for environmental and engineering applications. First Break, 14, 275-283.

Example 2 : Train tunnel project

The figure below shows part of the inversion model obtained together with the lithology log from the two boreholes. There is a good correlation between the location of the low resistivity region and the weathered sedimentary and igneous/metamorphic rocks. The proposed tunnel route is shown by the pair of lines between elevation levels of about 20 to 40 meters.

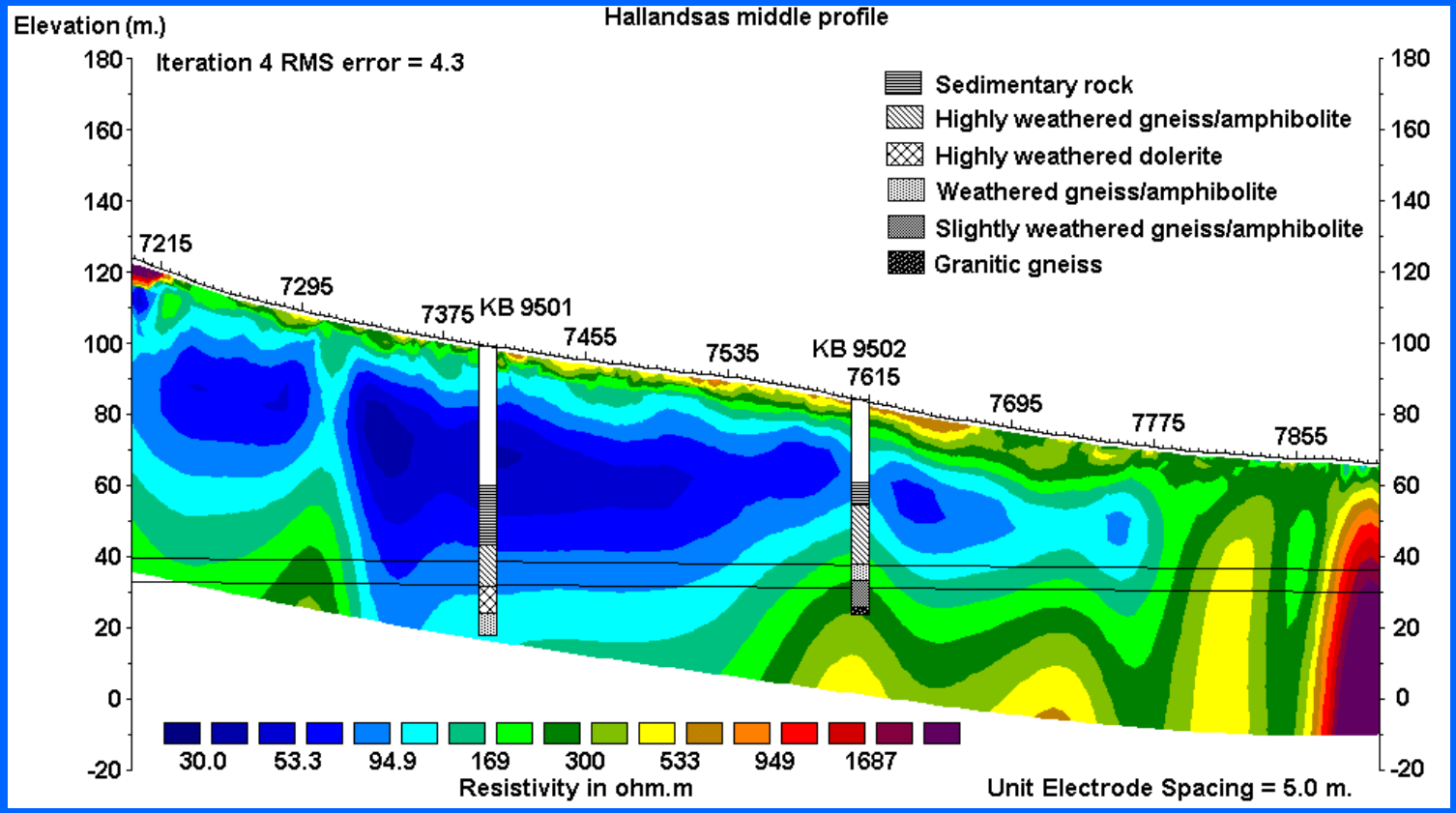

Ref. : Dahlin, T., 1996, 2D resistivity surveying for environmental and engineering applications. First Break, 14, 275-283.

Break for questions and discussion

IP surveys

A brief look at the I.P. effect and its applications

The I.P. effect

Many multi-electrode resistivity meter system now support Induced Polarization (I.P.) measurements. The I.P. effect is caused by two main mechanisms, the membrane polarization and the electrode polarization effects. The membrane polarization effect is largely caused by clay minerals in the soil or rock, which is used in environmental/engineering/hyrological surveys. The electrode polarization effect is caused by conductive minerals in rocks, which is used in mineral exploration surveys.

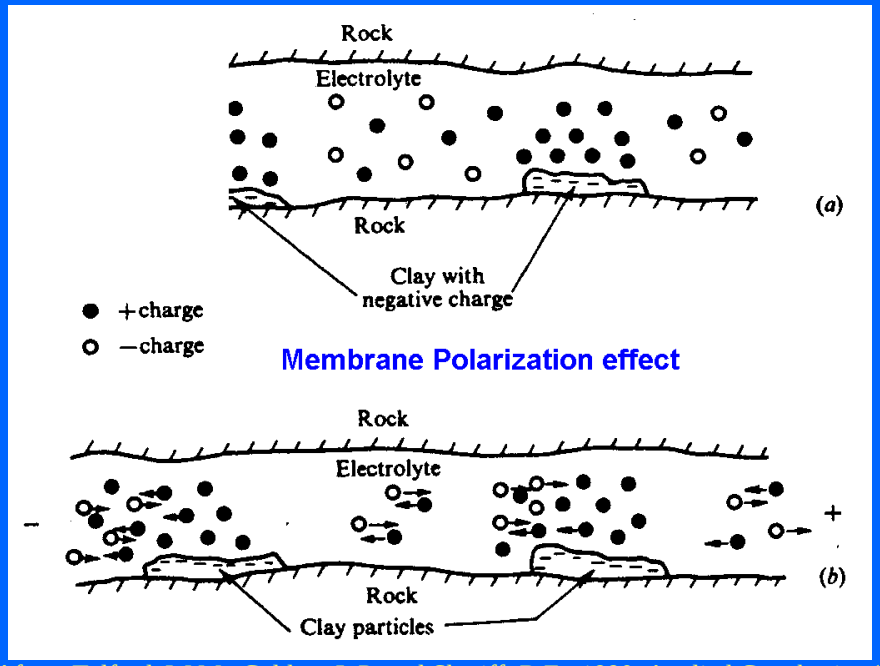

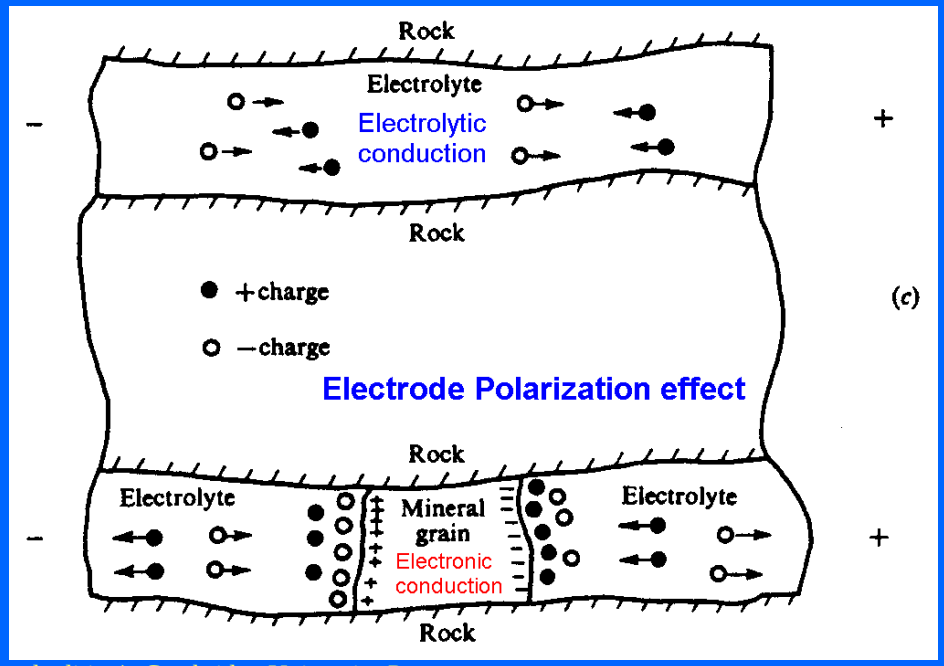

After : Telford, W.M., Geldart, L.P. and Sheriff, R.E., 1990. Applied Geophysics (second edition). Cambridge University Press.

I.P. properties of rocks and minerals

One characteristic of the I.P. method is the use of different parameters in the time and frequency domains used to represent the I.P. effect. One commonly used parameter is the time domain chargeability effect which is given in mV/V or milliseconds. The figure below shows the I.P. values for some minerals and rocks. Note the I.P. effect for conductive minerals (sulfides) is much greater than that due to clay in sedimentary rocks and sediments. It is particularly useful for detecting disseminated minerals that is difficult to detect using resistivity alone.

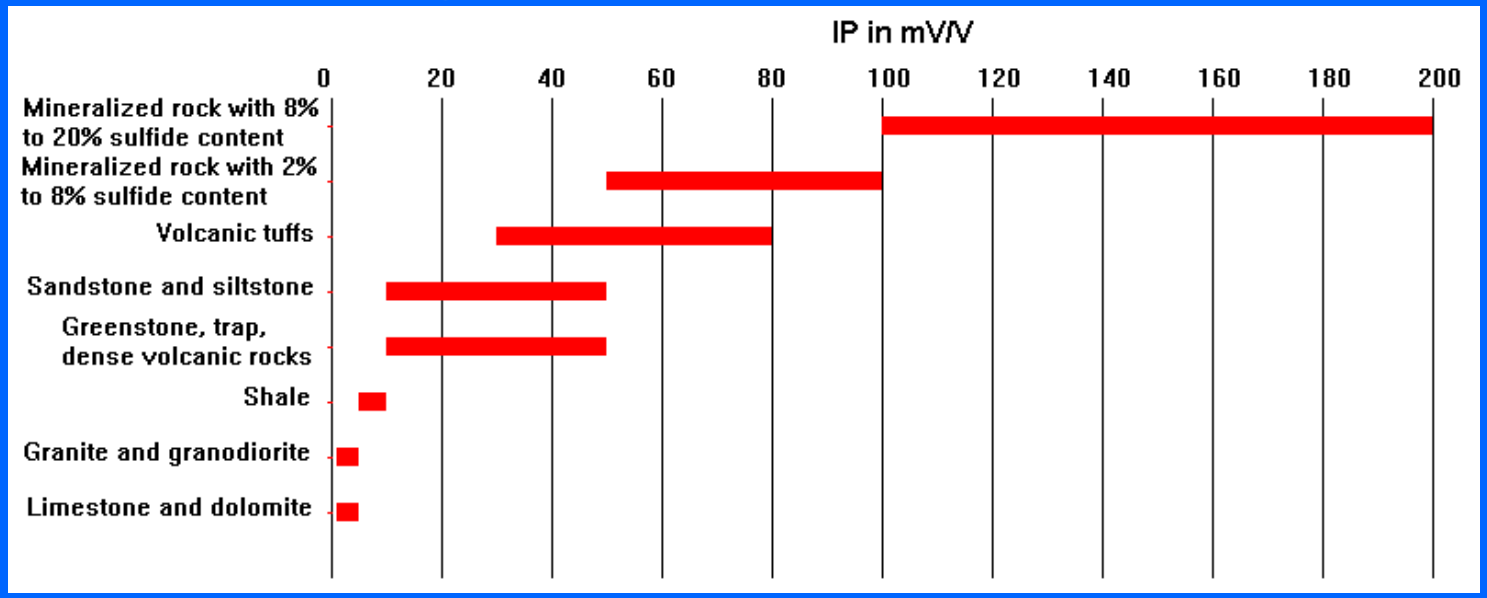

I.P. time domain measurements

In the time-domain method, the residual voltage after the current cut-off is measured. Some instruments measure the amplitude of the residual voltage at several time intervals after the current cut-off. A common method is to integrate the voltage electronically for a standard time interval. In the Newmont standard, the chargeability, m_t, is defined as

$$m_t = 1870 \frac{\int_{0.15}^{1.1} V_s \, dt}{V_{DC}}$$

The decay curve and the measurement of the I.P. value is shown in this figure. Normally the measured I.P. value is given in mill-seconds (msecs).

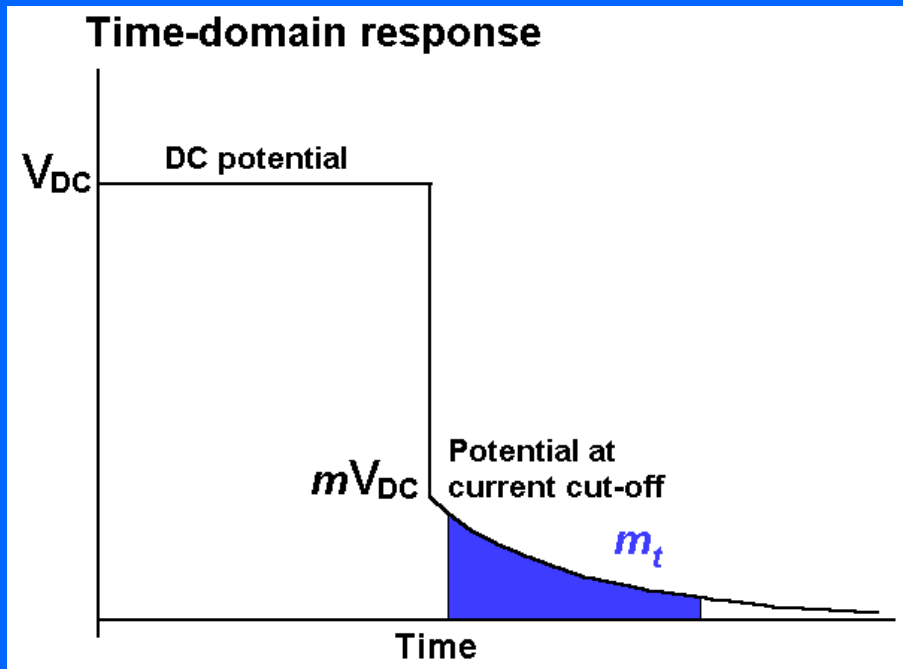

I.P. frequency domain measurements

Frequency domain I.P. measurements use an alternating current source. In one method, the phase shift between the transmitted current and the measured voltage is used. The measured I.P. is given in terms of milli-radians (mrad).

Another technique compares the amplitudes of the voltage for two different AC frequencies, such as 1 Hz and 10 Hz. The I.P. value given as Percent Frequency Effect (PFE).

As a general rule, a chargeability value of M = 100 mV/V is approximately equal to 10*PFE*, or 70*mrad*, or 70*msec*.

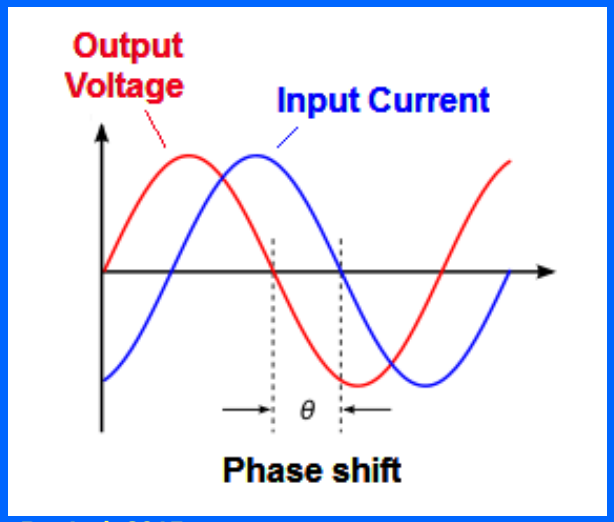

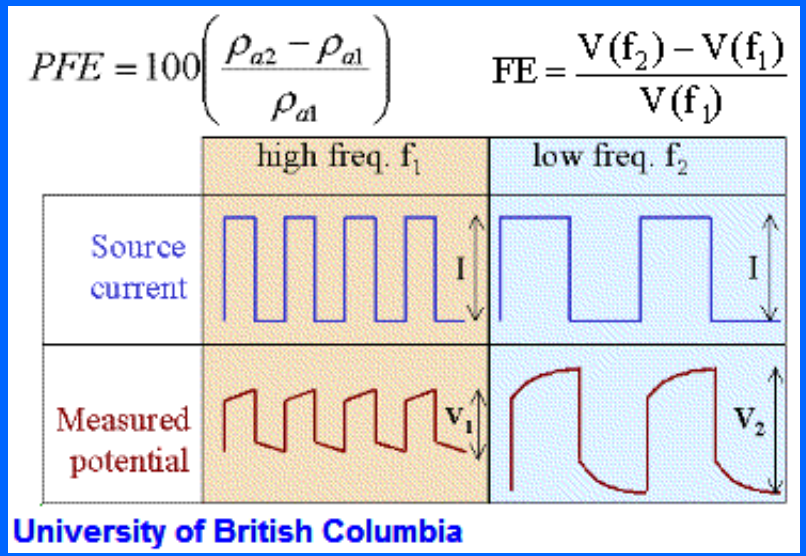

I.P. instrumentation

Many multi-electrode systems now offer an I.P. measurement option. The maximum current from battery-based systems is usually 1 Amp or less. This is usually too low to give reliable I.P. data when the electrode spacing is more than a few meters. However there has been recent improvements in the electronic circuitry and use of separate current and potential cables that have improved the quality of the I.P. data.

For large spacings of 10 meters or more used in mineral exploration surveys, a more powerful current transmitter powered by a petrol based power generator and a series of separate I.P. receivers is normally used.

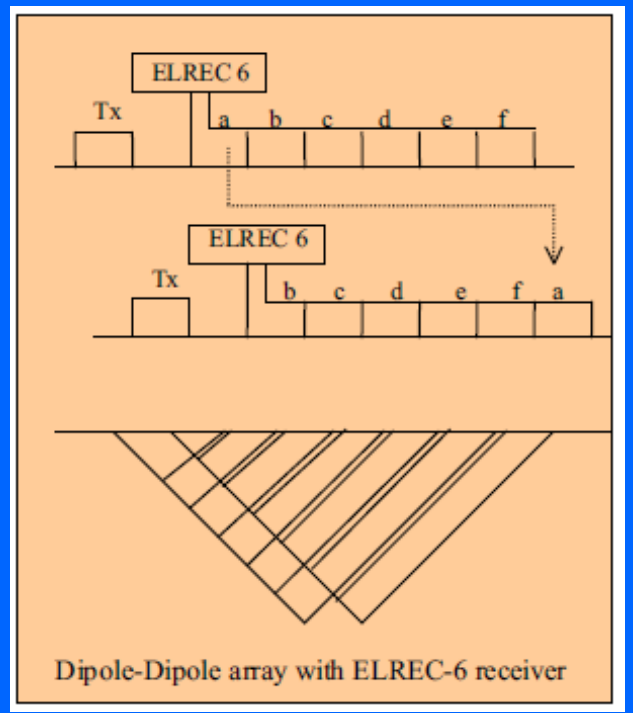

Dipole-Dipole array with ELREC-6 receiver

I.P. survey with multi-electrode system

One method to improve the quality of I.P. data from conventional multi-electrode systems that has two separate cables is by using different cables for the current and potential electrodes. This reduces the EM coupling between the current and potential cables.

The possible current and potential electrodes positions are reduced and special control files are needed for this configuration. However, this method can be used with any multi-electrode system that uses a two cable arrangement.

Note the two cables are placed as far as possible from each other in the field survey.

Actual field layout during survey

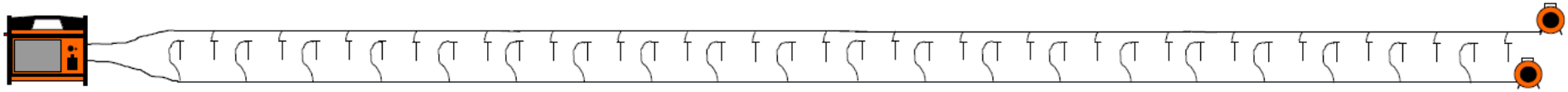

Sketch of cables setup with the Abem Terrameter LS system.

Example of I.P. survey

The results from a multi gradient array survey are shown below. The resistivity section shows an upper 3 to 4 meters sandy layer underlain by lower resistivity saline mud sediments. The I.P. section shows a top 1 to 2 meters layer with chargeability values of 4 to 8 mV/V which is probably sandy sediments with some organic content. The low I.P. values below this layer is probably due to high salinity that tends to reduce the I.P. effect.

Note the apparent resistivity pseudosection shows fairly regular contour patterns, whereas the bottom part of the I.P. pseudosection has noisier data due to larger electrode spacings and weaker signals.

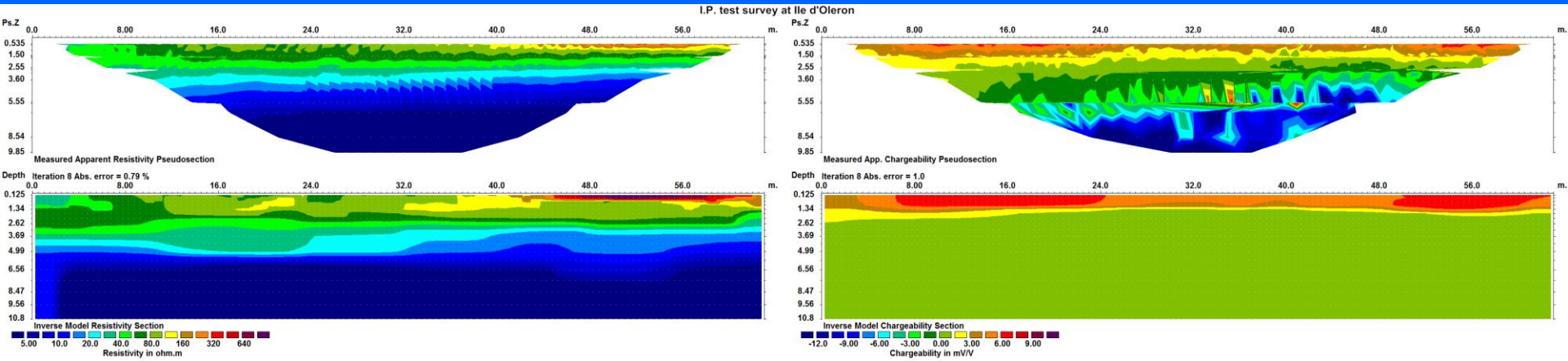

Part 4

3-D surveys, data and inversion

3-D Electrical Imaging Surveys

Since all geological structures are 3-D in nature, a 3-D resistivity survey using a 3-D inversion model should give the most accurate results. However 3-D surveys are not as commonly carried out as 2-D surveys. The main reason is that the survey cost is higher for a 3-D survey.

There are two recent developments that should make 3-D surveys a more cost-effective option. The new multi-channel resistivity meters significantly reduces the survey time. The second development is faster microcomputers to enable the inversion of very large data sets.

Many of the inversion concepts discussed for 2-D surveys are directly applicable for 3-D surveys and data inversion. This section will concentrate more on new features that are more relevant to 3-D surveys and models.

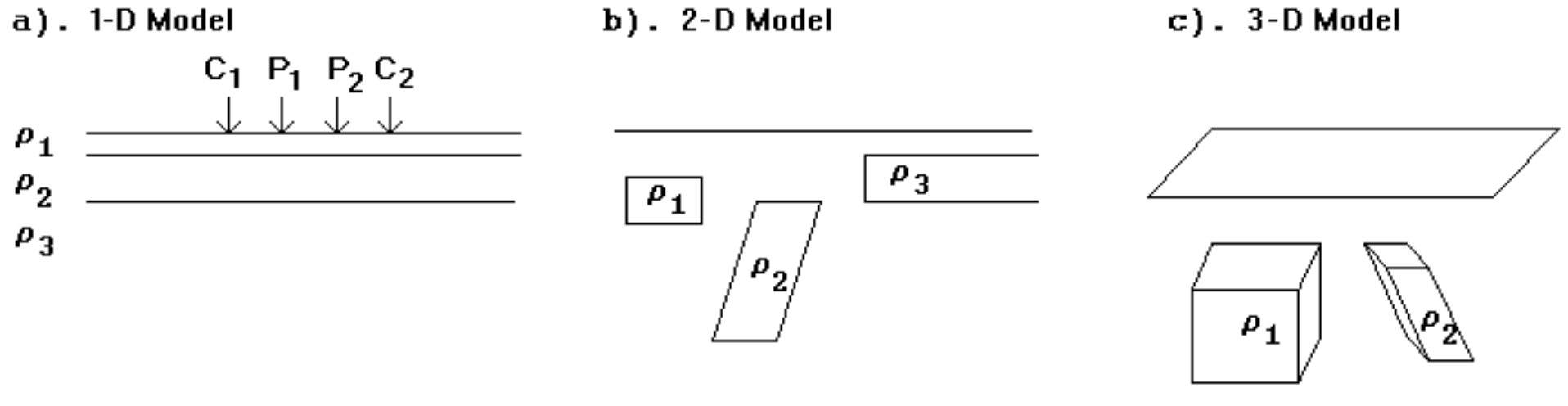

Types of arrays for 3-D surveys

Most arrays that are used in 2-D surveys can also be used in 3-D surveys. However the following array types seem to be more widely used for 3-D surveys.

Pole-pole : 2 active electrodes

Pole-dipole : 3 active electrodes

Dipole-dipole : 4 active electrodes

Wenner-Schlumberger : 4 active electrodes

The arrangement of the electrodes for these arrays together with their geometric factors are shown below.

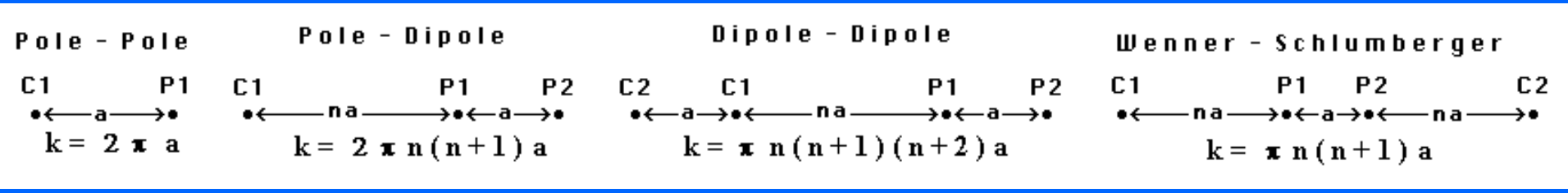

The Pole-Pole array : Electrode layout

Only two active electrodes, C1 and P1, and used. The second current and potential electrodes, C2 and P2, are fixed throughout the survey and must be placed at a distance of at least 20 times the maximum C1-P1 spacing. If the distances of the remote electrodes is less, the positions must be recorded and included in the data file. Different pairs of electrodes in the grid are selected as the C1 and P1 electrodes.

The depth of investigation is about 0.87 times the C1-P1 (or '*a*') spacing.

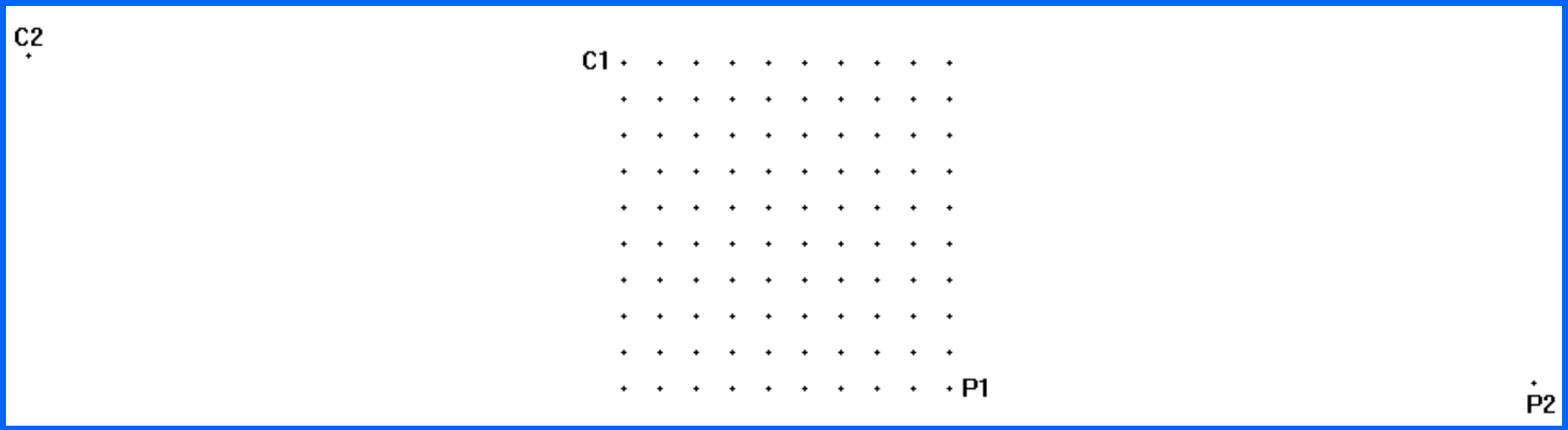

The pole-pole array - 3D sensitivity sections

The figure shows the sensitivity values on horizontal slices through the earth. The electrodes are at the 0 and 1 meter marks along the *x*-axis. Near the surface, there is an approximately circular region with negative sensitivity values in the top two slices at depths of 0.07 and 0.25 meter. The zone with the largest sensitivity extends in the *y*-direction to slightly over half the electrode spacing. To get a complete 3-D coverage, if the measurements are only made in the *x*-direction, the spacing between the lines should not be much more than the smallest electrode spacing used.

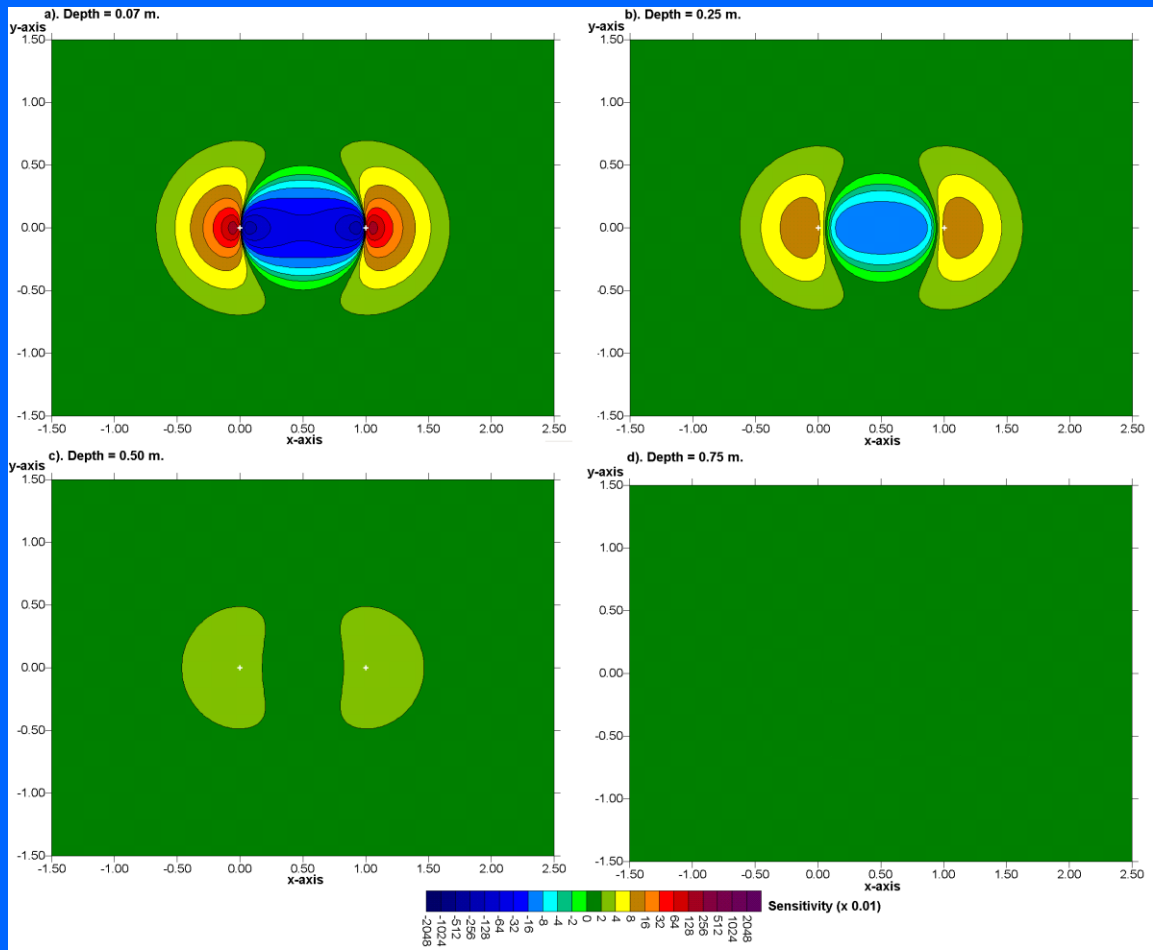

The pole-pole array for 3D surveys - summary

The pole-pole array has two main disadvantages.

Firstly it has a much poorer resolution compared to other arrays.

The second disadvantage is that the second current electrode and potential electrode must be placed at sufficiently large distances from the survey grid. This could be a challenging task for large grid sizes.

The main advantage of the pole-pole array is that it gives a better horizontal coverage than other arrays. It also has the deepest depth of investigation (0.87 times the C1-P1 spacing). For this reason, it is popular in small surveys grids of 15x15 electrodes or smaller.

In remote areas where cultural telluric noise is not a problem, it has been used for mineral surveys with fairly large spacings.

The Pole-Dipole array : Electrode layout

Three active electrodes are used; C1, P1 and P2. The second current and electrode, C2, is at a fixed position must be placed at a distance of at least 5 times the maximum C1-P2 spacing. Different groups of electrodes in the grid are selected as the C1, P1 and P2 electrodes.

The depth of investigation is about 0.35 times the C1-P2 spacing.

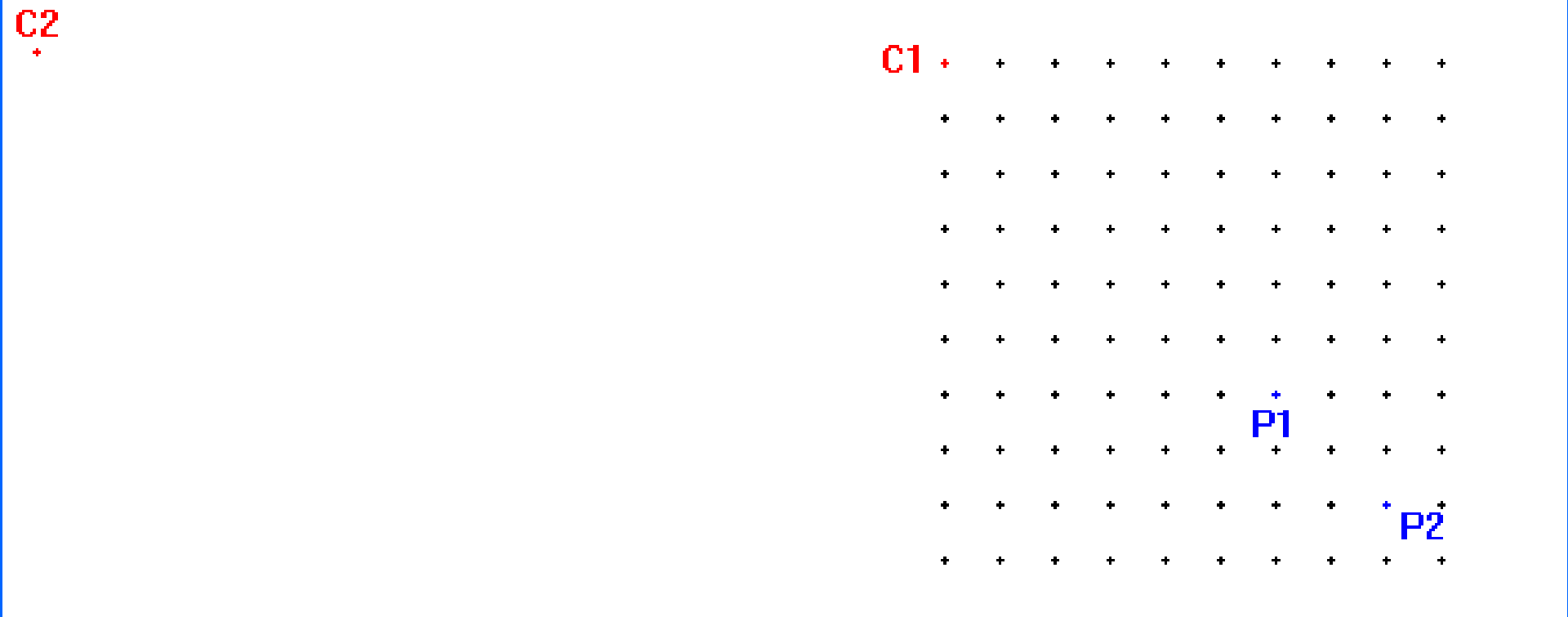

The pole-dipole array - 3D sensitivity sections

The figures below shows the sensitivity patterns with the dipole separation factor "*n*" is equals to 1 and 4. There is prominent area with negative sensitivity values between the C1 and P1 electrodes. The array is more sensitive to structures off the array axis (i.e. in the *y*-direction) compared to the pole-pole array. The area with the higher sensitivity values extends to about 0.8 times the array length, or 1.6 times the unit electrode spacing for n=1. When n=4, the array is more sensitive to off-axis structures near the P1-P2 dipole. This sensitivity to off-axis structures is useful if the survey is conducted along a series of parallel lines. The distance between the lines should be within 2 times the unit electrode spacing.

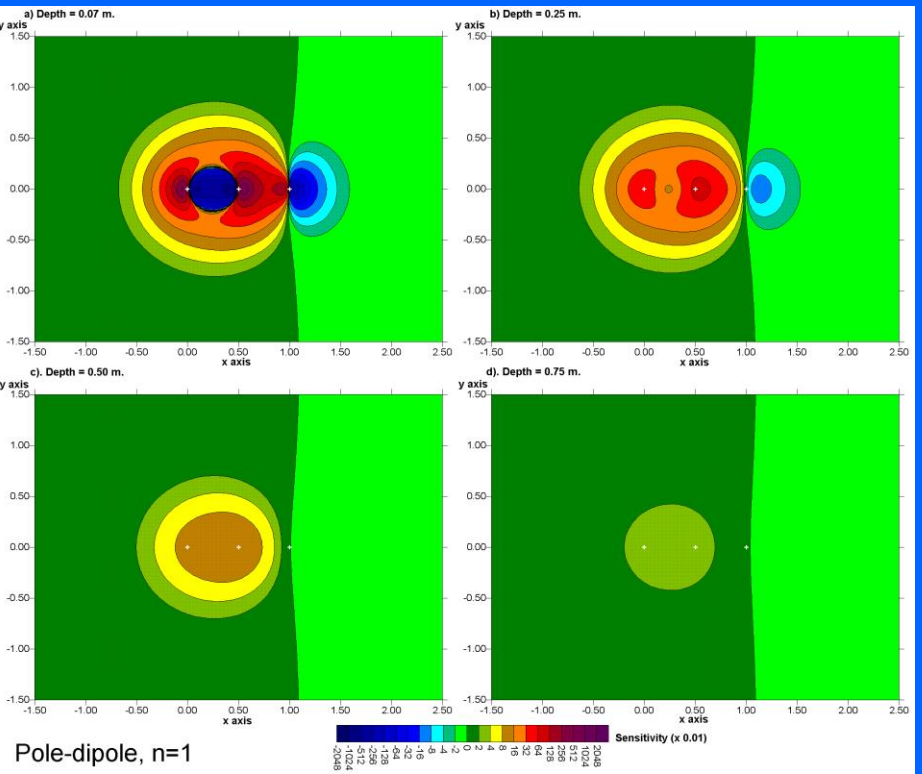

Pole-dipole, n=1

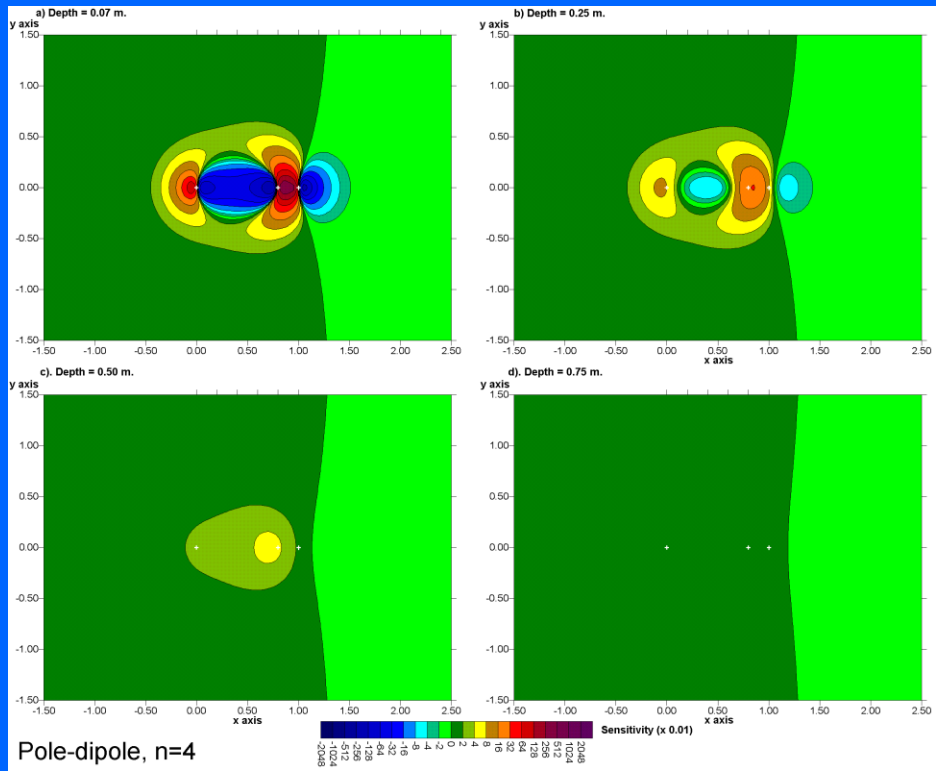

Pole-dipole, n=4

The pole-dipole array for 3D surveys - summary

This array is useful for surveys with medium and large survey grids.

It has a better resolving power than the pole-pole array, and is less sensitive to telluric noise since both potential electrodes are kept within the survey grid.

It has a stronger signal strength than the dipole-dipole array.

Although it has one "remote" electrode (the C2 electrode), the effect of this electrode on the measurements is much smaller compared to the pole-pole array. The effect can be included in the modeling by recording the position of this electrode.

This array is now widely used for 3-D I.P. surveys where very large survey grids (about 1000 electrodes and 50m spacing) are used. The offset pole-dipole array, where the C1 electrode is on a different line from the P1-P2 electrodes, is frequently used.

The Dipole-Dipole array : Electrode layout

All four electrodes are used.

The depth of investigation is about 0.20 times the array length (C2-P2 spacing). Measurements are usually made along the x and y lines, frequently in only one direction.

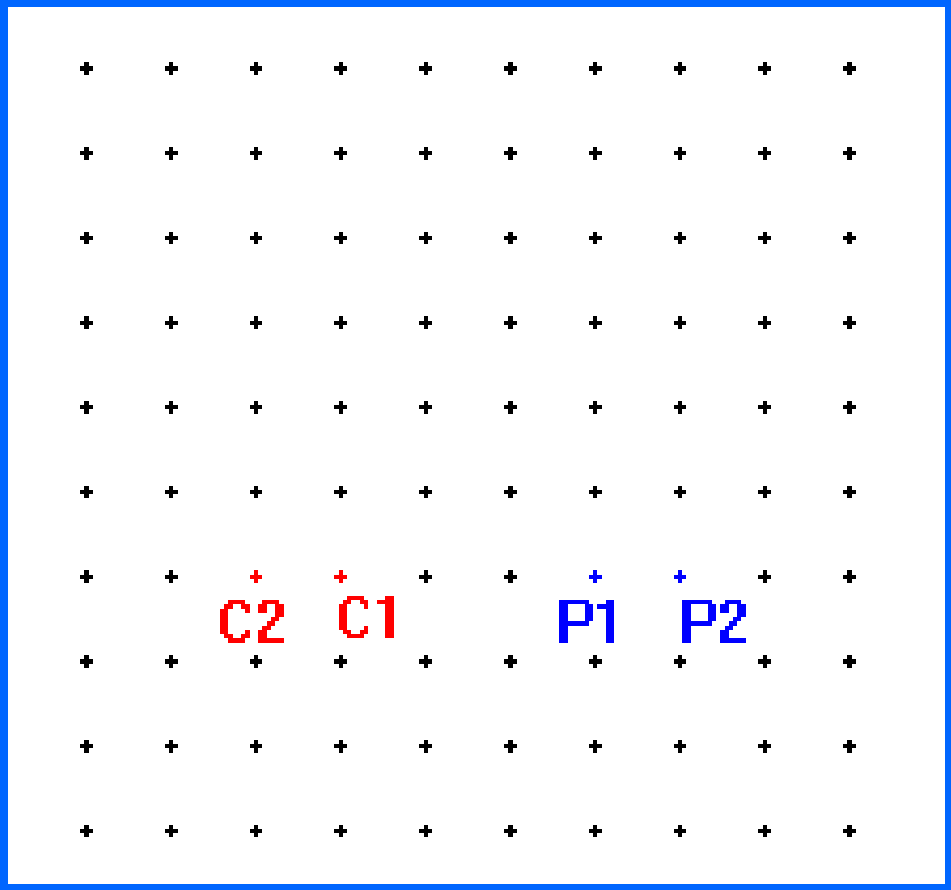

The dipole-dipole array - 3D sensitivity sections

The figures below shows the sensitivity patterns with the dipole separation factor "*n*" equals to 1 and 4. The sensitivity contours are elongated in the *y*-direction, particularly for the larger "*n*" value. The high sensitivity area extends to about 0.6 times the array length in the *y*-direction, or about 1.8 times the unit electrode spacing. This sensitivity of the dipole-dipole array to off-axis structures is a problem in 2-D surveys, but is useful in 3-D surveys if the survey is conducted along a series of parallel lines. A larger spacing between the survey lines (to about 3 times the electrode spacing) can be used for 3-D surveys.

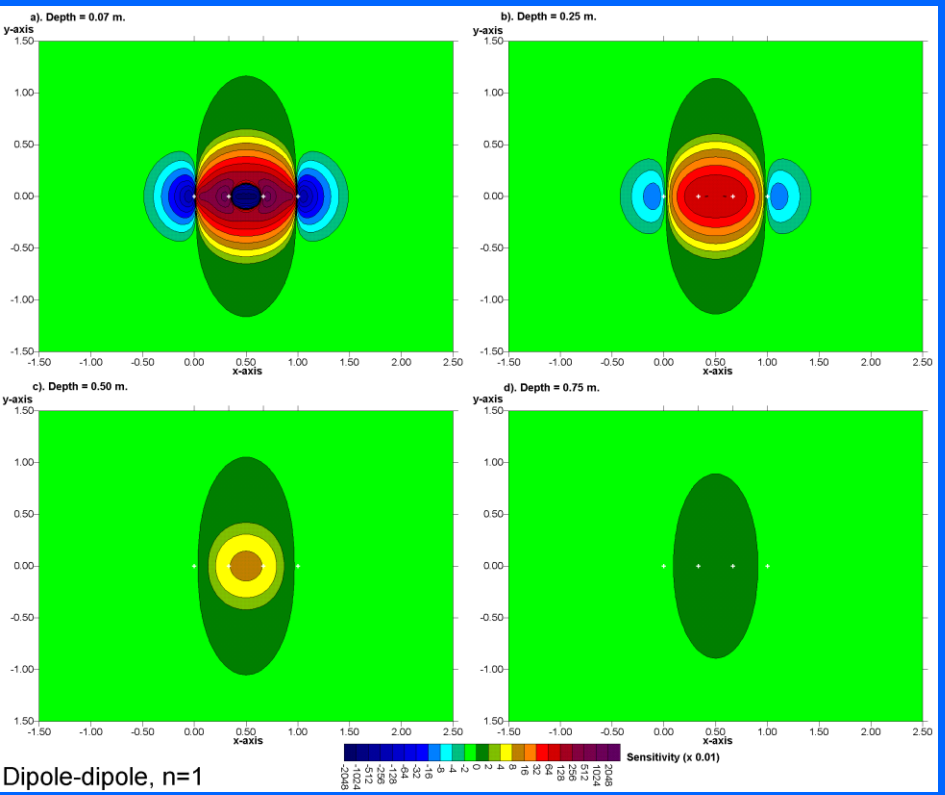

Dipole-dipole, n=1

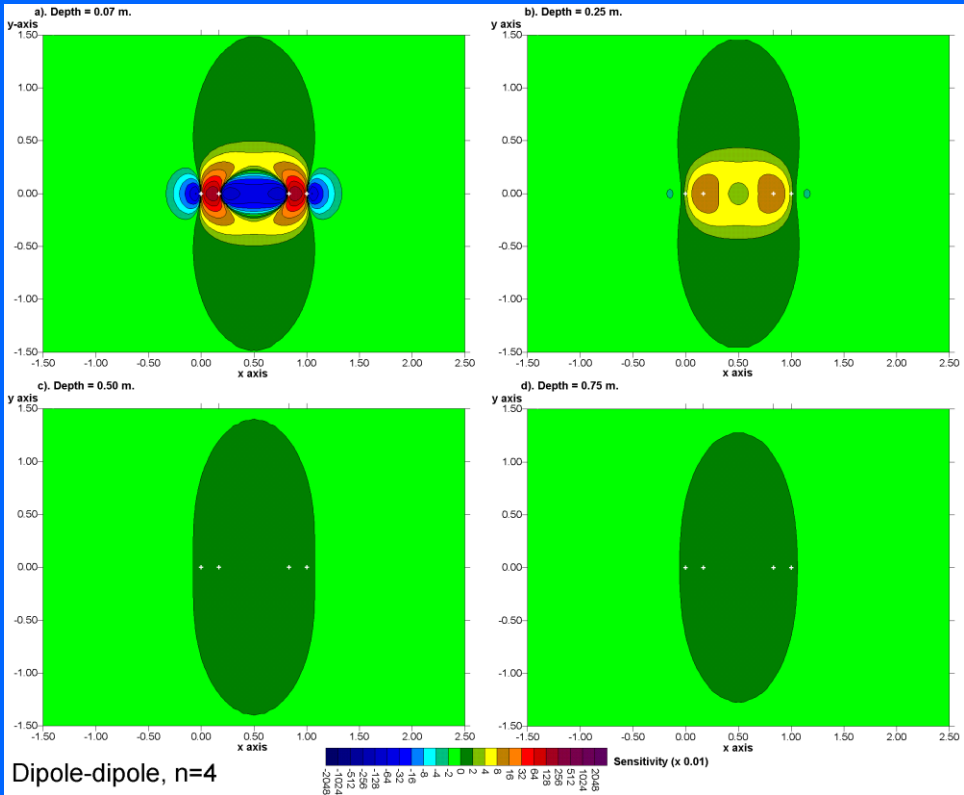

Dipole-dipole, n=4

The dipole-dipole array for 3-D surveys - summary

This array is widely used with large grids.

The main problem that is likely to be faced with this array is the comparatively low signal strength. This problem can be overcome by increasing the "a" spacing between the P1-P2 dipole to get a deeper depth of investigation as the distance between the C1-C2 and P1-P2 dipoles is increased.

It might be a useful array if the "3-D" survey actually consists of measurements along a series of 2-D lines. It has a sensitivity pattern that is elongated perpendicularly to the array direction, and thus provide more information on structures that are off the line axis.

In some large 3-D I.P. surveys with multi-channel instruments, a non-symmetrical form of the dipole-dipole array is sometimes used. The P1-P2 dipole length can be increased at larger distances to get a stronger signal strength for the same C1-C2 current dipole. In some cases, the C1-C2 dipole is offset from the P1-P2 dipole.

The Wenner array - 3D sensitivity sections

The sensitivity contours for the Wenner array (W-S with n=1), outside of the immediate vicinity of the electrodes, are elongated in the direction of the line of electrodes. This means that the Wenner alpha array is less sensitive to off-line structures than the dipole-dipole array, i.e. it is less sensitive to 3-D effects.

This is an advantage in 2-D surveys, but makes it less useful for 3-D surveys carried out with a series of 2-D lines.

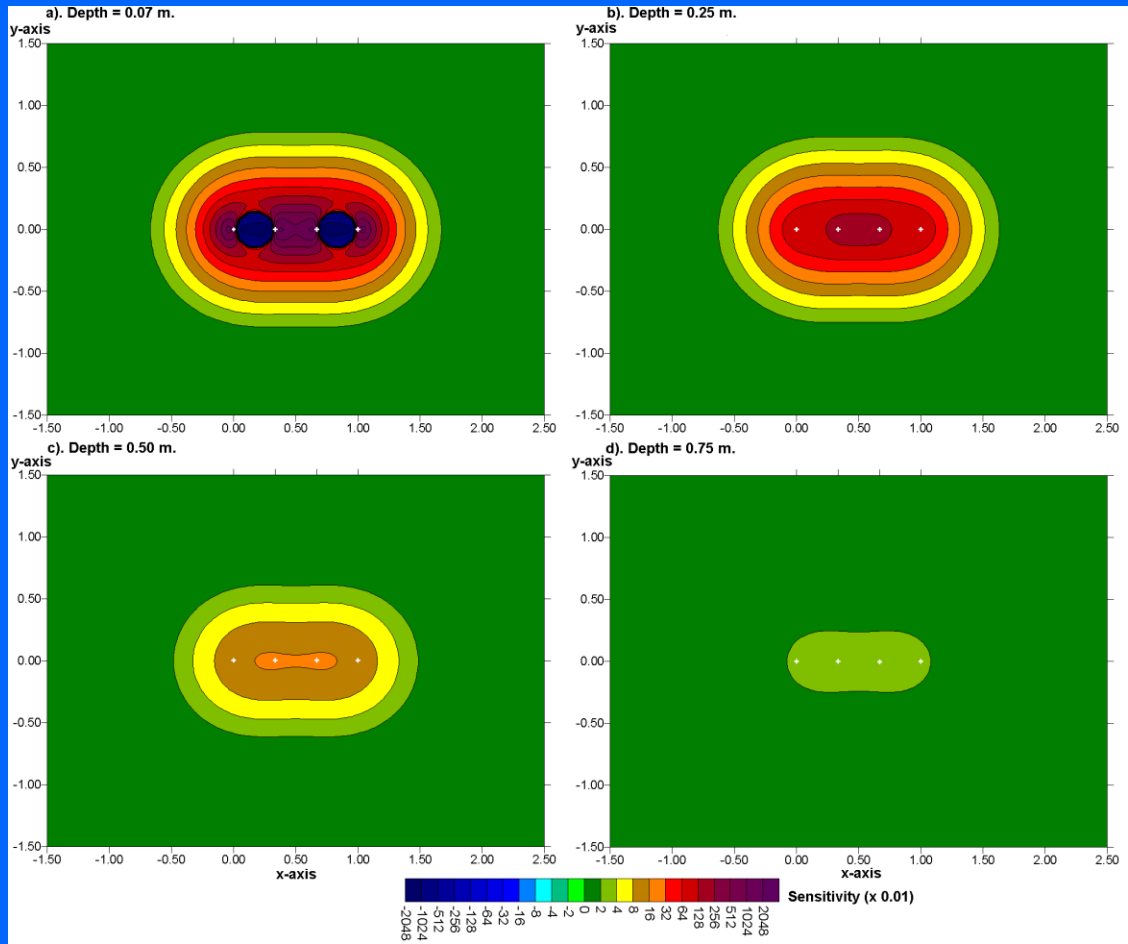

The Schlumberger array - 3D sensitivity sections

The sensitivity pattern for the Wenner-Schlumberger array (n=4) is generally elongated in the direction of the line of electrodes with a slight bulge near the center of the array. It is less sensitive to off-line structures than the dipole-dipole array (i.e. it is less sensitive to 3-D effects). However, the wider zone of off-axis high sensitivity values as the 'n' factor increases makes it is more useful for 3-D surveys than the Wenner (n=1).

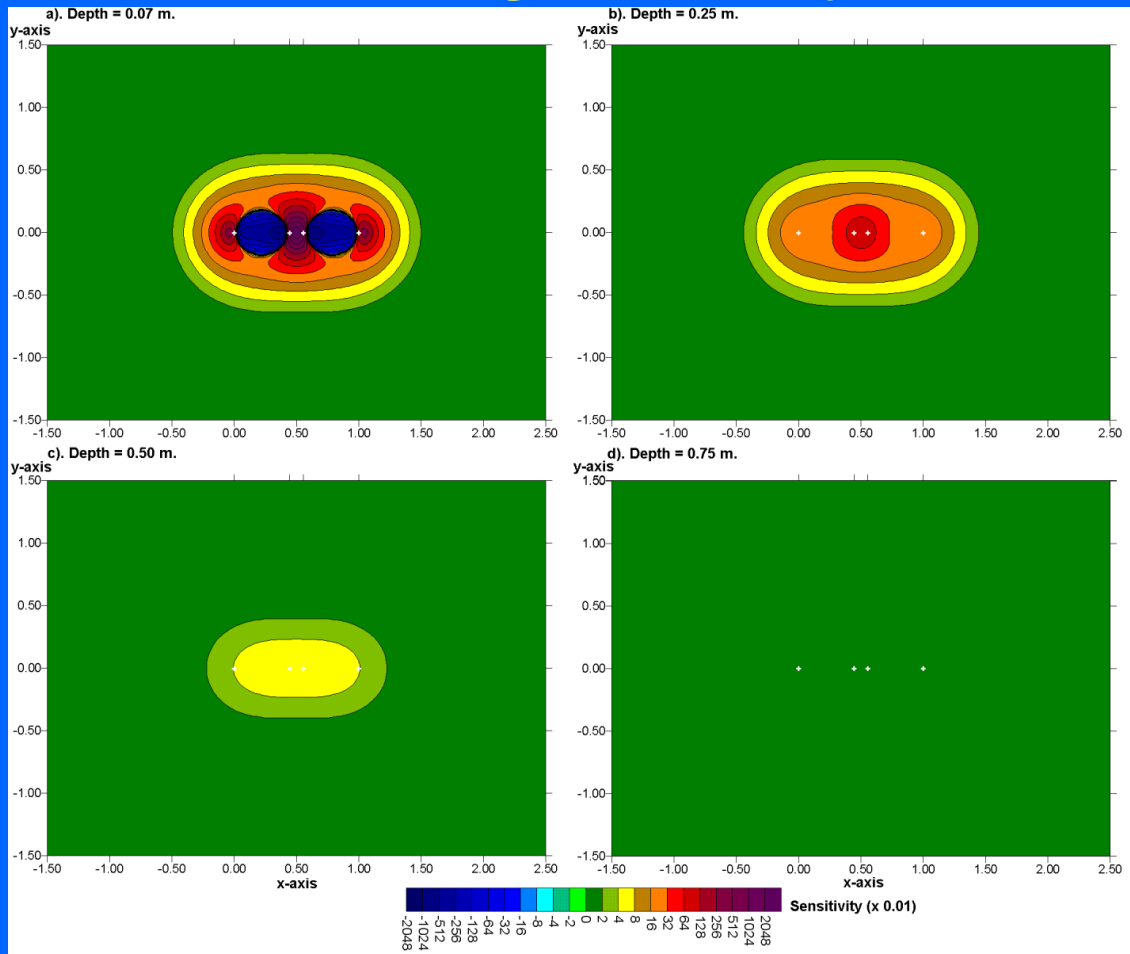

Summary of array types for 3-D surveys

For relatively small grids of less than 15 by 15 electrodes, the pole-pole array is popular since it provides better horizontal data coverage compared to other arrays. For large spacings, it has been used in areas with low cultural telluric noise.

The pole-dipole array has been widely used in recent years with large survey grids, particularly the offset version for I.P. surveys. It has a higher resolution than the pole-pole array. It requires only one remote electrode and is much less sensitive to telluric noise.

The dipole-dipole array is widely used for large survey grids, particularly if there is no convenient location for a remote electrode.

For very large survey grids with resistivity only surveys the Wenner-Schlumberger has been used. This array is frequently used when the survey is carried out along a series of parallel 2-D lines, particularly in environmental/engineering surveys.

3-D surveys and data inversion

Methods for carrying out 3-D surveys, and different model discretizations used for data inversion

3-D inversion models

What is 3-D inversion? An inversion model is 3-D if the resistivity values are allowed to vary in all three directions (in the *x*-, *y*- and *z*-directions) at the same time. In 2-D inversion the subsurface resistivity is assumed to vary only in the *x*- and *z*-directions but constant in the *y*-direction. A model constructed from a series of 2-D inversions along parallel lines is not a true 3-D inversion model. A 3-D forward modeling subroutine (the finite-difference and finite-element method) is used to calculate the model apparent resistivity and Jacobian matrix values.

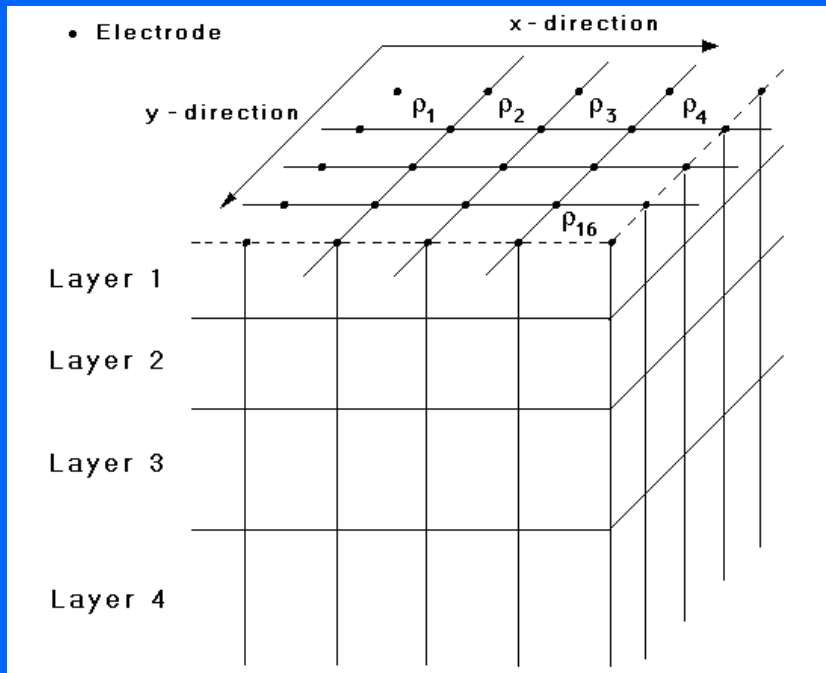

3-D data sets – measurements with a rectangular grid

The simplest 3-D survey layout is with the electrodes arranged in a rectangular grid. Measurements are sometimes made in diagonal directions, but more commonly are only made along the grid lines particularly if the data was collated from a series of 2-D survey lines. It is usually recommended that the spacing between the lines should not be more than 2 times the inline electrode spacing.

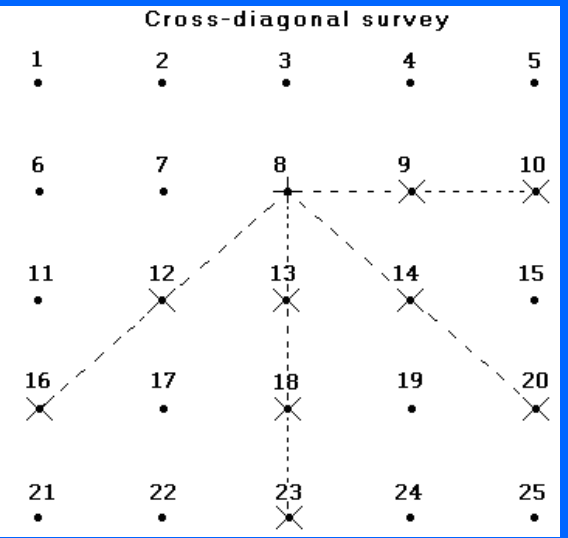

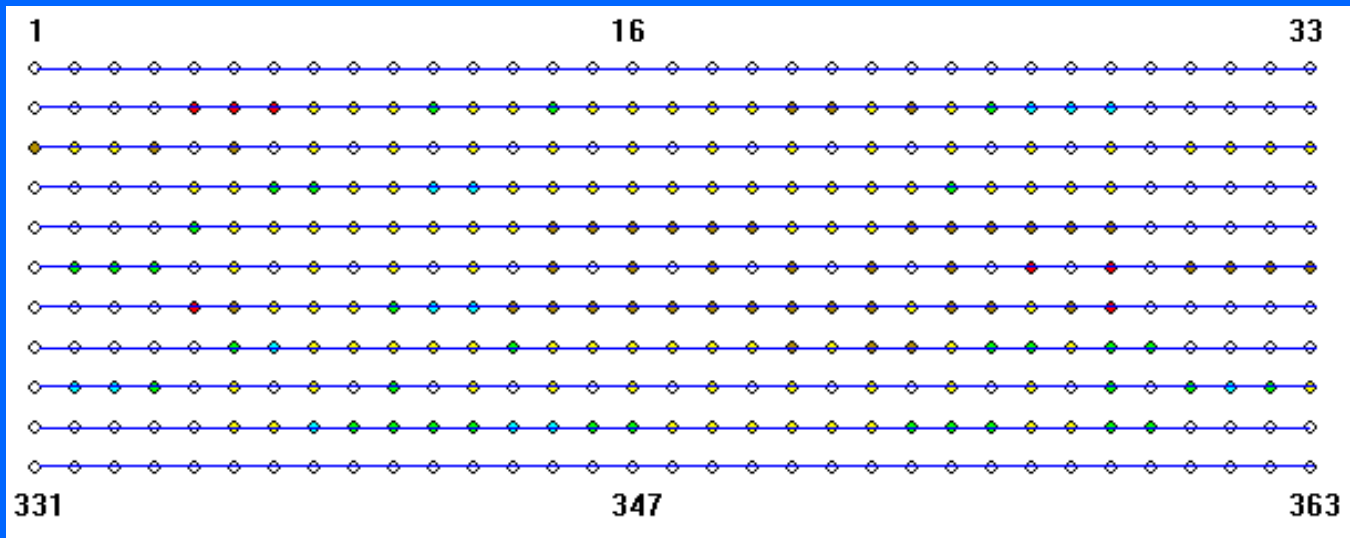

3-D data sets – non-rectangular layouts

Measurements can also be combined from 2-D lines that can run in different directions. This is common when the '3-D' data set was created from old 2-D surveys.

In this example, not only the lines have different directions, they also have different spacings.

Note the model used in this example has smaller cells sizes in the areas with more data, and larger cells towards the left and rights sizes where larger electrode spacings are used.

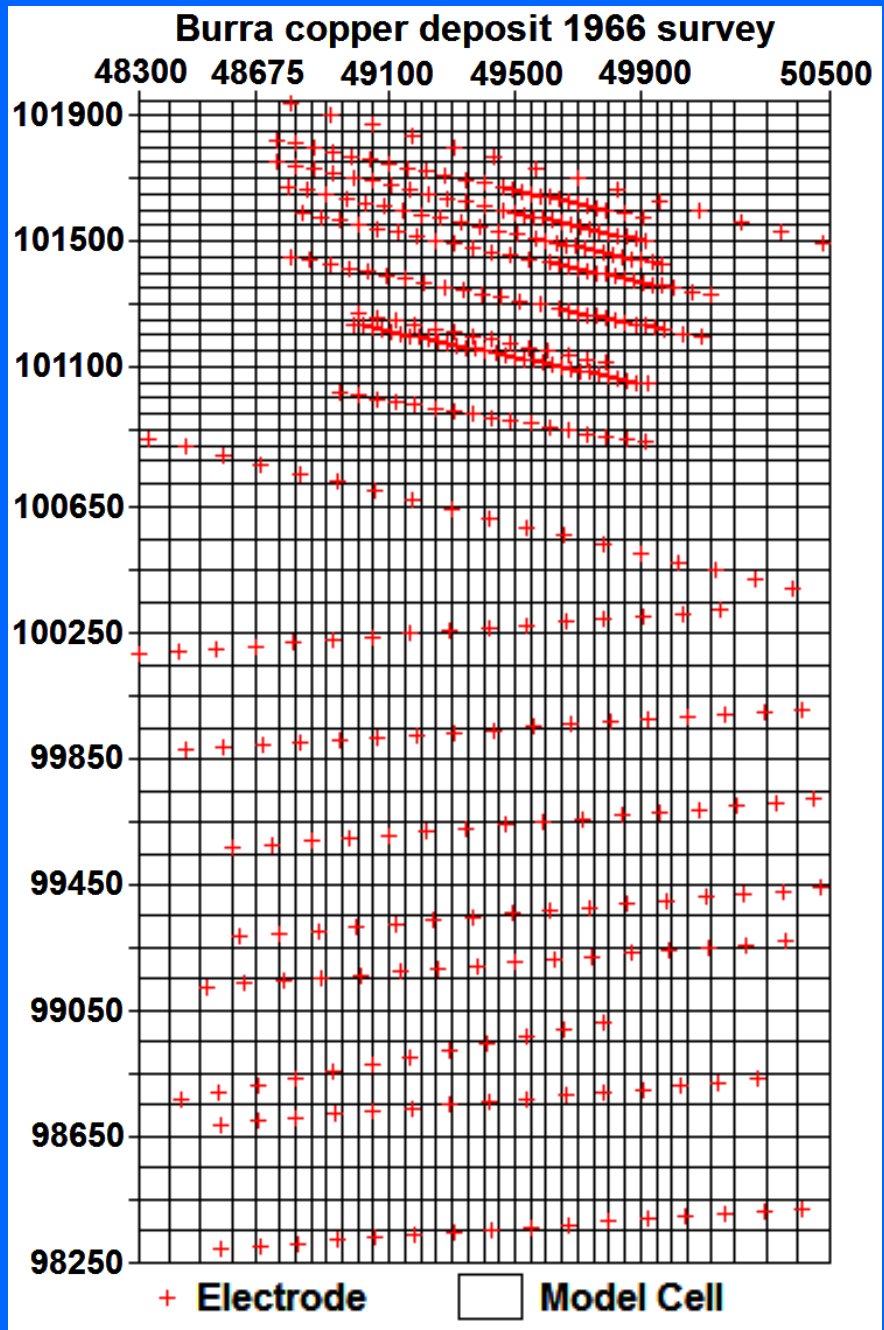

3-D model discretizations

To convert the 3-D of field data set into a resistivity model for the subsurface, we divide the subsurface into a number of blocks. Depending on the complexity of the survey setup, there are a few methods used.

They range from simple rectangular grids, to trapezoidal grids and finally to arbitrary grids.

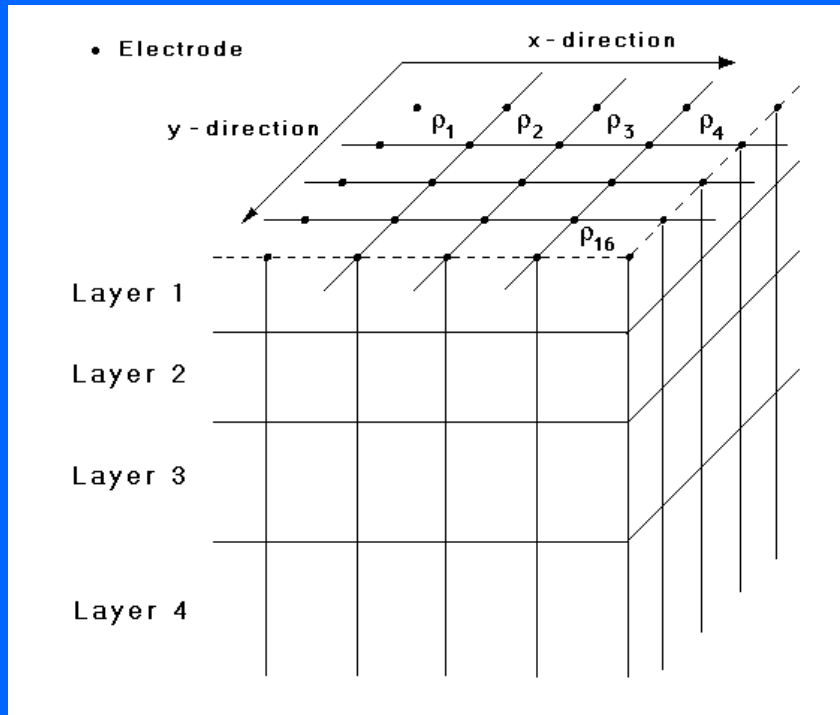

Rectangular and Trapezoidal Grids

A rectangular grid, possibly with non-uniform spacing, can be used when the data was measured using electrodes in a rectangular grid, such as from a series of parallel 2-D lines.

Due to physical obstructions, it is sometimes not possible to run straight survey lines. The next grid model allows for this. It still assumes each line has the same number of electrodes.

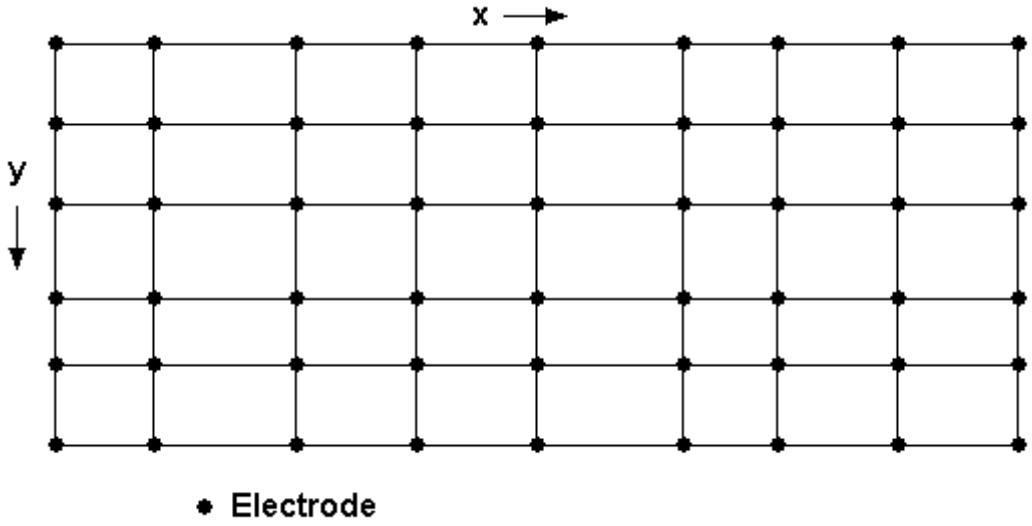

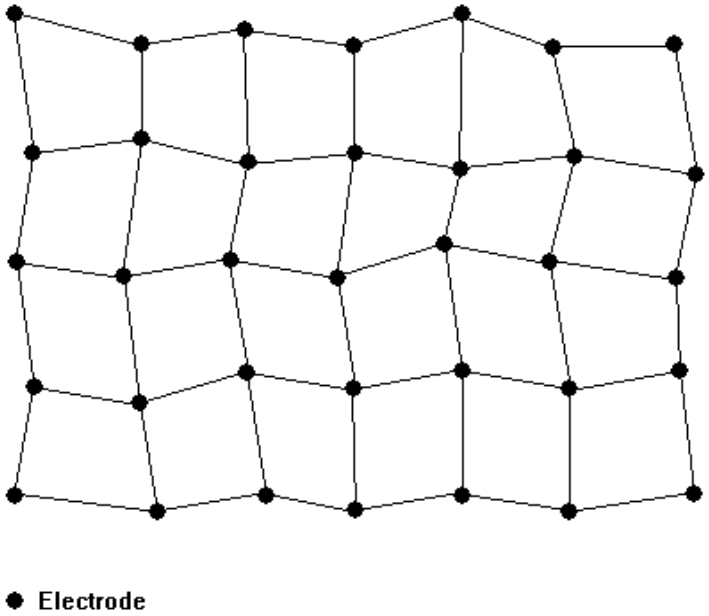

3-D models with arbitrary electrode positions

In some surveys, the positions of the electrodes cannot fit into a simple rectangular or even trapezoidal grid. This situation occurs because of physical obstructions such that straight surveys lines cannot be used, or the data is collated from surveys over different periods. This is particularly common in mineral exploration surveys where there were different survey phases, usually using a series of quasi-parallel 2-D survey lines. It is possible to invert such data sets by separating the model discretization grid from the survey grid.

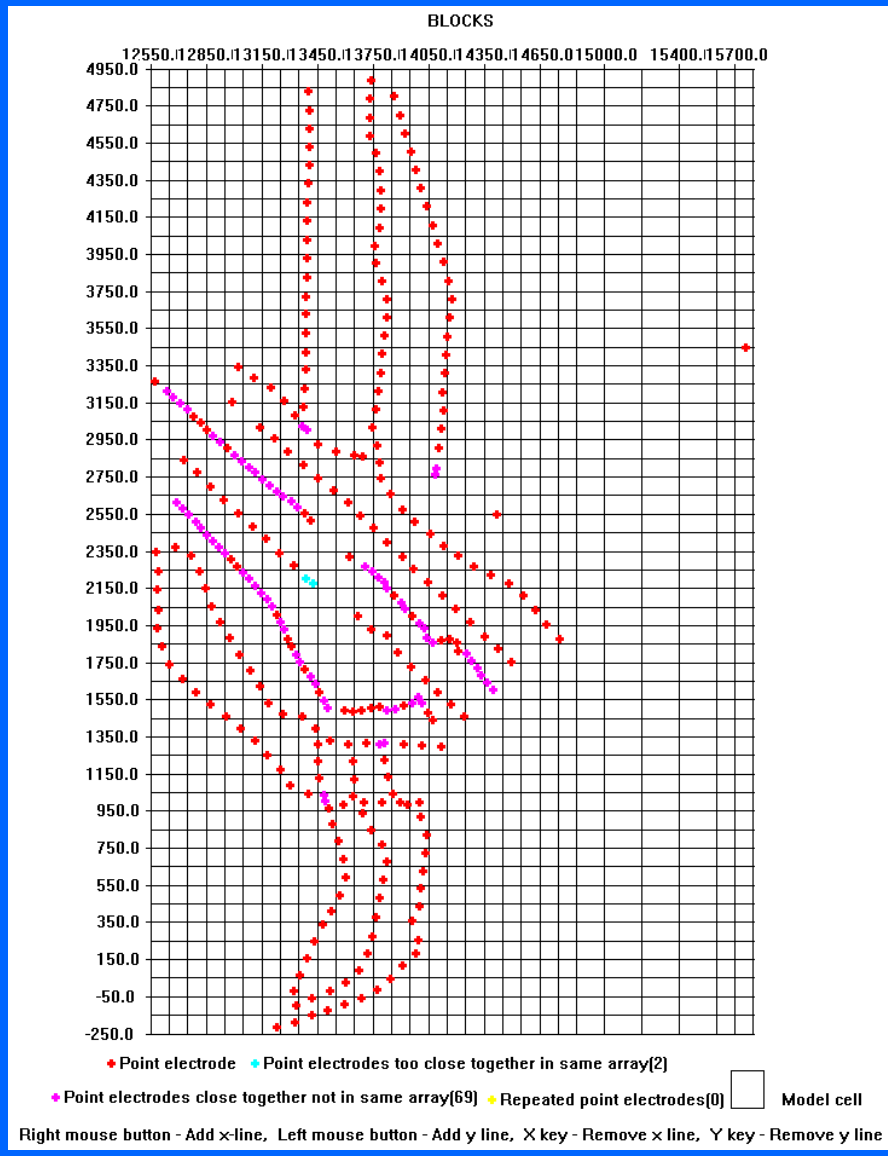

Methods to handle arbitrary electrode positions

There are two methods to model the effect of an electrode at an arbitrary position. The first is to calculate the potential at the electrode by interpolating the potentials at the four nearest nodes in the mesh (and replace a single current electrode by four equivalent current sources). It's advantage is that the finite-difference method can be used (if there is no topography) which requires less computer time and memory than the finite-element method.

The second method moves the nearest node to the location of the electrode using a distorted finite-element mesh. It's advantage is that it gives more accurate results for arrays such as the dipole-dipole that uses small potential differences between electrodes that are close together.

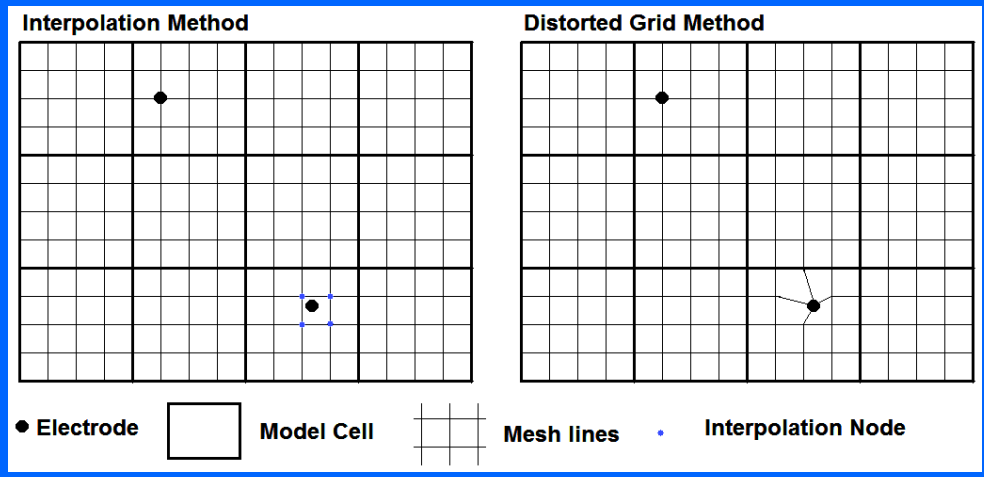

Example field survey with lines in different directions

This example is from the Hanford site where the waste material was stored in trenches and concrete cribs. Different resistivity survey phases were carried out using 2-D lines. The distribution of the electrodes does not fit into a simple rectangular grid. This data set had 5598 electrode positions and 86697 data points. The pole-pole array was used in this survey. While most of the lines used an electrode spacing of 3 meters, there were some readings that had closer spacings due to survey site constraints.

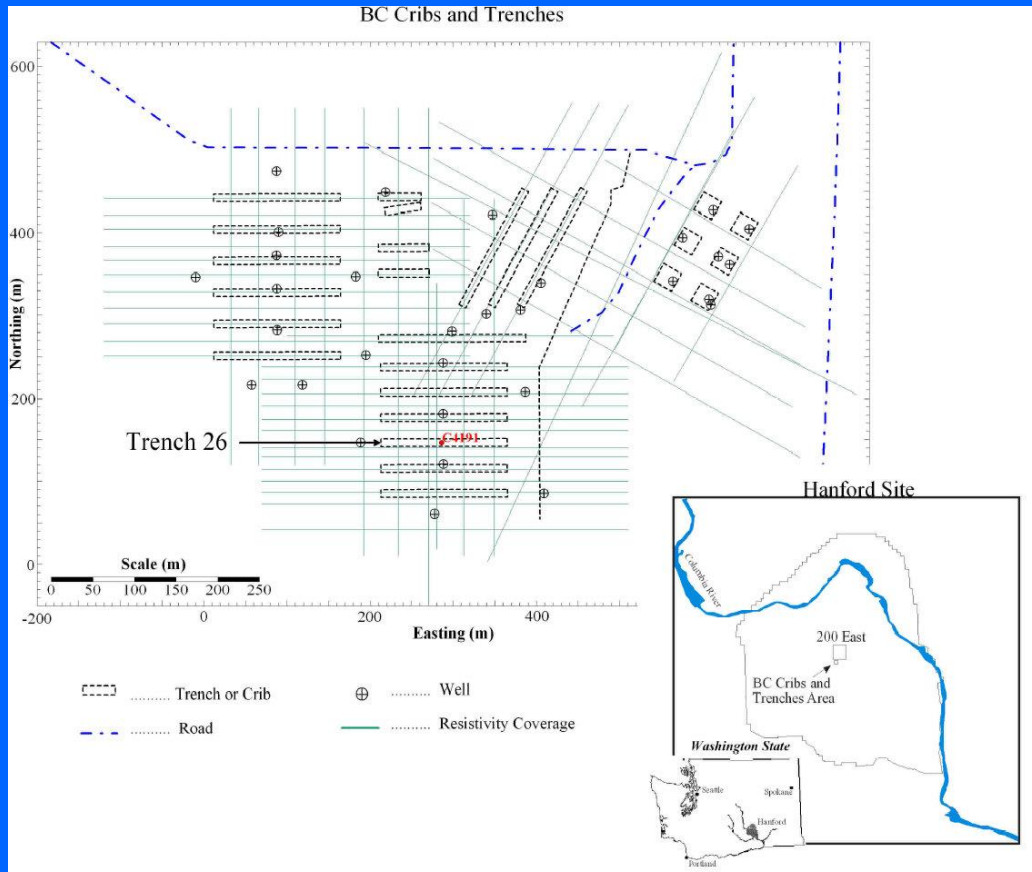

Inversion model for Hanford data set

Below is an inversion model of the data set. Note the prominent low resistivity zones indicating leakage zones. The linear features in the 2nd and 3rd layers are due to the trenches and concrete cribs.

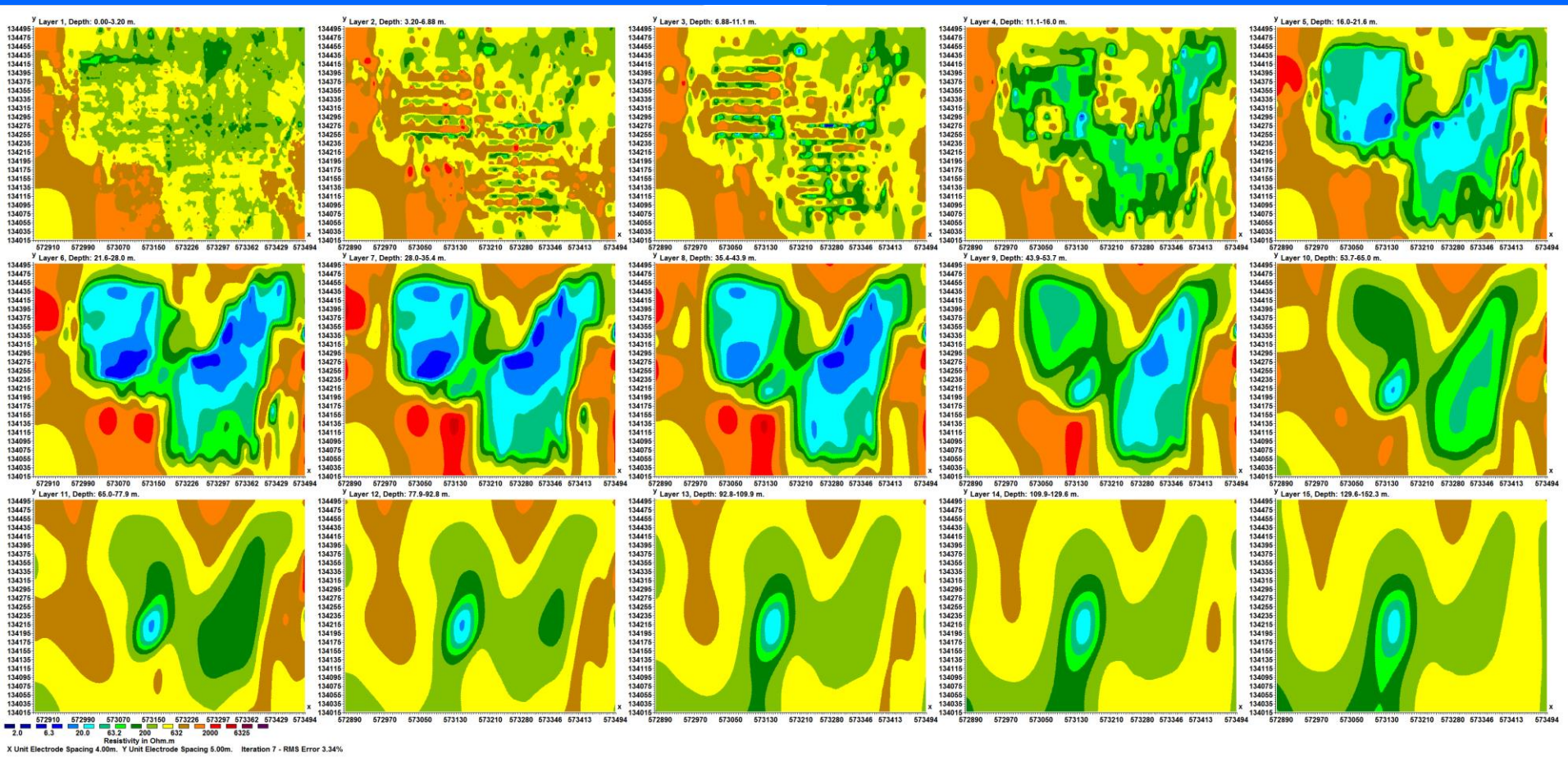

3-D electrical imaging surveys : Summary

3-D surveys now play an increasingly important role in very complex areas, particularly for mineral exploration where the extra cost is justified. In many cases the 3-D data set is collated from a series of parallel 2-D survey lines to reduce the survey time and cost.

The pole-dipole and dipole-dipole arrays are widely used in mineral exploration surveys particularly with multi-channel I.P. systems. The Wenner-Schlumberger array is used in many engineering and environmental surveys, although the multiple gradient array will play an increasingly important role with multi-channel multi-electrode systems.

Fast computer software, and PCs with multi-core CPUs or multiple CPUs and at least 32 GB RAM, have reduced the computer processing time such that it has become practical to process 3-D data sets with thousands of electrode position, tens of thousands of measurements and model cells within hours.

3-D Case Histories

Examples of 3-D field surveys

Example 1 – Landfill site, Sweden

The surveyed area is a former sludge disposal site, where liquid industrial waste was disposed in several shallow ponds. The site was later covered by earth resulting in a more or less flat surface. The site is situated in southern Sweden, at the abutment of the Öresund bridge, and has been previously investigated with DC resistivity imaging and electromagnetic profiling.

The figure below shows a geological cross-section of the survey site. Note the mound from the construction of the landfill site, and the boundary between the brackish and fresh water.

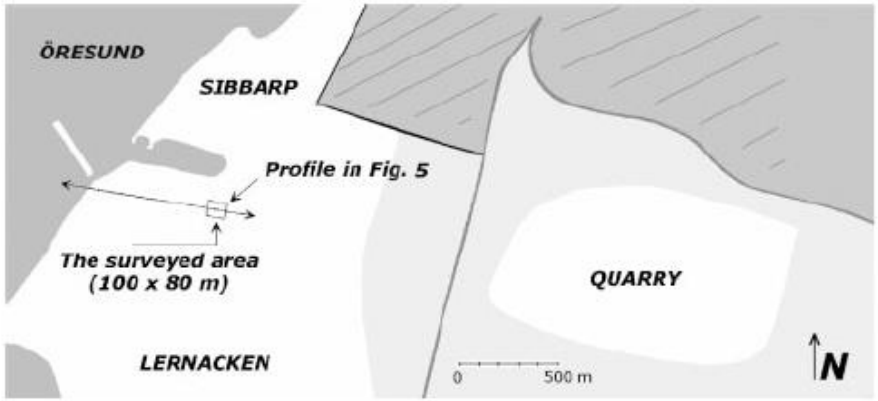

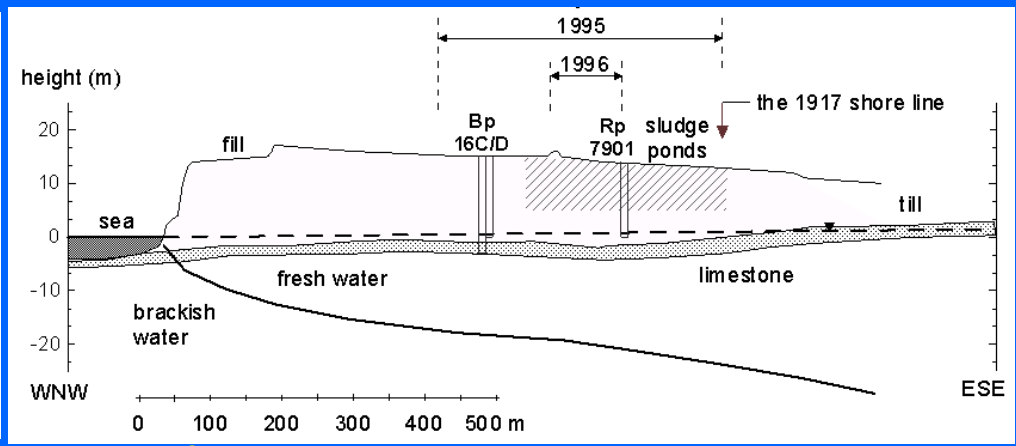

Dahlin, T., Bernstone, C. and Loke, M.H., 2002, A 3D resistivity investigation of a contaminated site at Lernacken in Sweden. Geophysics, 67, 1692-1700.

Example 1 - Field survey procedure

The Abem system was used with 3 cables each with 21 electrodes. The pole-pole array was used. The roll-along method in a direction perpendicular to the lines was carried out to extend the survey coverage.

Seven parallel multi-electrode cables were used to cover a 21 by 17 grid with a 5 metres spacing between adjacent electrodes. There were a total number of 3840 data points in this data set.

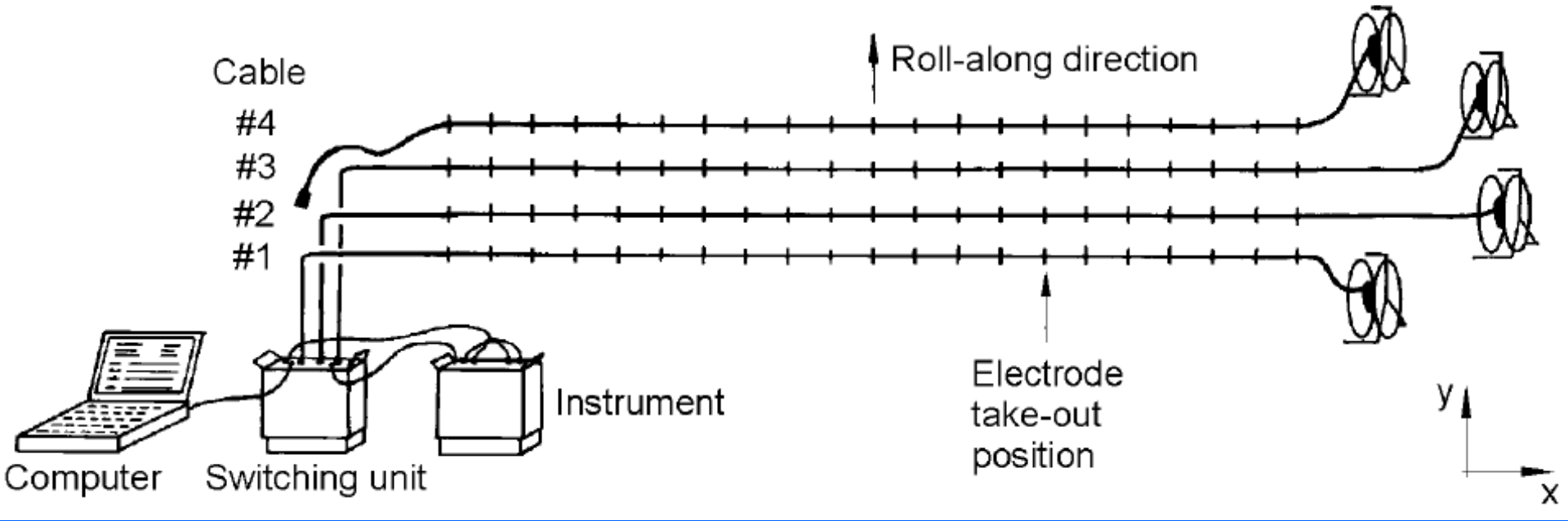

Example 1 – Landfill site, Sweden (model depth sections)

The model obtained from the inversion of this data set is shown below. The former sludge ponds containing highly contaminated ground water show up as low resistivity zones in the top two layers. This was confirmed by chemical analysis of samples. The low resistivity areas in the bottom two layers are due to saline water from a nearby sea.

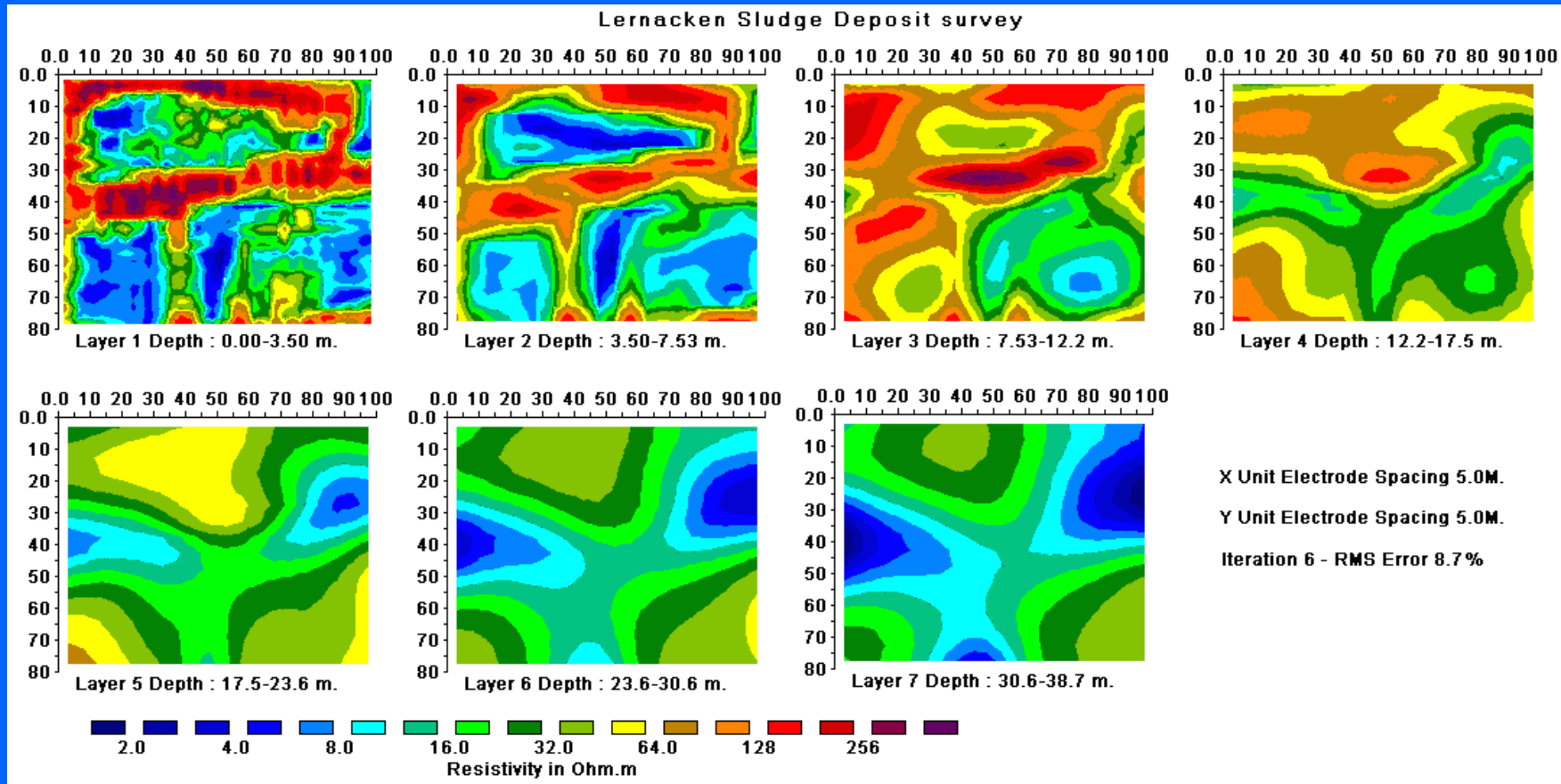

Example 1 – Landfill site, Sweden (Model 3-D view)

The figure below shows a 3-D plot of the inversion model using a 3-D contouring program.

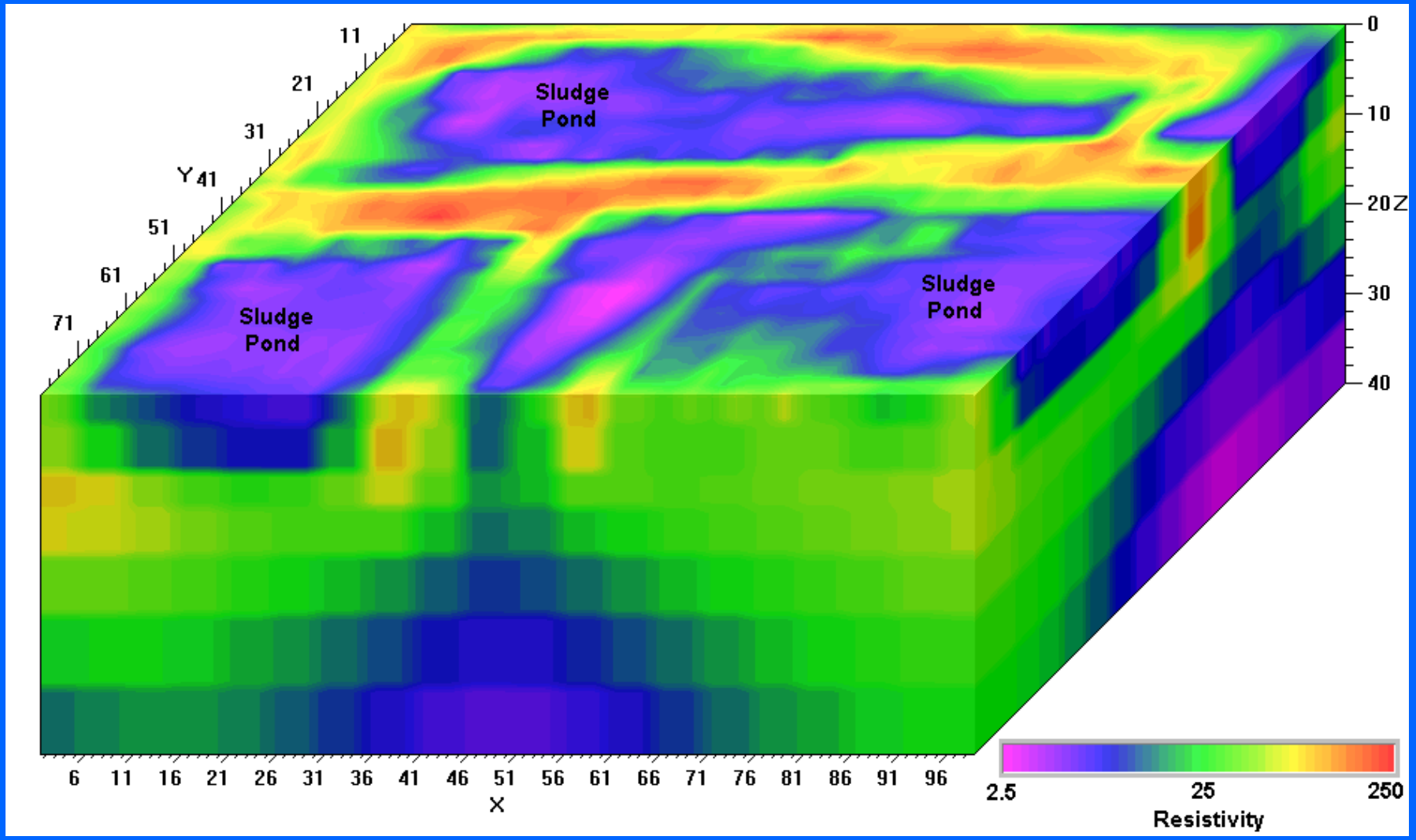

Example 2 – Base metal deposit, Australia (location)

Copper Hill is the oldest copper mine in NSW, Australia. An earlier survey was conducted in 1966 using mapping, rock chip sampling, an I.P. survey and 7 drill-holes. Gold and copper were found to occur in structurally controlled fractures and quartz veins. However, due to the very complex geology, large differences in ore grades were found in drill-holes that were less than 200 meters apart.

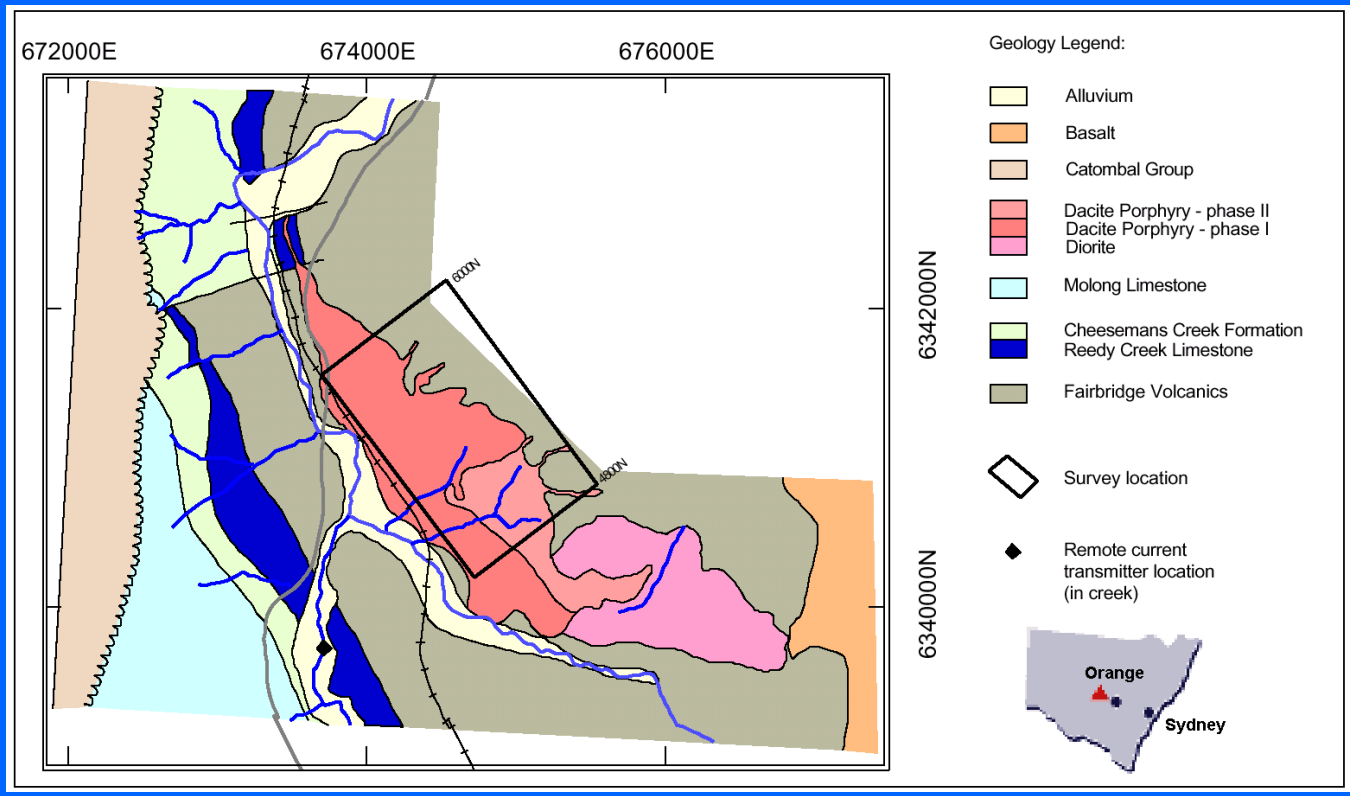

Denne, R., Collin, S., Brown, P., Hee, R. and White, R.M.S. 2001. A new survey design for 3D IP inversion modelling at Copper hill. ASEG 15th Geophysical Conference and Exhibition, August 2001, Brisbane.

Example 2 – Base metal deposit, Australia (survey)

To map the ore deposit more accurately, a new 3-D resistivity and I.P. survey using the offset pole-dipole array was used. The survey covered a large (1.6 x 1.1km) area using a series of 1.6 km lines with a spacing of 25m between adjacent electrodes. The figure below shows the survey layout. Currents of up to 7 Amps were used. The entire survey took 10 days giving a total of over 7000 measurements.

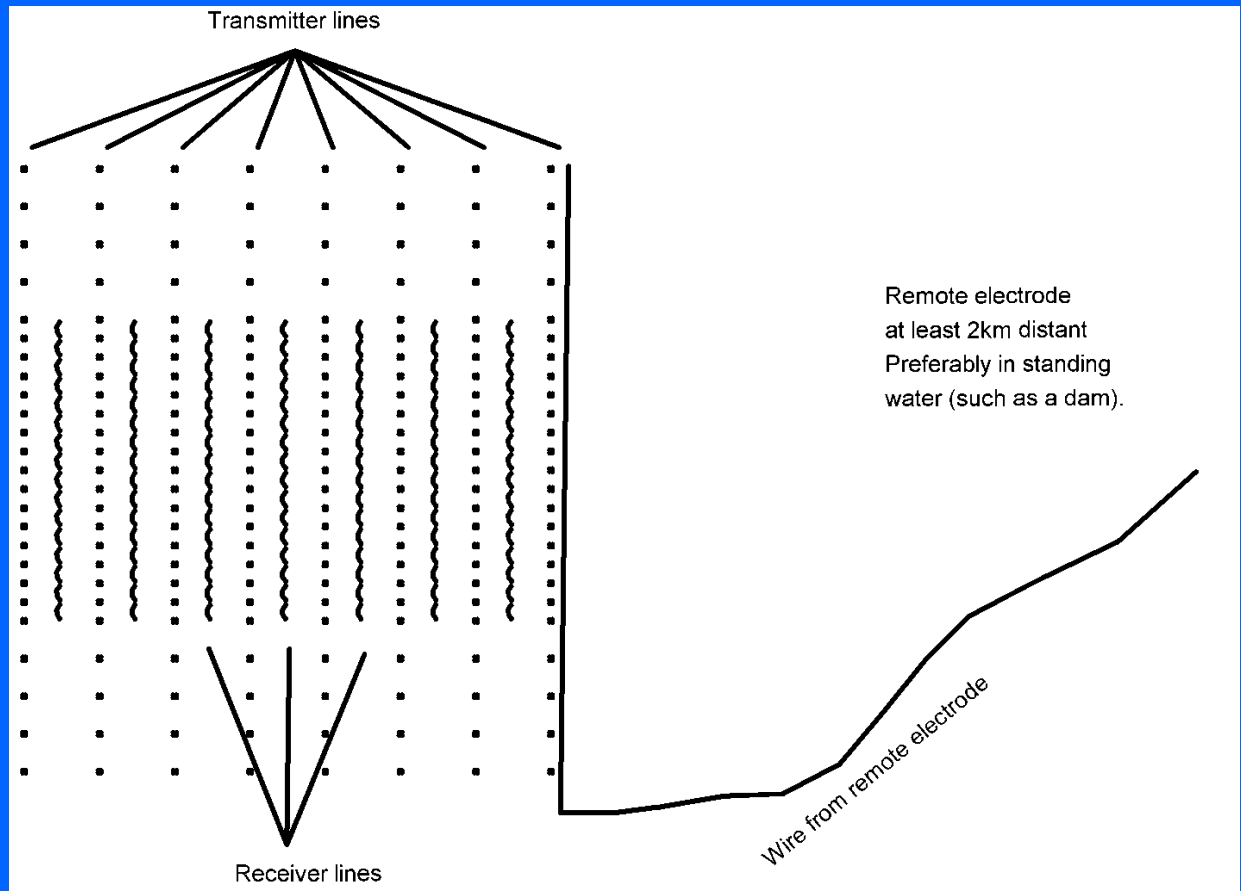

Example 2 – Base metal deposit, Australia (3-D model)

The 3-D I.P. model shows two north-south trends and two approximately east-west trends forming an annular zone of high chargeability. The results from existing drill-holes which had targeted the shallower part of the western zone agrees well with the resistivity and IP model. A drill-hole, CHRC58, intersected a 217m zone with 1.7 g/t gold and 0.72% copper coincided well an an I.P. zone of greater than 35mV/V.

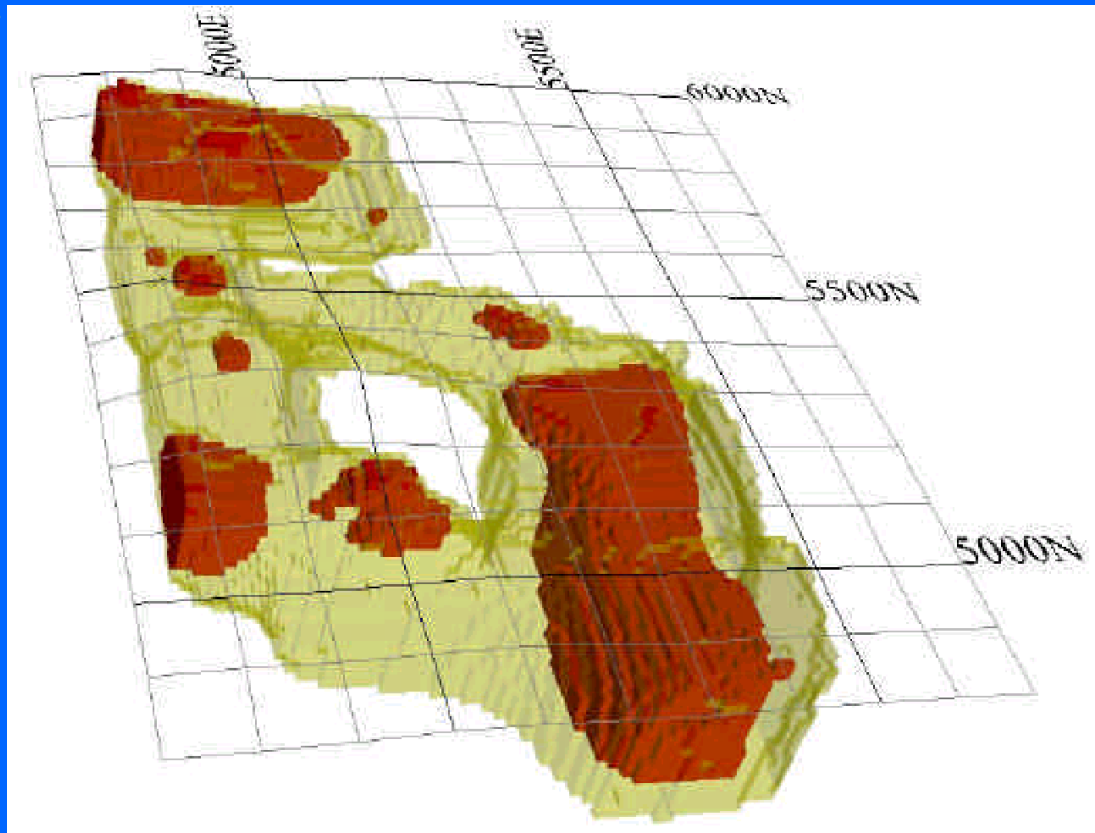

Part 5

4-D surveys data and inversion

Time-lapse surveys

The measurements are repeated on the same site, using the same survey parameters, at different times. The surveys can be repeated along 2-D lines, or a grid of electrodes for a 3-D survey. The purpose is to monitor changes of the subsurface resistivity with time. Examples include mapping the flow of contaminants, change of water saturation due to water extraction, flow of water from the surface to the water table, production of methane gas in landfills, geological changes such as landslides.

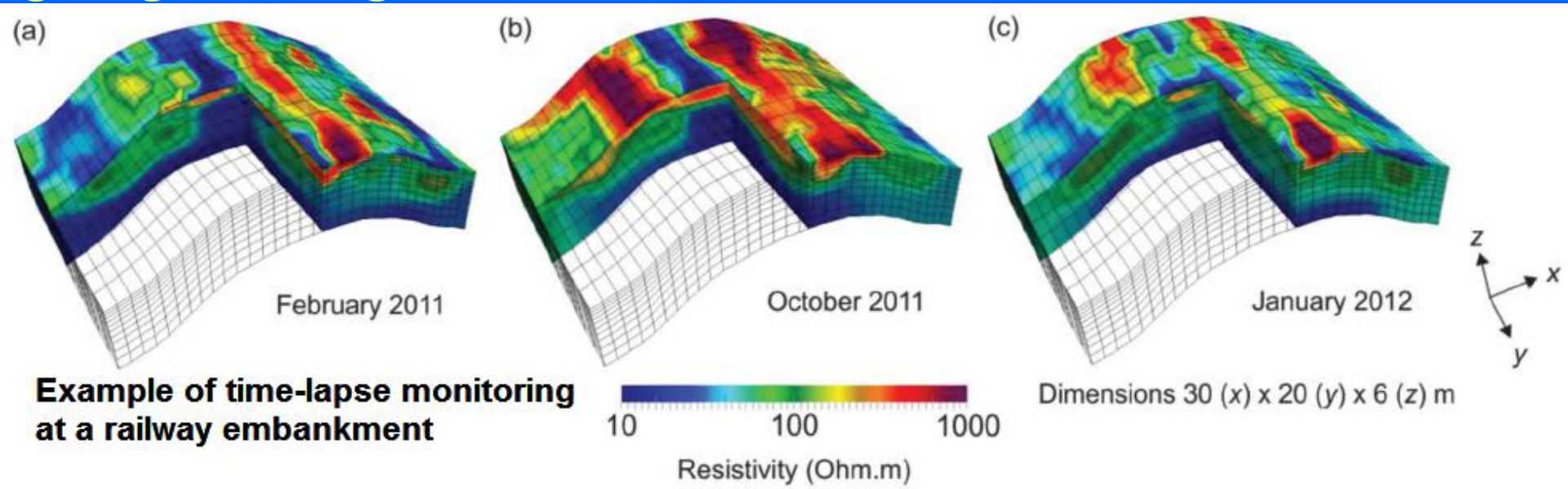

After Chambers, J.E., Gunn, D.A., Wilkinson, P.B., Meldrum, P.I., Haslam, E., Holyoake, S., Kirkham, M., Kuras, O., Merritt,A. and J. Wragg. 2014. 4D electrical resistivity tomography monitoring of soil moisture dynamics in an operational railway embankment. Near Surface Geophysics, 12, 61-72.

Time-lapse surveys - inversion

The data from surveys at different times are inverted jointly using a constraint to minimize the change in the resistivity with time. We make use of the fact that the changes usually occur in a smooth manner with time. The equation used is as follows. $$\left[\mathbf{J}_i^T\mathbf{J}_i + \lambda_i\left(\mathbf{W}^T\mathbf{W} + \alpha\mathbf{M}^T\mathbf{M}\right)\right]\Delta\mathbf{r}_i = \mathbf{J}_i^T\mathbf{g}_i - \lambda_i\left(\mathbf{W}^T\mathbf{W} + \alpha\mathbf{M}^T\mathbf{M}\right)\mathbf{r}_{i-1}$$

The time domain is incorporated into the regularization procedure through the **M** difference matrix that is applied across the time models. It minimizes the difference in the resistivity of each model cell and the corresponding cell for the next temporal model. The parameter α is the temporal damping factor that gives the relative weight for minimizing the change in the resistivity between one temporal model and the next model.

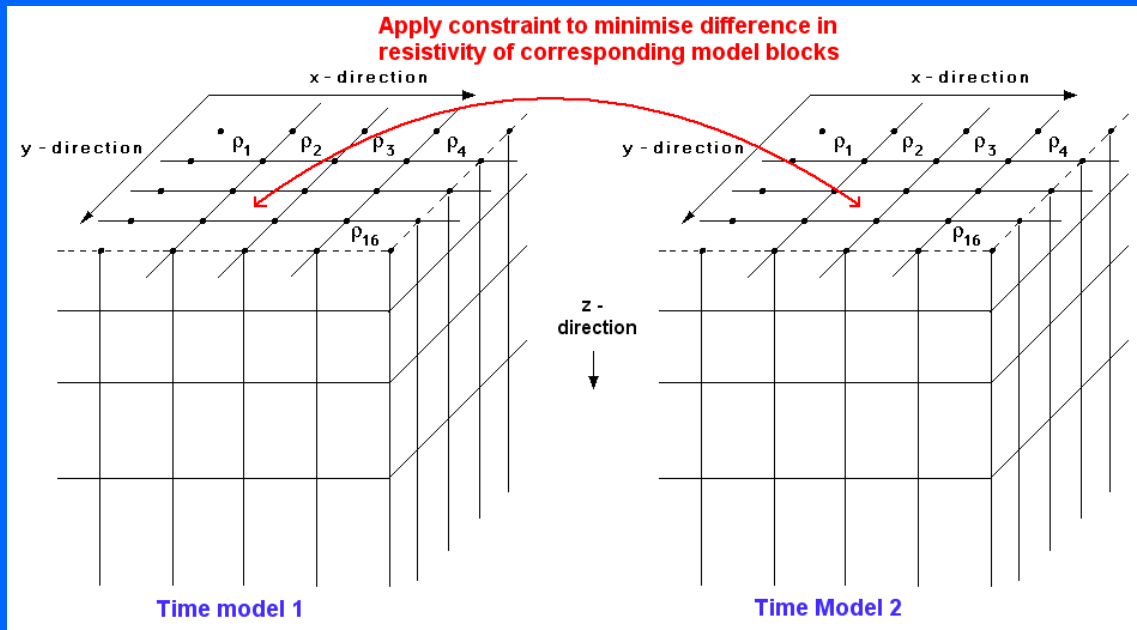

4-D Case Histories

Example of 4-D field survey

Example 1 : Pumping test at Hoveringham area, U.K.

This survey was from an experiment to map the change in the groundwater level during a pumping test in a farm in Western Central England.

Water was pumped for about 220 minutes from a borehole. Measurements were made before, during and after the pumping.

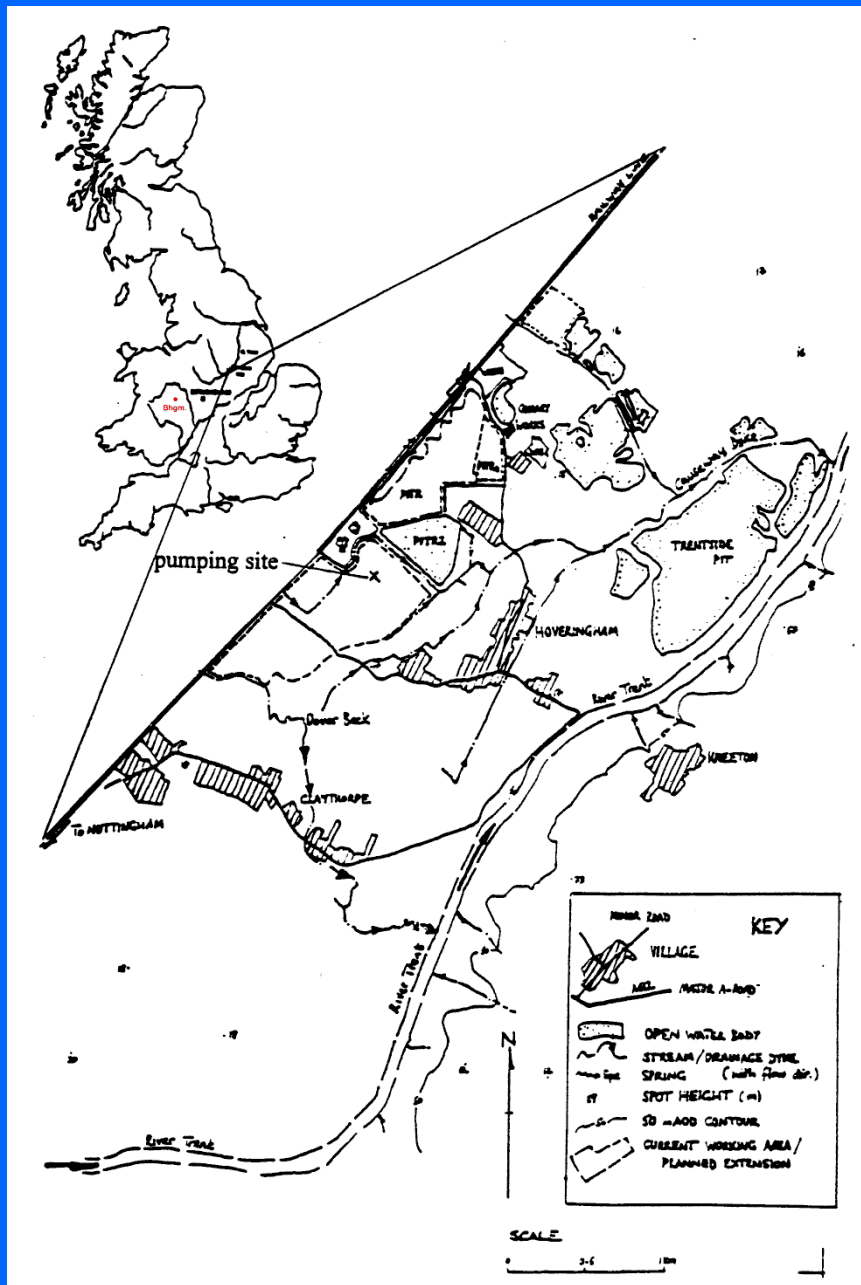

Hoveringham data set – data and models

(a) Apparent resistivity pseudosection and

(b) inversion model for data set before the start of the pumping test.

(c) Apparent resistivity pseudosection and

(d) inversion model for data set after 220 minutes of continuous pumping.

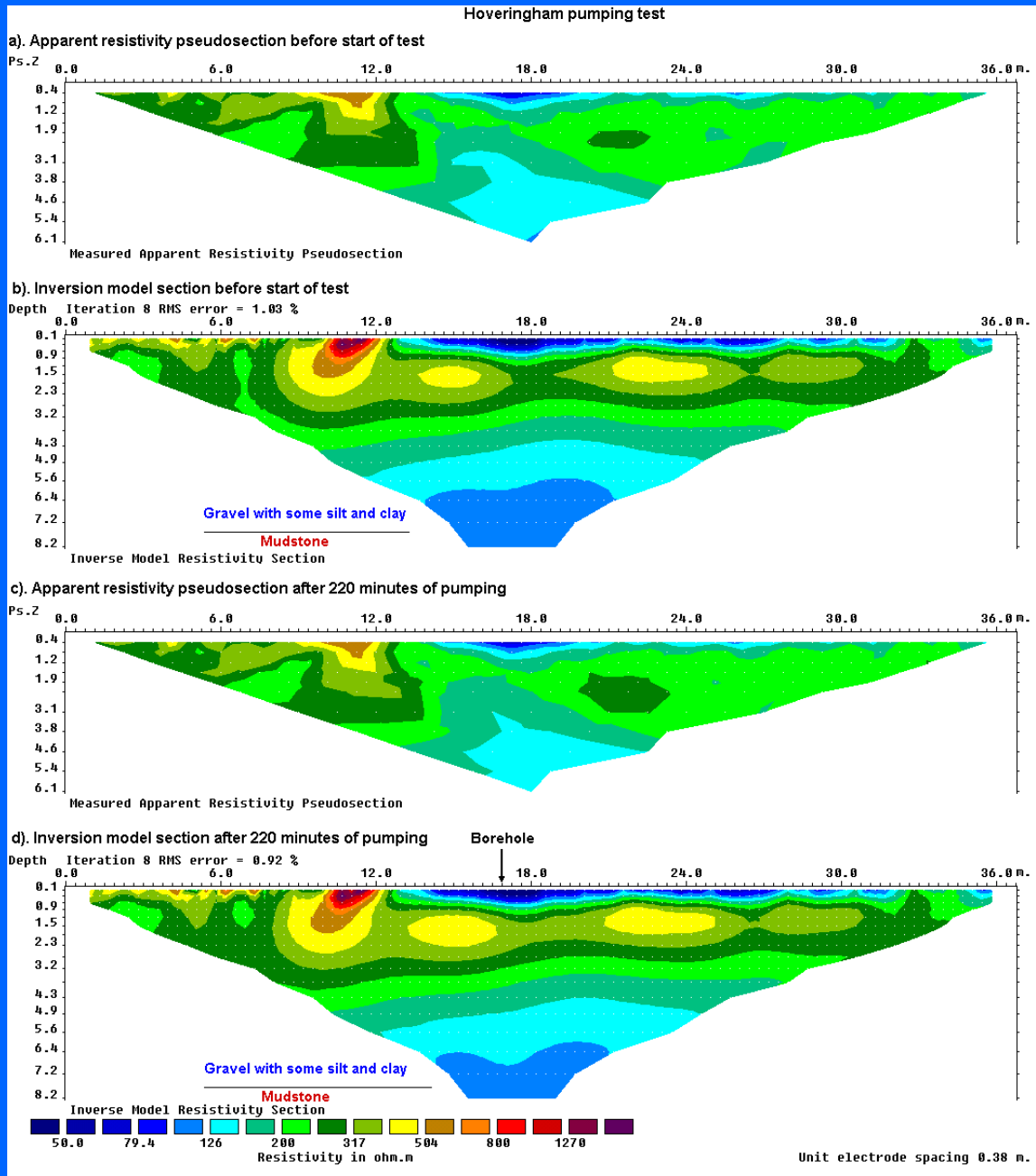

Hoveringham data set : change in resistivity

To show the change in resistivity more clearly, we take the difference in the logarithm of the model resistivity values.

Sections showing the percentage relative change in the subsurface resistivity values with time obtained from the inversion of the data sets collected during the different stages of the Hoveringham pumping test.

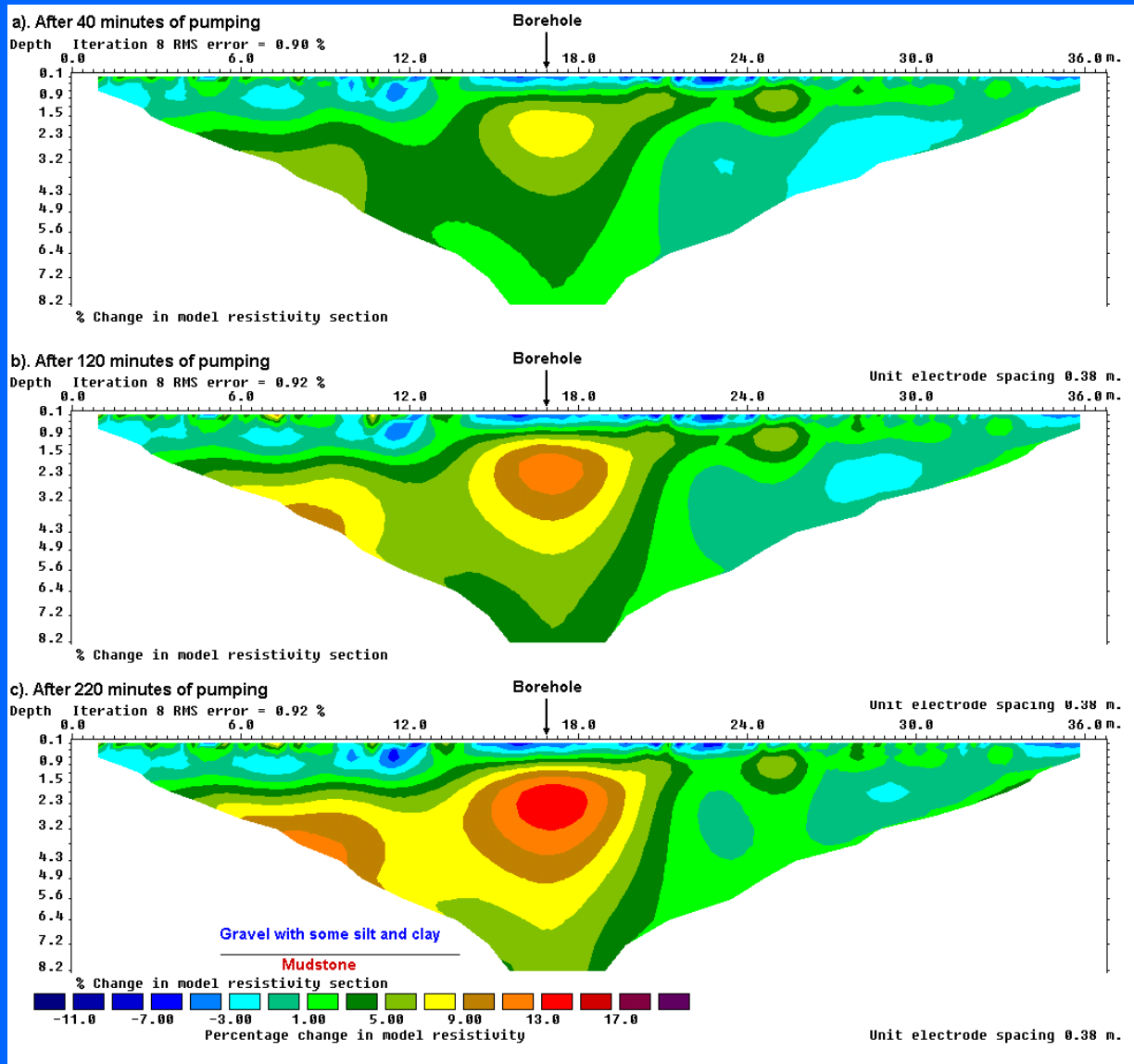

Hoveringham data set : change in saturation

We can also calculate the change in the water saturation from the change in the resistivity using Archie's Law.

Sections showing the percentage desaturation values obtained from the inversion models of the data sets collected during the different stages of the pumping test.

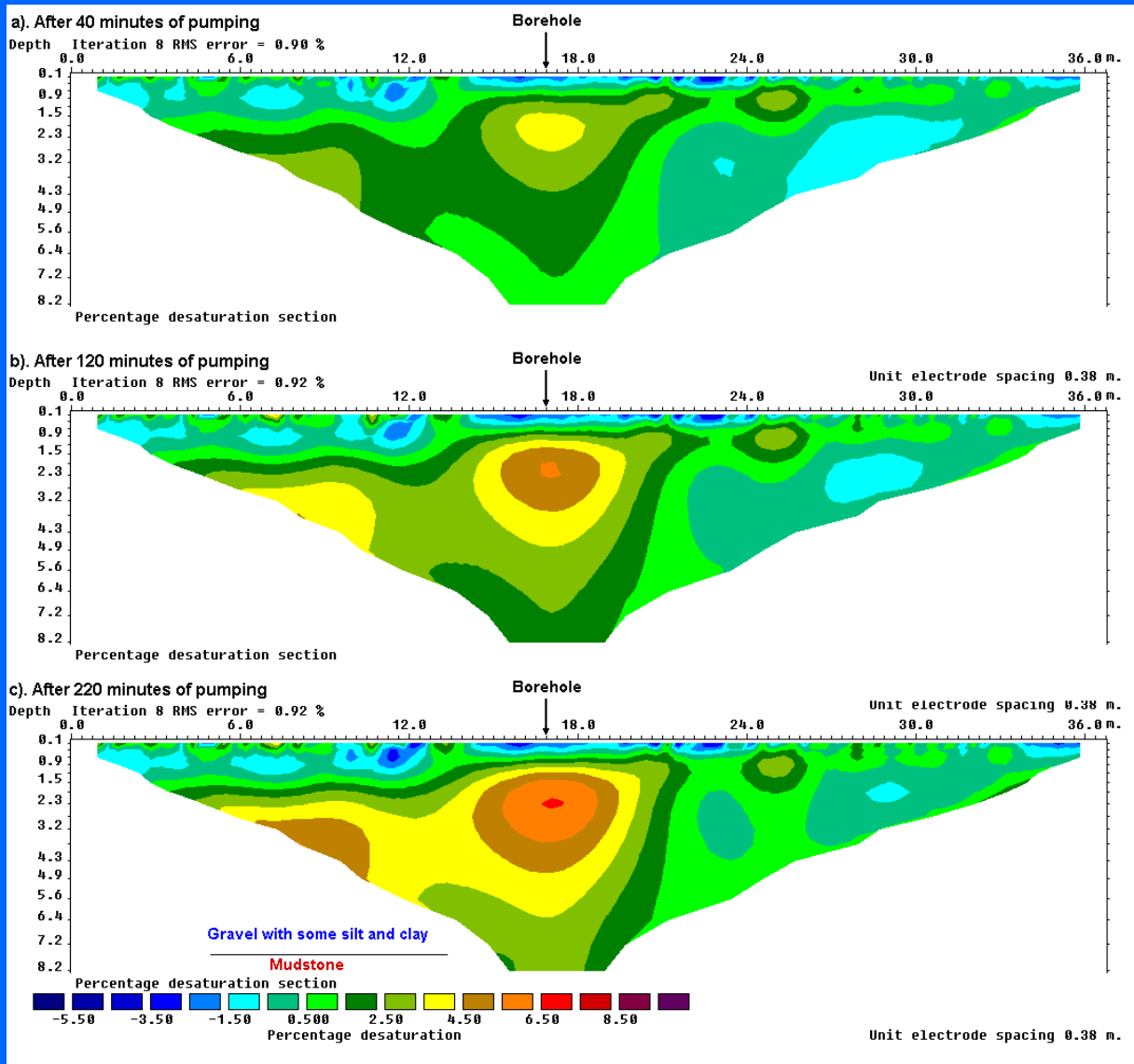

Closing remarks on 2-D, 3-D and 4-D surveys

2-D surveys constitute the bulk of field surveys. They are simple and inexpensive to carry out. Using model cells with widths of half the unit electrode spacing seems to give the best results. The inversion settings that control of nature of the model should be selected based on available information about the subsurface.

3-D surveys are necessary to resolve complex structures. Most 3-D data sets are collated from 2-D surveys lines that are sufficiently close to each other. This provides a practical method to obtain a 3-D model of the subsurface in an inexpensive manner. Ideally, the distance between the lines should not be more than 2 times the inline electrode spacing.

4-D surveys are used to map temporal changes in areas such as landslide monitoring, subsurface movement of fluids. A coupled least-squares inversion method reduces inversion artefacts from noise.

Break for questions and discussion

Part 6

Special Topics.

1). Least-squares inversion theory and methods

2). Banding effects in 3-D surveys

3). Model reliability

Least-squares inversion theory and methods

Why we carry out inversions, the least-squares optimization method with different constraints and their effects on the model.

What is inversion?

The purpose of an inversion program is to convert the apparent resistivity values into the true resistivity of the subsurface.

$$\rho_a \rightarrow \rho_{true}$$

The relationship between the apparent resistivity and the true resistivity is a very complex relationship. It depends on whether the subsurface is assumed to be 1-D, 2-D or 3-D.

We first must define what is meant by '<u>data</u>' and '<u>model</u>'.

Example of a typical 1-D inversion.

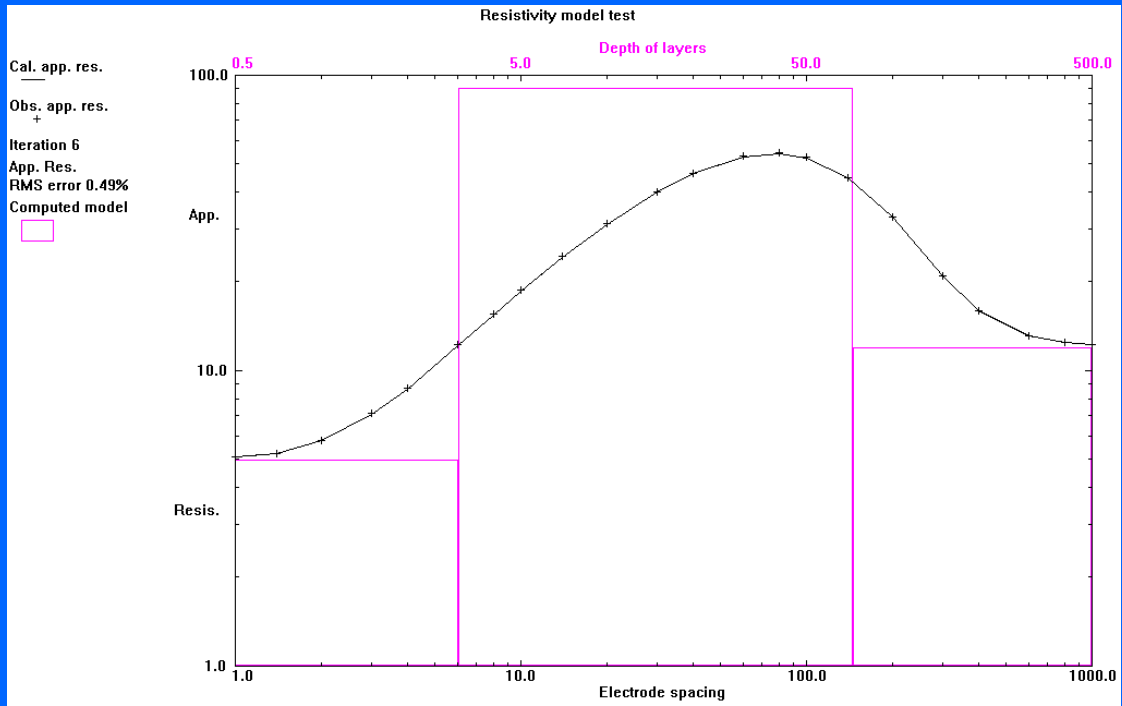

Data and models

Data (y) :- What we measure in an experiment.

Model (q) :- The physical quantity we want to estimate from the data. The model usually has more than one value – parameters.

The connection between them : Model response (f) :- A mathematical relationship between the model and data.

Simple case of measurement on a homogeneous half-space with Wenner array. Data = V/I = R. Model = ρ.

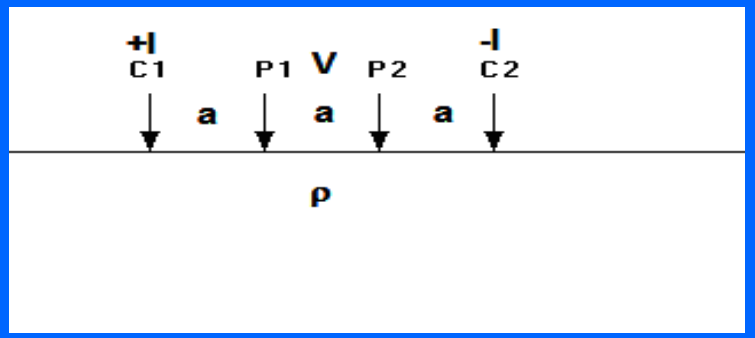

Model response : $R = \rho / 2\pi a$

The model response equation has a simple linear form, so a direct inversion is possible.

Inversion equation : $\rho = 2\pi a R$

Types of models

Model (q) :- The physical quantity we want to estimate from the data. We use 1-D, 2-D and 3-D models.

1-D models – Thickness can be allowed to vary (few layers), or fixed (many layers).

2-D and 3-D models – Usually only the cells resistivity is allowed to vary.

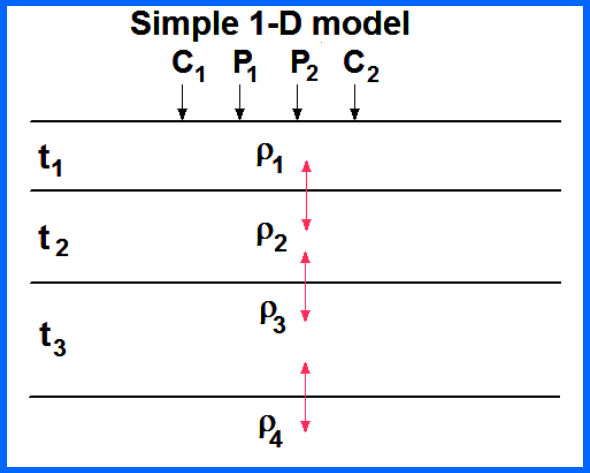

2-D model with fixed cell sizes and positions, and variable resistivity

ρ_1	ρ_2	ρ_3								
ρ_{13}										
ρ_{25}										
ρ_{37}										
ρ_{49}										
ρ_{61}										ρ_{72}

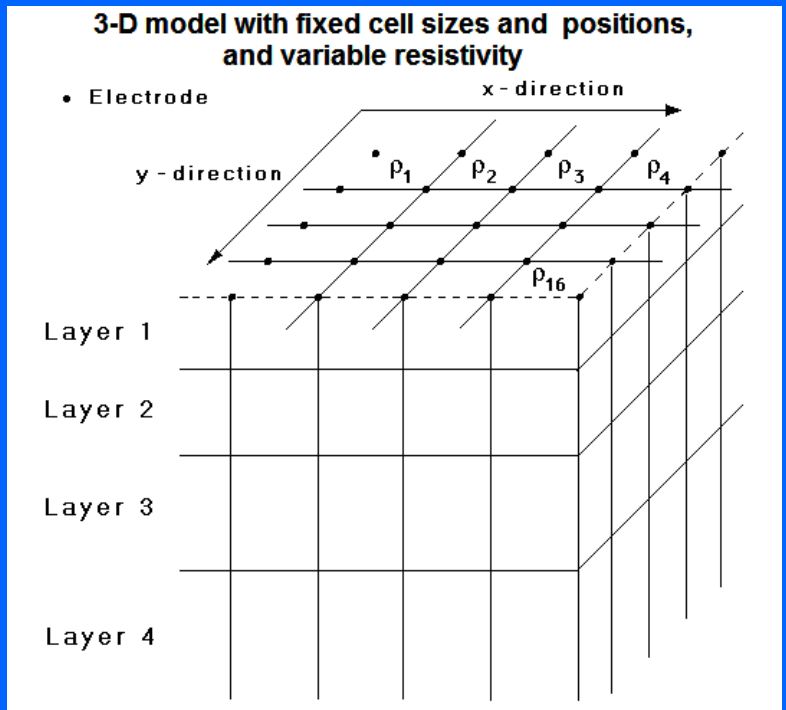

1-D layered earth model – nonlinear model response

Unfortunately other than the case of a homogeneous half-space, the relationship between the model parameters and the data is a complex non-linear equation, even in the case of a simple 1-D layered model. It is given as an integral of Bessel functions.

$$\varphi_l\left(r_S^h, z\right) = \frac{\rho_1 I}{2\pi}\int_0^{+\infty}\left(\left(1 + a_l\left(\theta\right)\right)\mathrm{e}^{-\theta z} + b_l\left(\theta\right)\mathrm{e}^{\theta z}\right)\mathrm{J}_0\left(\theta r_S^h\right)d\theta$$

For 2-D and 3-D models the finite-difference or finite-element is normally used to calculate the apparent resistivity values, thus there is no simple analytical formula.

Thus a non-linear iterative method is normally used to derive the model parameters from the survey measurements.

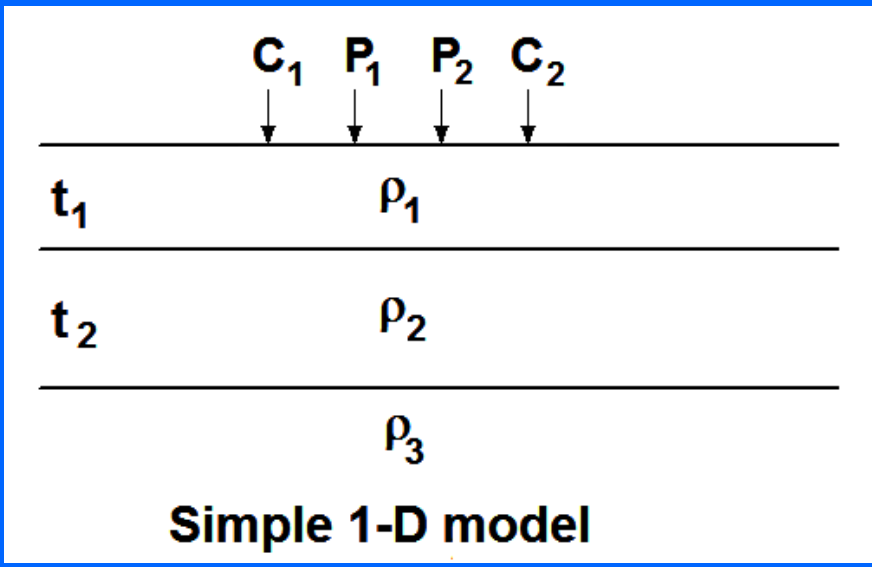

Simple 1-D model

Inversion and optimization

All inversion methods try to determine a model for the subsurface whose response agrees with the measured data subject to certain restrictions. The model parameters are the resistivity values of the model cells, while the data is the measured apparent resistivity values. We want to find a model that reduces the difference or data misfit , $\mathbf{g = y - f}$, between the calculated (f) and measured (y) apparent resistivity values is reduced. If the difference is sufficiently small, then we have an 'acceptable' model. In resistivity problems, we normally use the logarithm of the resistivity.

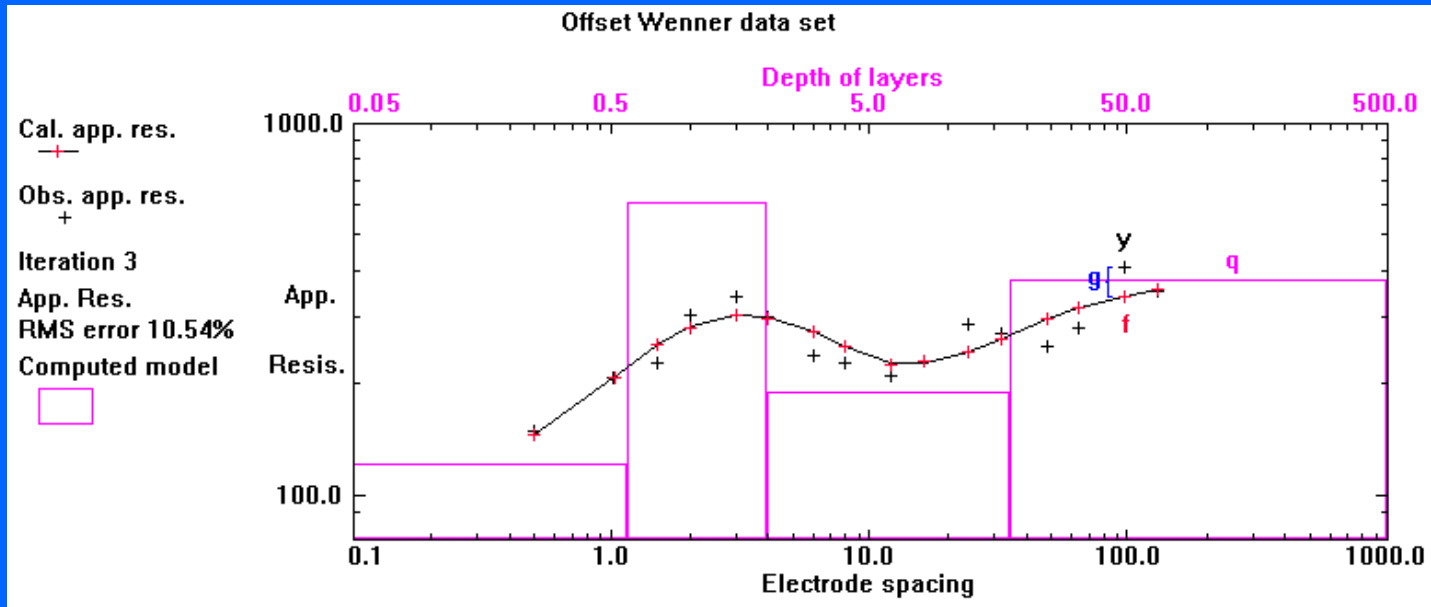

Example of measured and calculated apparent resistivity

We first use a 1-D sounding survey that makes it easier to illustrate the different quantities. In this case

y = input data is the (log) measured apparent resistivity values

f = model response, (log) calculated apparent resistivity values

g = **y** – **f** = data misfit, difference between (log) measured and calculated apparent resistivity values

q = model parameters, the (logarithm of) resistivity and thickness of layers that we want to adjust so as to reduce **g**

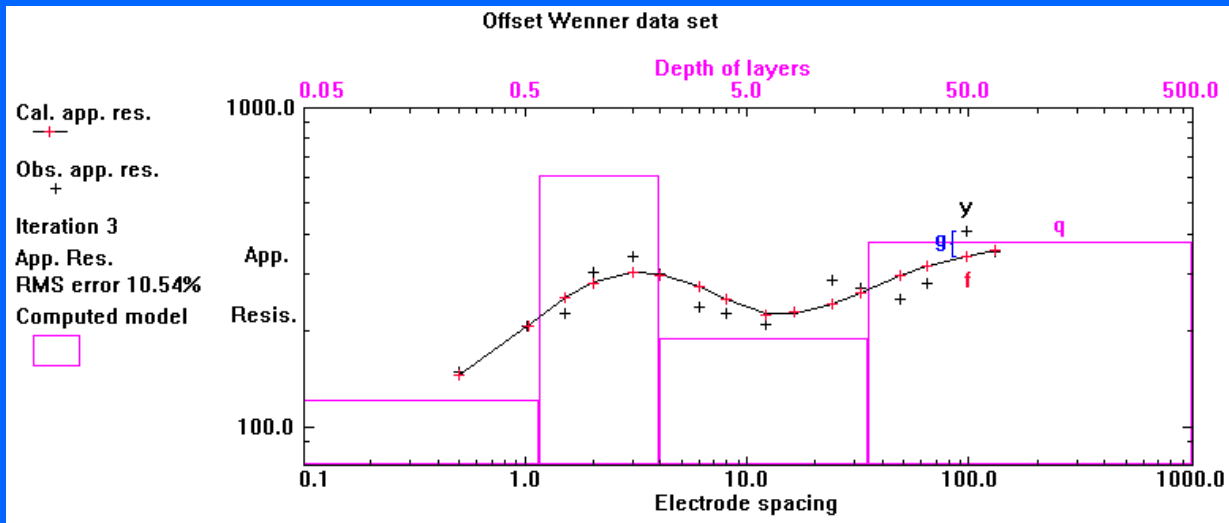

The least-squares criterion

A data set has a number of measurements. A common method to quantify the accuracy of a model is by using the sum of squares error ***E***. This is calculated by summing the square of the difference between the model response and the observed data values (**g = y - f**).

$$E = \mathbf{g}^{\mathrm{T}}\mathbf{g} = \sum_{\mathbf{i}=1}^{\mathbf{n}} g_{\mathbf{i}}^{2}$$

where **n** is the number of data points. When ***E*** is small, the model obtained (**q**) is a possible solution.

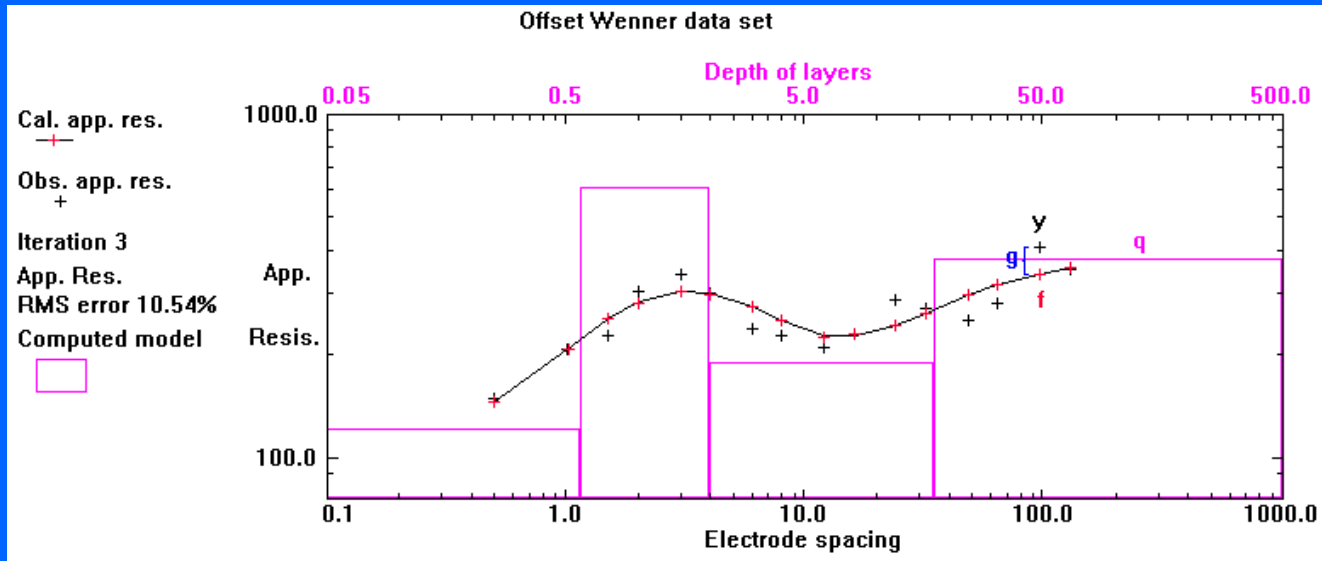

The iterative inversion algorithm

The simplest initial model q_0 is a homogenous earth model, set to the average apparent resistivity value.

The main difference in an inversion method is in step 4, i.e. the method used to determine the change in the model Δq that should improve the current model.

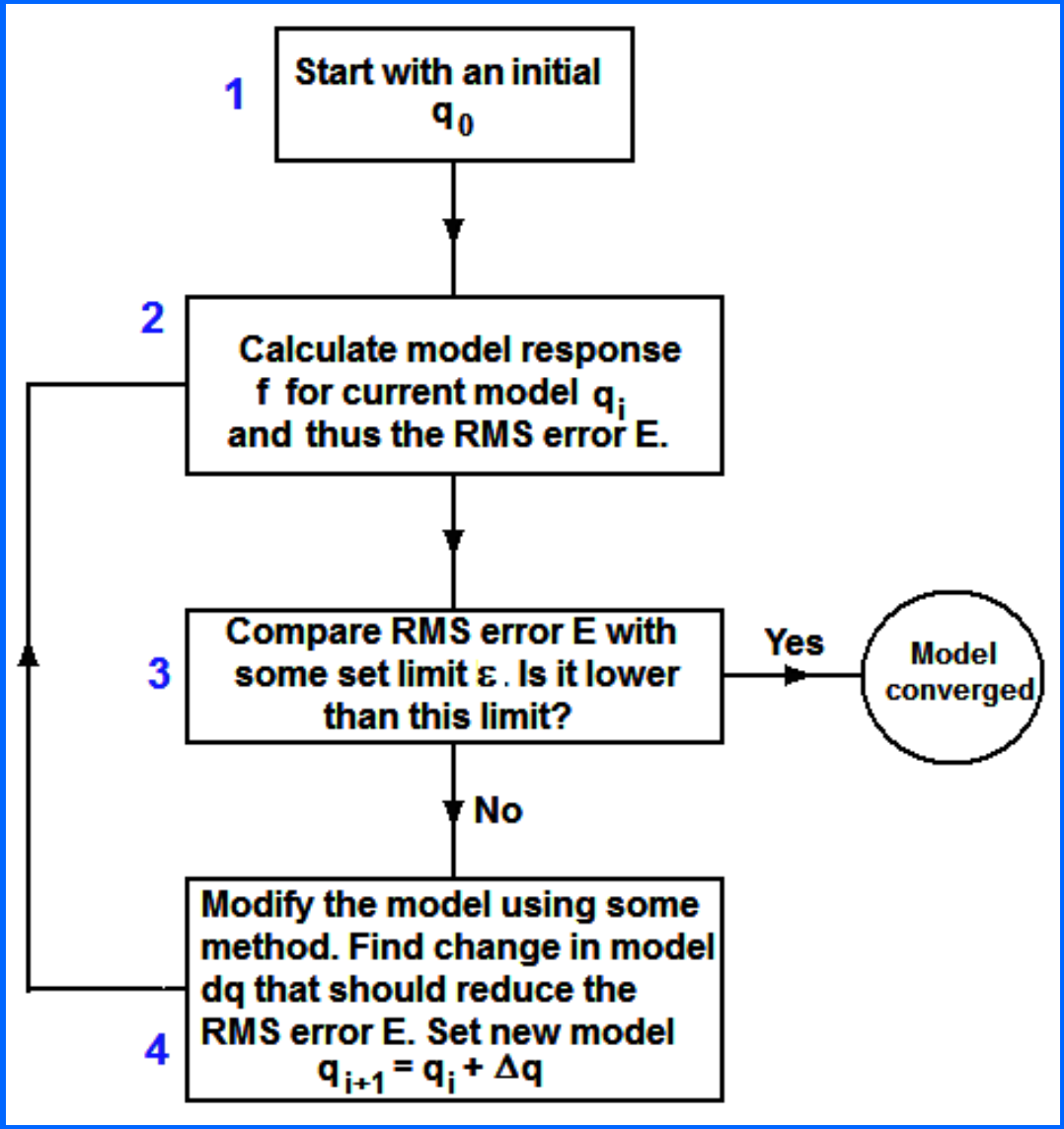

Inversion and optimization

In an inversion program, we want to find a model that minimizes the RMS error, given by the sum of squares of the difference between the measured data and model response.

$$E = \mathbf{g}^{\mathrm{T}}\mathbf{g} = \sum_{i=1}^{n} g_i^2$$

We want to find the minimum of an objective function E. Many nonlinear optimization techniques have been developed. In the case where the objective function E has a sum of squares form, the most efficient is the least-squares optimization method.

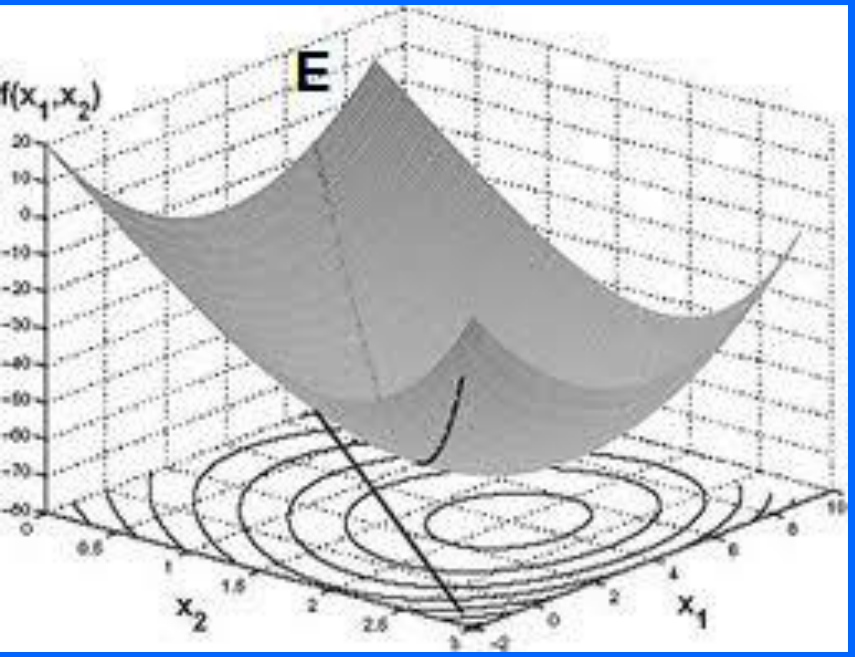

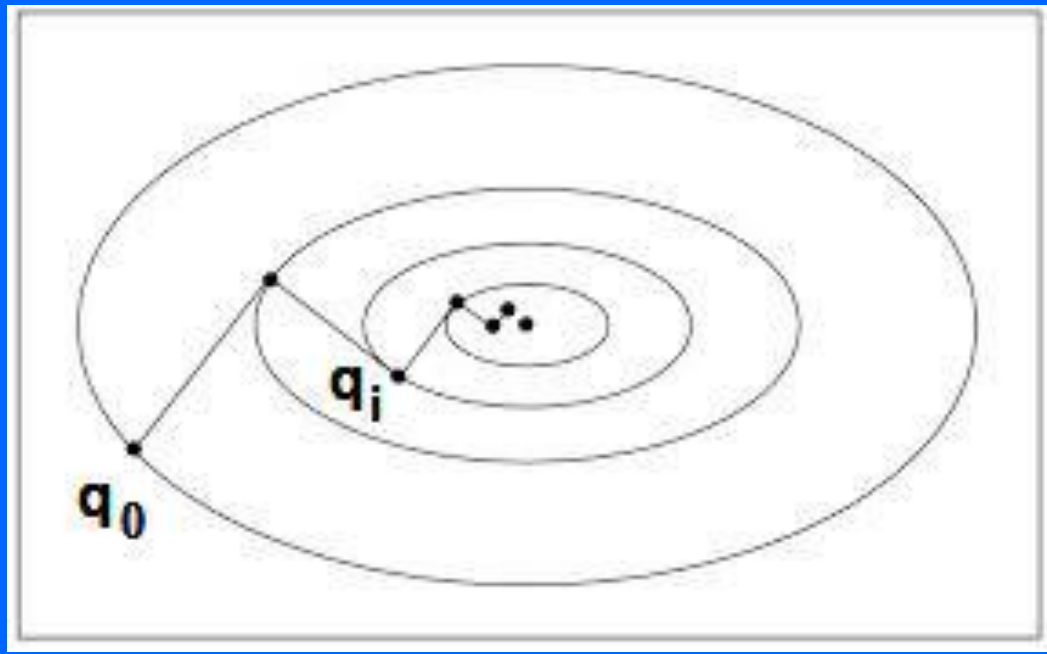

The least-squares inversion method

The Gauss-Newton least-squares method uses the equation

$$\mathbf{J}^{\mathrm{T}}\mathbf{J}\,\Delta\mathbf{q}_i = \mathbf{J}^{\mathrm{T}}\mathbf{g}$$

to calculate the change in the model resistivity values (**Δq**) that will reduce the sum of squares error **E**. **J** is the Jacobian matrix (of size **m** by **n**) of partial derivatives, **m** is the number of model parameters. The elements of the Jacobian matrix are given by

$$J_{ij} = \frac{\partial f_i}{\partial q_j}$$

that is the change in the *i* th calculated apparent resistivity value due to a change in the *j* th model resistivity value. After calculating the parameter change vector, a new model is obtained by

$$\mathbf{q}_{k+1} = \mathbf{q}_k + \Delta\mathbf{q}_k$$

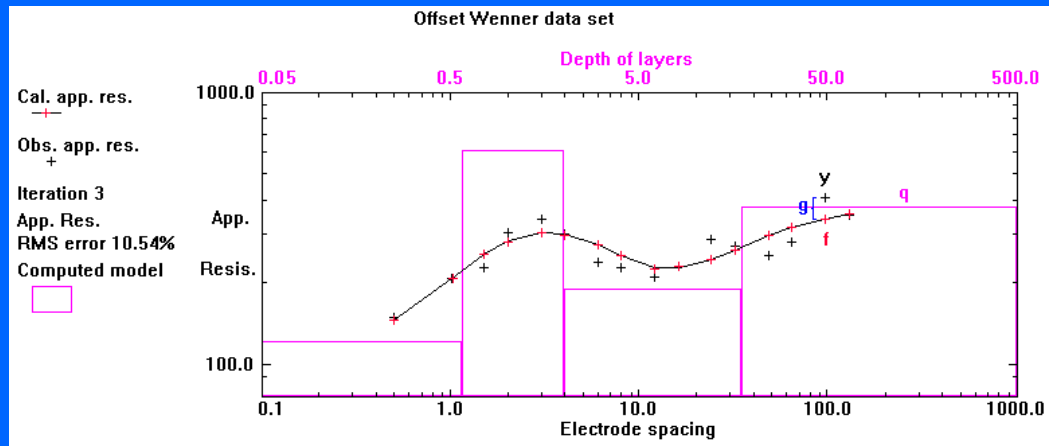

The least-squares inversion method - assumptions

The simple least-squares method uses the equation

$$\mathbf{J}^T\mathbf{J}\,\Delta\mathbf{q}_i = \mathbf{J}^T\mathbf{g} \qquad \mathbf{q}_{k+1} = \mathbf{q}_k + \Delta\mathbf{q}_k$$

The least-squares method is based on the assumption that the current model is close to the minimum, and that the objective function has a quadratic shape. It uses the minimum of the quadratic approximation to estimate Δq. When the current model is far from the minimum, this assumption might not be accurate, so the value for Δq might not be accurate.

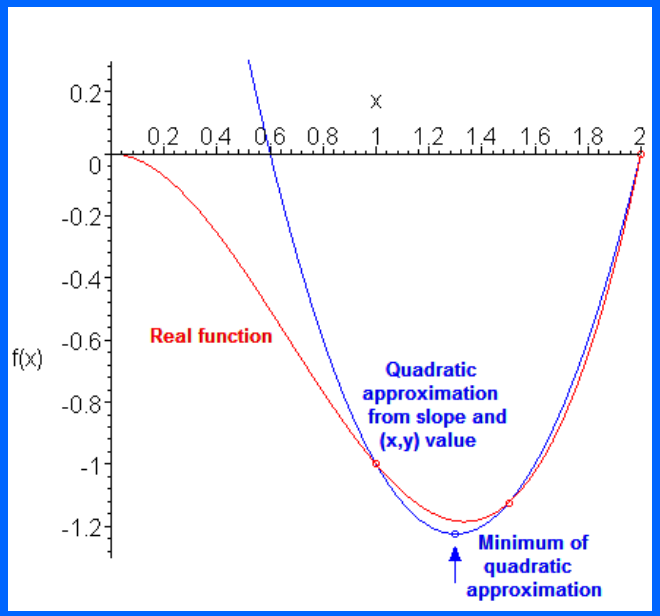

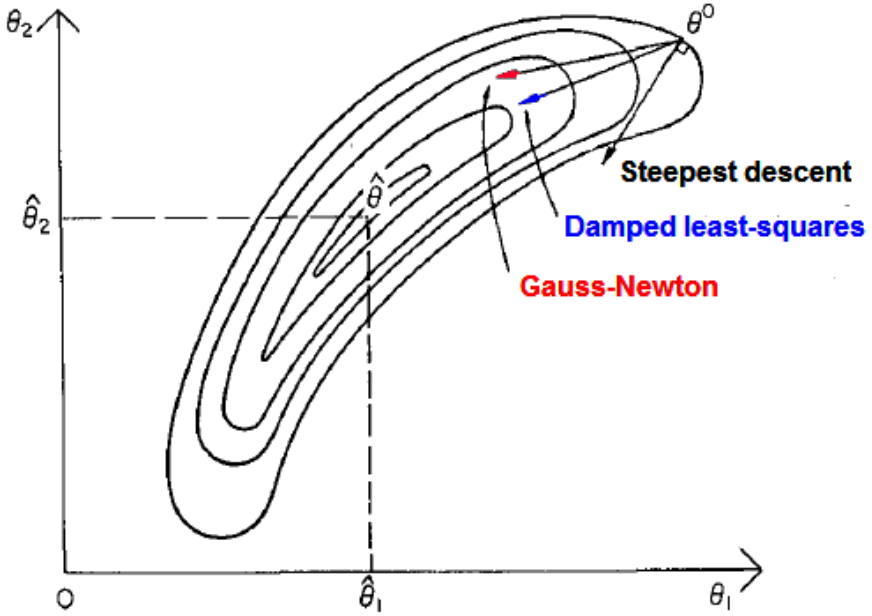

The least-squares inversion method - problems

One problem with this method is that it can become unstable where the calculated change in the model Δq becomes too large, and the new model q_{k+1} has unrealistically too small or too large values. This can happen when the data is very noisy or the initial model is far from the optimum model (g has large values). It can also happen if the $J^T J$ matrix is nearly singular, this occurs if the data has very little information about some of the parameters. It can cause the change Δq to head in a direction away from the minimum.

$$J^T J \, \Delta q_j = J^T g$$

$$q_{k+1} = q_k + \Delta q_k$$

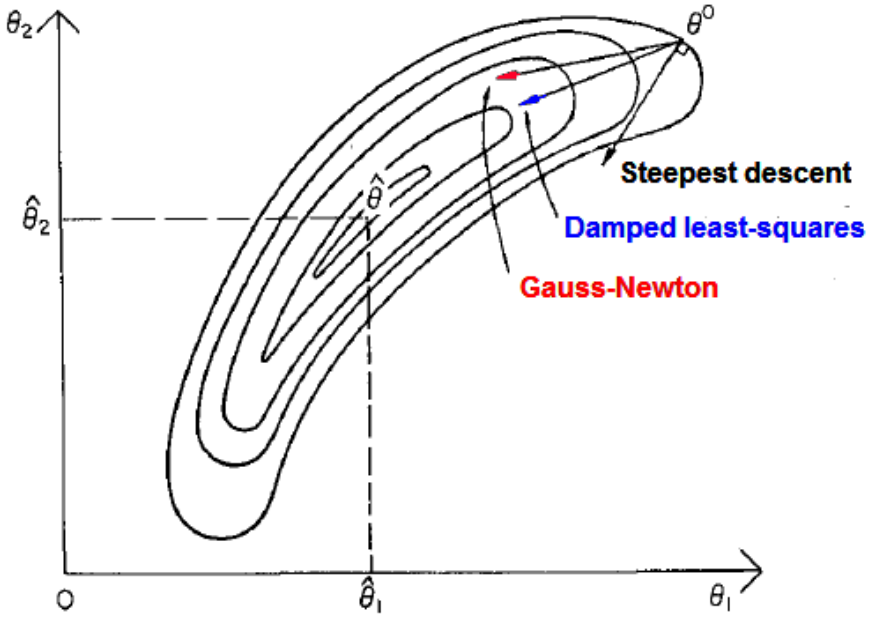

The damped least-squares inversion method

To overcome the problem of instability in the Gauss-Newton method, the damped least-squares or "ridge-regression" method is used.

$$\left(\mathbf{J}^{\mathrm{T}}\mathbf{J}+\lambda\mathbf{I}\right)\Delta\mathbf{q}_{\mathbf{k}}=\mathbf{J}^{\mathrm{T}}\mathbf{g}$$

λ is the damping factor that reduces the change in model resistivity values (Δq). It ensures that Δq is not too large, and modifies its direction towards that of the steepest descent direction. It has been successfully used in cases with a small number of model parameters, such as in resistivity sounding inversions.

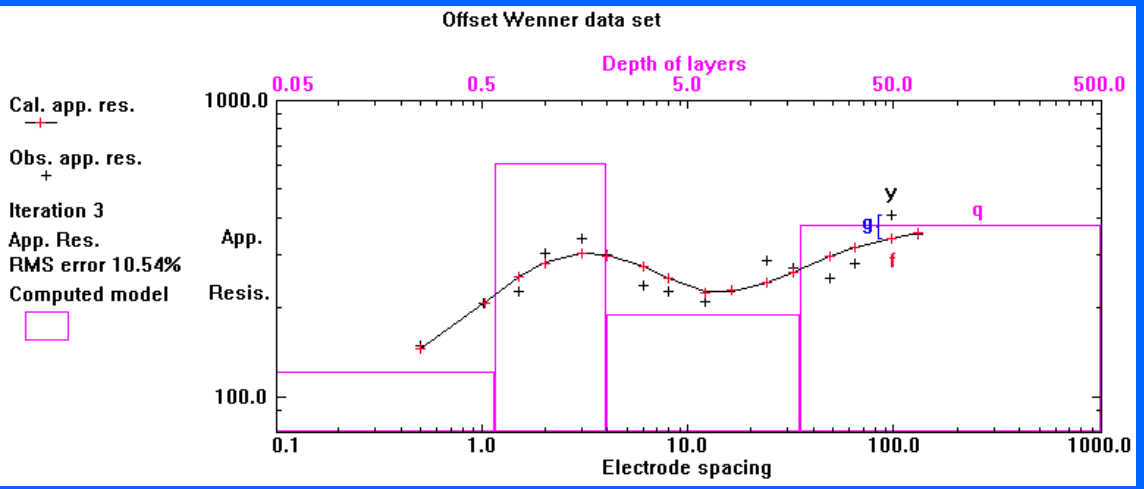

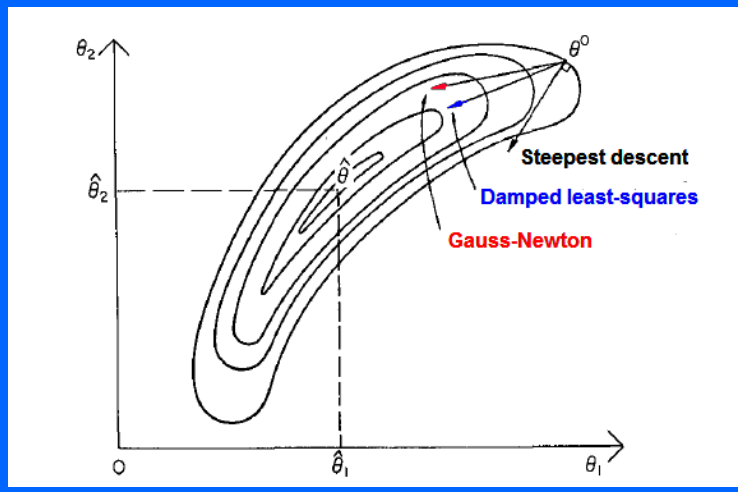

Damped least-squares inversion method - limitations

The damped least-squares (Marquardt) method uses the equation.

$$\left(\mathbf{J}^{\mathrm{T}}\mathbf{J}+\lambda\mathbf{I}\right)\Delta\mathbf{q}_{\mathrm{k}}=\mathbf{J}^{\mathrm{T}}\mathbf{g}$$

It is useful for models with a small number of model parameters, eg. 7 parameters in the example below. However, for models with a large number of parameters, it can lead to very large and abrupt changes in model resistivity values, such as the 1-D model with a large number of layers example. The damping factor ensures that the 'average' change in $\Delta\mathbf{q}$ is limited, but does not ensure it changes slowly from one layer to the next.

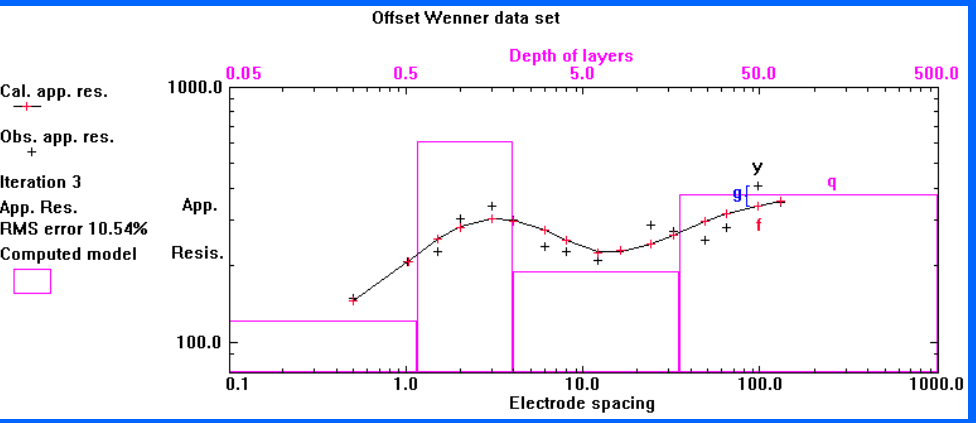

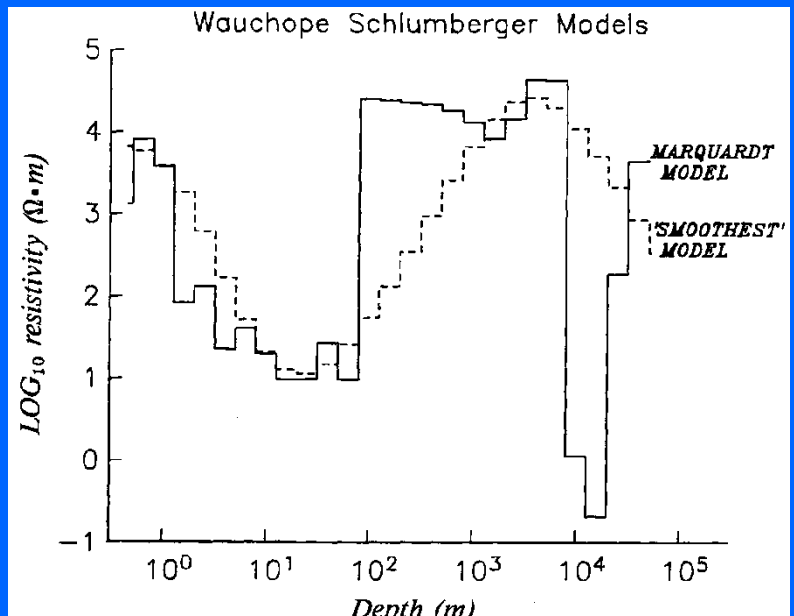

The smooth least-squares inversion method

For models with a large number of parameters, the following smoothness-constrained least-squares equation can be used to ensure that the model resistivity changes in a smooth manner.

$$\left(\mathbf{J}^{\mathrm{T}}\mathbf{J} + \lambda\mathbf{F}\right)\Delta\mathbf{q}_{\mathbf{k}} = \mathbf{J}^{\mathrm{T}}\mathbf{g} - \lambda\mathbf{F}\mathbf{q}_{\mathbf{k}},$$

$$\text{where} \quad \mathbf{F} = \alpha_x \mathbf{C}_{\mathbf{x}}^{\mathrm{T}}\mathbf{C}_{\mathbf{x}} + \alpha_y \mathbf{C}_{\mathbf{y}}^{\mathrm{T}}\mathbf{C}_{\mathbf{y}} + \alpha_z \mathbf{C}_{\mathbf{z}}^{\mathrm{T}}\mathbf{C}_{\mathbf{z}}$$

$\mathbf{C}_x$, $\mathbf{C}_y$ and $\mathbf{C}_z$ are the roughness filter matrices in the *x*-, *y*- and *z*-directions. A first-order difference matrix is commonly used as the roughness filter matrix.

$$\mathbf{C} = \begin{bmatrix} -1 & 1 & 0 & 0 & .. & .. & .. & 0 \\ 0 & -1 & 1 & 0 & .. & .. & .. & 0 \\ 0 & 0 & -1 & 1 & 0 & .. & .. & 0 \\ & & & .. & & & & \\ & & & & .. & & & \\ & & & & & .. & & \\ & & & & & & .. & \\ & & & & & & & \mathbf{0} \end{bmatrix}$$

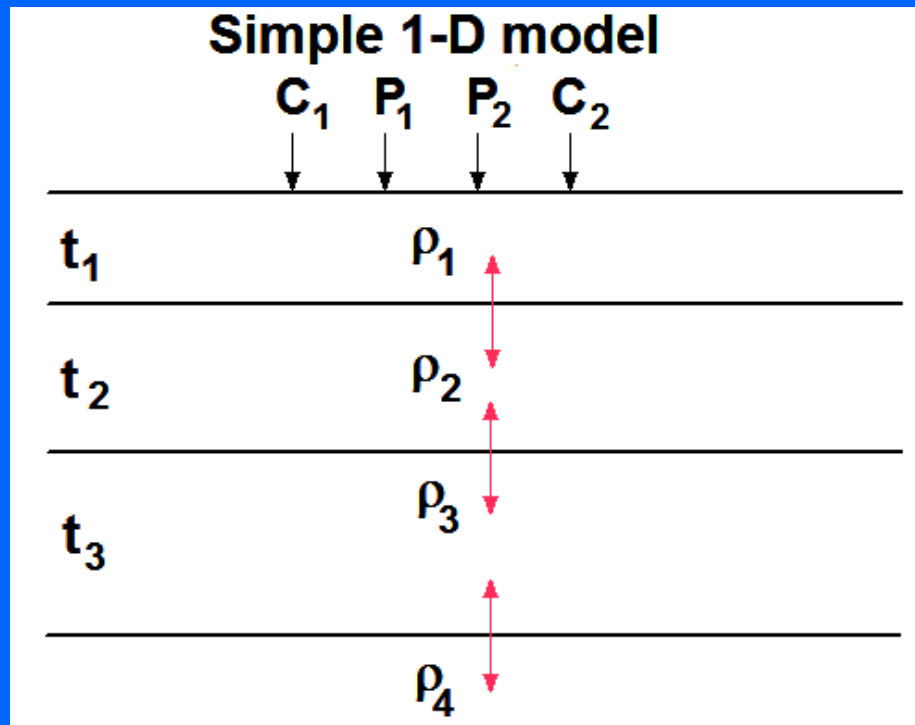

The L_2 norm least-squares inversion method

The smoothness-constrained least-squares equation.

$$\left(\mathbf{J}^{\mathrm{T}}\mathbf{J} + \lambda\mathbf{F}\right)\Delta\mathbf{q}_k = \mathbf{J}^{\mathrm{T}}\mathbf{g} - \lambda\mathbf{F}\mathbf{q}_k ,$$

$$\text{where} \quad \mathbf{F} = \alpha_x \mathbf{C}_x^{\mathrm{T}}\mathbf{C}_x + \alpha_y \mathbf{C}_y^{\mathrm{T}}\mathbf{C}_y + \alpha_z \mathbf{C}_z^{\mathrm{T}}\mathbf{C}_z$$

For the simple case of a 1-D model, the $\mathbf{C}_z$ matrix takes the difference between the (logarithm) of the resistivity of adjacent layers. Applying the $\mathbf{C}_z$ matrix will form terms of the type $(q_{i+1}-q_i)$, and since we use $\mathbf{C}^{\mathrm{T}}\mathbf{C}$ we actually get $(q_{i+1}-q_i)^2$, i.e. we minimize the square of the changes so it is call a L_2 norm method.

$$\mathbf{C} = \begin{bmatrix} -1 & 1 & 0 & 0 & .. & .. & .. & 0 \\ 0 & -1 & 1 & 0 & .. & .. & .. & 0 \\ 0 & 0 & -1 & 1 & 0 & .. & .. & 0 \\ & & & .. & & & & \\ & & & & .. & & & \\ & & & & & .. & & \\ & & & & & & .. & \\ & & & & & & & 0 \end{bmatrix}$$

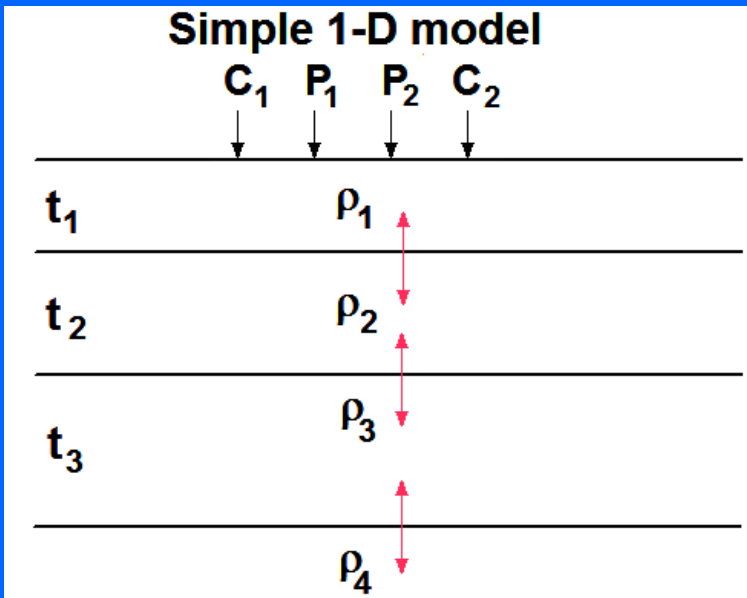

Roughness filters for the smooth least-squares method

The smoothness-constrained least-squares equation is given by :-

$$\left(\mathbf{J}^{\mathrm{T}}\mathbf{J} + \lambda\mathbf{F}\right)\Delta\mathbf{q}_{\mathbf{k}} = \mathbf{J}^{\mathrm{T}}\mathbf{g} - \lambda\mathbf{F}\mathbf{q}_{\mathbf{k}},$$

$$\text{where} \quad \mathbf{F} = \alpha_x \mathbf{C}_{\mathbf{x}}^{\mathrm{T}}\mathbf{C}_{\mathbf{x}} + \alpha_y \mathbf{C}_{\mathbf{y}}^{\mathrm{T}}\mathbf{C}_{\mathbf{y}} + \alpha_z \mathbf{C}_{\mathbf{z}}^{\mathrm{T}}\mathbf{C}_{\mathbf{z}}$$

The diagrams below shows the coupling introduced by the C_x, C_y and C_z filters for 2-D and 3-D models. In 2-D models, the coupling is applied to adjacent cells horizontally and vertically. In the 3-D model, there is an additional coupling in the y-direction.

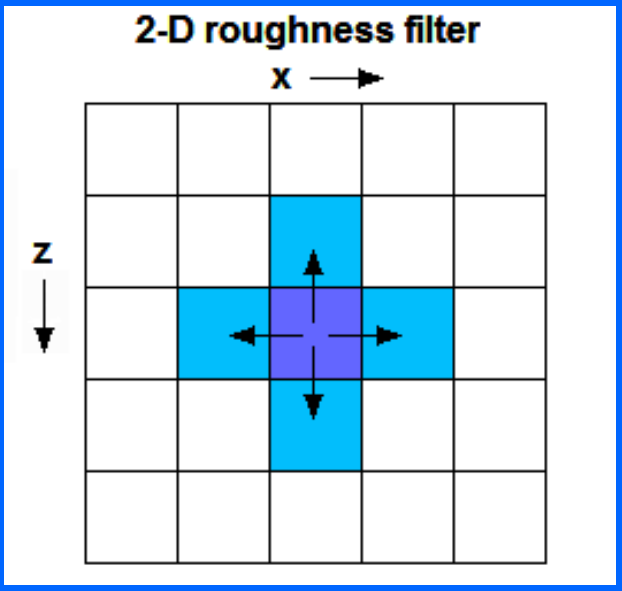

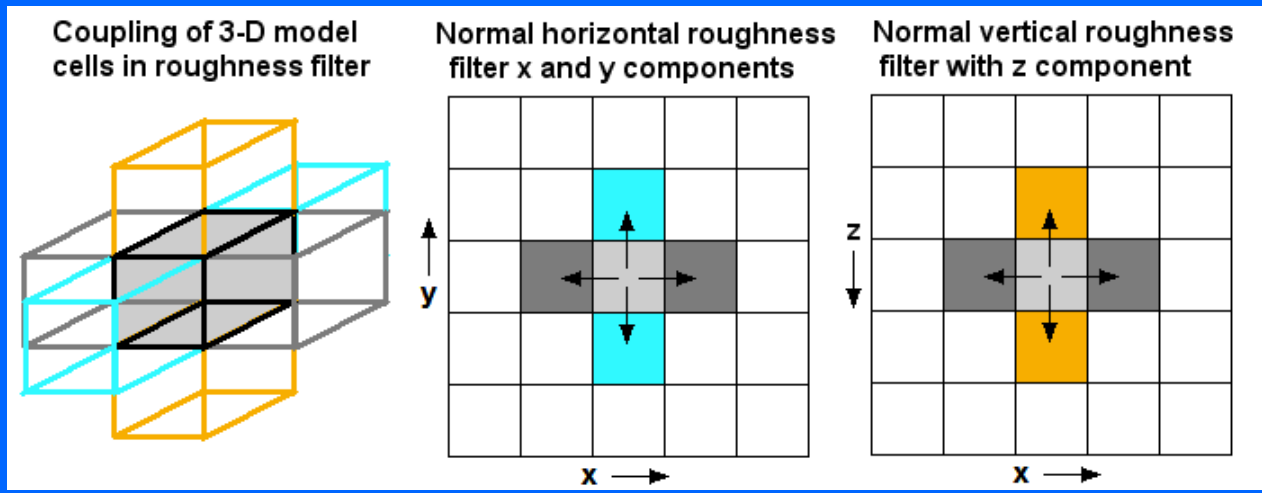

A smooth 1-D model

The smooth inversion method minimizes the sum-of-squares (a L_2 norm) of the change in the model resistivity values (through the $\mathbf{C^TC}$ term). It tries to minimize the square of the change in the resistivity from one model layer to the next in a 1-D model. It basically assumes the resistivity changes in a 'smooth' manner. The example below is from a 1-D inversion of TEM data. The L_2 norm method gives accurate results in situations where the subsurface resistivity changes in a gradual manner. In situations with sharp boundaries, the results are less accurate. The L_2 norm model shows a smooth gradual change at the location of the sharp boundary between two layers.

Note all the models differ from the true resistivity for the deepest layer where there is less information.

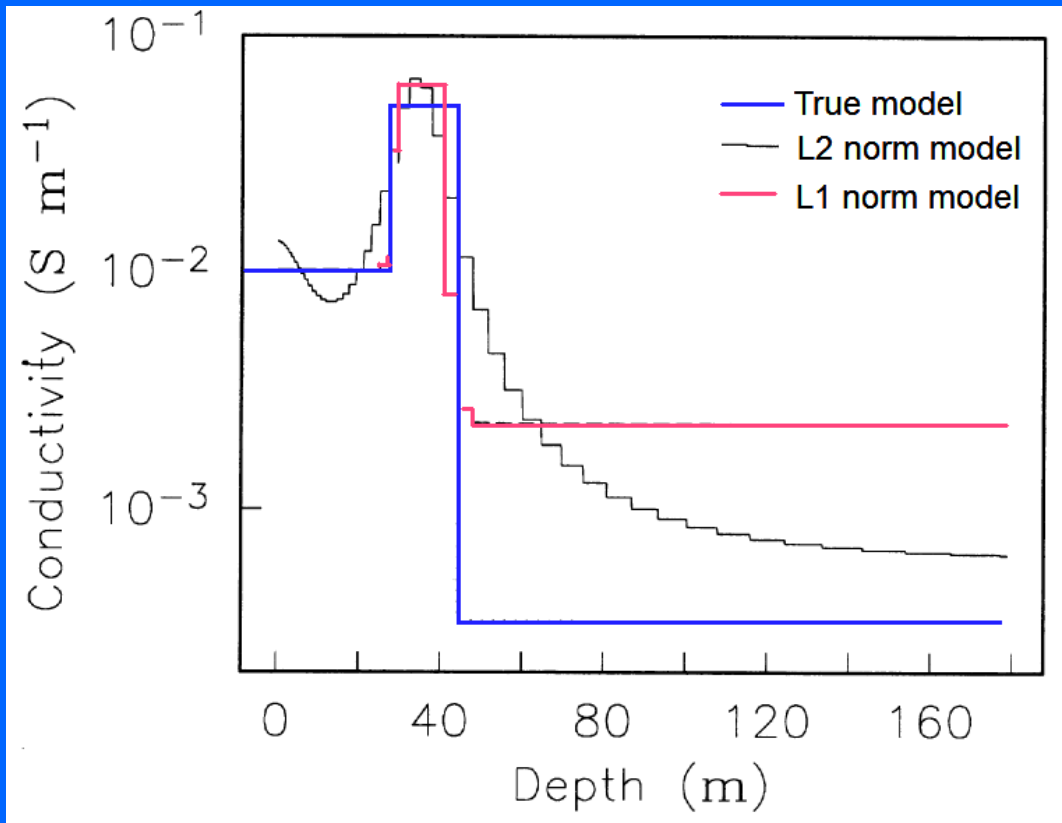

After 'Farquharson, C.G., and D.W. Oldenburg, 1998. Nonlinear inversion using general measures of data misfit and model structure, Geophysical Journal International, **134**, 213-227'.

Smooth 2-D models

The example below shows a 2-D rectangular block model with sharp boundaries. The smooth inversion method produces a model (b) with smeared boundaries at the true edges of the block. The anomaly is spread out over a larger area than the true block.

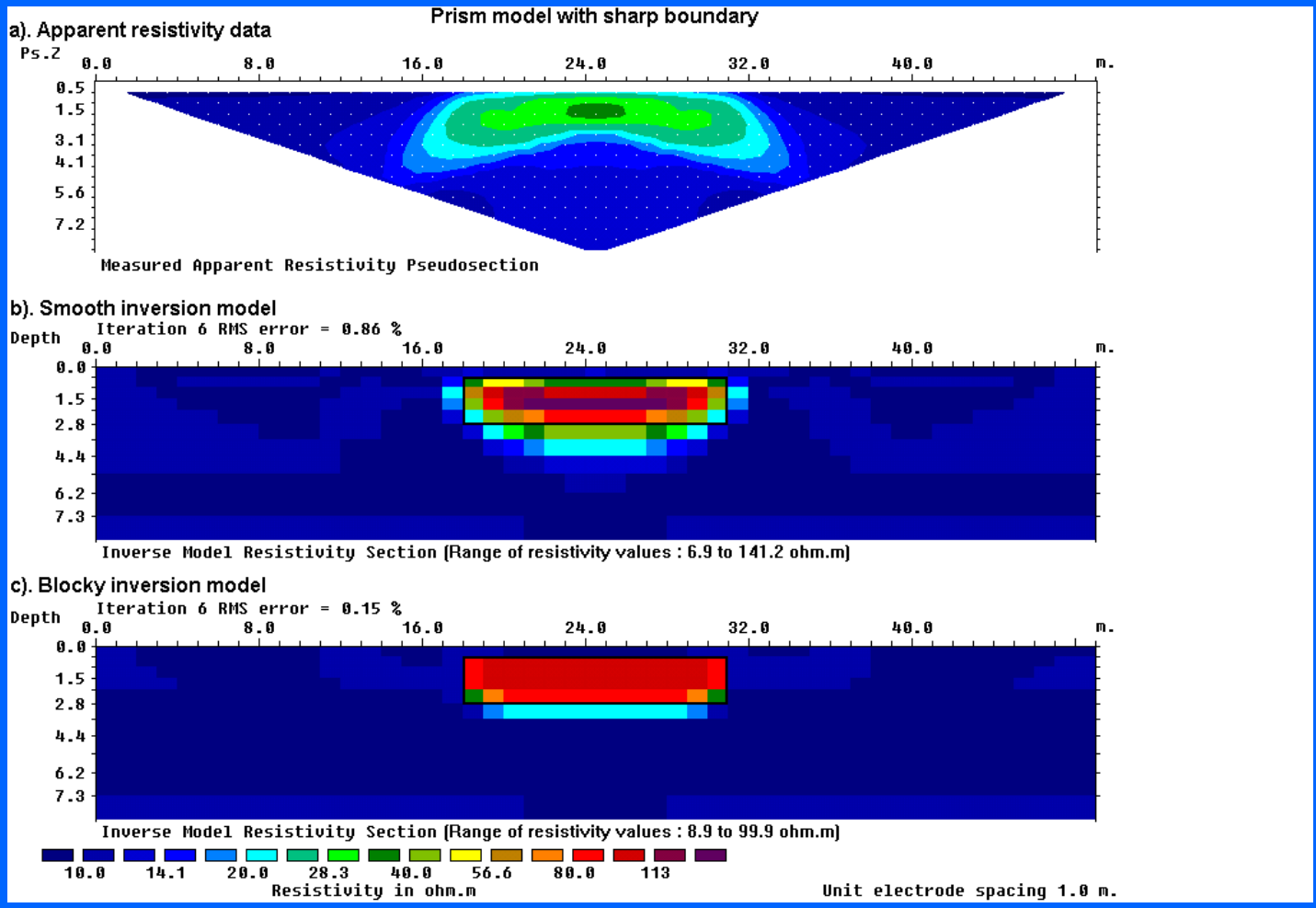

The blocky least-squares inversion method

To overcome the problem of boundaries that are too smooth, the "blocky" inversion method is one possible solution. The least-squares equation is further modified to

$$\left(\mathbf{J}^{\mathrm{T}}\mathbf{J} + \lambda\mathbf{F}_{\mathbf{R}}\right)\Delta\mathbf{q}_{\mathbf{k}} = \mathbf{J}^{\mathrm{T}}\mathbf{g} - \lambda\mathbf{F}_{\mathbf{R}}\mathbf{q}_{\mathbf{k}},$$

$$\mathbf{F}_{\mathbf{R}} = \alpha_x \mathbf{C}_{\mathbf{x}}^{\mathrm{T}}\mathbf{R}_{\mathbf{m}}\mathbf{C}_{\mathbf{x}} + \alpha_y \mathbf{C}_{\mathbf{y}}^{\mathrm{T}}\mathbf{R}_{\mathbf{m}}\mathbf{C}_{\mathbf{y}} + \alpha_z \mathbf{C}_{\mathbf{z}}^{\mathrm{T}}\mathbf{R}_{\mathbf{m}}\mathbf{C}_{\mathbf{z}}$$

$\mathbf{R}_{\mathbf{m}}$ is a weighting matrix used so that different elements of the model roughness vector are given equal weights in the inversion process. It is a L_1 norm (robust) method in that it attempts to minimize the absolute value of the model changes. It basically tries to minimize the sum of the absolute change $\Sigma|q_{i+1}-q_i|$ in the resistivity from one layer to the next in a 1-D model.

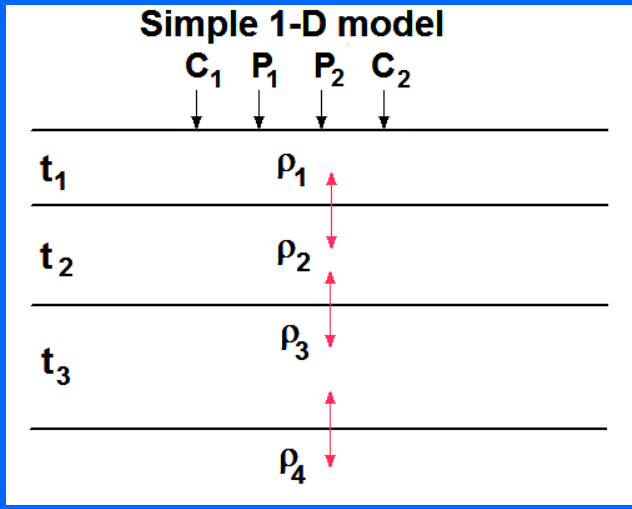

Applying the blocky least-squares inversion method in 1-D

In the 1-D TEM model, the L_1 norm model shows a more rapid change in the resistivity near the positions of the top and bottom surface of the high-resistivity layer.

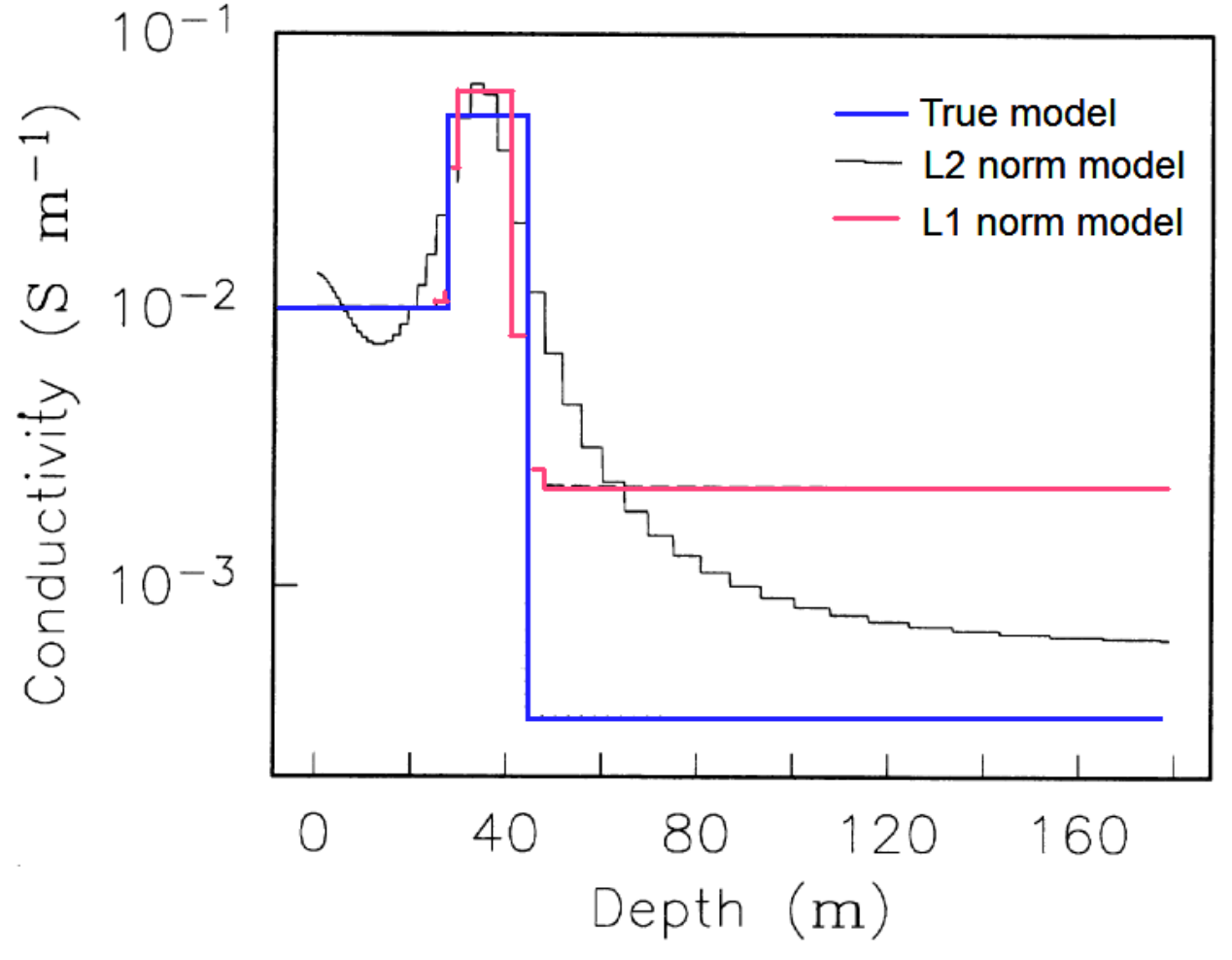

The blocky least-squares inversion method in 2-D

In the L_1 norm 2-D model the high resistivity anomaly is concentrated in a smaller area within the actual boundaries of the block. There is a sharper transition to the low resistivity background.

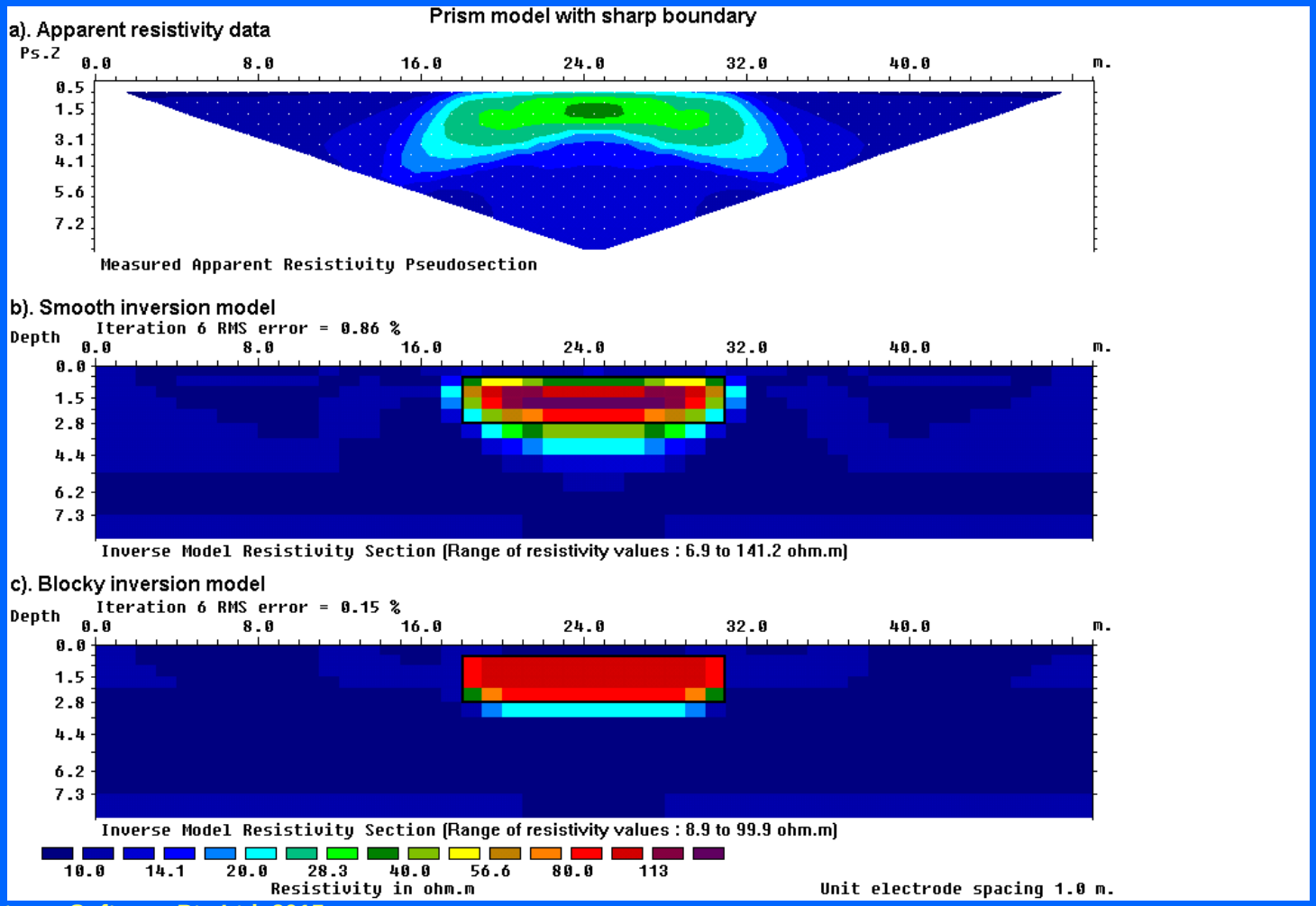

The L_1 norm for the data misfit – line fitting example

The example fits a straight line through 10 data points with *(x,y)* coordinates. The L_2 norm method finds a line this minimizes the sum of the squares of the differences in the y values, $\sum_{i=1}^{m}(y_i - f_i)^2$

This is greatly affected by the 2 outlier data points. The L_1 norm method tries to minimize the sum of the absolute differences.

$$\sum_{i=1}^{m}|y_i - f_i|$$

It is less affected by the 2 outlier data points. For example, the weight of distance of point A from the straight line is 60 units in L_1 norm, but 3600 units in L_2 norm.

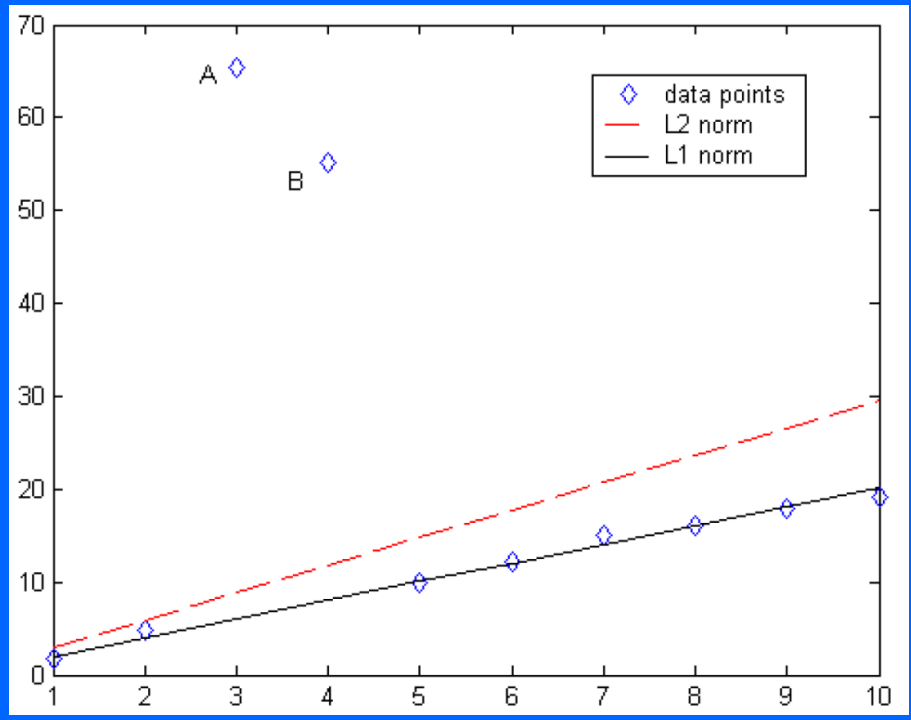

Applying the L1 norm data misfit

The least squares equation can be modified so that it minimizes the absolute value of the difference between the measured and calculated apparent resistivity.

$$\left(\mathbf{J}^T\mathbf{R}_d\mathbf{J} + \lambda\mathbf{F}_R\right)\Delta\mathbf{q}_k = \mathbf{J}^T\mathbf{R}_d\mathbf{g} - \lambda\mathbf{F}_R\mathbf{q}_k,$$

$\mathbf{R}_d$ is a data misfit weighting matrix used so that different elements of the data misfit vector $\mathbf{g}$ are given equal weights.

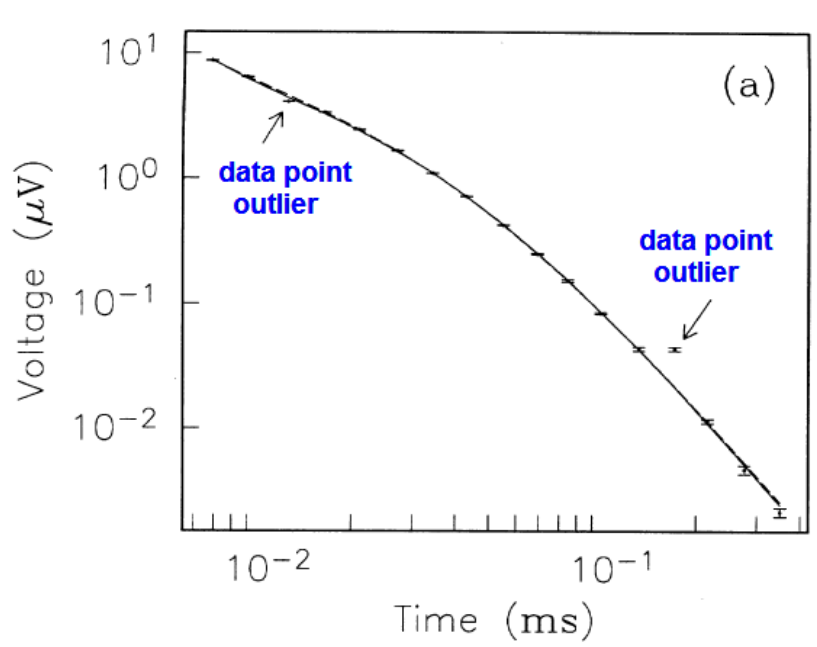

Data with noise added at two points

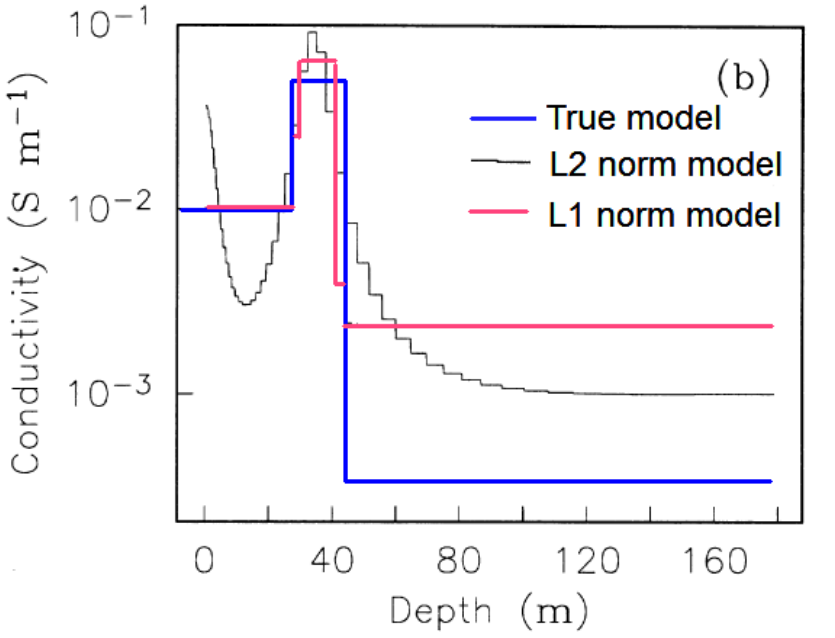

Models with L1 and L2 norms used for model roughness and data misfit.

Other variations of the least-squares method

There are other possible variations, usually made by adding different terms to the least-squares equation. One common addition is to add a constraint so that the resulting model is "close" to some background model $\mathbf{q}_0$.

$$\left(\mathbf{J}^T\mathbf{R}_d\mathbf{J} + \lambda\mathbf{F}_R\right)\Delta\mathbf{q}_k = \mathbf{J}^T\mathbf{R}_d\mathbf{g} - \lambda\mathbf{F}_R(\mathbf{q}_k - \mathbf{q}_0),$$

$$\mathbf{F}_R = \alpha_x\mathbf{C}_x^T\mathbf{R}_m\mathbf{C}_x + \alpha_y\mathbf{C}_y^T\mathbf{R}_m\mathbf{C}_y + \alpha_z\mathbf{C}_z^T\mathbf{R}_m\mathbf{C}_z + \alpha_s\mathbf{I}$$

Another variation is to modify the roughness filters so that features in a desired direction are emphasized. To avoid a bias in the vertical and horizontal directions, the filter can be modified to include diagonal components. We will look at an example later.

If the data errors are known, they can also be used as 'weights' to reduce the effect of the noisy data points.

Different ways to subdivide the subsurface - cells

(a) A cell based model. The positions of the cells are fixed and only the resistivities of cells are allowed to vary. The model parameters consist of the resistivity of the cells. The resistivity is assumed to change in a "smooth" manner.This is the most commonly used method. It has the advantage that practically any structure can be accommodated.

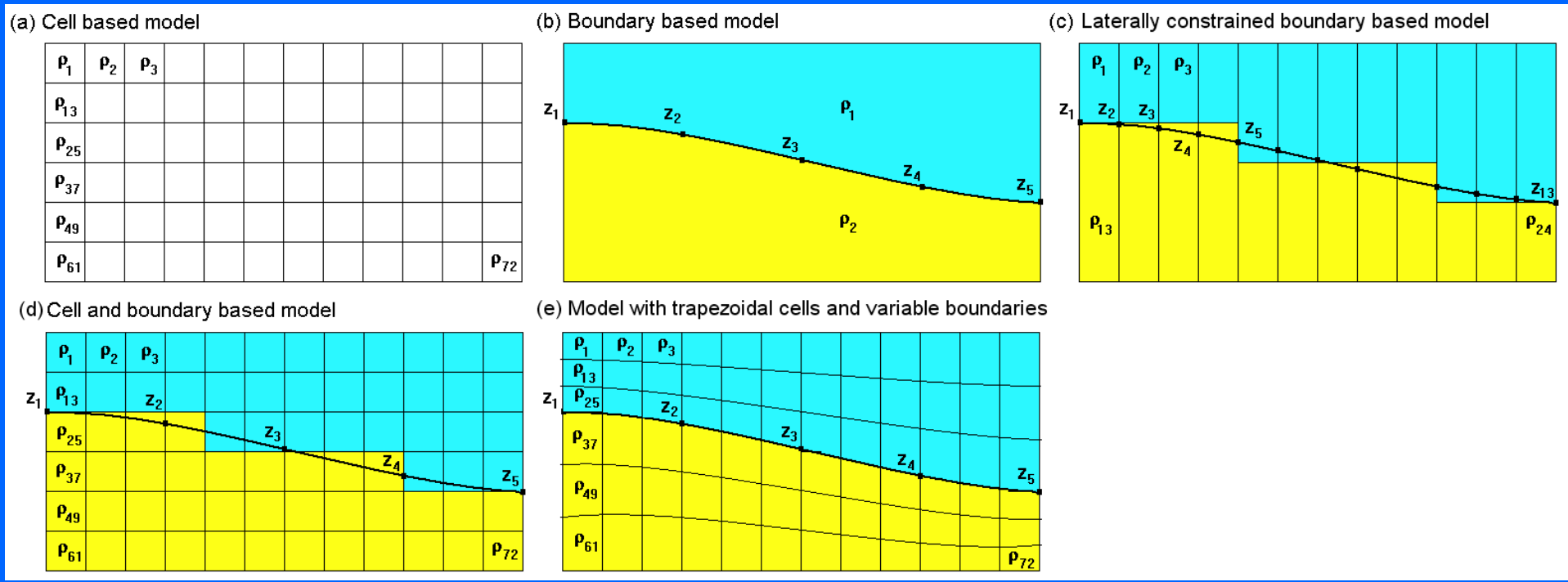

Different ways to subdivide the subsurface - boundaries

(b) A boundary based model. The subsurface is subdivided into different regions. Model parameters are the depths to the boundary and resistivity of each region. The resistivity can change quickly across the boundary, but cannot change within a layer. The main problem is that lateral changes near the surface have a very large effect on the apparent resistivity values. It does not take into account lateral changes, that are then mistakenly modeled as changes in the depths of the boundaries.

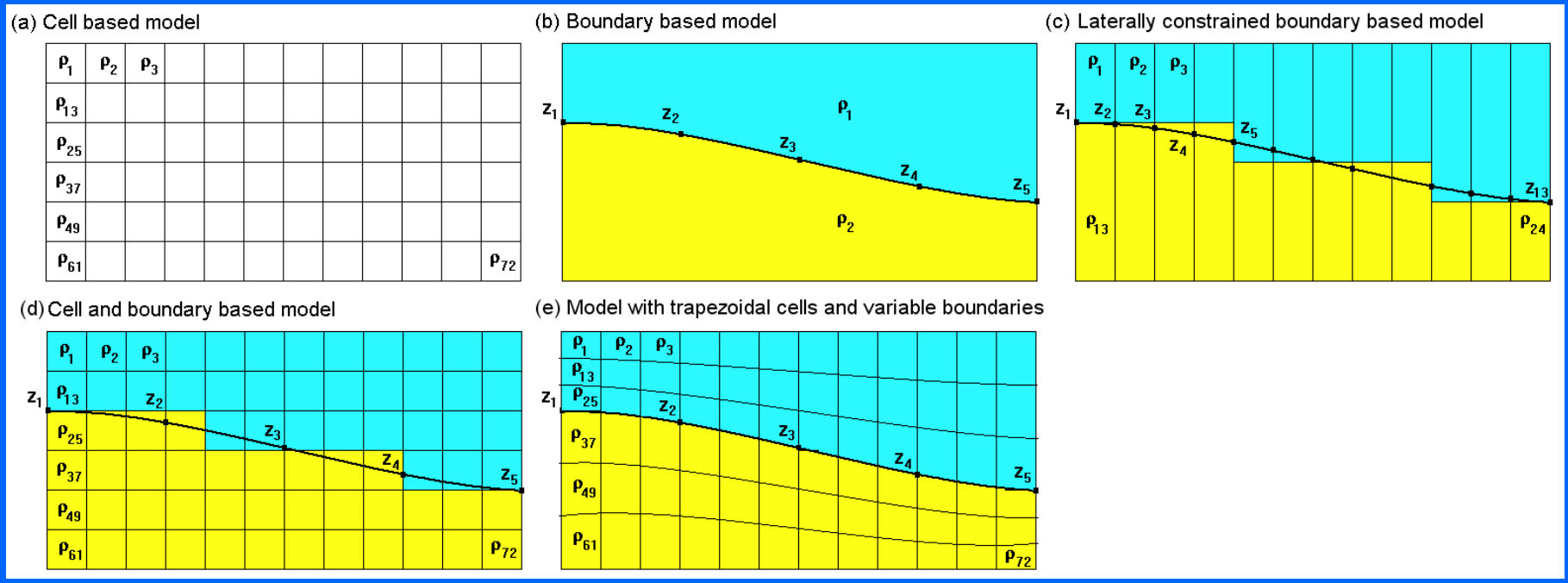

Laterally constrained method

(c) To overcome the instability in the "boundary based method", we allow horizontal (but not vertical) changes in the model resistivity. The laterally constrained method is a big improvement over the purely boundary based method. It works particularly well in areas with sedimentary layers with lateral changes in the resistivity.

Can we improve on the laterally constrained method? In some areas, there could be large vertical changes as well.

(a) Cell based model

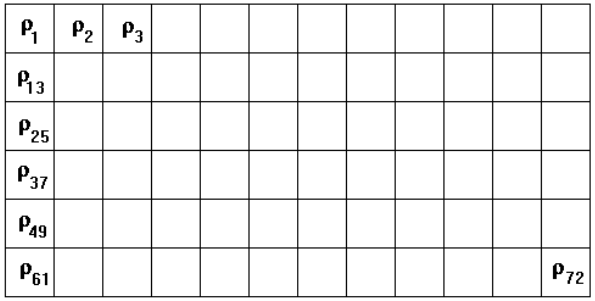

(b) Boundary based model

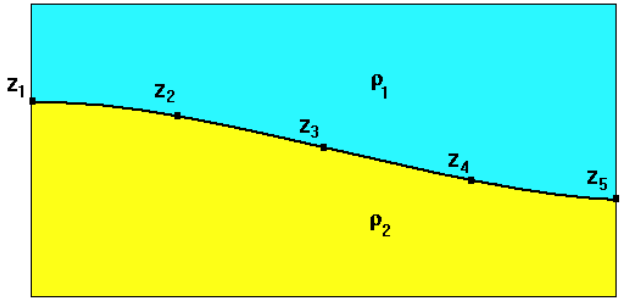

(c) Laterally constrained boundary based model

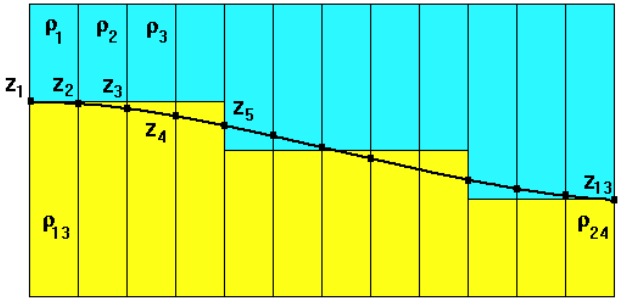

(d) Cell and boundary based model

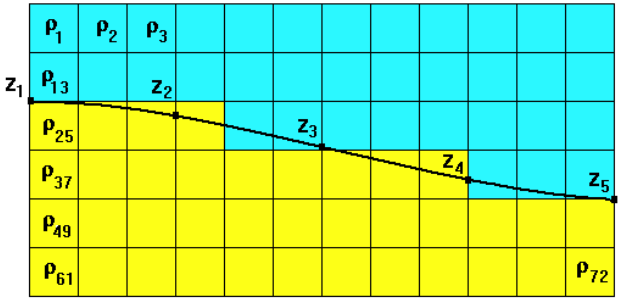

(e) Model with trapezoidal cells and variable boundaries

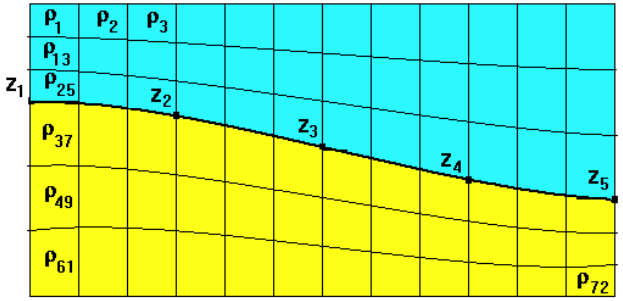

Cell and boundary based method

(d) Allow vertical as well as horizontal changes in the resistivity, and sharp changes across the boundary. This should take into account situations with large vertical changes as well. Rectangular model cells are used. The cells are grouped into different regions, with smooth variation between cells in the same region but allow sharp changes between cells in different regions.

A final possibility (e) is to use non-rectangular cells.

(a) Cell based model

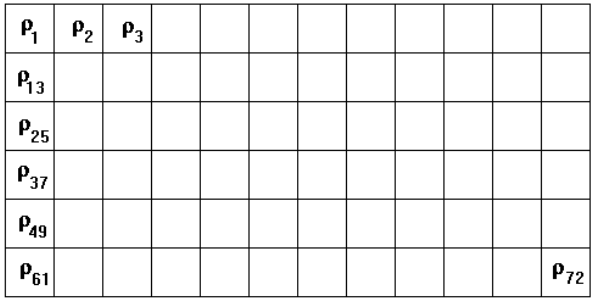

(b) Boundary based model

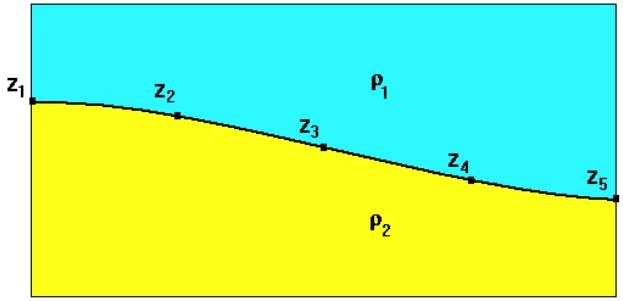

(c) Laterally constrained boundary based model

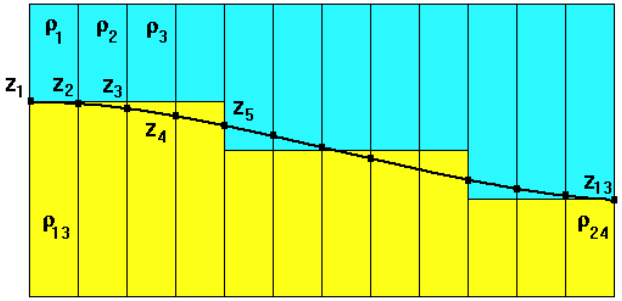

(d) Cell and boundary based model

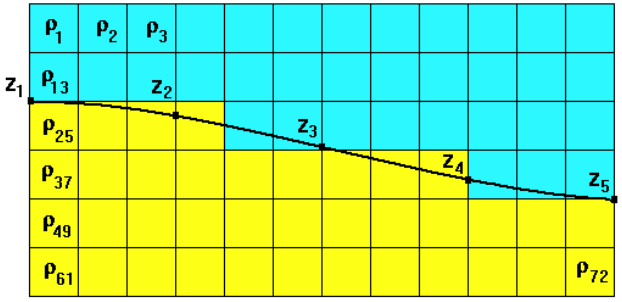

(e) Model with trapezoidal cells and variable boundaries

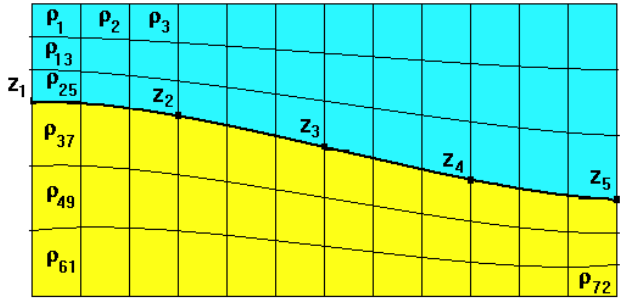

Example of cell and boundary inversion

This shows an example of the method where the model cell resistivities, as well as a boundary between 2 region, are allowed to change (the (d) method). The initial model has a homogeneous resistivity and a flat boundary. Both the resistivity and depth to boundary at a number of points are then automatically adjusted.

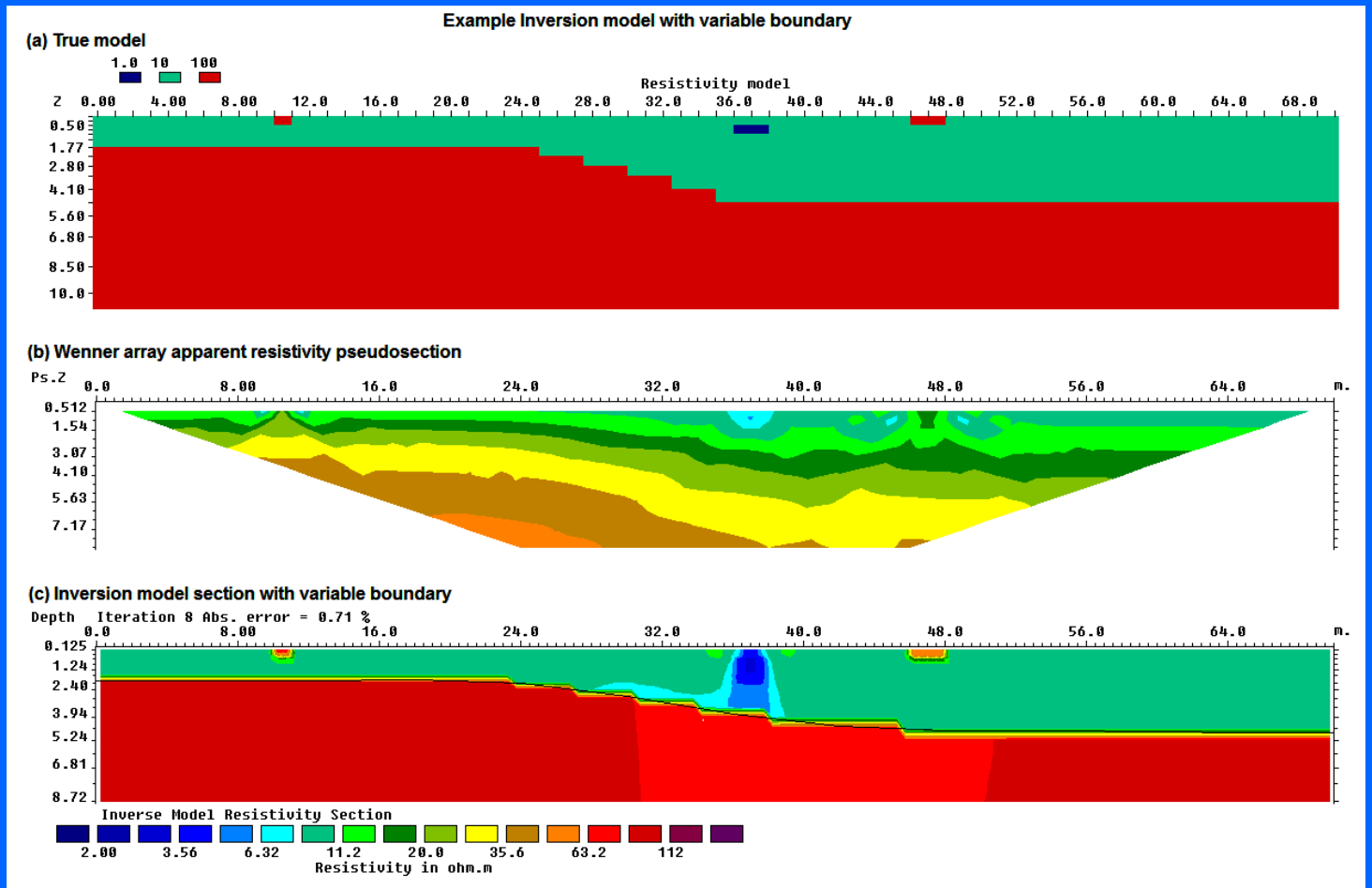

Inversion settings

Some common settings used to optimize the inversion model.

1). Robust or L_1 norm inversion method

2). Including known boundaries

3). Methods to select the damping factor

RES2DINV - INVERSION METHODS

One commonly used option is the 'Robust' or 'Blocky' inversion method which should be used if the subsurface resistivity has sharp boundaries. Clicking the 'Select robust inversion' option will show the dialog box below. The 'Robust model constrain' will apply the blocky model inversion method. The 'Robust data constrain' should be used if the data is very noisy.

Standard = L_2, Robust = L_1

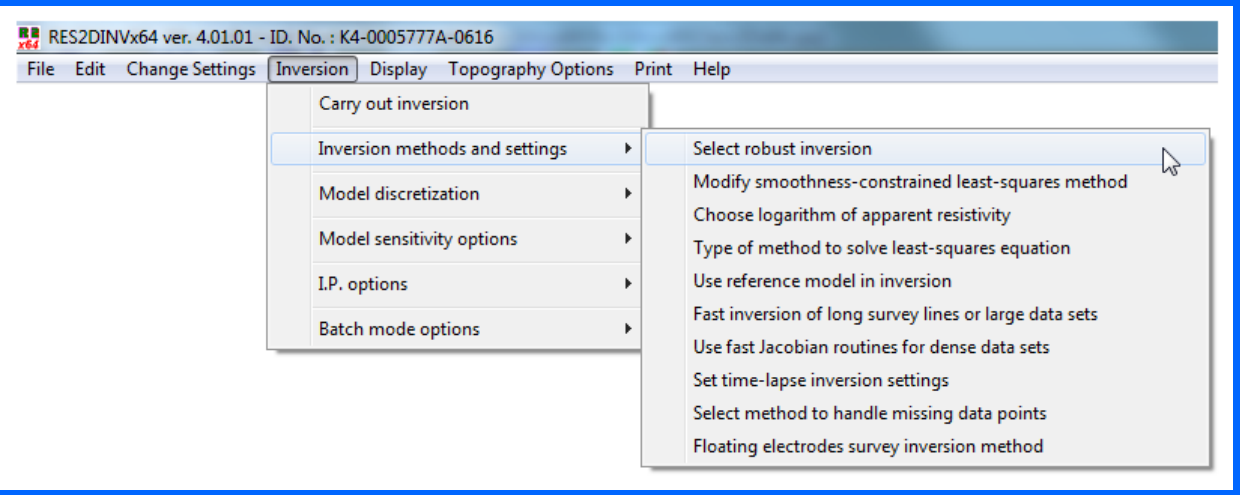

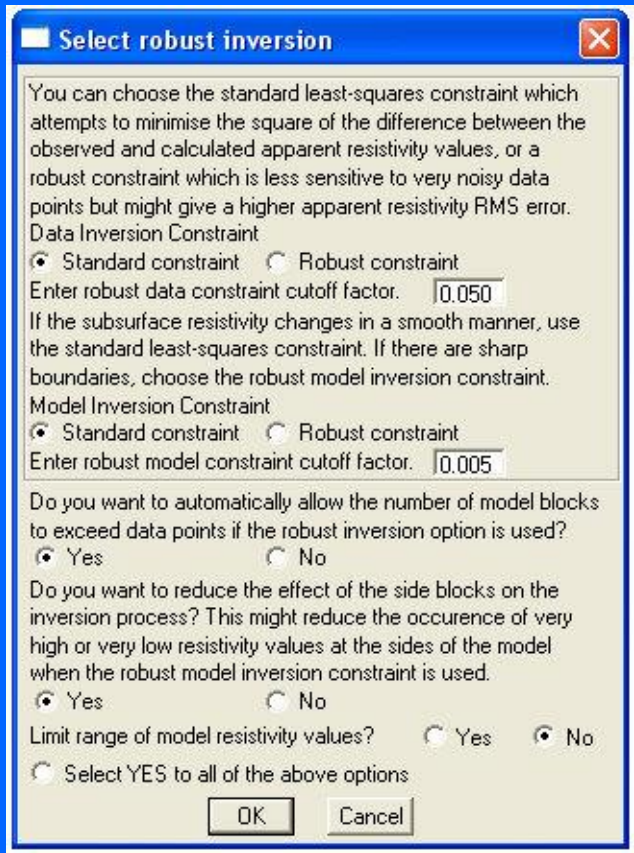

Example of robust or blocky model inversion

The figure below shows the inversion results for data from a synthetic model with sharp boundaries. In this case, the robust inversion method gives significantly better results since the true model consists of three regions with sharp boundaries between them. The model consists of a faulted block (100 ohm.m) and a small rectangular block (1 ohm.m) in a 10 ohm.m medium.

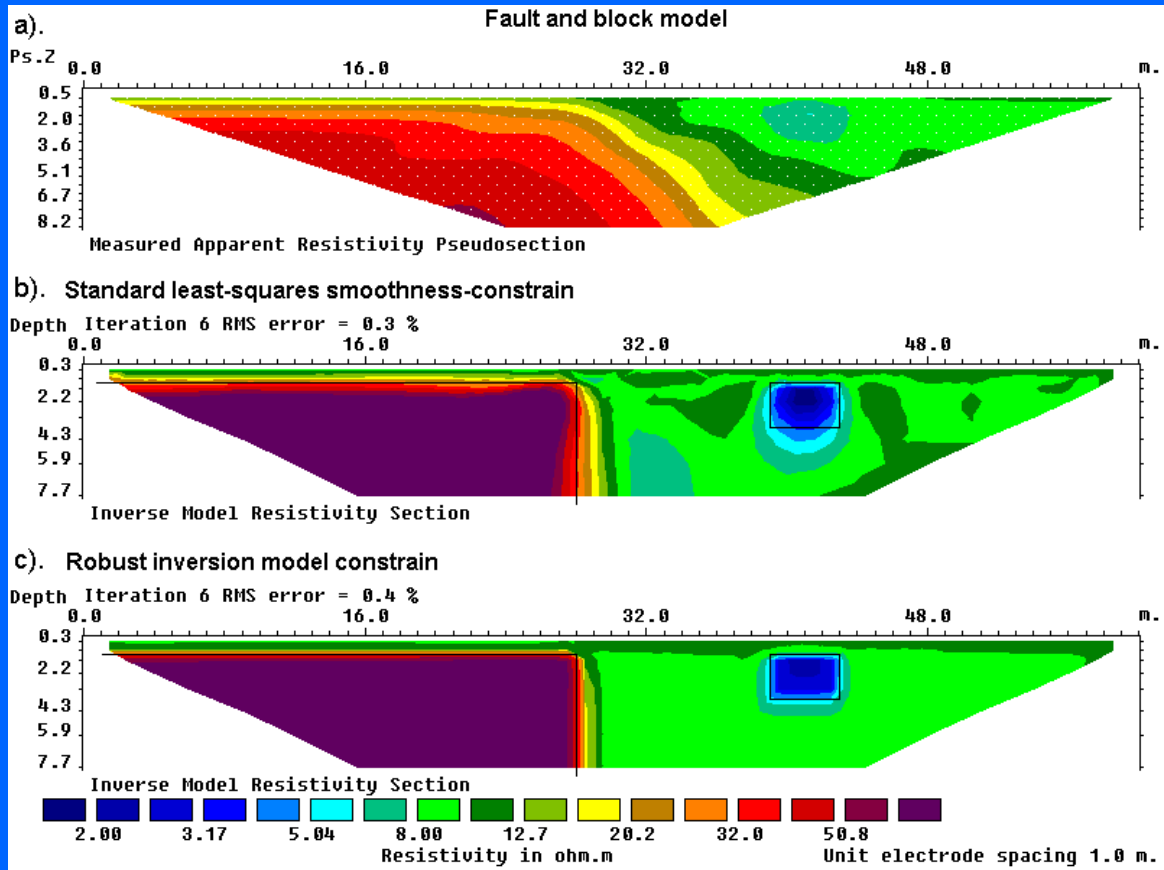

Including known boundaries into the model

In some cases the position of the boundaries between 2 regions is known, such as from borehole or seismic data. The depth to the boundary can be included into te model through the data file.

The models cells are divided into different regions that are separated by the boundaries. Within each region (highlighted by the same color) the resistivity of the model cells are constrained to change in a 'smooth' or 'blocky' manner. However, across a boundary, the resistivity between model cells in two different regions is allowed to change abruptly. This option is useful when the boundaries coincide with boundaries between geological units with very different resistivities.

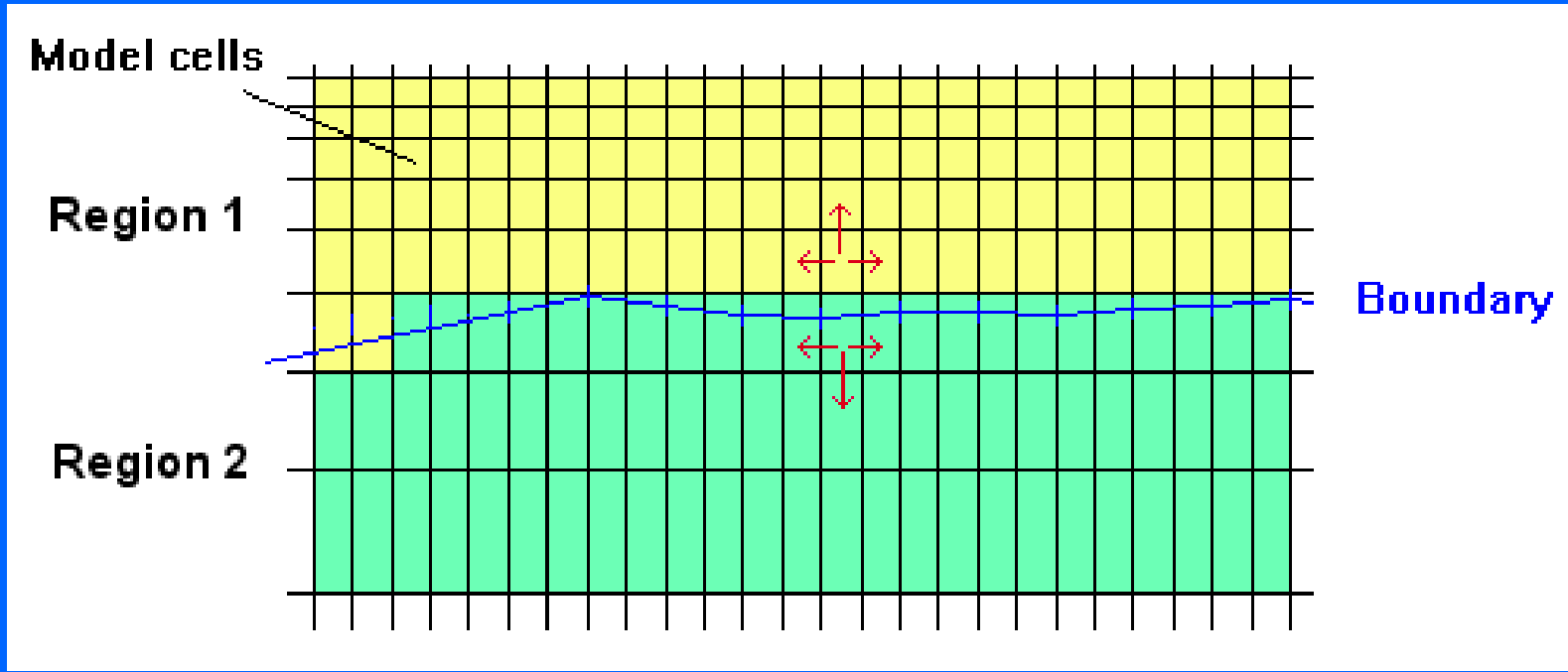

Sharp boundary inversion example

The survey was carried out in Clifton, Birmingham, U.K. to map a sand layer over clay. The boundary between the sand and clay layers is known from a seismic refraction survey. First the results using normal smoothness-constrained inversion is shown. Note the boundary between the higher resistivity sand layer and the underlying lower resistivity clay layer is not well resolved n the model using the L_2 norm.

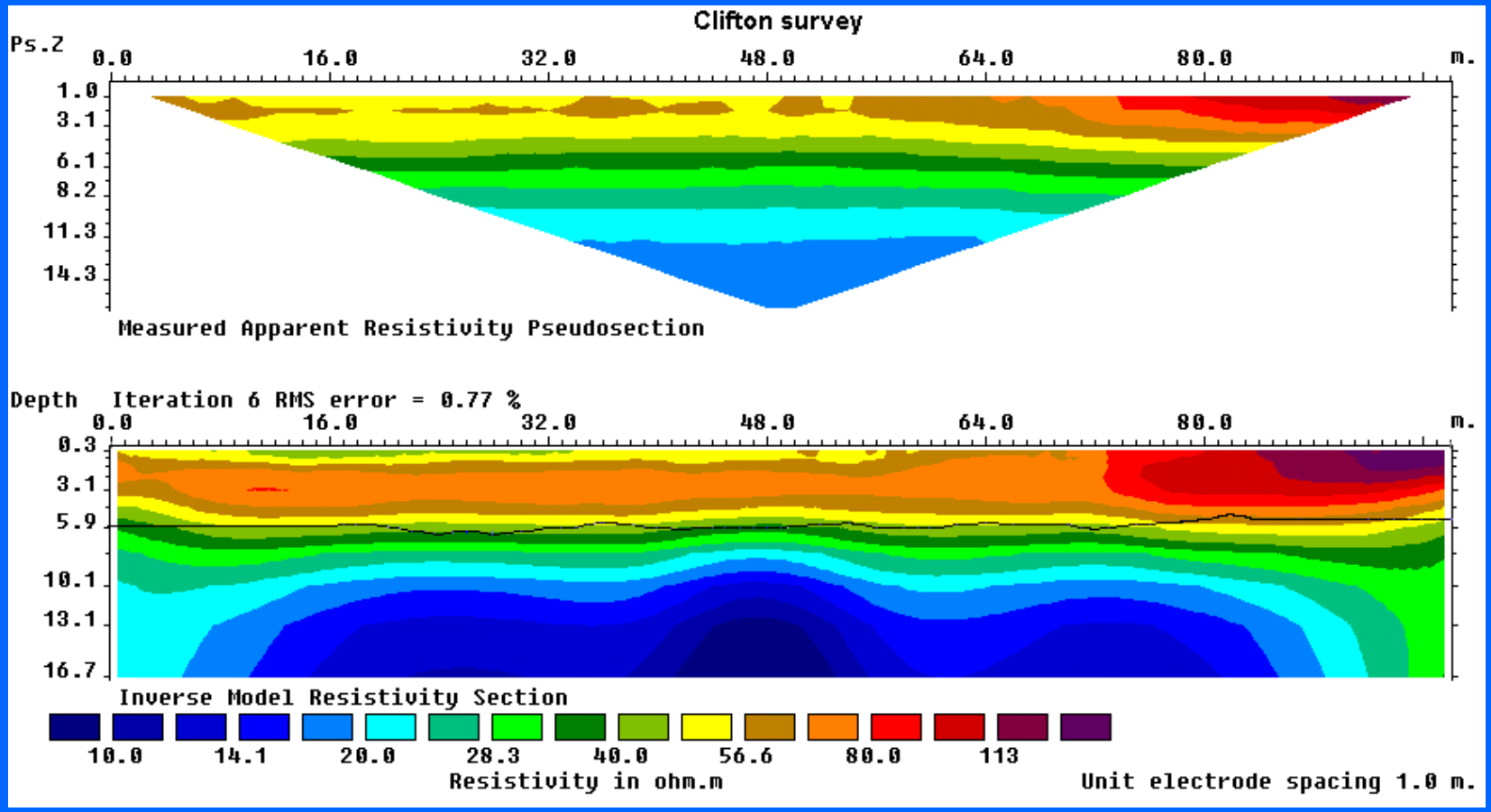

Sharp boundary inversion – Clifton survey example

Models from the different inversion methods are shown together. The boundary is much better resolved in the blocky and sharp boundary inversion methods.

Note the slightly better performance of the sharp boundary method compared to the blocky method alone at the left and right ends of the profile.

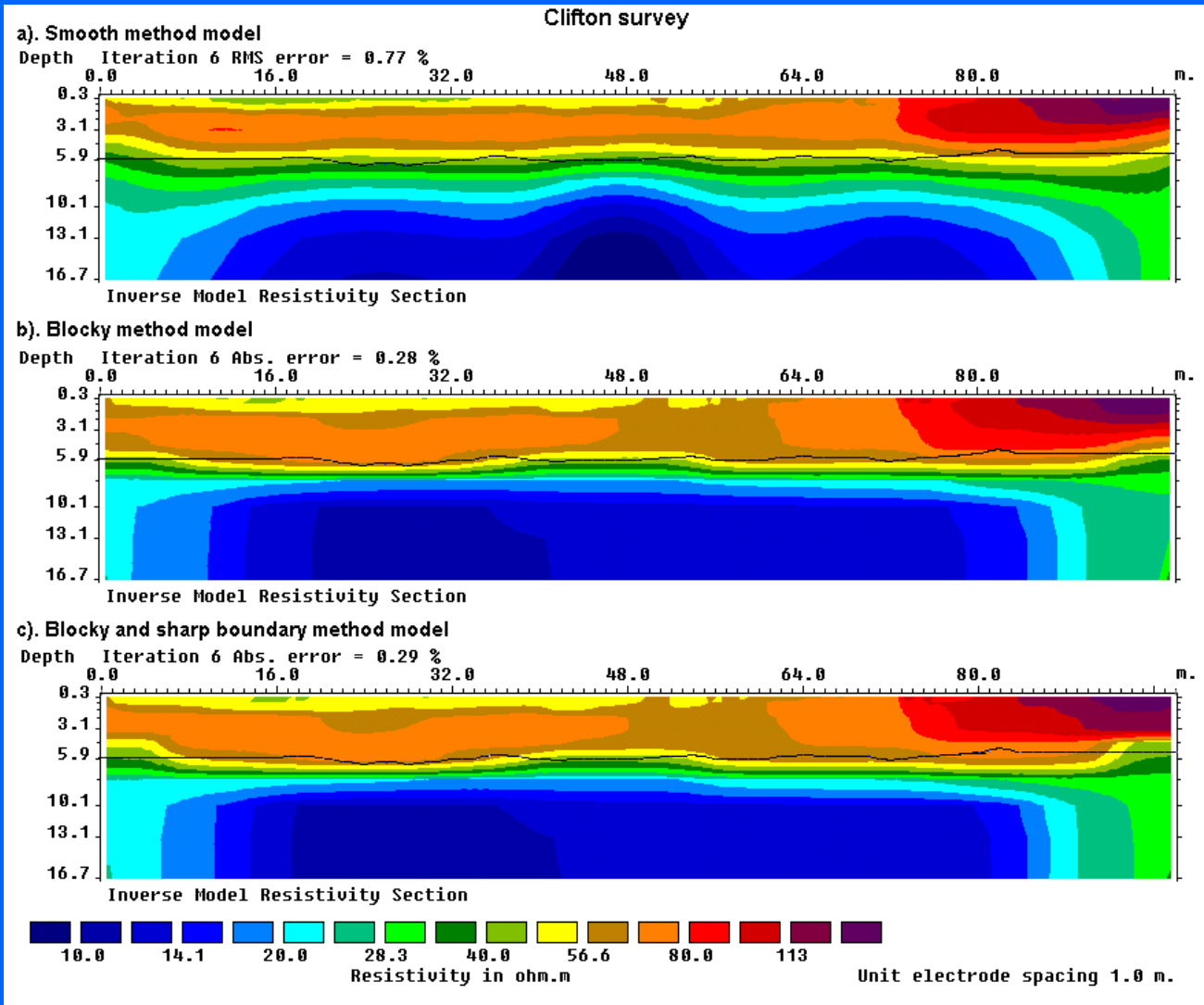

Data provided by Julian Scott, School of Earth Sciences, Un. of Birmingham, U.K.

Setting the damping factor

The λ damping factor in the least-squares optimization equation

$$\left(\mathbf{J}^{\mathrm{T}}\mathbf{J} + \lambda\mathbf{F}\right)\Delta\mathbf{q}_{\mathbf{k}} = \mathbf{J}^{\mathrm{T}}\mathbf{g} - \lambda\mathbf{F}\mathbf{q}_{\mathbf{k}},$$

$$\text{where} \quad \mathbf{F} = \alpha_x \mathbf{C}_{\mathbf{x}}^{\mathrm{T}}\mathbf{C}_{\mathbf{x}} + \alpha_y \mathbf{C}_{\mathbf{y}}^{\mathrm{T}}\mathbf{C}_{\mathbf{y}} + \alpha_z \mathbf{C}_{\mathbf{z}}^{\mathrm{T}}\mathbf{C}_{\mathbf{z}}$$

controls the relative importance in obtaining a 'smooth' model and in reducing the data misfit. The following menu has a list of option that control the use of this parameter.

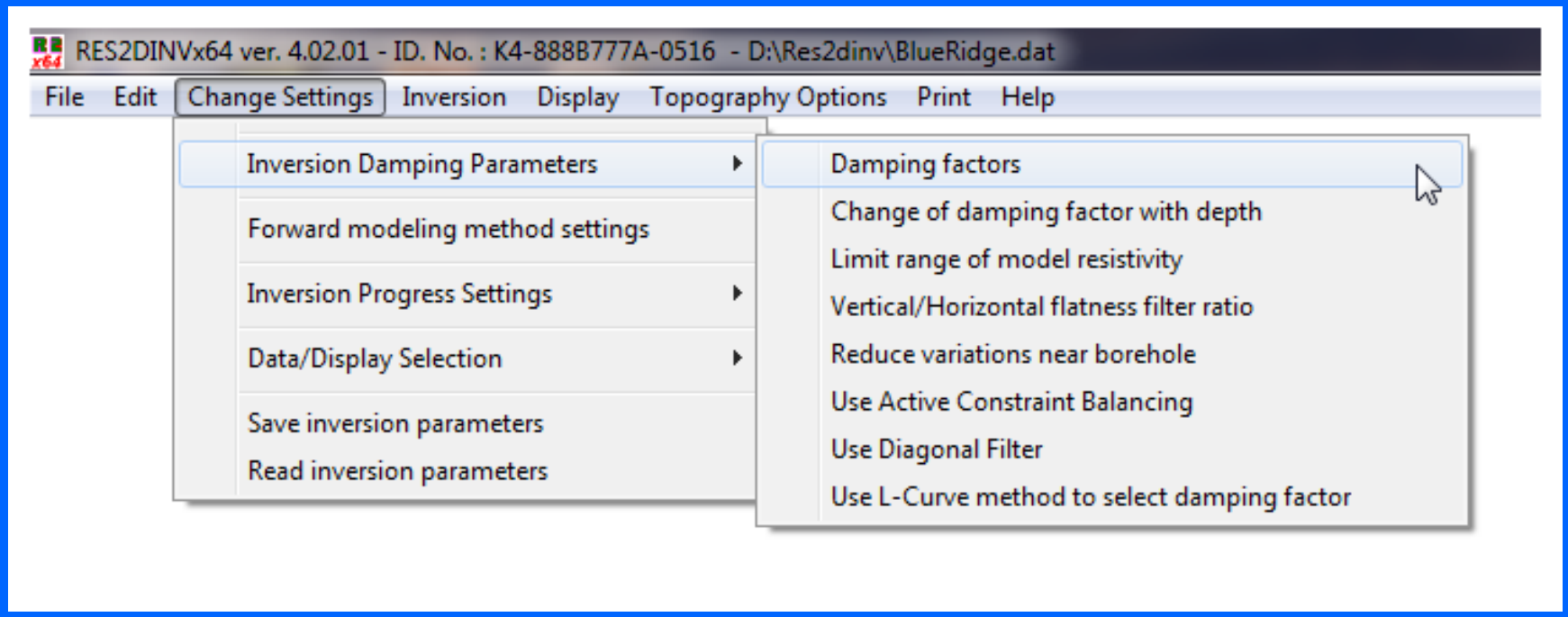

Selecting the damping factor

In the program, the inversion starts with a relatively large value for the damping factor λ which is reduced by about half in each iteration until it reaches a minimum value set. Setting too large a value for the minimum value might result in a model that is too smooth and some anomalies might be missed. Setting a value that is too small might introduce artifacts in the model. In general, the more noisy the data, the larger value is used. One method is to select the inversion model where the data misfit is 'close' to the expected error in the data if this is known.

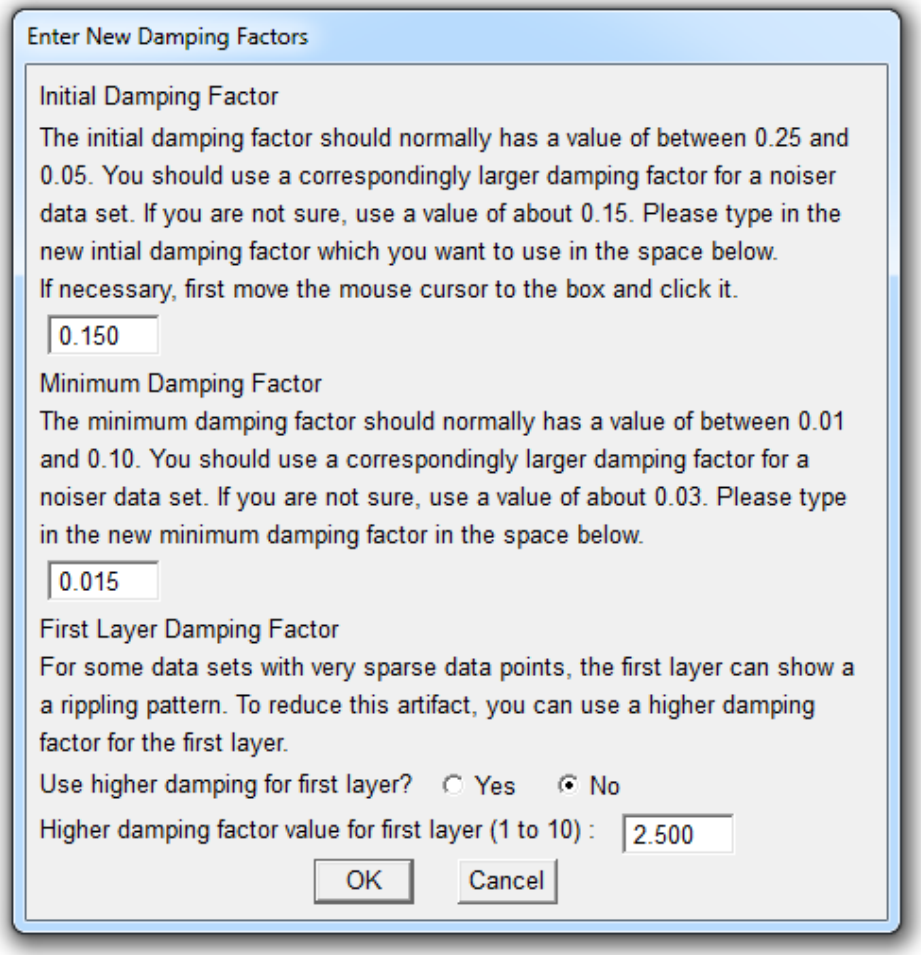

Use of L-curve method

In many cases, the data error is not accurately known. The L-curve method tries to find the optimum balance between reducing the data misfit and the model roughness. It calculates the data misfit and model roughness for different test values of the damping factor. The plot of the model roughness versus the data misfit typically has a L type shape. For large damping factor values, the model roughness is small while the data misfit is large, and vice-versa. The L-curve method uses the point of maximum curvature in the curve to estimate the optimum damping factor. Below are example plots for the BLUERIDGE.DAT data set, with optimum λ value of 0.014.

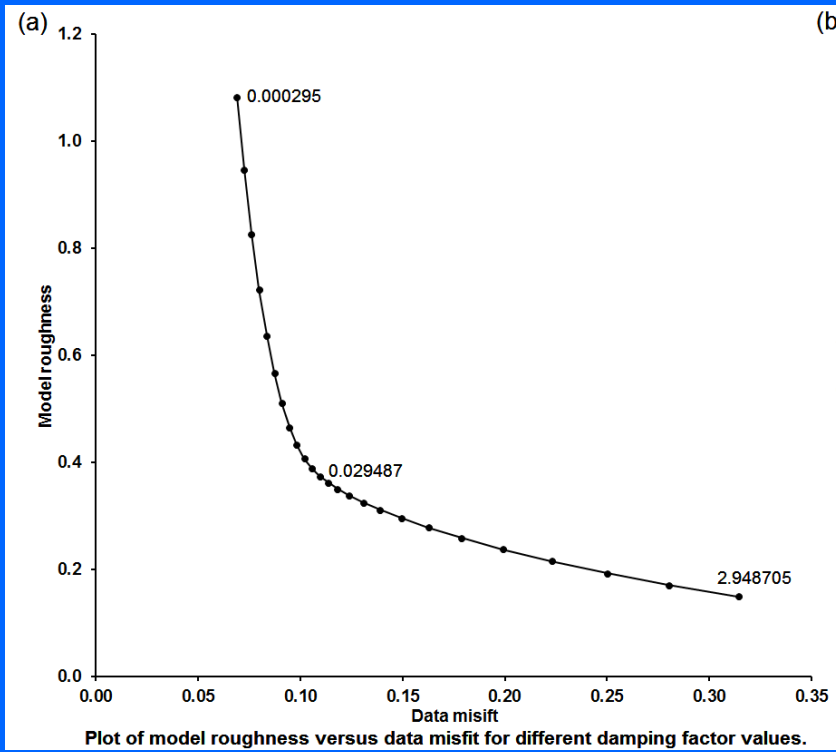

Plot of model roughness versus data misfit for different damping factor values.

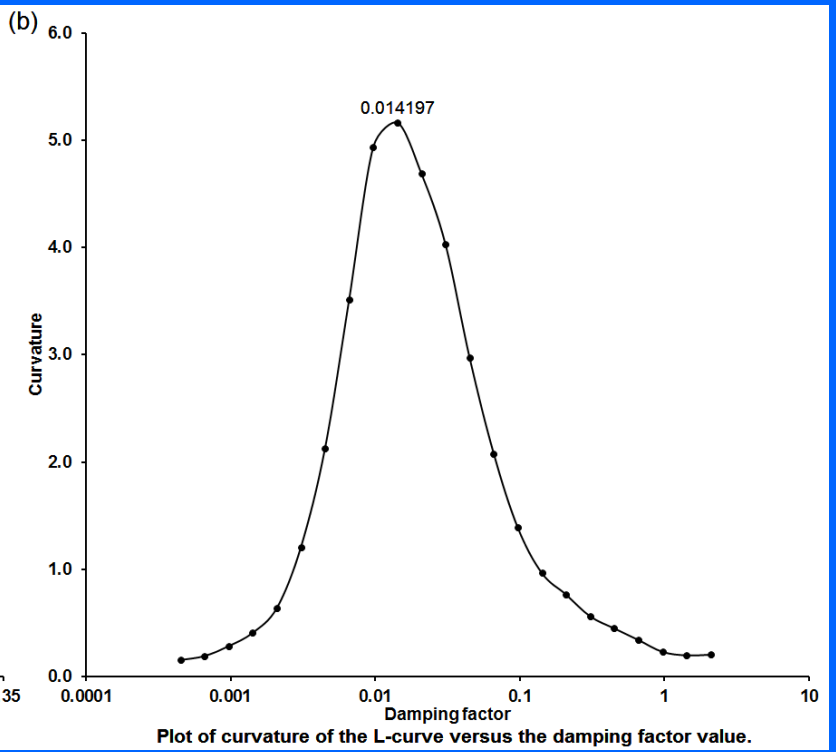

Plot of curvature of the L-curve versus the damping factor value.

Banding effects in 3-D models

Methods for reducing banding effects in 3-D inversion models for data collated from 2-D surveys lines.

3-D data sets – banding effects

To reduce the survey costs, some surveys are carried out where the spacing between the lines is twice (or more) the electrode spacing along the lines. This leads to a situation where there is not much information on the material midway between the lines. This can lead to a 'banding' effect with the structures aligned along the two axes of the survey grid. The example below has data from 11 parallel lines with an inline spacing of 0.25 m. and distance of 0.5 m. between the lines over a test site in University of Leicester, U.K. The target is a resistive sand block buried in boulder clay. The sand body is well outlined in the 3-D inversion model, but there are prominent striations in the top two layers due to banding effects.

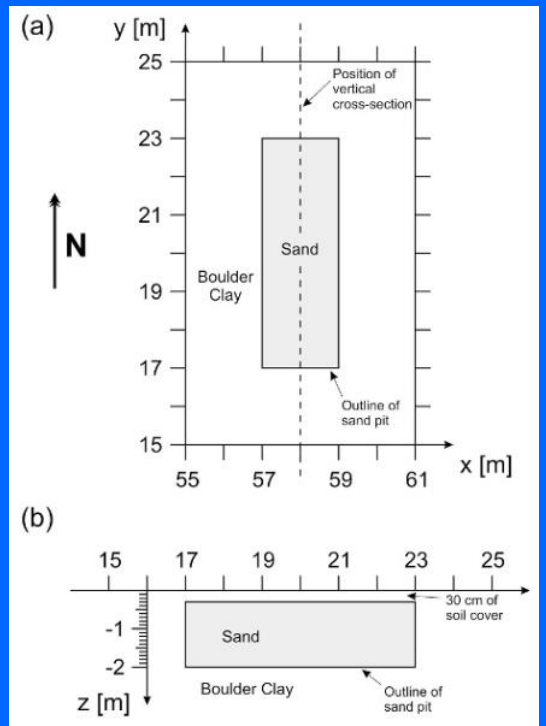

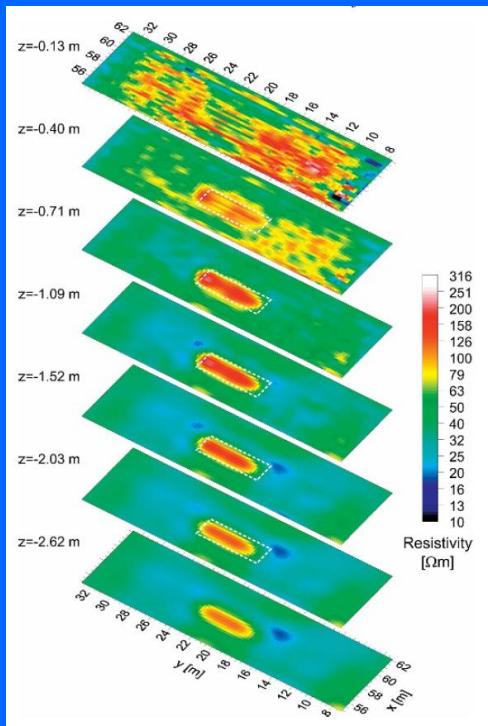

Kuras, O., Meldrum, P. I., Beamish, D., Ogilvy, R. D., and Lala, D., 2007. Capacitive resistivity imaging with towed arrays. *Journal of Environmental and Engineering Geophysics*, 12: 267-279.

Field example of 3-D effects

This survey was over the Ekeboda landfill (Sweden) has 10 parallel 2-D lines. The low resistivity area in the 2-D model due to leachate downward migration at 95 m. elevation is much smaller than the 3-D model. Other known structures such as a buried culvert on the eastern side at 98 m. elevation shows up better in the 3-D model. However the 3-D model shows prominent linear artefacts that are aligned along or perpendicular to the direction of the survey lines.

The artefacts are due to the survey setup and the arrangement of model cells and the smoothness-constrained least-squares method used. The measurements are made in only one direction. The x and y axis of the model cells are arranged along and perpendicular to the direction of the survey lines. There is a directional bias in both the data and the model cells setup.

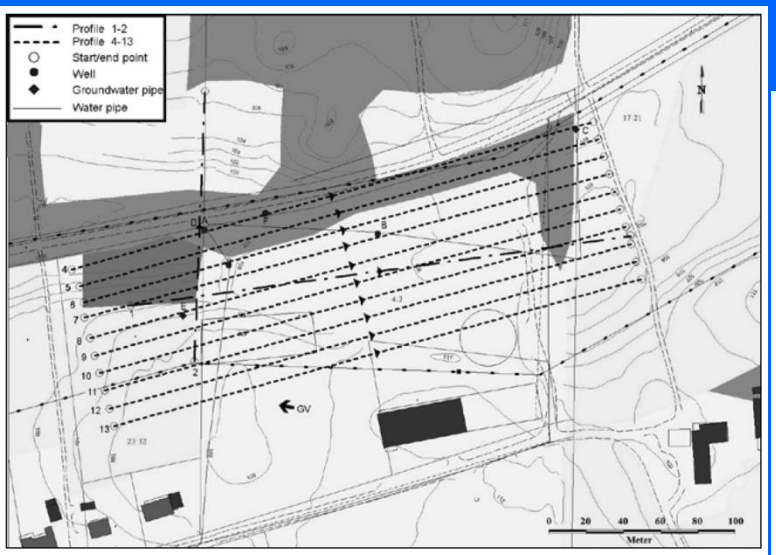

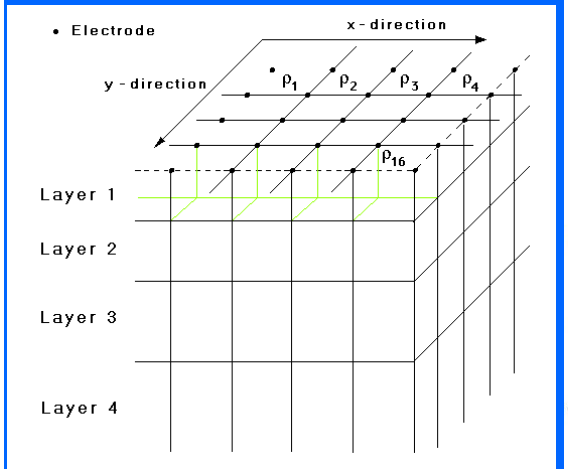

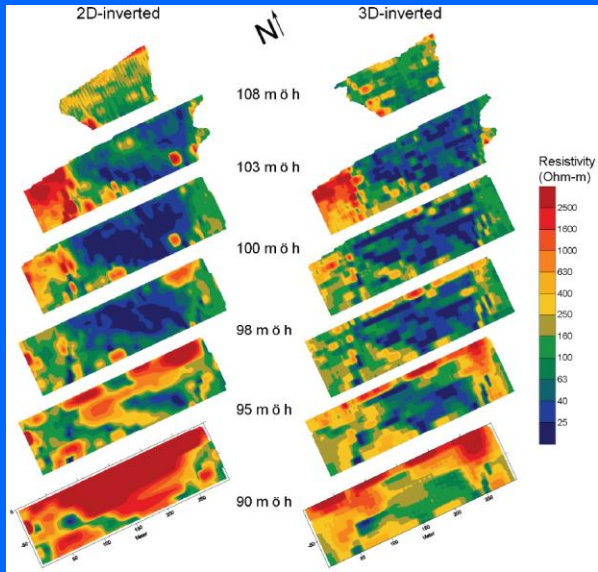

Structure of the roughness filter

The roughness filter has the form $$F = \delta x^T \delta x + \delta y^T \delta y + \delta z^T \delta z$$

δx, δy and δz are the first-order difference matrices in the x, y and z directions. It minimizes the change the resistivity between adjacent model cells in the x, y and z directions. It has a bias to produce structures that are aligned along the x, y and z directions particularly if the L_1-norm (blocky) inversion method is used.

A modification to the horizontal roughness filter to include components in the diagonal x-y directions is made to reduce the bias.

Coupling of 3-D model cells in roughness filter

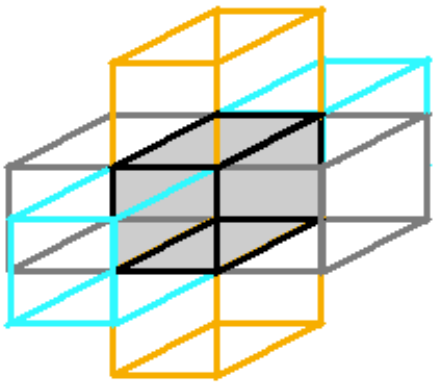

Normal horizontal roughness filter x and y components

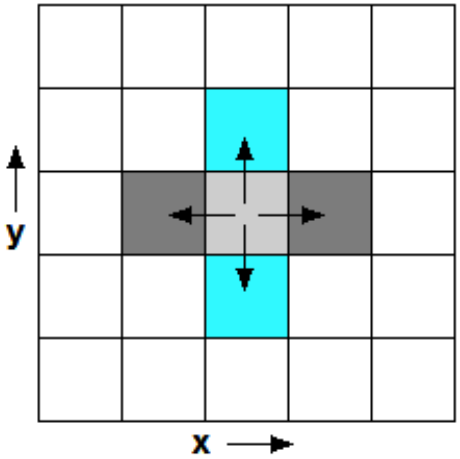

Normal vertical roughness filter with z component

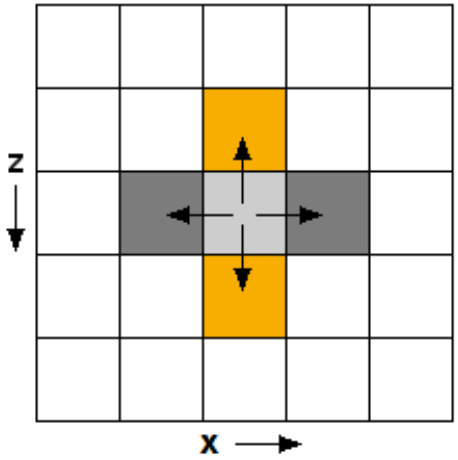

Horizontal roughness with diagonal x-y components

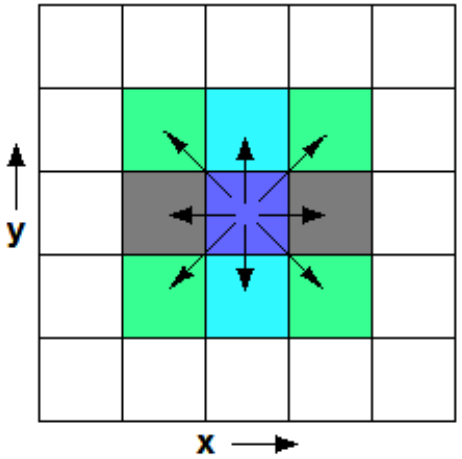

Ekeboda landfill data set – default model

The field survey data set consists of 10 parallel lines with 61 electrode positions along each line using the multiple gradient array. The in-line electrode spacing is 5 meters, and the spacing between the lines is 10 meters. The model has prominent structures in the top two layers that are elongated in the *y* direction as the model cells are twice as long in this direction.

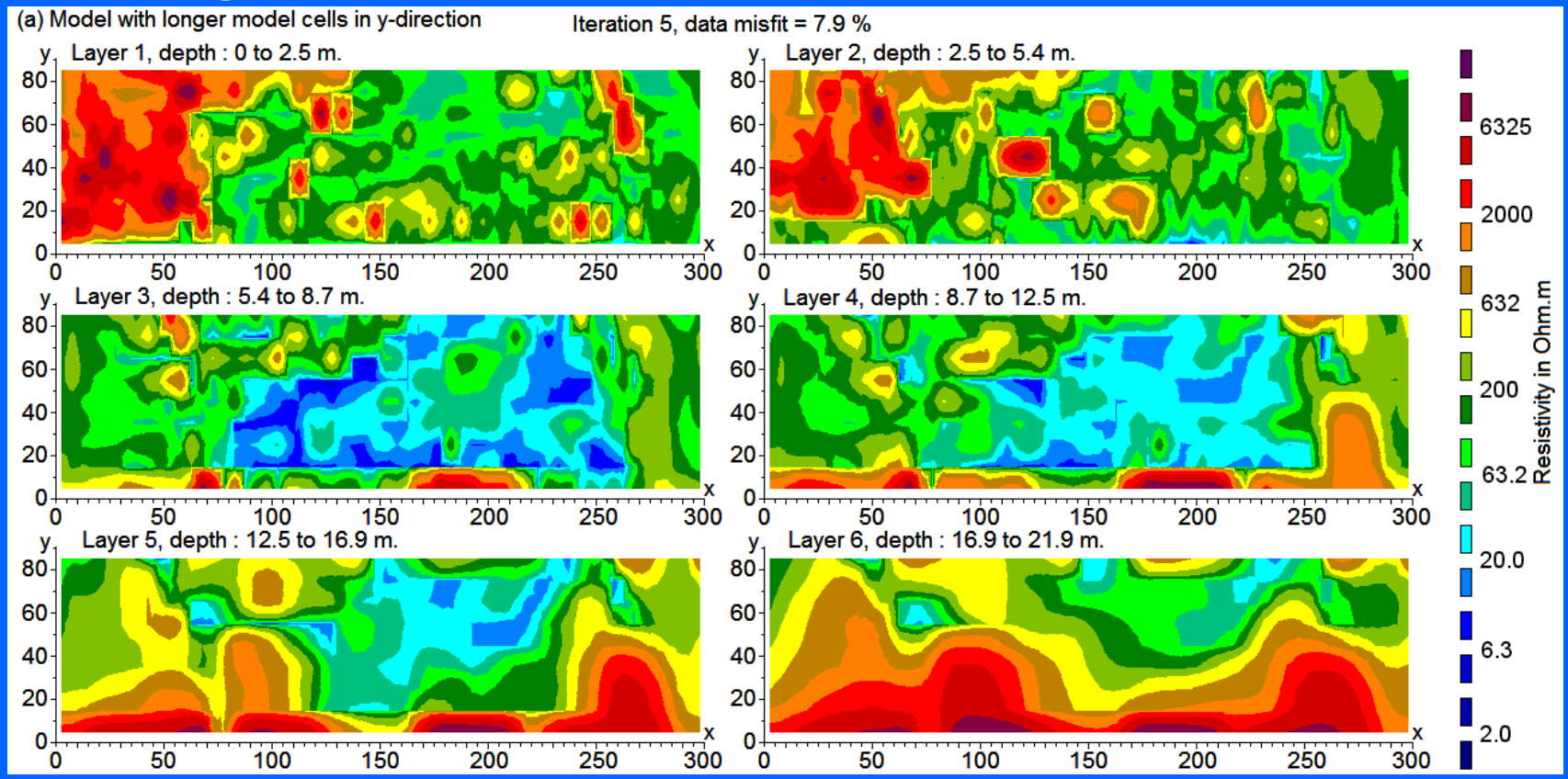

Ekeboda landfill – model with uniform cell lengths

The inversion model with cells of the same lengths in the *x* and *y* directions removes the elongated structures in the *y* direction. The banding effect in the *x* direction is more clearly shown in the top three layers, such as in the low resistivity (blue) landfill.

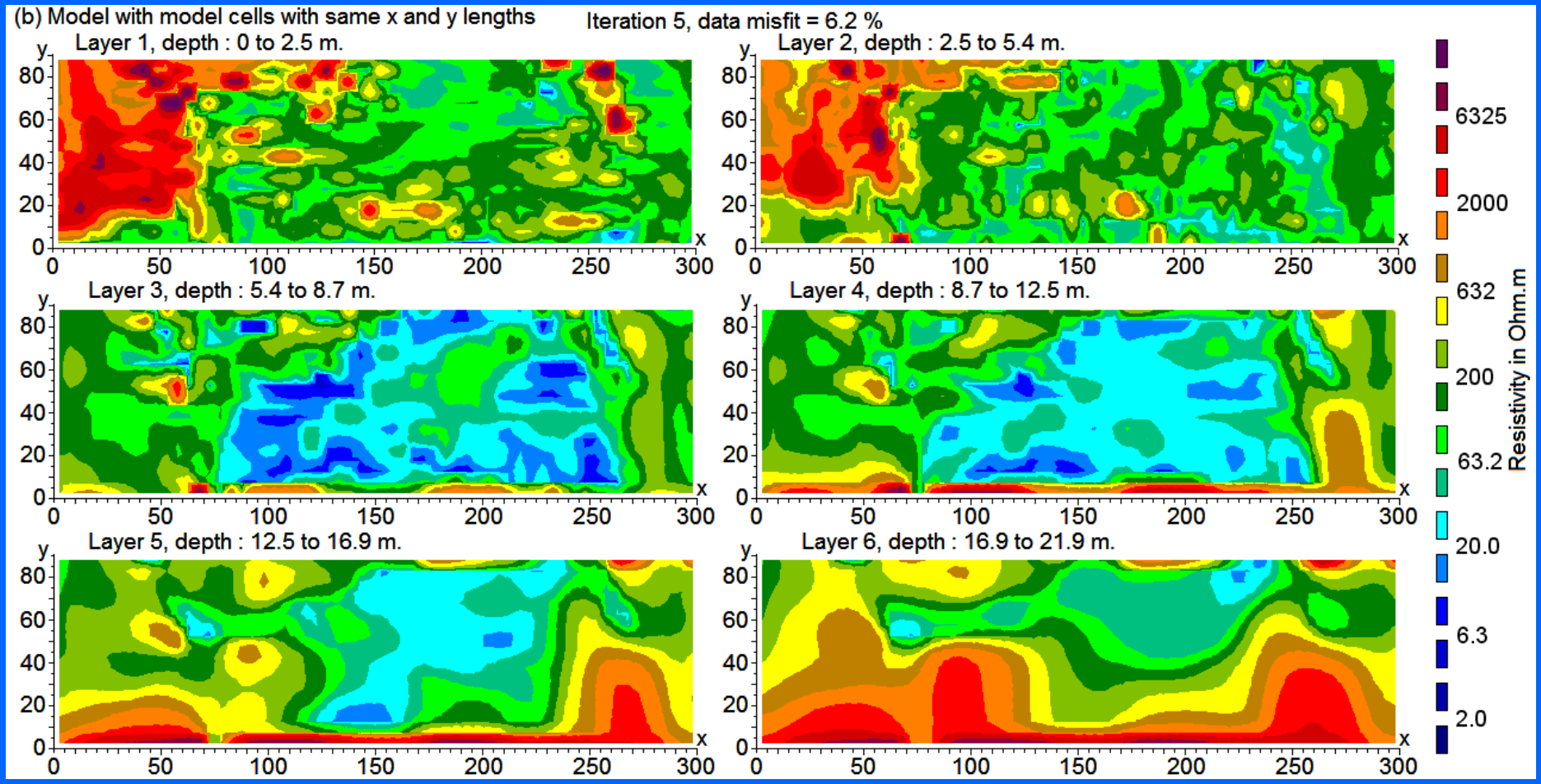

Ekeboda landfill – model with higher damping factors

The elongated structures in the *x* direction are greatly reduced by using a higher damping factor for the top layers. The more slanting left boundary of the low resistivity landfill is now more clearly shown.

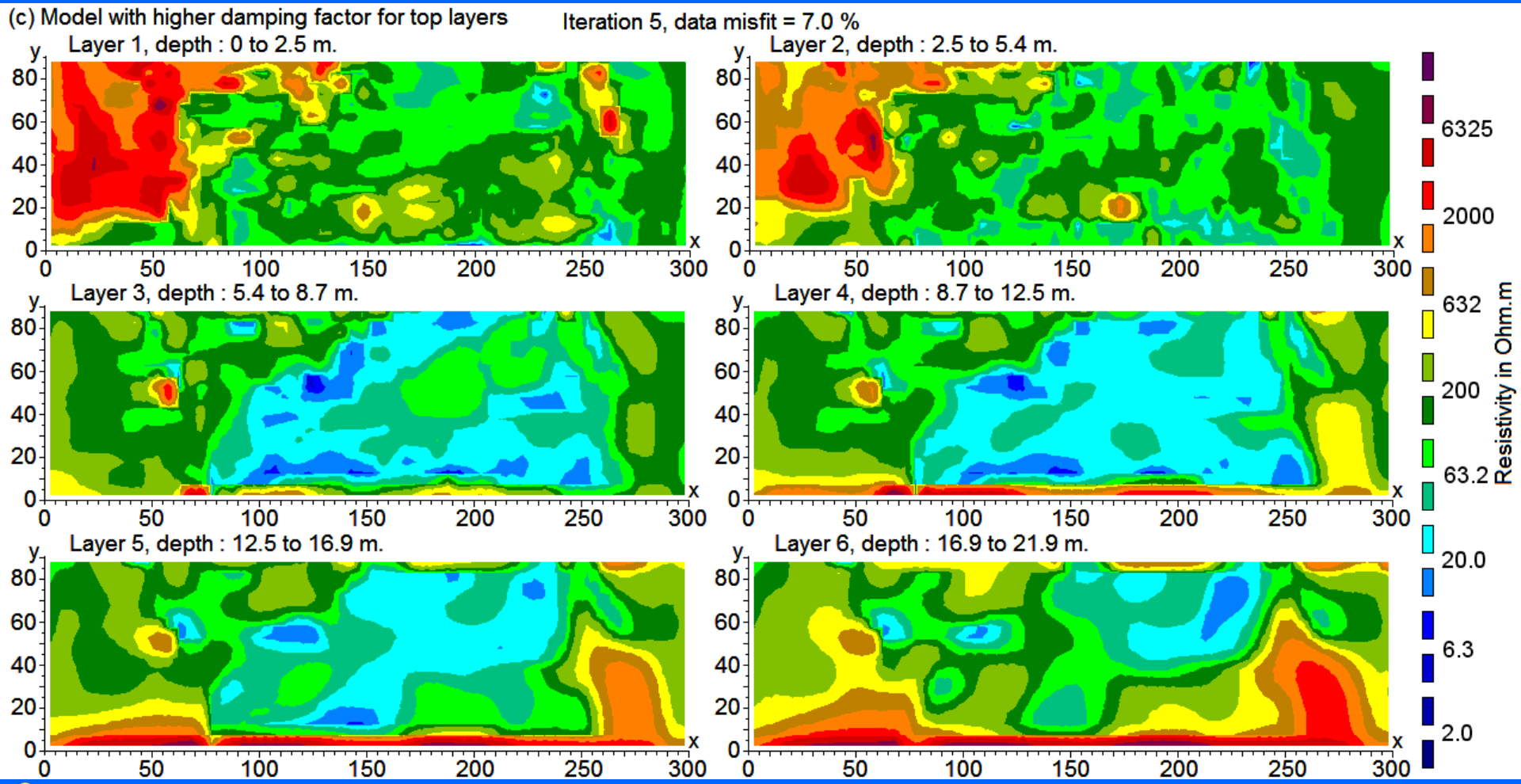

Ekeboda landfill data set – model with diagonal filters

The elongated structures in the *x* direction is are almost completely removed when the horizontal roughness filter with diagonal *x-y* components is used.

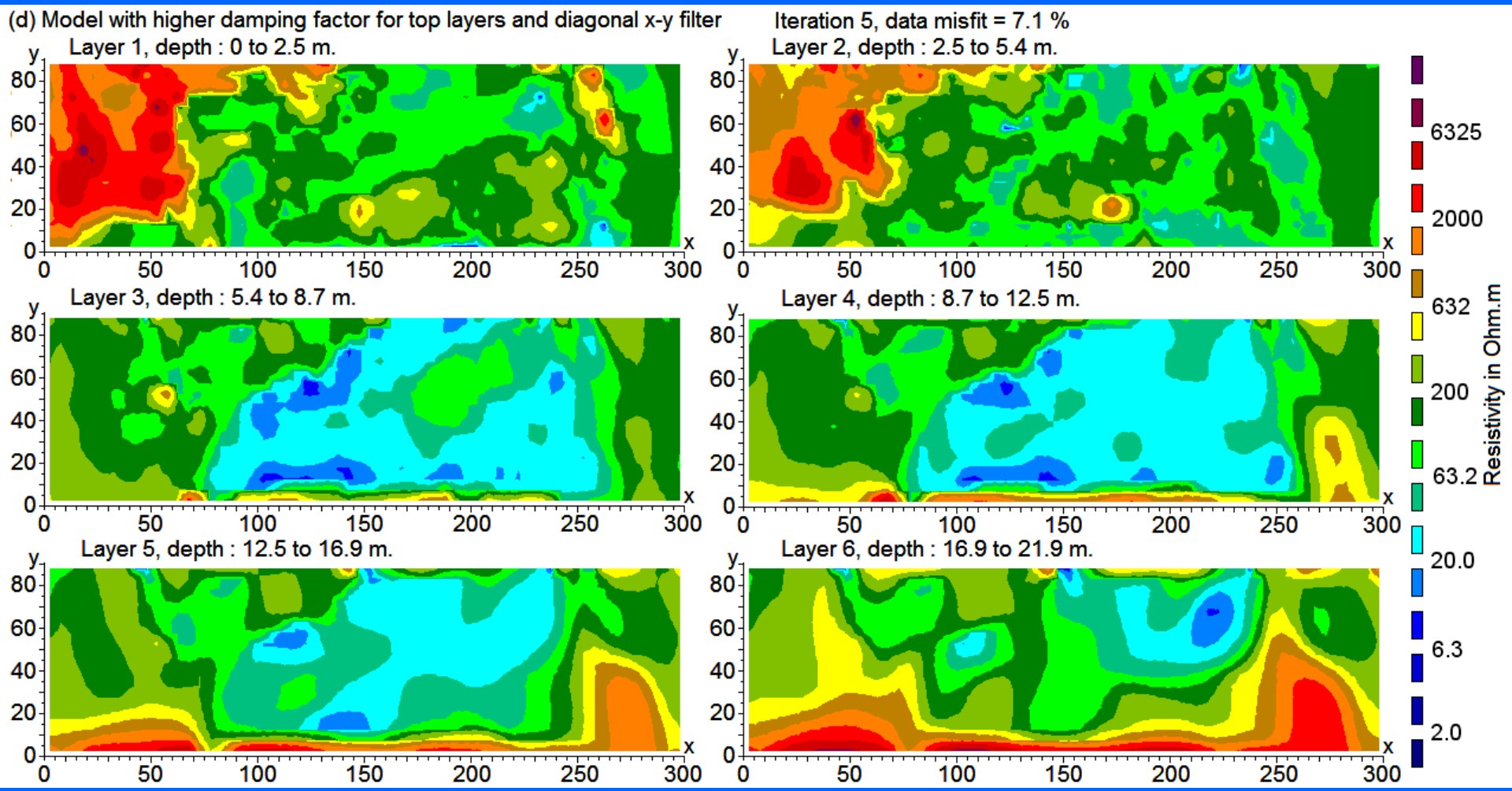

Other types of diagonal filters

Roughness filters with diagonal components in the *x-z* and *y-z* directions can be used to reduce bias in the vertical direction. The roughness filter can also be applied between the central and corner cells as well (only 2 out of 8 corner cells are shown).

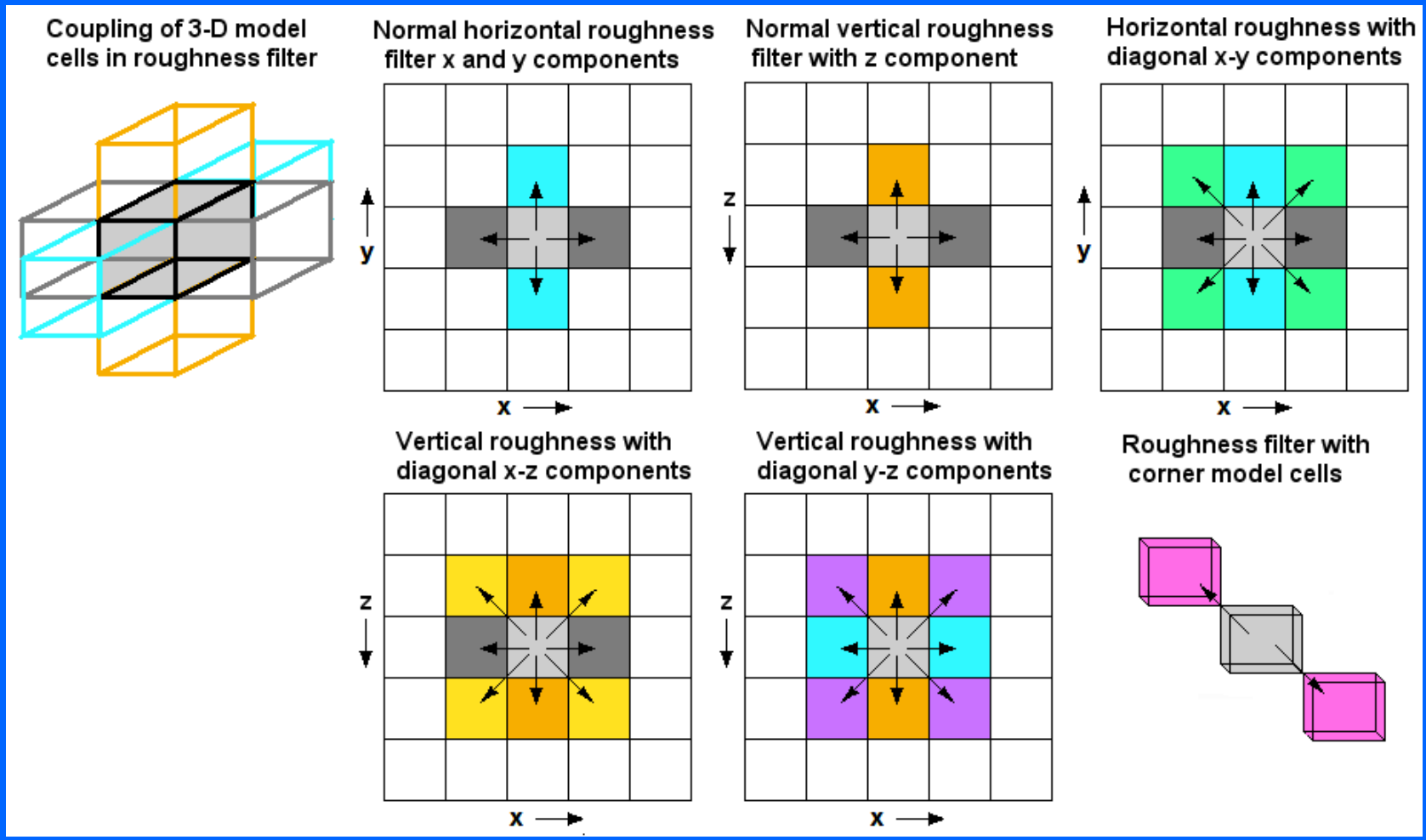

Banding effects conclusions

Many 3-D data sets are collated from a series of parallel 2-D survey lines. The distance between the lines is often two or more times the in-line electrode spacing.

Inversion models for such 3D data sets can display artefacts in the top layers elongated along the axes of the survey grid.

The artefacts are reduced by using a model discretization where the cells have about the same lengths in both horizontal directions.

Further reductions in the artefacts are achieved by using a higher damping factor for the top few layers together with a horizontal roughness filter with diagonal components.

Model reliability

Different estimates of model reliability

Sensitivity

Covariance matrix

DOI

Model Resolution

Model reliability

A 2-D survey typically has hundreds of data points collected with electrodes at different locations and spacings. We want to know the regions of the subsurface sensed by the survey, and the reliability of the results.

Sensitivity values

One method is to use the ‘sensitivity’ values, i.e. elements of the Jacobian matrix associated with the model cells. In the RES2DINV, the sum of the absolute values of the sensitivity values associated with the model cell is used. The sensitivity value is a measure of the amount of information about the resistivity of a model block cell in the measured data set. The higher the sensitivity value, the more reliable is the model resistivity value. In general, the cells near the surface usually have higher sensitivity values because the sensitivity function has very large values near the electrodes.

Model reliability - sensitivity

Figure shows the model section obtained from the inversion of a data set for a survey to map leakage of pollutants from a landfill site. The model sensitivity section in shows high sensitivity values near the surface with decreasing values with depth. This is to be expected as the near surface materials have a larger influence on the measured apparent resistivity values. The large values at the sizes are due to the larger sizes of the side model cells (the sensitivity values have not been normalized for the size of the cells).

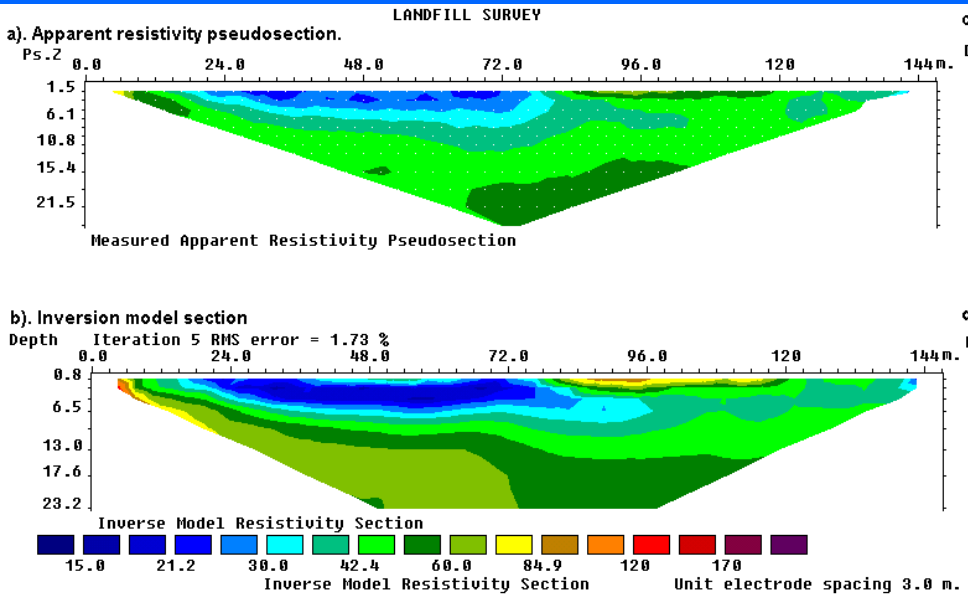

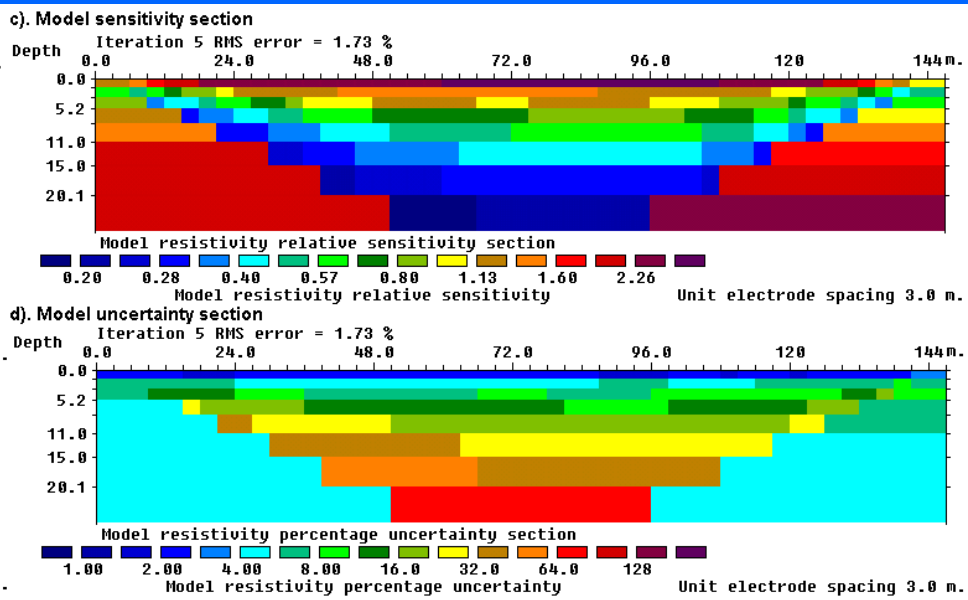

Model reliability – covariance matrix

Another approach is by using the model covariance matrix which is given by $[\text{cov } m]=\sigma_d^2(J^TJ+\lambda F)^{-1}$, where σ_d^2 is the variance of the data misfit. Figure (d) shows the model uncertainty values obtained from this method where the smoothness constraint is included in the model uncertainty estimate. However the uncertainty values are only meaningful if the subsurface resistivity varies in a smooth manner as assumed by the smoothness constraint.

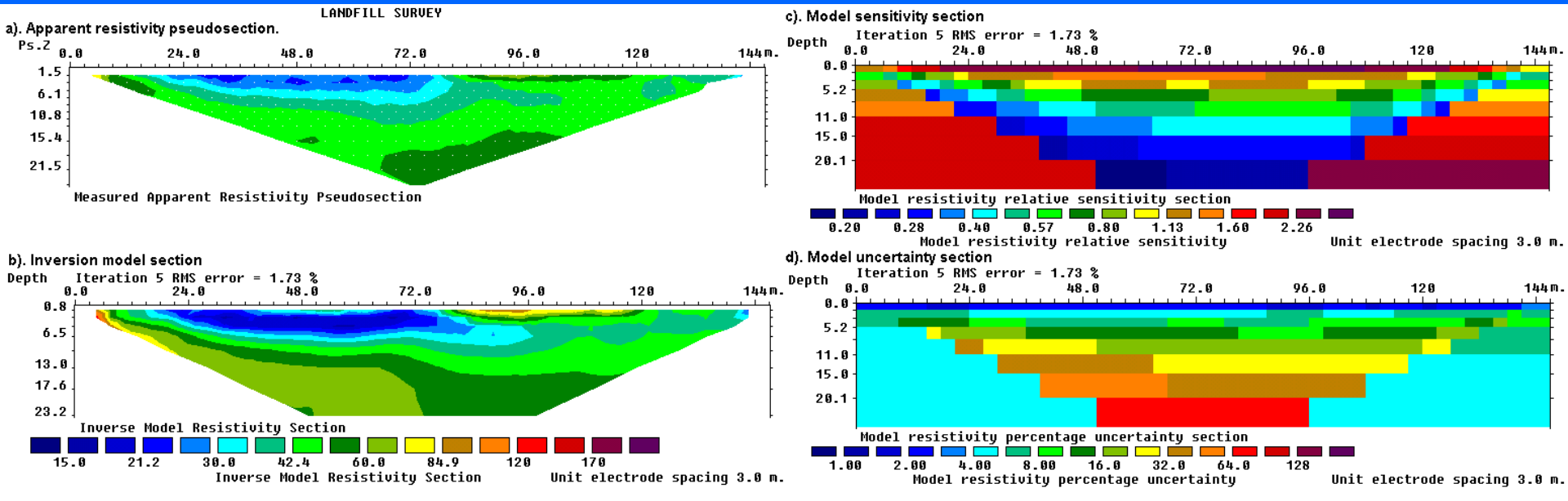

Model reliability – DOI

The depth of investigation (DOI) method carries out two inversions of the data set using different reference models using the following least-squares equation.

$$\left(\mathbf{J}^{\mathrm{T}}\mathbf{J} + \lambda\mathbf{F}_{\mathrm{R}}\right)\Delta\mathbf{q}_{\mathrm{k}} = \mathbf{J}^{\mathrm{T}}\mathbf{R}_{\mathrm{d}}\mathbf{g} - \lambda\mathbf{F}_{\mathrm{R}}(\mathbf{q}_{\mathrm{k}} - \mathbf{q}_{\mathrm{o}}),\ \textit{where}\ \mathbf{F}_{\mathrm{R}} = \alpha_s + \alpha_x\mathbf{C}_{\mathrm{x}}^{\mathrm{T}}\mathbf{R}_{\mathrm{m}}\mathbf{C}_{\mathrm{x}} + \alpha_z\mathbf{C}_{\mathrm{z}}^{\mathrm{T}}\mathbf{R}_{\mathrm{m}}\mathbf{C}_{\mathrm{z}}$$

$\mathbf{q}_o$ is a homogeneous half-space reference model and α_s is an additional "self" damping factor that has a value of about 0.01 times the α_x and α_z damping factors. Two inversions are carried out using different resistivity values for the reference model. The second reference model usually has a resistivity of 10 to 100 times the first reference model. The DOI value is calculated using the following equation.

$$R(x,z) = \frac{m_1(x,z) - m_2(x,z)}{m_{1r} - m_{2r}}$$

m_{1r} and m_{2r} are the resistivity of first and second reference models, $m_1(x,z)$ and $m_2(x,z)$ are model cell resistivity obtained from the first and second inversions. R will approach a value of 0 where the inversion will produce the same cell resistivity regardless of the reference model resistivity. In such areas, the cell resistivity is well constrained by the data. In areas where the data do not have much information about the cell resistivity, R will approach a value of 1 as the cell resistivity will be similar to the reference resistivity. The model resistivity in areas where R has small values are considered to be "reliable", while in areas with high R values are not reliable.

Model reliability – Landfill DOI example

The model cells extend to the ends of the survey line and a depth of about 3 to 5 times the maximum median depth of investigation of the data set. This ensures that the data has little information about the resistivity of the cells at the bottom of the model and have DOI values of almost 1.0. The figure below shows the inversion model and DOI section for the landfill survey data set. A value of 0.1 is used as the cut-off limit for the effective depth of investigation. The depth to the 0.1 DOI contour is about 27 m. along most of the survey line, compared to 25 m. for the maximum median depth of investigation. The shallower regions with high DOI values below the 50 m. mark is probably due to the low resistivity plume that limits the amount of current flowing into the deeper sections below it. The regions at the sides of the section have high DOI values because of less data coverage.

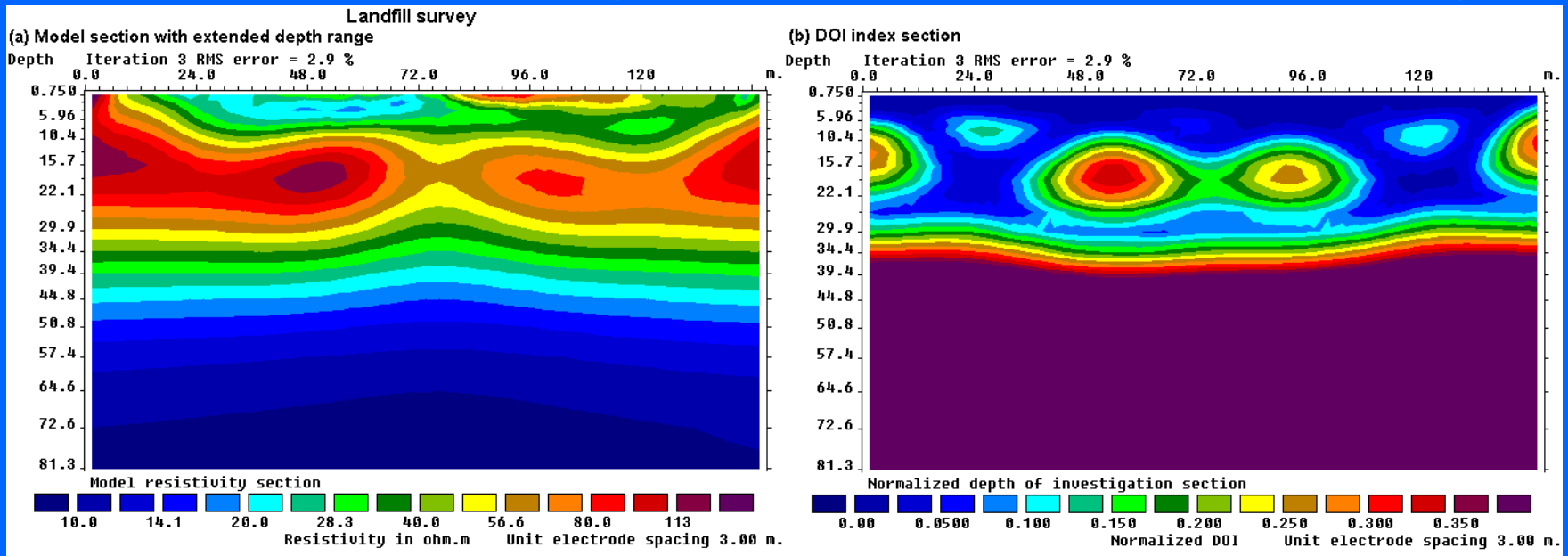

Model reliability – Saline boundary DOI example

The figure below shows the DOI plot from a survey to map the boundary between the salt and fresh water zones across a beach in Denmark. The profile is perpendicular to the seashore and the electrodes 1 to 16 are under the seawater, while the rest of the profile is above the water. Note the increase in DOI values on the left part of the profile that is covered with seawater. In this section most of the current flows within the seawater and does not penetrate into the subsurface. Thus the depth of investigation there is much shallower.

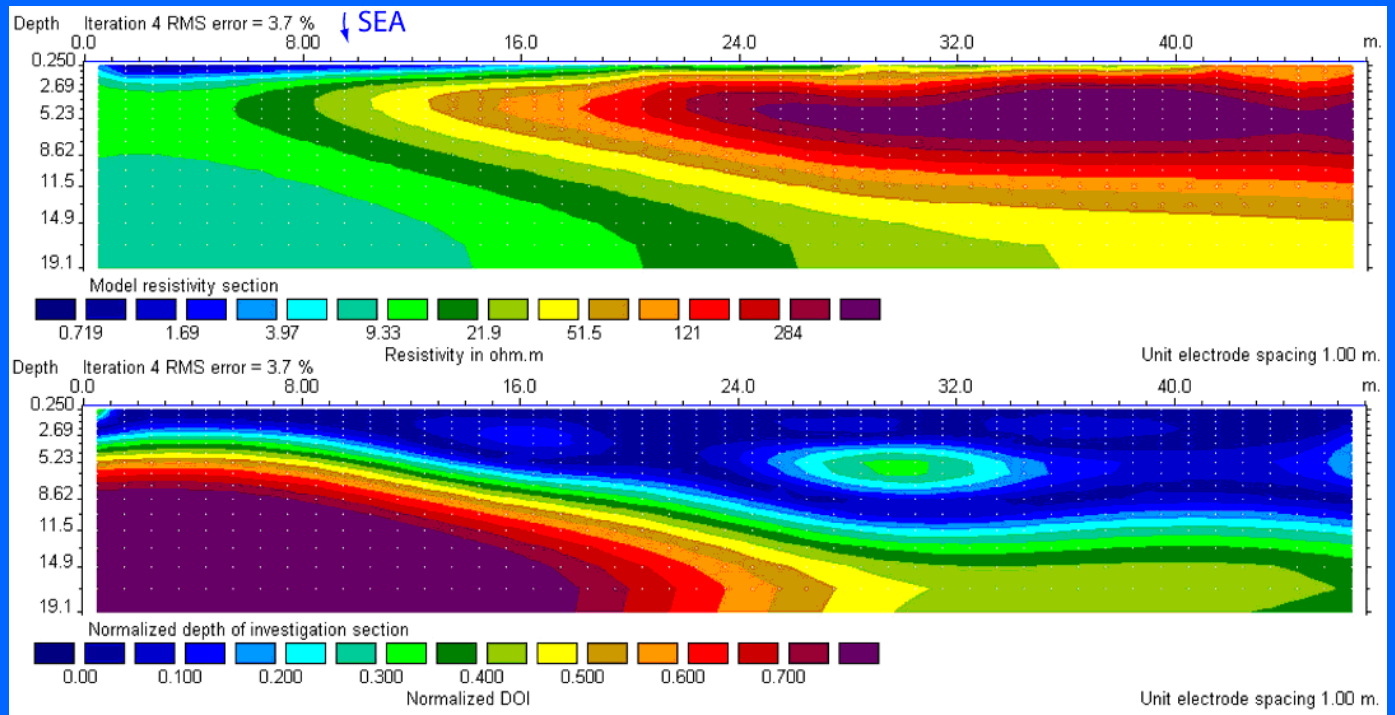

Model reliability –DOI remarks

The DOI method is useful in marking the regions where the model values are well constrained by the data set, and thus greater confidence can be placed on the model resistivity values at such regions.

The DOI method may be considered an empirical method to determine the regions where we can reasonably resolve the subsurface.

Resolution of data sets and models

Use of model resolution to quantify the information in a data set and inversion model sections.

Information in a data set

The sensitivity section shows the areas where a single array gives the most information about the subsurface. However, a survey consists of data collected using many arrays with electrodes placed at different locations, and with different spacings.

For example, the diagram below shows a Wenner array survey with 58 data points. What are the sections of the subsurface where this survey gives reliable information?

One method to determine this is the model resolution section.

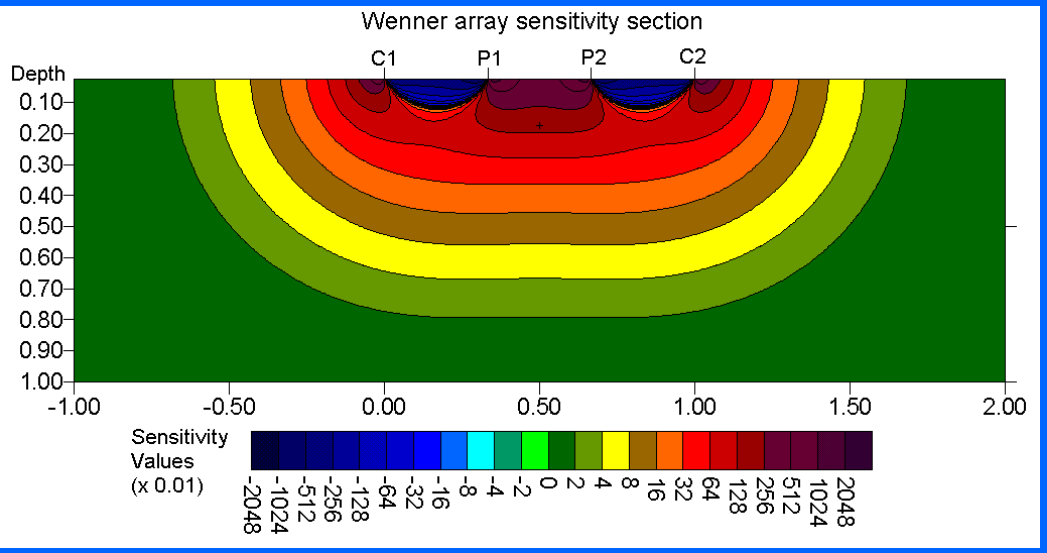

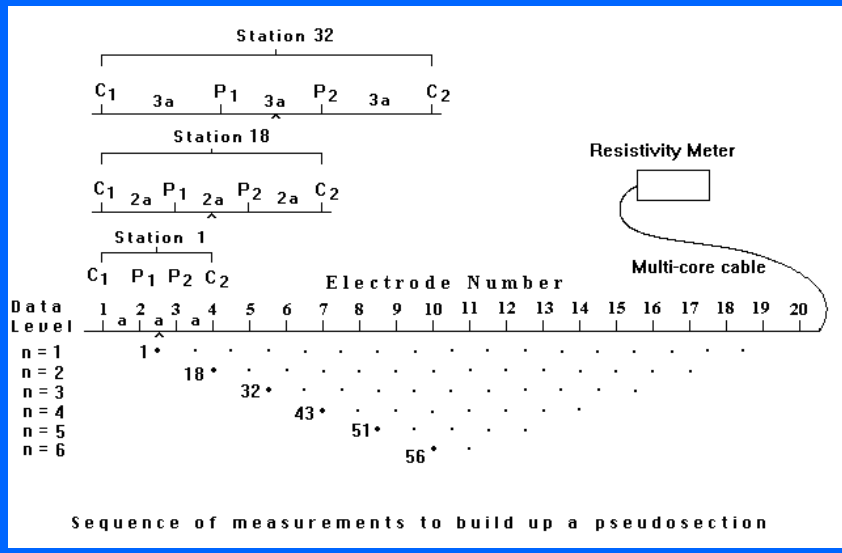

Model resolution equation

The model resolution equation is related to the least-squares equation which is given by

$$\left(\mathbf{J}^{\mathbf{T}}\mathbf{J}+\lambda\mathbf{F}\right)\Delta\mathbf{q}_{\mathbf{k}}=\mathbf{J}^{\mathbf{T}}\mathbf{g}-\lambda\mathbf{F}\,\mathbf{q}_{\mathbf{k}}$$

The relation between the calculated model resistivity and the true resistivity is approximately given by

$$\mathbf{q}_{\mathbf{Model}}\approx\left(\mathbf{J}^{\mathbf{T}}\mathbf{J}+\lambda\mathbf{F}\right)^{-1}\mathbf{J}^{\mathbf{T}}\mathbf{J}\,\mathbf{q}_{\mathbf{Actual}}$$

To show the relationship better, we rewrite it as

$$\mathbf{q}_{\mathbf{Model}}\approx\mathbf{R}\,\mathbf{q}_{\mathbf{Actual}}\ ,\quad\mathbf{R}=\left(\mathbf{J}^{\mathbf{T}}\mathbf{J}+\lambda\mathbf{F}\right)^{-1}\mathbf{J}^{\mathbf{T}}\mathbf{J}$$

The **R** matrix is called the resolution matrix.

It can be considered as a ‘filter’ or ‘distorting lens’ through which we see the subsurface.

Model resolution – seeing through a distorting lens

The effect of the model resolution matrix can be shown qualitatively below. Consider an original image, such as

A person with less than perfect eyesight might see it as

Someone with very poor eyesight might see it as

The matrix R can be considered as a 'blurring' matrix that contaminates the calculated model value with values from nearby cells.

Model resolution – simple example

Consider as simple model with only 4 cells.

The relationship between the calculated resistivity value for each cell and the true cell resistivity value is given by

$$\mathbf{q}_{\text{Model}} \approx \mathbf{R}\,\mathbf{q}_{\text{Actual}}\ ,\quad \mathbf{R} = \left(\mathbf{J}^{\mathrm{T}}\mathbf{J} + \lambda\mathbf{F}\right)^{-1}\mathbf{J}^{\mathrm{T}}\mathbf{J}$$

Model with 4 cells

q_1	q_2
q_3	q_4

This can be written in matrix form as

$$\begin{pmatrix} q_{M1} \\ q_{M2} \\ q_{M3} \\ q_{M4} \end{pmatrix} = \begin{pmatrix} R_{11} & R_{12} & R_{13} & R_{14} \\ R_{21} & R_{22} & R_{23} & R_{24} \\ R_{31} & R_{32} & R_{33} & R_{34} \\ R_{41} & R_{42} & R_{43} & R_{44} \end{pmatrix} \begin{pmatrix} q_{A1} \\ q_{A2} \\ q_{A3} \\ q_{A4} \end{pmatrix}$$

$$\mathbf{q}_{\text{Model}} = \mathbf{R}\,\mathbf{q}_{\text{Actual}}$$

Perfect model resolution example

So far we have the model resolution matrix

$$\begin{pmatrix} q_{M1} \\ q_{M2} \\ q_{M3} \\ q_{M4} \end{pmatrix} = \begin{pmatrix} R_{11} & R_{12} & R_{13} & R_{14} \\ R_{21} & R_{22} & R_{23} & R_{24} \\ R_{31} & R_{32} & R_{33} & R_{34} \\ R_{41} & R_{42} & R_{43} & R_{44} \end{pmatrix} \begin{pmatrix} q_{A1} \\ q_{A2} \\ q_{A3} \\ q_{A4} \end{pmatrix}$$

$$\mathbf{q}_{\text{Model}} = \mathbf{R}\, \mathbf{q}_{\text{Actual}}$$

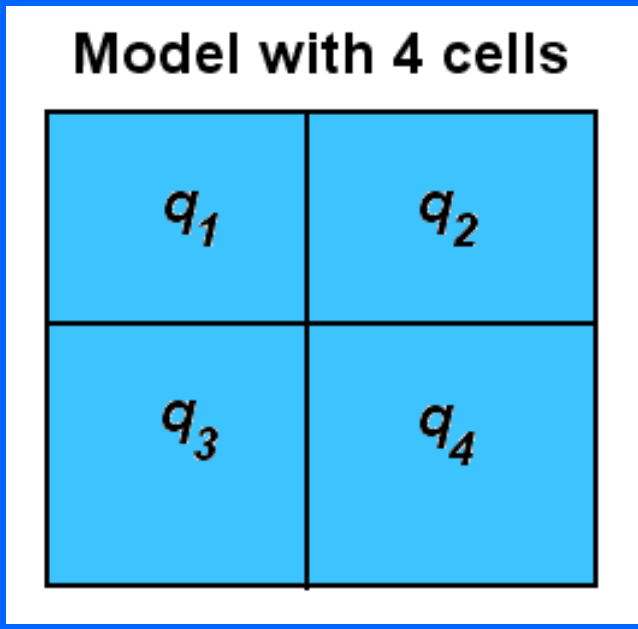

If the cells are perfectly resolved, the diagonal elements of the resolution matrix are 1.0 and other elements are 0.0.

This means the calculated value for each cell only depends on the true value.

$$\begin{pmatrix} q_{M1} \\ q_{M2} \\ q_{M3} \\ q_{M4} \end{pmatrix} = \begin{pmatrix} 1.0 & 0.0 & 0.0 & 0.0 \\ 0.0 & 1.0 & 0.0 & 0.0 \\ 0.0 & 0.0 & 1.0 & 0.0 \\ 0.0 & 0.0 & 0.0 & 1.0 \end{pmatrix} \begin{pmatrix} q_{A1} \\ q_{A2} \\ q_{A3} \\ q_{A4} \end{pmatrix}$$

Imperfect model resolution example

In the case with imperfect resolution, we might have something like

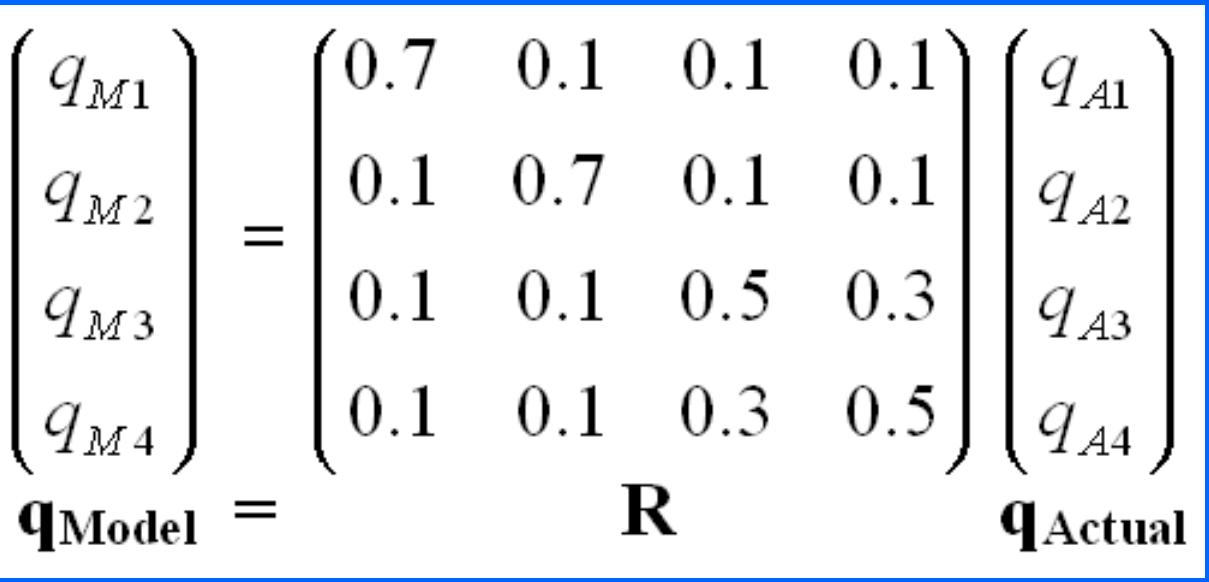

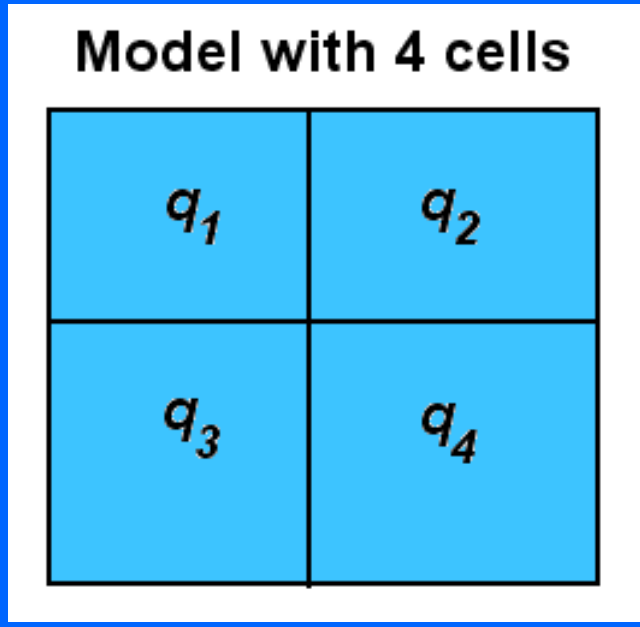

The diagonal elements give the 'degree' of resolution, while the off diagonal elements give the degree of 'contamination' or cross-correlation with the neighboring model cells. One way to illustrate the resolution is to plot the values of the diagonal elements of the R matrix. This shows the degree at which the calculated model value depends on the true value. A value of about 0.05 (5%) is sometimes chosen as the 'cutoff' value.

Model resolution – Wenner array survey

As an example, we use a survey line with 30 electrodes with 1 meter spacing. First we look at the model resolution for a Wenner array survey with the '*a*' spacing ranging from 1 to 9 meters.

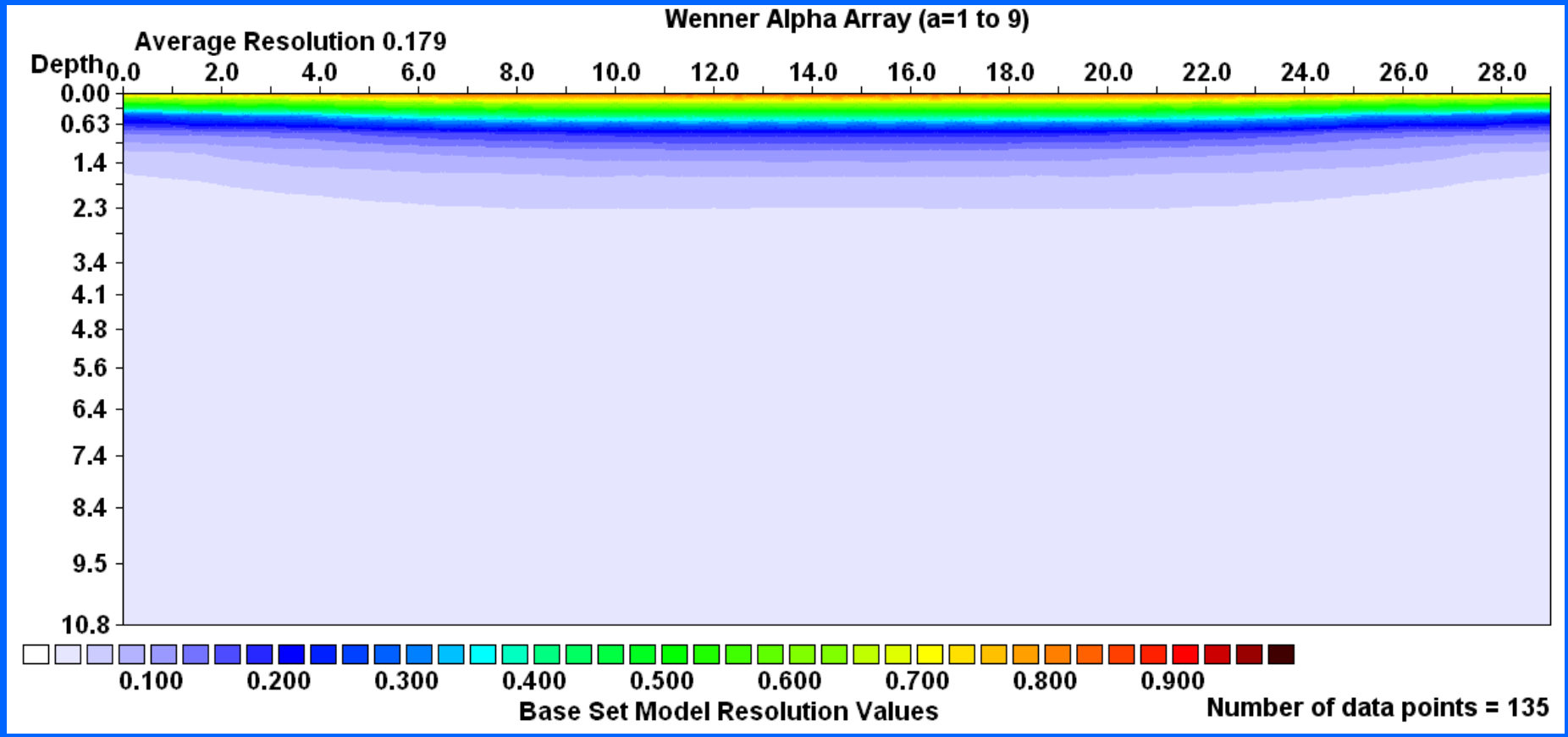

The resolution is greatest near the surface, decreases rapidly with depth, and is very small below a depth of about 2.0 meters.

Model resolution – dipole-dipole survey

Next we check the resolution for a dipole-dipole survey carried out with a=1, and n=1 to 6.

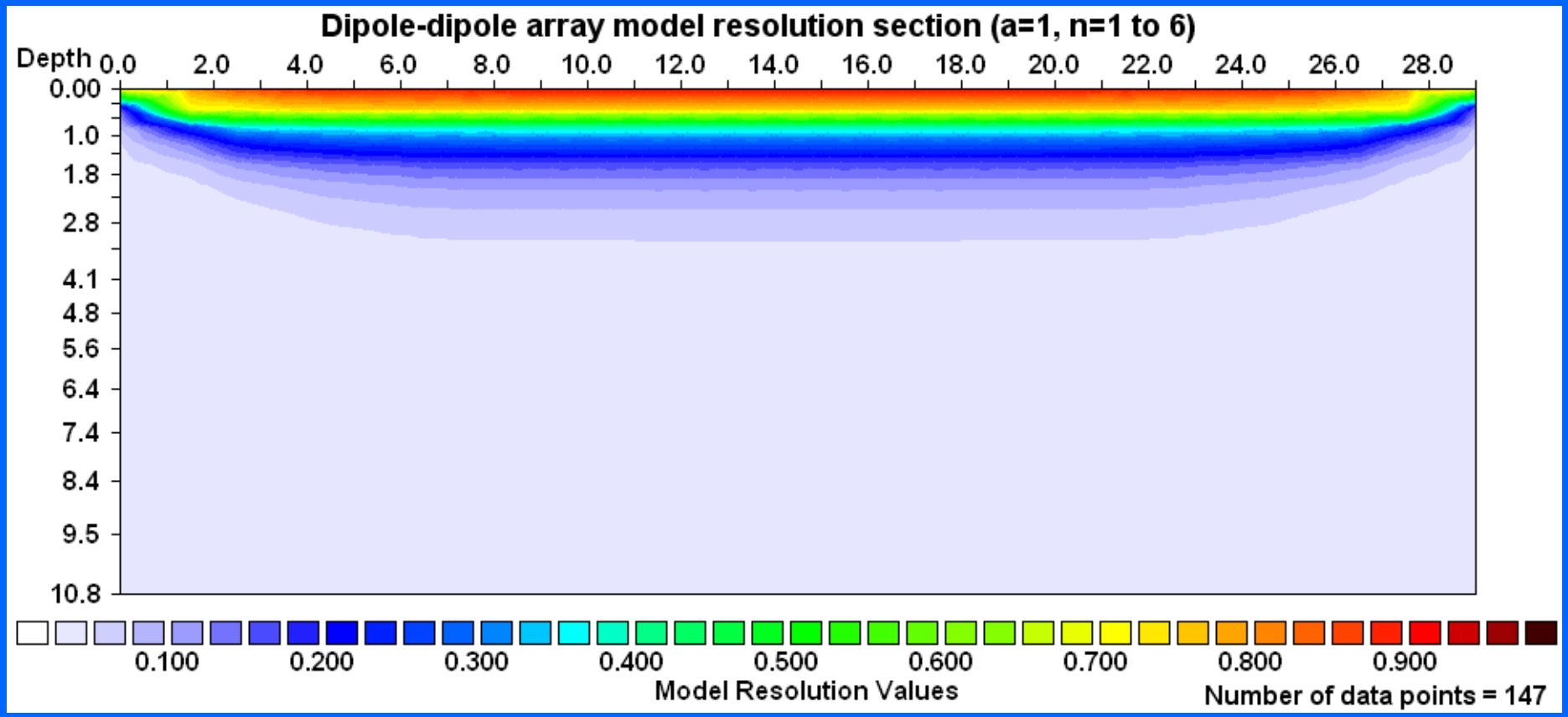

Note that the resolution is greatest near the surface, decreases rapidly with depth, and is not significant below a depth of about 3.0 to 3.5 meters. It has slightly more data points than the Wenner, and performs significantly better.

Dipole-dipole survey with multiple dipole spacings

Now, lets see what happens if we use the method of overlapping data levels with the dipole length a =1 to 3 meters, and n=1 to 6.

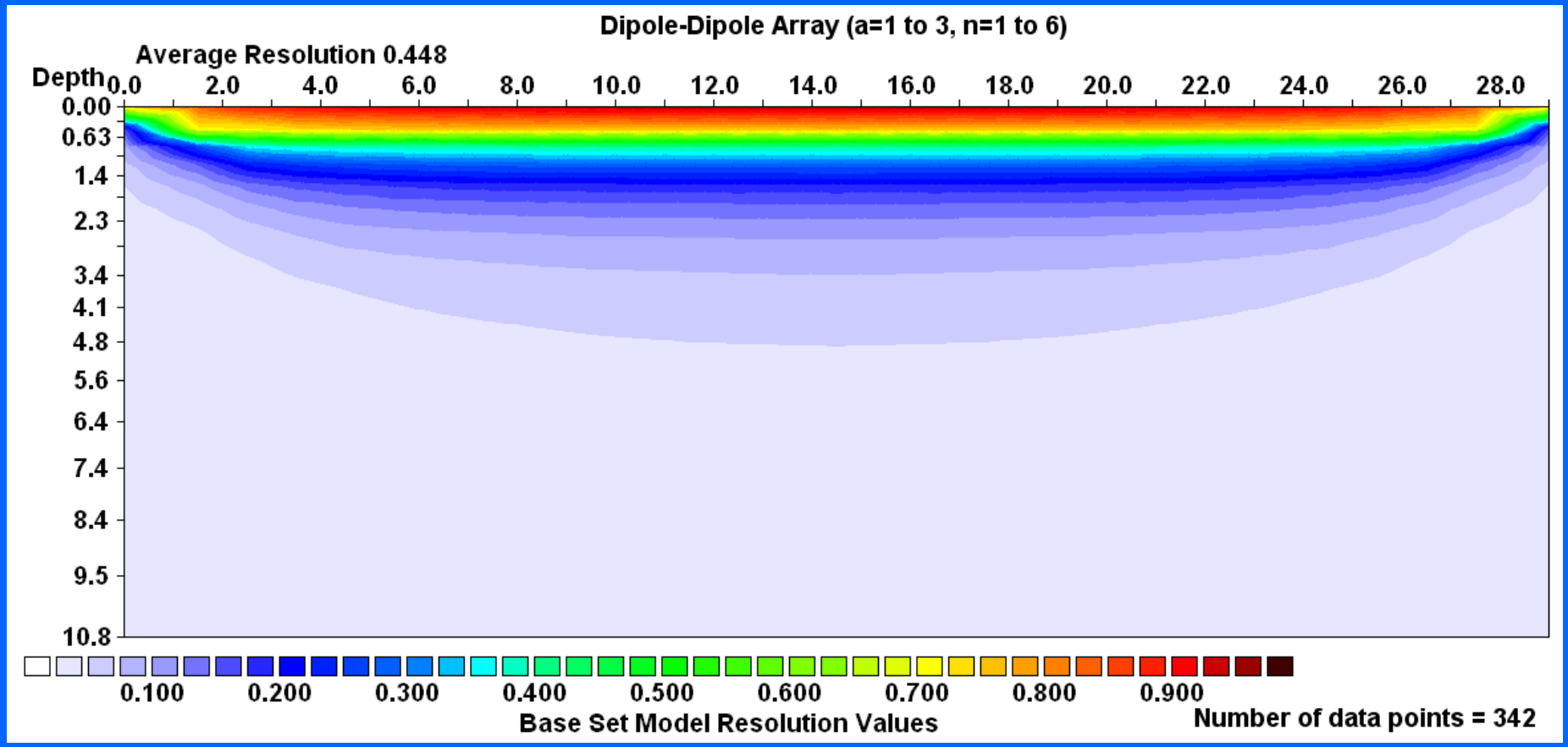

The region with significant resolution values increases to about 5 meters, an improvement from the 3.5 meters limit with a single ‘a’ dipole length (although it is mainly concentrated near the center).

Wenner-Schlumberger survey with multiple spacings

The dipole-dipole array has the disadvantage of low signal strength. An alternative is the Wenner-Schlumberger array. The resolution section if we use a =1 to 3 meters, and n=1 to 8 is shown below.

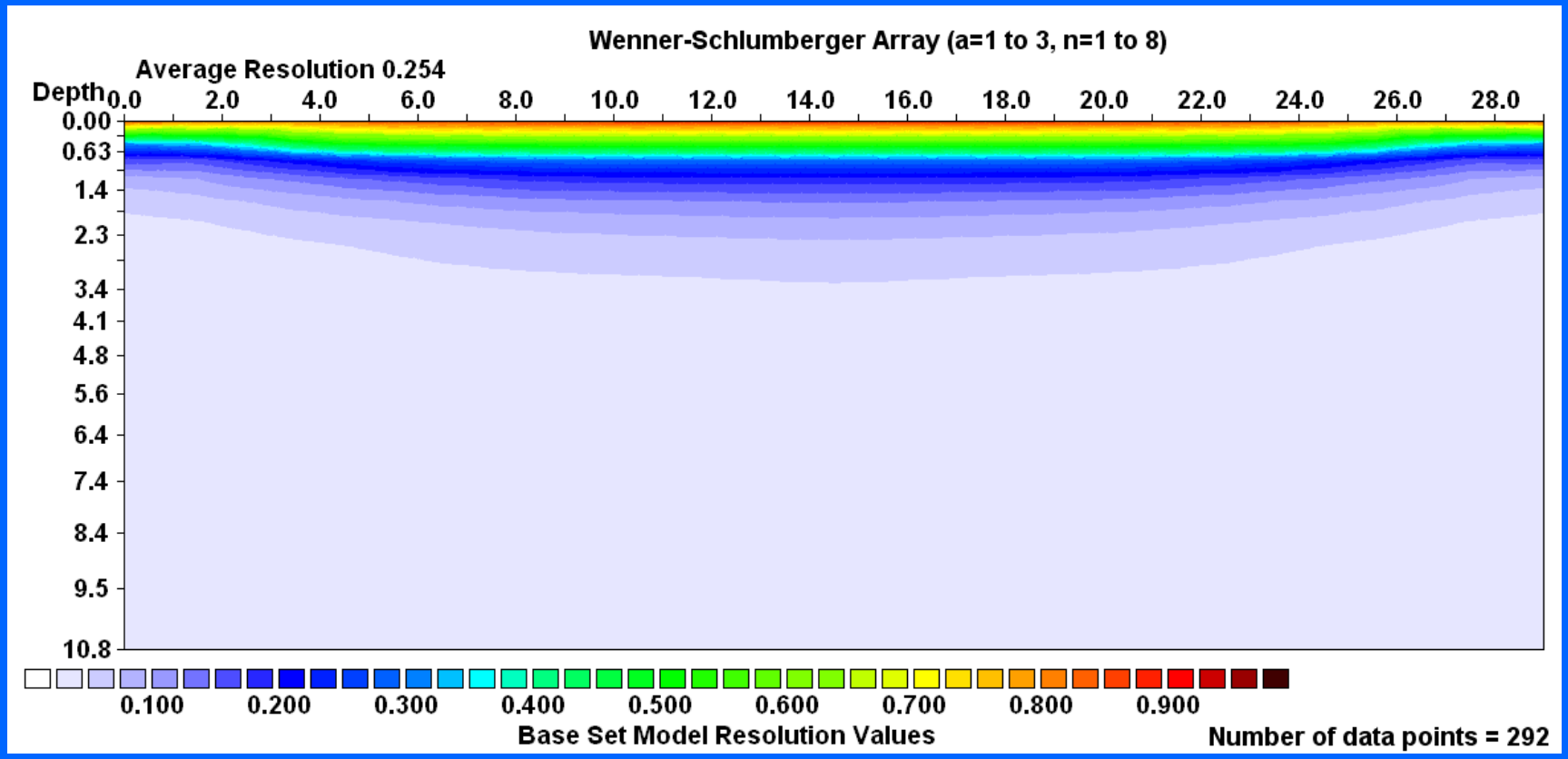

The region with significant resolution values extends to about 3 meters, an improvement from the Wenner, but poorer than the dipole-dipole.

Example of model resolution – landfill survey

This example is from a Wenner array survey over a landfill site with a region of low resistivity values in the landfill. (c) shows the model resolution section normalized by the cell size. (d) shows the model resolution multiplied by the number of model cells to give an index value, i.e. R_{ii}.m, to remove the effect of how finely we subdivide the subsurface.

If a cut-off value of 5 is used for the index value, the depth with significant information is about 19 to 22 meters. The slightly lower depth in the resolution contours below the low resistivity zone due to the zone that blocks more of the current from flowing below it. Note the resolution values do not taper off towards the ends of the lines as rapidly as the pseudosection.

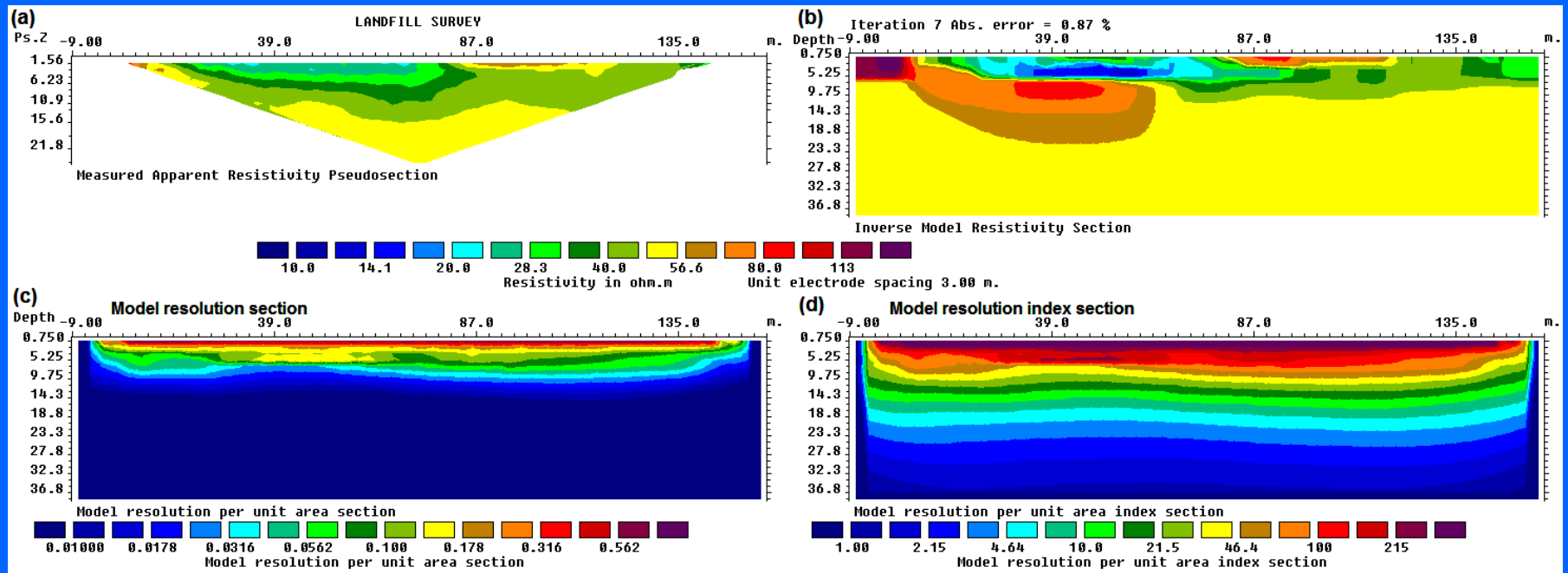

Blanking out model using model resolution index

The model resolution values can be used to blank out parts of the model with low resolution values and are not reliable.

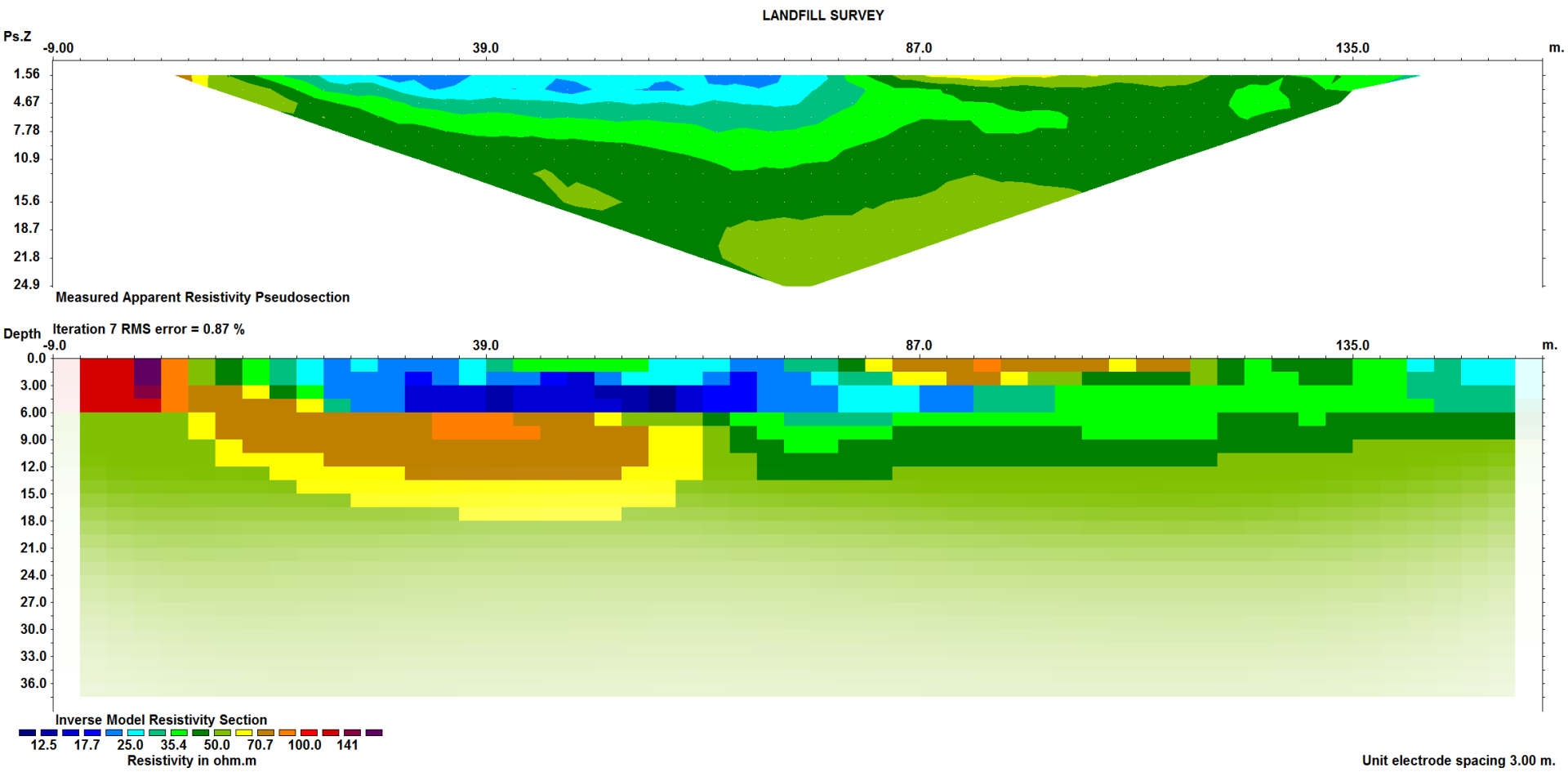

Model reliability – Resolution and DOI

The model resolution shows a more gradual change with depth (and also laterally) in the resolution values compared to the DOI. The 5 model resolution index contour (about 19 to 21 m depth) is slightly shallower than 0.1 DOI index lower contour at about 27 m. The model resolution section avoids the localized regions with high DOI index values. It is less empirical in nature compared to the DOI index method.

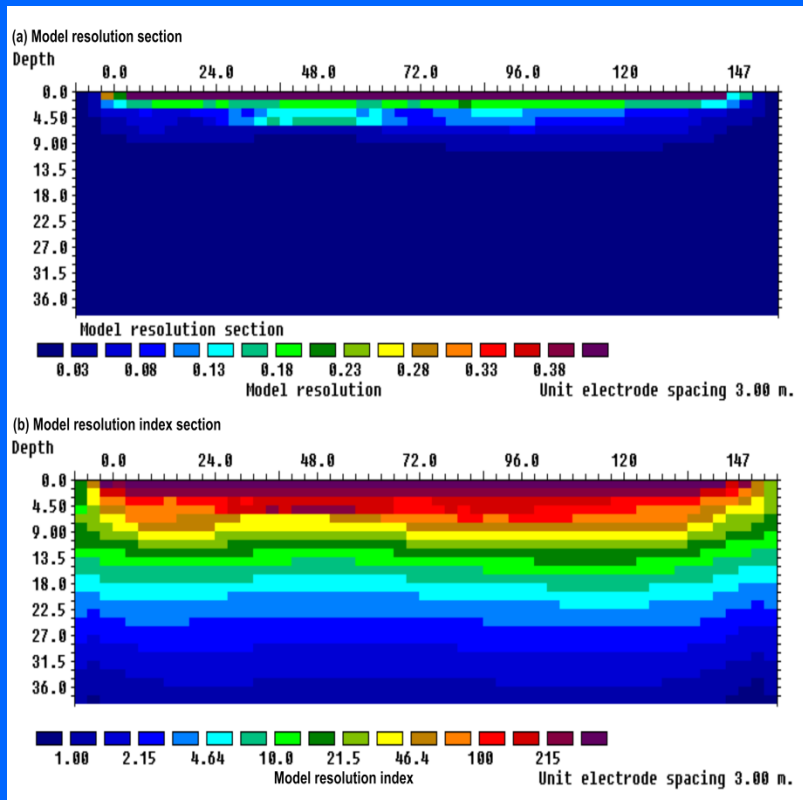

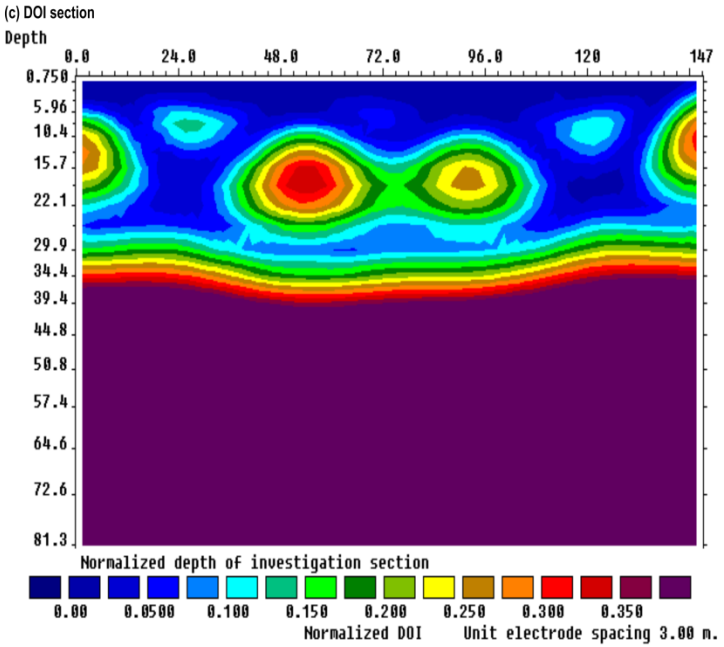

Comparison of methods to assess model reliability

Method	Advantages	Disadvantages
Sensitivity	Simple and fast to calculate.	A very crude measure. Does not take into account data redundancy.
DOI	Can be used for any inversion model. Only requires two inversions of the same data set. It can be used for very large 3-D models.	Can have localized regions with high or low DOI values, caused by noise or local anomalies. Sensitive to stability of inversion method used.
Covariance matrix and resolution section	Less subjective, shows a smoother variation than DOI.	Calculation time is proportional to cube of number of model cells. Limitations in using for very large 3-D models (over 100,000 model cells).